The effect of Distributed Generation on the Quality of Power

A dissertation presented to

The School of Electrical, Electronic
and Computer Engineering

North-West University

In partial fulfilment of the requirements for the degree

Magister Ingeneriae
(Electrical & Electronic Engineering)

by

Chris J. Viljoen

Supervisor: Prof. G. van Schoor

May 2006

Potchefstroom Campus

Declaration

I hereby declare that all the material incorporated in this thesis is my own original unaided work except where specific reference is made by name or in the form of a numbered reference. The work herein has not been submitted for a degree at another university.

Signed: _____

Chris Viljoen

Executive Summary

This document presents a study of the effects distributed generation (DG) has on the power quality (PQ) of electrical power networks. At the time the study was proposed the scheme of DG was speculative by nature and the initiative to employ it was eagerly anticipated. The aim of the study is to explore the possibilities of DG. More specifically, the impact DG has on PQ in power networks is best studied and described by practical measurements of real existing systems in accordance with the purposes and goals of this study. Unfortunately, such systems (termed scenarios) are uncommon given that the technologies associated with DG were not widely operational at the time of writing the dissertation.

The alternative is to simulate the DG scenarios and lay a foundation for a well defined knowledge base sketching the behaviour of DG scenarios. This could aid with predictions and provide realistic boundaries for DG performance expectations. The effects are observed, documented, motivated and apt conclusions drawn and guidelines are proposed for the effective utilization of DG. In this document the development of three experimental simulation scenarios will be described. The reader will also encounter the proposed and adopted methods for simulation of the developed scenarios.

It is shown that a strategic application of DG is accompanied by numerous beneficial influences, all of which are advantageous effects and ensures improved long-term scenario performance. These effects include, but are not limited to, the isolation of waveform disturbing loads (sources), the reduction of impedance paths leading to these non-linear loads, and the attenuation of harmonics by coincidental passive filtering paths in a network, to name an important few. Proof of these advantageous effects is found in the comprehensive study and investigation of accurately developed computer simulation scenario models and the generated results thereof. Finding correlations between the researched literature and the responses of the simulated scenarios support the validity of the simulation results and will aid in truthfully describing the observed effects. Precise conclusions are drawn and form the basis of the suggested strategy for PQ improving DG applications.

A cost function is proposed, developed and presented. The generated data is scrutinized and after careful perusal key factors are identified that play a major part in the cost function. The identified crucial factors are incorporated in the assembly of three indicators that collectively quantify the performance of the scenario being investigated. A cost function is thus applied to fittingly quantify the total performance of each of the three individual scenarios. The cost function is tested and shown to respond appropriately if any of the three indicators are intentionally disturbed – i.e. reset one indicator to a new value while keeping the other two constant. The cost function relays the value change returning a new performance index, reflecting the change in the concerned indicator.

The generated cost function data is carefully studied in conjunction with the simulation results and further conclusions are drawn based on motivations supported by the researched literature. These final conclusions complement the initial findings and provide guidelines for the strategic application of DG maximizing the effect DG has on the performance of the optimized scenario. The observed effects are summarized and detailed presentations of each are made in cause-related categories. Recommendations are made for improvements to the present study and future work linked to the study is proposed.

Opsomming

Hierdie dokument beskryf 'n studie aangaande die effekte van verspreide generasie (VG) op die drywingskwaliteit (DK) van elektriese kragnetwerke. Met die aanvang van die projek was VG nog 'n vae konsep en was die gebruik en toepassing daarvan spekulatief van aard. Die doel van hierdie studie is om die moontlikhede van VG binne die raamwerk van DK verbetering en die toepaslikheid daarvan te ondersoek. Die beste manier om die impak van VG op DK in kragnetwerke te ondersoek is met behulp van praktiese en realistiese metings van werklike stelsels terwyl daar streng gehoor gegee word aan die doel en uitkomste van hierdie studie. Ongelukkig is sulke stelsels (ook genoem scenario's) ongewoon omdat die tegnologieë wat daarmee gepaard gaan nie in algemene gebruik was toe hierdie dokument geskryf is nie.

Die alternatief is om gesimuleerde VG scenario's te ondersoek en die verwerkte resultate te gebruik om 'n goed-gedefinieërde fondasie te lê vir die gedrag van VG scenario's. Hierdie kennis-basis kan gebruik word om voorspellings te maak en gepaste grense vir die gedrag van VG vas te stel. Die waargenome effekte word volledig gedokumenteer, gemotiveer en daar word tot gepaste gevolgtrekkings gekom wat lei tot die voorstel van riglyne vir die effektiewe toepassing van VG. In hierdie dokument word die ontwikkeling van drie scenario's bespreek waartydens die leser die voorgestelde en aangewende simulasiemetodes sal teëkom.

Dit word bewys dat die strategiese toepassing van VG gepaard gaan met verskeie voordelige effekte; verbeterde lang-termyn gedrag vir die kragnetwerk word ook verseker. Hierdie effekte sluit in die isolering van golfvorm-versteurende laste (-bronne), vermindering van die toevoer impedansie van nie-lineêre laste, en die demping van harmonieke as gevolg van toevallige passiewe filternetwerke in 'n netwerk. Bewyse van hierdie voordelige invloed word gevind in die volledige studie en ondersoek van die akkuraat-ontwikkelde scenario rekenaarmodelle en die resultate daardeur gegenereer. Ooreenkomste tussen die literatuurstudie en die respons van die gesimuleerde scenario's ondersteun die geldigheid van die simulasieresultate en help om die waargenome effekte te bespreek. Presiese gevolgtrekkings word gemaak en dien as basis vir die voorgestelde strategie om DK met VG te verbeter.

'n Kostefunksie word voorgestel, ontwikkel en geïllustreer. Die gegenereerde data word ondersoek en na versigtige oorweging word sleutelfaktore geïdentifiseer vir die kostefunksie. Hierdie faktore word in die samestelling van die indikators gebruik wat as 'n geheel die gedrag van die scenario beskryf. Die kostefunksie word dus op gepaste wyse gebruik om die algehele gedrag van elk van die drie scenario's te kwantifiseer en te beskryf. Die kostefunksie word getoets om te bepaal of dit 'n verandering in enige van die drie indikators akkuraat weerspieël. Die algehele gedragsindeks moet ook die verandering weerspieël.

Die verkrygde kostefunksie-resultate word noukeurig bestudeer saam met die simulasieresultate en lei tot verdere gevolgtrekkings wat gebaseer is op motiverings wat deur die literatuurstudie ondersteun word. Die waargenome effekte word opgesom en deeglik voorgestel in kategorieë wat verdeel is in oorsake van die effek. Aanbevelings word gemaak vir verbeterings aan die huidige studie en vir verdere werk rakende die studie.

Acknowledgements

First of all, I am absolutely grateful to my Heavenly Father for blessing me with the abilities to have attempted this study. All thanks and glory to Him and I am overjoyed to confess that He is our divine Creator and Saviour.

Next, I would like to thank M-Tech Industrial and PBMR (by means of bursary) and THRIP for funding this research and granting me the opportunity to further my studies.

I would also like to acknowledge the following people, in no particular order, for their contributions during the course of this project:

- My study leader and mentor, Professor George van Schoor, for his guidance, advice, support and patience that stood central to the success of this project.
- My parents, Hennie and Maritha Viljoen, for their love, support and understanding. They have truly been exceptional in motivating and promoting me throughout my studies.
- My brothers, Henk and Marius Viljoen, for their company and support.
- My loving partner and confidant, Alretha Matthee. Thank you for encouraging me to persist and for bringing out the best in me.
- My friends, Neil Kemp, Jan Prinsloo, and the rest who'll remain anonymous, for their belief and confidence in my abilities.
- Mrs. Isabel Delport (on behalf of M-Tech Industrial) for her services during my studies.

"A good name is rather to be chosen than great riches, and loving favour rather than silver and gold". Proverbs 22:1

"Gratitude is not only the greatest of virtues, but the parent of all others."
Cicero (106 BC - 43 BC)

Table of Contents

DECLARATION I
EXECUTIVE SUMMARY II
OPSOMMING III
ACKNOWLEDGEMENTS IV
CHAPTER 1 INTRODUCING DISTRIBUTED POWER GENERATION 1
1.1 INTRODUCTION 1
1.2 BACKGROUND 1
1.2.1 DISTRIBUTED GENERATION VERSUS CENTRAL STATION GENERATION 1
1.2.2 DEFINING DISTRIBUTED POWER GENERATION 3
1.2.3 THE STANDARD: IEEE P1547 6
1.2.4 BRIEF OVERVIEW OF EXISTING DG TECHNOLOGY 6
1.2.5 MORE APPLICATIONS OF DISTRIBUTED GENERATION 7
1.2.6 POWER QUALITY 8
1.3 PROBLEM STATEMENT 8
1.4 ISSUES TO BE ADDRESSED, ASSUMPTIONS AND METHODOLOGY 9
1.4.1 DESIGN PROCESS 9
1.4.2 SYSTEM SPECIFICATION 9
1.4.3 SYSTEM MODELLING 10
1.4.4 DESIGN IMPLEMENTATION 10
1.4.5 SYSTEM EVALUATION 10
1.4.6 DELIMITATIONS 10
1.5 OVERVIEW OF THE DISSERTATION 10
1.6 SUMMARY 11
CHAPTER 2 LITERATURE STUDY 12
2.1 INTRODUCTION 12
2.2 DISTRIBUTED GENERATION TECHNOLOGY OVERVIEW 12
2.2.1 THE PEBBLE BED MODULAR REACTOR (PBMR) 14
2.3 POWER QUALITY OVERVIEW 16
2.3.1 ELECTRICAL UNBALANCE AND ASYMMETRICAL COMPONENTS 16
2.3.2 HARMONICS 18
2.3.3 IMPROVING GRID PERFORMANCE BY CONNECTING DISTRIBUTED RESOURCES 27
2.3.4 POWER QUALITY ISSUES IN DISTRIBUTED GENERATION 28
2.3.5 POWER QUALITY AND DISTRIBUTED GENERATION 31
2.4 RELIABILITY, COST AND PLANNING – THE ANTAGONIZED RELATIONSHIP 32
2.5 SUMMARY AND CONCLUSION(S) 32
CHAPTER 3 POWER SYSTEM SCENARIOS 34
3.1 INTRODUCTION 34
3.2 METHODS AND ASSUMPTIONS 34
3.3 THE SCENARIOS AND THEIR DEVELOPMENT 36
3.3.1 THE FIRST SCENARIO 37
3.3.2 THE SECOND SCENARIO 39
3.3.3 THE THIRD SCENARIO 41
3.4 RESULTS OF THE SCENARIOS 44
3.4.1 THE RESULTS OF SCENARIO 1 46
3.4.2 THE RESULTS OF SCENARIO 2 47
3.4.3 THE RESULTS OF SCENARIO 3 48
3.5 SUMMARY AND CONCLUSIONS 49
CHAPTER 4 MEASURING SCENARIO PERFORMANCE 50
4.1 INTRODUCTION 50
4.2 THE MATHEMATICS: SINUSOIDAL & NON-SINUSOIDAL CALCULATIONS 50
4.2.1 SINUSOIDAL MATHEMATICS 50
4.2.2 NON-SINUSOIDAL MATHEMATICS 54
4.3 THE COST FUNCTION 59

4.4 TESTING AND VERIFICATION OF THE COST FUNCTION 64
4.5 SUMMARY 66
CHAPTER 5 SIMULATION RESULTS AND SCENARIO PERFORMANCE IMPROVEMENT 67
5.1 INTRODUCTION 67
5.2 GENERATED SIMULATION RESULTS DATA STRUCTURE 67
5.3 SCENARIO 1 RESULTS 70
5.4 SCENARIO 2 RESULTS 77
5.5 SCENARIO 3 RESULTS 81
5.6 SUMMARY AND CONCLUSIONS 87
CHAPTER 6 OVERVIEW, CONCLUSIONS AND RECOMMENDATIONS 88
6.1 INTRODUCTION 88
6.2 OVERVIEW 88
6.2.1 WAVEFORM DISTORTION (HARMONIC DISTORTION): 88
6.2.2 VOLTAGE REGULATION (GENERATED- AND TRANSMITTED VOLTAGE LEVELS): 89
6.2.3 SYSTEM EFFICIENCY – LINE LOSSES (AND TRANSFORMERS, ETC.): 89
6.2.4 MORE OBSERVATIONS (POWER FLOW, *POWER FACTOR*, RELIABILITY, ETC.): 90
6.3 CONCLUSIONS 90
6.4 RECOMMENDATIONS 92
6.4.1 THE STUDY AT PRESENT 92
6.4.2 FUTURE WORK 93
APPENDIX 94
APPENDIX A REMAINING DISTRIBUTED GENERATION TECHNOLOGIES 94
A.1 FUEL CELL POWERED DISTRIBUTED GENERATORS 94
A.2 RENEWABLE RESOURCE DISTRIBUTED GENERATORS 96
A.3 DISTRIBUTED GENERATION AND ENERGY STORAGE 103
APPENDIX B RELIABILITY, COST AND PLANNING CONTINUED 105
B.1 POWER SYSTEM RELIABILITY 105
B.2 PLANNING- AND DEVELOPMENT COST 106
B.3 COST VERSUS RELIABILITY 106
B.4 VALUE-BASED PLANNING 107
APPENDIX C DEVELOPED MATLAB® SIMULINK® MODELS 108
C.1 POWER SYSTEM SCENARIOS 108
C.2 DEVELOPED MATLAB® SIMULINK® MODELLING BLOCKS 116
APPENDIX D MATHCAD® 2001 WORKSHEETS 120
APPENDIX E DATA PROVIDED BY ESKOM FOR SCENARIO 3 133
APPENDIX F COMPARING LOAD FLOW ANALYSIS AND SIMULATION RESULTS 134
BIBLIOGRAPHY 143

List of Figures

FIGURE 2-1: SOLID MODEL ILLUSTRATION OF THE MPS [23]..... 14
FIGURE 2-2: PBMR SYSTEM LAYOUT AND BRAYTON CYCLE [24]..... 15
FIGURE 2-3: BALANCED THREE-PHASE NETWORK..... 16
FIGURE 2-4: UNBALANCED THREE-PHASE NETWORK..... 17
FIGURE 2-5: UNBALANCED PHASE WAVEFORMS..... 17
FIGURE 2-6: DISTORTION OF THE FUNDAMENTAL WAVEFORM BY A HARMONIC WAVEFORM [27]..... 19
FIGURE 2-7: THE WAVEFORMS OF A SINGLE-PHASE TWO-PULSE DIODE BRIDGE CONVERTER [28]..... 19
FIGURE 2-8: AN EXAMPLE OF A TYPICAL POWER SYSTEM IN PRACTICE WITH A SOURCE AND LOADS [29]..... 23
FIGURE 2-9: A SUGGESTION FOR THE USE OF DG IN THE EXAMPLE DISCUSSED IN SECTION 2.3.2.1 [29]..... 28
FIGURE 2-10: TYPICAL OVER-VOLTAGE WAVEFORM [36]..... 30
FIGURE 2-11: VARIABLE SPEED DRIVE INPUT CURRENT WAVEFORM AND HARMONIC SPECTRUM [36]..... 30
FIGURE 3-1: SCENARIO 1 CONSISTS OF A SERIES OF MEDIUM-LENGTH LINES WITH LOADS AT INTERVALS..... 38
FIGURE 3-2: SCENARIO 2 IS A SYSTEM WITH TRANSMISSION LINES MEETING AT A COMMON POINT..... 40
FIGURE 3-3: THE TRANSMISSION SYSTEM AS PROVIDED BY ESKOM – SCENARIO 3..... 42
FIGURE 3-4: TYPICAL MEASUEMENTS FOR A MEASUREMENT BUS..... 45
FIGURE 3-5: FFT-ANALYSIS OF THE A-PHASE VOLTAGE WAVEFORM IN FIGURE 3-4..... 46
FIGURE 4-1: PHASOR DIAGRAM AND POWER TRIANGLE FOR A LAGGING POWER FACTOR (INDUCTIVE LOAD)..... 52
FIGURE 4-2: PHASOR DIAGRAM AND POWER TRIANGLE FOR A LEADING POWER FACTOR (CAPACITIVE LOAD)..... 53
FIGURE 4-3: MATHEMATICAL CALCULATION FLOWCHART DEPICTING THE VARIABLE INTERRELATIONSHIPS..... 60
FIGURE 4-4: COST FUNCTION FLOWCHART..... 63
FIGURE 4-5: *VOLTAGE REGULATION INDICATOR* INFLUENCE ON THE *PERFORMANCE INDICATOR*..... 64
FIGURE 4-6: *HARMONIC DISTORTION INDICATOR* INFLUENCE ON THE *PERFORMANCE INDICATOR*..... 65
FIGURE 4-7: *LINE LOSS INDICATOR* INFLUENCE ON THE *PERFORMANCE INDICATOR*..... 66
FIGURE 5-1: PERFORMANCE INDEX PLOT FOR PLACEMENT OF A DG UNIT AT THE LABELLED BUS..... 75
FIGURE 5-2: SUGGESTED PLACEMENT OF THE DG UNITS RESULTING IN AN OPTIMUM SOLUTION..... 76
FIGURE 5-3: DG PLACEMENT SOLUTION FOR SCENARIO 2..... 77
FIGURE 5-4: PERFORMANCE INDEX PLOT FOR SCENARIO 2..... 78
FIGURE 5-5: BAR PLOTS OF THE PERFORMANCES FOR THE TWO CONDITIONS OF SCENARIO 3..... 85
FIGURE 5-6: DG PLACEMENT FOR THE SUGGESTED SOLUTION FOR SCENARIO 3..... 86
FIGURE A-1: ILLUSTRATION OF THE ELEMENTS OF A FUEL CELL [2]..... 95
FIGURE A-2: TWO TYPES OF SOLAR THERMAL POWER, TROUGH- AND PARABOLIC MIRROR [2]..... 97
FIGURE A-3: THE STIRLING CYCLE ILLUSTRATED HERE WITH A "SINGLE CYLINDER" STIRLING ENGINE [2]..... 100
FIGURE A-4: STRUCTURE OF A TYPICAL PV CELL [2]..... 101

List of Tables

TABLE 0-1: LIST OF ABBREVIATIONS. IX
TABLE 0-2: LIST OF SYMBOLS. X
TABLE 1-1: TECHNOLOGIES FOR DG [18], [19], [20]. 7
TABLE 2-1: RESULTS AND CAUSES OF HARMONICS [28]. 20
TABLE 2-2: COMPATIBILITY LEVELS FOR HARMONIC VOLTAGES IN LV AND MV NETWORKS [32] 25
TABLE 2-3: RECOMMENDED LIMITS FOR HARMONIC VOLTAGES IN HV AND EHV NETWORKS [32]. 26
TABLE 2-4: LIMITS FOR HARMONIC VOLTAGES IN MEDIUM-VOLTAGE (MV) AND HV NETWORKS [33]. 27
TABLE 2-5: PQ PHENOMENA CLASSIFICATION. 29
TABLE 3-1: SUMMARY OF THE RELEVANT MATHEMATICAL EQUATIONS. 35
TABLE 3-2: POWER FLOW ANALYSIS BUS TYPES [35] 37
TABLE 3-3: DETAILED DATA SUMMARY OF SCENARIO 1. 39
TABLE 3-4: DETAILED DATA SUMMARY OF SCENARIO 2. 41
TABLE 3-5: DETAILED DATA SUMMARY OF SCENARIO 3. 43
TABLE 3-6: SIMULATION PARAMETERS USED FOR THE SIMULATIONS. 44
TABLE 3-7: SUMMARIZED DATA RESULTS FOR SCENARIO 1. 47
TABLE 3-8: SUMMARIZED DATA RESULTS FOR SCENARIO 2. 47
TABLE 3-9: SUMMARIZED DATA RESULTS FOR SCENARIO 3. 48
TABLE 5-1: SELECTED CALCULATED AND MEASURED RESULTS FOR THE SWING BUS OF SCENARIO 2. 68
TABLE 5-2: CALCULATED AND MEASURED RESULTS FOR LINE 1 IN SCENARIO 2. 68
TABLE 5-3: COMPARATIVE SUMMARY OF SELECTED RESULTS FOR SCENARIO 2. 69
TABLE 5-4.1: SUMMARIZED RESULTS FOR ALL THE BUSES SCENARIO 1. 71
TABLE 5-5.1: SUMMARIZED BUS RESULTS FOR SCENARIO 1 WITH DG CONNECTED TO BUS 3 LOAD. 73
TABLE 5-6: CALCULATED PERFORMANCE INDICES FOR ALL POSSIBLE DG PLACEMENT PERMUTATIONS. 75
TABLE 5-7: CALCULATED PERFORMANCE INDICES FOR DIFFERENT DG PLACEMENTS IN SCENARIO 2. 79
TABLE 5-8: RESULTS FOR SCENARIO 2 WITH A DG UNIT CONNECTED TO BUS 4 LOAD. 80
TABLE 5-9.1: SUMMARIZED BUS DATA RESULTS FOR THE INITIAL CONDITION OF SCENARIO 3. 81
TABLE 5-10: PERFORMANCE INDEX INFORMATION FOR INITIAL- AND SUGGESTED CONDITIONS. 84
TABLE A-1: THE THREE MAJOR APPLICATIONS OF ENERGY STORAGE WITH DG [2] 103

Nomenclature

Following is a list of abbreviations and acronyms used in the following document. The reader is encouraged to study the list before continuing and can consult this section when uncertainty arises regarding any of the abbreviations while reading the text.

Table 0-1: List of abbreviations.

Abbreviation	Meaning
ac	Alternating current
AI	Artificial intelligence
ANSI	American National Standards Institute
BCP	Budget-constrained planning
CAD	Computer-aided design
CHP	Combined heat and power
CIGRE	International Council on Large Electric Systems
CSG	Central station generation
dc	Direct current
DG	Distributed generation
DR	Distributed resource
DSM	Demand-side management
EHV	Extra high-voltage
EPRI	Electric Power Research Institute
EPBS	Electric power back-up system
EPS	Electric power system
ESBS	Electric stand-by system
GWh	Gigawatt hour (1 000 000 000 watt/hour)
HV	High-voltage
IEEE	Institute of Electrical and Electronic Engineers
IEA	International Energy Agency
IRP	Integrated resource planning
ISO	Independent system operators
kWh	Kilowatt hour (1 000 watt/hour)
LV	Low voltage
MPS	Main power system
MTBF	Mean time between failures
MTTR	Mean time to repair
MV	Medium voltage
MWh	Megawatt hour (1 000 000 watt/hour)
NEPAD	New Partnership for Africa's Development
PBMR	Pebble bed modular reactor
PCC	Point of common coupling
PQ	Power quality
pu	Per-unit
PV	Photovoltaic
rms	Root-mean-square
SMES	Superconducting magnetic energy storage
STES	Solar thermal energy storage
SVR	Step voltage regulators
T&D	Transmission and distribution
VBP	Value-based planning

Table 0-2 is a list of symbols used during the study

Table 0-2: List of symbols.

Symbol	Meaning
α_1	Fundamental voltage component phase angle
α_{ah}	Phase angle of the harmonic phase voltage component in phase *a*
β_1	Fundamental current component phase angle
β_{ah}	Phase angle of the harmonic line current component in phase *a*
DPF	Displacement power factor
$i(t)$	Instantaneous line current
$i_a(t)$	Instantaneous a-phase line current
I	Rms current
I_1	Rms fundamental harmonic current component
I_H	Rms harmonic current component
I_0	Zero-sequence current component
I_1	Positive-sequence current component
I_2	Negative-sequence current component
I_{a0}	Average (or dc) value line current in phase *a*
I_a	Line-a current (current through phase-a)
I_{ah}	Harmonic line current component in phase *a*
I_b	Line-b current
I_c	Line-c current
I_e	Effective three-phase current
I_{e1}	Effective three-phase fundamental harmonic current component
I_{eH}	Effective three-phase harmonic current component
$Index_{performance}$	Performance indicator
$Index_{Ploss}$	Line loss indicator
$Index_{THD}$	Harmonic distortion indicator
$Index_V$	Voltage regulation indicator
I_p	Line current
$ITHD$	Total harmonic current distortion
$ITHD_e$	Total harmonic effective current distortion
N	Total single-phase non-active power
N_H	Harmonic single-phase non-active power
P	Active power
P_1	Fundamental single-phase active power
$P_{3\Phi}$	Total three-phase active power
$P_{3\Phi 1}$	Total three-phase fundamental active power
$P_{3\Phi H}$	Total three-phase harmonic active power
PF	True apparent power factor
P_H	Total harmonic single-phase active power
$P_{loss\,i}$	Three-phase active power loss for line *i*
$p(t)$	Instantaneous active power
$p_R(t)$	Instantaneous active power component
$p_X(t)$	Instantaneous reactive power component
Q	Reactive power
$Q_{3\Phi}$	Total three-phase reactive power
$q(t)$	Instantaneous reactive power
S	Apparent power
S_1	Fundamental apparent power
S_e	Three-phase effective apparent power
S_{e1}	Effective fundamental apparent power
S_{eN}	Effective non-fundamental apparent power
S_{eN}/S_{e1}	Harmonic pollution indicator
S_{ieN}/S_{ie1}	Harmonic pollution indicator for bus *i*
S_H	Total harmonic single-phase apparent power
S_N	Non-fundamental apparent power
θ	Phase angle
θ_1	Phase angle difference between fundamental voltage and -current components
θ_i	Current phase
THD	Total harmonic distortion
θ_v	Voltage phase

$v(t)$	Instantaneous phase voltage
$v_a(t)$	Instantaneous a-phase voltage
$v_{bc}(t)$	Instantaneous line-line voltage (b- and c-phase)
V	Rms voltage
V_1	Rms fundamental harmonic voltage component
V_H	Rms harmonic voltage component
V_0	Zero-sequence voltage component
V_1	Positive-sequence voltage component
V_2	Negative-sequence voltage component
V_{a0}	Average value for the *a*-phase voltage
V_{ag}	A-phase voltage (between line a and ground)
V_{ah}	Harmonic phase voltage component in phase *a*
V_{bg}	B-phase voltage
V_{cg}	C-phase voltage
V_e	Effective three-phase voltage
V_{e1}	Effective three-phase fundamental harmonic voltage component
V_{eH}	Effective three-phase harmonic voltage component
$V_{e1}I_{eH}$	Current distortion power
$V_{eH}I_{e1}$	Voltage distortion power
$V_{eH}I_{eH}$	Harmonic distortion power
V_{ie1}	Effective three-phase fundamental voltage magnitude for bus *i*
V_p	Phase voltage
$VTHD$	Total harmonic voltage distortion
$VTHD_e$	Total harmonic effective voltage distortion

Chapter 1

Introducing Distributed Power Generation

1.1 Introduction

In this chapter the reader is introduced to the available definitions, key specifications (standards) and descriptions of DG. First, the reader needs to be familiar with the meaning of distributed generation. After this initial introduction to DG the available technologies employed as distributed resources are briefly discussed. A more in-depth discussion of the technologies is left for Chapter 2 and Appendix A, but the pebble bed modular reactor (PBMR) is of primary concern. Finally, the problem statement is presented, followed by the issues to be addressed, assumptions, methodology and a terse overview of the whole document.

1.2 Background

Since the emergence of distributed generation resources, and considering the recent developments of the generation technologies, it has been expected that the industry would apply the trend, now commonly known as distributed generation (DG). This concept is current and modern and, as such, has not been able to develop any formal standards or definitions that accurately describe it [1]. There are a few short definitions available as of late, and there is talk of an eagerly awaited published draft for the standards of this concept.

DG technologies provide energy solutions to customers that are more cost-effective, environmentally friendly, or provide higher power quality and reliability than conventional solutions. Power quality (PQ) plays an important role in DG and with the aid of analysis tools – possibly incorporating the use of artificial intelligence (AI) – PQ can be analyzed and controlled. Different scenario's of how DG can be applied exist; each having a unique effect on the PQ.

1.2.1 Distributed Generation versus Central Station Generation

As mentioned earlier, central station generation (CSG), also known as the conventional power generation method, consists of a few large power stations. Strategic placement as close as possible to the majority of consumers allows convenient delivery of power, while simultaneously enabling an efficient route for the fuel supply of the station (coal stations), or the availability of adjacent cooling masses such as large masses of water (nuclear stations) [2]. Other factors also include the potential for hydro-electric power from rivers and other large masses of moving water (hydro-electric power stations and tidal power stations), etc.

The rest of the consumers, and in most instances, the entire consumer load relies on electric power provided via transmission lines over long distances delivering the required electricity. This is consequence of power stations remotely connected to the power grid due to the technology employed and the location of the "energy pool" (hydro-electric power stations, nuclear, etc.). Quite often the power quality deteriorates after transmission over these long inefficient lines. The lines themselves

become very complex due to their respective lengths, and these complexities only increase as the line lengths do.

Conventional generation does however have the advantage of physical size and in terms of size the utility always profits with regards to improved efficiency, generating capacity, reliability and expanding potential; while enjoying lowered running costs, generation costs and maintenance. The drawback of conventional generation is the relatively high transmission and distribution (T&D) costs. The utility is solely responsible for the distribution and transmission of electricity to the customer. The customer pays for both the T&D service and the amount of electrical power used (generation cost of the electrical energy). Since the utility provides this service to customers as a whole, the rate is fixed depending on the type of customer (residential-, commercial- and industrial client) and intervals of power usage.

Recent developments in the power industry have lead to the development of smaller and more efficient sources of electrical power. The newly developed sources are more fuel-efficient owing to the modern technology employed in their construction. The traditional power sources remain in use thanks to their inherently large power capacities. The expected general efficiencies of these power stations linger in the area of 28 to 35% while the developed higher efficient power sources range from 40 to 55% [2].

In an age where availability of fuel is continually growing in concern it's merely logical that these newly developed sources be used. Furthermore, T&D costs are constantly rising and conventional methods of power generation and transmission are becoming more expensive as a result. The new generating units have smaller impacts on the environment than large central power stations. The final, and rather pre-eminent fact being investigated, is that a power network consisting of these smaller interconnected generating units will exhibit an improved power quality (PQ) delivering a much more "useful" and economical power to the consumer.

Considering the above, it could be stated then that distributed generation (DG) is the strategic and beneficial utilization of the newly developed smaller generating technologies. This is achieved by the "rearrangement" of an electric power supply grid consisting of the existing utility grid and optimized/supplemented by interconnection with the smaller available generating units able to act as DG units at strategic points in the system. The smaller units are placed conveniently close to the customer causing power problems, such as poor power quality; or at customers who experience poor PQ, lack of reliability, expensive power and inefficient power as a result of being remote or isolated (power loss over long lines and propagated distortion).

The advantages of these smaller units are, to name an eminent few, higher efficiency due to modern technology, lowered T&D costs, improved PQ and reliability (depending on the type of technology employed), less environmental impacts, providing a "type" of technology or power source that is preferred by the customer and reducing aesthetic impacts due to noisy, dirty and excessively large generation methods.

The use of distributed generation (DG) and, more generally, distributed resources (DR) – which includes DG and energy storage systems – has the potential to provide more reliable and lower-cost energy for electricity customers as well as benefits for today's electric transmission and distribution (T&D) systems. This may prove to be particularly true for customer-sited generation. Further, increased interest in the use of DR is evolving as a result of potential opportunities envisioned with the modernization of T&D systems and the advanced development of improved small, modular generation technologies such as fuel cells, photovoltaics, and micro-turbines (pebble bed modular reactor – PBMR). In addition, the potential environmental benefits of DR (for example, for renewable resources and combined heat and power systems) are substantial.

Combining the two concepts would be the optimum solution; as already discussed. A system comprised of the smaller generating units alone would give rise to reliability problems and effective control and administration of such a system would necessitate the development of stringent governing laws/guidelines and treaties to ensure that the unsuspecting customer would have a reliable source of power year round. Power interruptions due to administrative problems are unacceptable and these problems are likely if a number of companies/persons each own a generating unit while they all attempt to sell the most possible power in order to insure a greater profit from their investment.

A symbiotic relationship between the existing utility supply and any newly introduced generating unit, either owned by a third party or just another asset to the utility, is possible as long as the established utility remains the governing body. The utility is then responsible for drawing up the necessary contractual agreements for safe and reliable generation and supply of electrical power to the respective customers. The other remaining issue would be standards for the interconnection of DG to the electric power system (EPS). A draft of such a standard exists and is known as IEEE P1547 Series of Standards for Interconnection [3]. At the time of writing the whole standard was not available for the author's perusal, but the draft was obtained and proved to be sufficiently accurate for the purposes of the study. A brief discussion emphasizing the key points is given in Section 1.2.3.

1.2.2 Defining Distributed Power Generation

Distributed generation (DG) is a newly developed approach in the electric power industry and the available literature regarding the subject shows that there is no general definition for DG as yet. From the literature sources, a widely varying group of terms and definitions used for DG is identified, to name but an acceptable few:

1. The *Institute of Electrical and Electronic Engineers (IEEE)* defines DG as [1]: "The generation of electricity by facilities sufficiently smaller than central generating plants as to allow interconnection at nearly any point in a power system. A subset of distributed resources".

2. According to *Willis and Scott* [2] DG includes any of the following: "The use of small electric power generators, whether located on the utility system, at the site of a utility customer, or at an isolated site not connected to the power grid".

3. *Borbely and Kreider* [4] define DG as: "Power generation technologies below 10 MW electrical output that can be sited at or near the load they serve".

4. Distributed generation is defined as small power generation units strategically located near consumers and load centres that provide benefits to customers and support for the economic operation of the existing power distribution grid (from *Richard P. Bingham*) [5] and [6].

5. The *DG Monitor* defines DG as electric generating units less than 20 MW in size that are located close to the primary load being served or provide grid support. Backup powers, including emergency and standby power, are included in this definition, as are remote power, which is DG that is used at places located away from the distribution grid [7]. They also refer to the following definition: electric generation sited close to the load it serves, under 50 MW, with most of the output used by the host facility.

6. *Resource Dynamics Corporation*: Small power generating units that are close to load, under 50 MW, and most of the electrical output is used by the host facility. Includes: combined heat and power (CHP); backup power; niche applications such as premium power, peak shaving, and green power [8]. Another of their adopted definitions is: Resource Dynamics Corporation: Relatively small electricity generating units located close to the loads being served. In general, distributed generation covers units in the 5 kW to 30+ MW size range [9].

7. The *Public Utility Commission of Texas*: An electrical generating facility located at a customer's point of delivery (point of common coupling) of 10 MW or less and connected at a voltage less than 60 kV, which may be connected in parallel operation to the utility system. May include energy storage technologies as well as conventional generation technologies [10].

8. The *International Council on Large Electric Systems (CIGRE) Working Group* has set its definition of DG to be generation that is: not centrally planned; not centrally dispatched; usually connected to the distribution network; smaller than 50–100 MW [1].

9. *California Energy Commission*: distributed generation is defined as small-scale generation, typically less than 10 MW in capacity, inter-connected to the utility grid at distribution or sub-transmission voltages [11].

With respect to the rating of DG power units, the following different definitions are currently used:

1. The *Electric Power Research Institute (EPRI)* defines DG as generation from 'a few kilowatts up to 50 MW' [12];

2. The *Gas Research Institute* defines DG as being 'typically between 25 kW and 25 MW' [13];

3. *Preston and Rastler* defines the size as 'ranging from a few kilowatts to over 100 MW' [14];

4. *Cardell et al.* defines DG as generation 'between 500 kW and 1 MW' [15];

5. *The International Conference on Large High Voltage Electric Systems (CIGRE)* defines DG as 'smaller than 50–100 MW' [16];

The challenge now is to reach a sensible and logical synthesis of the above criteria in order to compile a definition of DG as it is applied in this study. This is a rather overwhelming undertaking due to the remarkable differences the above have and the evident lack of uniformity. Together with this it is quite necessary for the definition to comply with the IEEE standard mentioned mealier.

After careful consideration the author suggests that a concise and complete definition of distributed generation (DG) as applied in this investigation should define the following characteristics:

- ❖ Location of DG equipment.
- ❖ Connection level.
- ❖ Power quality (PQ) influences.
- ❖ Mode of operation.
- ❖ Operational parameters.
- ● A unified terminology of DG and related equipment and terms.

The definition does not need to explicitly define the following (delimitations):

- ❖ Type of generation; the technology applied.
- ❖ Size and power delivered.
- ❖ Ownership of the DG equipment.
- ❖ Financial compensation and monetary agreements.
- ❖ Connection types and -standards.

A suggestion for a definition of DG as intended for use in the study is:

Distributed generation (DG) is the generation topology using any generating technology to connect to the existing electric power system (EPS) infrastructure and provide a useful and appropriately beneficial source of electrical power to the system and its consumers. The generating equipment is strategically located near the problematic loads and available natural resources that aid the specific type of technology applied. The influences, or effects, of the additionally connected power sources should be beneficial to the overall power quality (PQ) of the electrical power grid. The equipment is connected to the required level, either distribution- or transmission network, depending on the requirements of the load and the generating equipment specifications. The equipment is intended to operate continually and in parallel with the EPS. This excludes islanding (load independently served by its own generating plant) and roll-over operation (commonly found in back-up power systems – BPS).

1.2.3 The Standard: IEEE P1547

Although the application of DG and storage can have many benefits, the technologies and operational concepts to properly integrate them into the existing power system must be developed to realize these benefits and avoid negative effects on reliability and safety. The electric distribution system traditionally was not designed to accommodate active generation and storage at the distribution level or, generally, at the sub-transmission level and, especially, it was not designed to allow distributed generators to supply energy to other distribution customers. The technical issues involved in readily interconnecting and effectively integrating these types of DR applications with grid operations are significant.

DR and uniform interconnection standards offer much promise in helping to modernize and improve distribution system and related transmission system performance. When DR are properly designed, interconnected, and integrated with the grid, the potential benefits include reduced electric line loss; reduced T&D congestion; grid investment deferment and improved grid asset utilization; improved grid reliability; ancillary services such as voltage support or stability, VAR's, contingency reserves, and black start capability; clean energy; lower cost electricity; reduced price volatility; greater reliability and power quality; energy and load management; and combined heat and power synergies. In summary, those benefits tend toward the evolution of a modernized electric power system that has greater flexibility and energy security for the future [17].

The draft suggest the following concerns as the major issues, in summarized form, related to the emergence of DG interconnection: system impacts and analysis (e.g., is it necessary and when), penetration (e.g., ideal allowable aggregation), safety (e.g., functional versus operational modes), re-fitting of electric power systems (e.g., what to do), cost of electric power system re-fits (e.g., how and who pays), operation (e.g., which standard and who is in control), and reliability (e.g., operational issues such as durability versus availability). Even broader DR interconnection concerns and T&D issues include standards for interface between the DER and the interconnection package (e.g., equipment manufacturing design standards), issues of scaling to different power levels, and lower interconnection system cost.

1.2.4 Brief Overview of existing DG Technology

Distributed generation (DG) is currently being used by some customers to provide some or all of their electricity needs. As mentioned, in some instances, DG technologies can be more cost effective than conventional solutions. There are many different potential applications for DG technologies. For example, some customers use DG to reduce demand charges imposed by their electric utility, while others use it to provide premium power or to reduce environmental emissions.

Current technologies for DG vary widely and will be discussed concisely in the following chapter, but a short summary of current technologies is shown in Table 1-1 and is given so the reader can familiarize with the technologies referred to in the proposed definition of DG. These technologies include a wide variety of natural resources & renewable resources. The current research is in the field of renewable

resource utilization while the remaining development concentrates on efficient use of energy-efficient non-renewable resources. The closed cycle multi-axial gas turbine pebble bed modular reactor (PBMR) developed in South Africa is a nuclear generating plant aimed at being the most energy-efficient method for generating electrical power over extended periods of time, therefore becoming a cost-effective solution to power grid problems.

Table 1-1: Technologies for DG [18], [19], [20].

	Type	Typical size per module
Technology	Combined gas turbine	35–400 MW
	Internal combustion engines	5 kW–10 MW
	Combustion turbine	1–250 MW
	Micro turbines	35 kW–1 MW
Renewable Sources	Small hydro	1–100 MW
	Micro hydro	25 kW–1 MW
	Wind turbine	200 W–3 MW
	Photovoltaic cells	20 W–100 kW
	Solar thermal	1–80 MW
	Biomass, e.g. based on gasification	100 kW–20 MW
	Fuel cells	1 kW–5 MW
	Geothermal	5–100 MW
	Ocean energy	100 kW–1 MW
	Battery storage	500 kW–5 MW

Also part of the technologies in Table 1-1 is the pebble bed modular reactor (PBMR). This is a South-African project (more specifically, ESKOM – the local utility) with international partners attempting to produce a closed cycle (Brayton-cycle) based nuclear power generation plant. The design is inherently safe and the modularity of it the renders it an ideal alternative to meet future energy needs. Part of the New Partnership for Africa's Development (NEPAD) initiative it also aims to provide for the rest of Africa's electrical power needs. The PBMR technology lends itself to the modular electrification of Africa, supplying energy where needed.

1.2.5 More Applications of Distributed Generation

Distributed generation (DG) can be used for a variety of applications and utilized as effective solutions for problematic scenarios. Presently the most common applications are:

- Electric power back-up system (EPBS) or electric stand-by system (ESBS).
- Islanded power sources for users who have exact power requirements.
- Improving power reliability and or quality for certain "sensitive" customers.
- Providing electrical power to remote customers.

DG is a practical solution to the common problem of poor power quality experienced worldwide. The generated power from each source has to have the effect that the power of the grid complies with the regulations set out by the regulatory bodies governing the power specifications.

Another advantage of DG, specifically with the aid of the PBMR system, is the reduction of pollutants. Air pollution is reduced as well as most other environmental pollutions, such as water-, ground-, noise-, etc.

1.2.6 Power quality

Electric power quality (PQ) has become a topic of increased interest since the late 1980's. This interest involves all the parties concerned with PQ in the power business: firstly the utility companies which are the origin of the electricity, the customers who use the electricity and the manufacturers of electric equipment. Much has been said about PQ up till now and according to *Ibrahim and Morcos* [21] the growing concern is due to the following reasons:

- ❖ End-user load equipment has become more sensitive to power quality due to many microprocessor-based controls.
- ❖ Complexity of industrial processes: The re-start-up of these industries is a very costly affair.
- ❖ Proliferation of large computer systems into many businesses and commercial facilities.
- ❖ Development of sophisticated power electronics equipment used for improving system stability, operation, and efficiency. These devices are a major source of bad power quality and are themselves vulnerable to poor PQ.
- ❖ Deregulation of the power industry.
- ❖ Complex interconnection of systems, which results in more severe consequences if any one component fails.
- ❖ Continuous development of high performance equipment: Such equipment is more susceptible to power disturbances.

Power quality problems can be defined as any problem in power due to current, voltage or frequency deviations that result in the failure or malfunction of the customers' equipment [22]. Alternative definitions for PQ are used within the power industry, reflecting the different viewpoints of the parties involved. From a supplier and equipment manufacturer's point of view, PQ is a perfect sinusoidal waveform with no distortion and no noise on the grounding system. A point of view from the customer may be that PQ is simply the power that works for their equipment without damaging it.

1.3 Problem Statement

The purpose and aim of this project (the study and investigation) is to prove that distributed generation (DG) resources can be applied in a beneficial and advantageous manner to improve the performance (largely power quality (PQ) orientated performance) of electrical power system scenarios. The effects of the applied DG on the power quality (PQ) are investigated and conclusions are drawn as to why the observed effects are experienced. The problem is that there aren't existing studies (or methods) that accurately predict these effects and the study attempts to coherently investigate these effects.

The conclusions are aimed at providing general guidelines for the planning, implementation, design and application of DG. These guidelines can only be

fashioned once there is a clear understanding of the effects DG has on the PQ of a certain power system scenario (commonly termed scenario henceforth). The applications of DG are primarily aimed at improvement of the scenario's power performance by means of optimization. By optimization it is meant that placement and quantity of the distributed resources (specifically PBMR units in this study) be studied in a cost-effective manner to determine optimal solutions.

Predictions are made for placement and amount of pebble bed modular reactors (PBMRs) in a given scenario once the observed effects have provided rules (guidelines) indicating how the effectiveness of the generating equipment is maximized during use.

1.4 Issues to be Addressed, Assumptions and Methodology

The research- and investigative experimental method relies heavily on certain assumptions made for the study. These are general assumptions for the entire study and are repeated occasionally when either relevance is adjusted or greater detail is desired. Since the nature of this project is mainly research oriented, there is no need for complicated formal design processes. The experimental research is solely based on computer simulations (mainly MATLAB® Simulink® SimPowerSystems blockset) of developed scenario models and the results from these simulations are considered to be the collected "raw" data.

1.4.1 Design process

Simulink® scenario models are developed (Chapter 3) in an accurate and comprehensive manner under advisement from experts (the local utility, ESKOM, was approached to provide input and assistance for possible scenarios). These scenarios are modelled, simulated and used to collect data. It is assumed that the intended computer simulation software package is reliable, accurate and provides realistic data and responses.

A cost function is developed (Chapter 4) to quantify and measure the performance of each scenario before and after the addition of DG to it. This also aids in studying the effects of distributed generation (DG) on the overall power quality (PQ). The pebble bed modular reactor (PBMR) is exclusively employed as the only DG resource.

1.4.2 System Specification

System specifications are largely influenced by the limits set for power quality standards by the governing authority (NRS 048 Power Quality Standards, South Africa [32]). These include that the given/developed scenario is intentionally altered to marginally exceed these power quality (PQ) limits for certain chosen buses if it initially does not.

Other specifications include those of the developed cost function. The individual components of the cost function should provide accurate, global indications of their respective chosen variables/effects and provide true representations.

1.4.3 System Modelling

The scenarios are modelled by means of simulation and the collected data is mathematically processed and analyzed. The effects of DG is modelled by connecting the developed pebble bed modular reactor (PBMR) Simulink® model at various points in the scenario and the data analysis is once again done in the same manner.

1.4.4 Design Implementation

The studied effects and responses are used to form the foundation for the conclusions, motivations and ultimately, the guidelines for distributed generation (DG) planning.

1.4.5 System evaluation

Results are compared to those of similar studies. Similar computer simulation software (PSAF®) is used to verify the results for one scenario, but the verification process and results will not be presented unless there are inconsistencies. Besides, Simulink® is universally accepted for its proven accuracy and realistic nature, thus no discrepancies are expected.

1.4.6 Delimitations

In this study the suggested optimization purposes of the study conclusions, findings and guidelines will not be developed. Optimization is a complex problem and relies on more techniques that also are not presented. These techniques include generator control; control was only implemented in purely intuitive, basic and simple measures in a few isolated instances during the study.

1.5 Overview of the Dissertation

Chapter 2 is a detailed literature study and the various distributed generation (DG) technologies are briefly discussed while primary focus is on the pebble bed modular reactor (PBMR). Key power quality (PQ) definitions are provided and the causes and sources of non-sinusoidal waveforms are discussed. Planning, cost and reliability are some of the remaining minor topics of Chapter 2.

Chapter 3 discusses the development of the chosen scenarios. Detailed assumptions and aims relevant to the development of the models are again presented. Finally preliminary results for the "problematic" pre-improved scenarios are provided.

Chapter 4 examines the development of the cost function that eventually leads to the formation of various indicators that collaborate to provide a final index that quantifies the performance of a scenario as a whole. The differences between the established conventional sinusoidal mathematic procedures and the adopted non-sinusoidal mathematics are illustrated.

Chapter 5 is the penultimate chapter that provides results for the effects of DG on the PQ of the developed scenarios. The effects are motivated and discussed in detail as observed in each scenario and the precise data analysis technique is tersely illustrated.

The final chapter, Chapter 6, summarizes the observed effects, the drawn conclusions are presented and discussed and recommendations are made for improvements to the present study as well as suggestions for future work relevant to the subject of this study.

1.6 Summary

The capability of distributed generation (DG) as an augmentation of the existing grid, delivering a higher system performance, therefore a higher quality of power to the consumer is introduced. This type of generation is able to discreetly solve power generation problems in a number of ways. The modern technology incorporated in the design of these small generators enable them to be efficient, reliable and simple enough to own and operate and compete with electric power systems delivering cheaper electrical power due to lowered transmission and distribution (T&D) costs. The absence of a sufficient definition is noted and an attempt is made to put forth a definition that meets the requirements of the industry, the field and the purposes of this study.

Chapter 2

Literature Study

2.1 Introduction

This chapter is aimed at equipping the reader with the general knowledge associated with distributed generation (DG). This includes discussion of the various technologies and their basic operating principles. Later on will follow a brief discussion of power quality (PQ) in general followed by a more in-depth explanation of PQ issues and concerns as intimately related to the purposes of this study. Finally, a short introduction of reliability, cost and planning is made.

Regarding the production of electrical energy with the technological means being discussed, it is important to remember that all the technologies rely on a source of energy that is applied in a certain process and in a specified manner to convert the source of energy to electrical energy. The energy sources are grouped in two main categories, namely non-renewable and renewable energy sources. Non-renewable sources are generally comprised of the common fossil fuels while examples of renewable sources include sun-, wind- and hydro-using power production [2].

As of late it is well-known that the natural resources responsible for the continued supply of fossil fuels are being depleted at an increasingly alarming rate. Non-renewable resources seem to hold the answer to this problem but have proved to rely on largely inefficient means of energy conversion [2]. Compounding the problem of effectively using these energy sources is the high costs involved in development, construction and implementation of these methods.

Bearing in mind that the aim of this study is to reliably and effectively improve the PQ of a chosen scenario while applying a suitable DG resource, it must be noted that the different types of technology employed have varying influences on the quality of the power delivered to consumers. Therefore, choice of DG technology, associated control thereof and strategic placement of the individual units are all factors that individually influence the "improved" power system scenario. Since the control measures of the different types of DG are not of concern for this study it will be ignored and as a result not be discussed or presented. Also, the main type of DG employed is the pebble bed modular reactor (PBMR) presented in more detail later on in this chapter.

As can be seen from the preceding paragraphs the issues of reliability, cost and planning were mentioned and therefore beg a brief discussion. In the study these concerns were given minor attention and led to trivial influences on the outcomes of the study.

2.2 Distributed Generation Technology Overview

It suffices to make brief mention of the known technologies employed as DG power sources or distributed resources (DR) [2]:

- ❖ Reciprocating Piston Engine generators
- ❖ Gas Turbine powered generators
- ❖ Fuel Cell powered generators
- ❖ Renewable Resource generators
- ❖ Stored Energy Resource generators

Each of these will be presented, but the intent is not to confuse the reader with the specifics and the detail of each one; only to develop an understanding of the technology and of the operating principles. This allows each technology to be used for a specific situation where it would be the most suitable option.

The differences in the generation methods are ideal and will meet the majority of the needs of present day consumers. Examples are: the most logical option would be reciprocating piston engine generators in noisy industrial areas where air pollution of an acceptable level is allowed and offering a reliable means of fuel supply; fuel cell generators or stored energy generators (battery storage) for medical and residential areas; in commercial areas the modern gas turbine powered generators are the desired solution; and in agricultural and rural areas renewable resource generators are to be used. The reader is encouraged to make use of the relevant references for any further information that may be needed.

These technologies invariably utilize any of a variety of conventional fossil fuels (mostly oil- or coal-based) in a certain applied method and manner to produce electrical energy – this process is most commonly facilitated by means of oxidation of the fuel in a controlled process.

The most commonly adopted method of electrical energy generation is where combustion of the desired fuel(s) results in heat an pressure that is easily converted to mechanical energy (usually rotation of the mechanical parts) that in turn is responsible for the generation of electrical power in a generator.

Another method is where oxidation is achieved without combustion – by means of chemically oxidizing the fuel with the aid of a catalyst. This is the process on which the operation of fuel cells relies. A fuel cell is likened to a "chemical fuel-powered battery" [2]. Electric energy is immediately produced via oxidation of hydrogen produced from the fuel in the fuel cell. The electrical power is direct current (dc) and is converted to alternating current (ac) with the aid of power electronics.

Reciprocating piston engine generators are by far the most popular type of DG generation units used worldwide [2]. The basics of the internal combustion engine operation are not presented and explained due to the universally familiar nature of the details (the four stroke Otto cycle and the two stroke cycle). Thanks to the rotating movement characteristics of these engines they are readily connected to electrical generating equipment via gearboxes, belts and a multitude of mechanical means to produce electrical power.

The basics of gas turbine powered generating equipment are also commonly known and byway of the above same reasons it follows that the inherent rotating nature of these mechanical systems is easily exploited to conveniently generate the

desired electrical power. The conversion process of the mechanically produced energy to the generated electrical power is essentially the same as for reciprocating piston engine generators as conversed earlier.

The rest of the DG technologies available for use as distributed electrical power resources are appended in Appendix A. These include fuel cells, renewable resources (such as *solar thermal-* and *solar photovoltaic power generation*, wind-, hydro-, and trash burning power generation, etc.), and energy storage for use with DG(*superconducting magnetic energy storage* (SMES), batteries, capacitors, etc.).

Because of the chosen approach of this study to exclusively employ the pebble bed modular reactor (PBMR) as a DG resource, it deserves to be described in more detail. The next section pithily presents the basics of the PBMR system and its operation.

2.2.1 The Pebble Bed Modular Reactor (PBMR)

The pebble bed modular reactor (PBMR) is a new type of nuclear power plant developed in recent years in South Africa by the local utility ESKOM and a number of other shareholders. It relies on the thermodynamics of a high temperature gas cycle and more specifically, the PBMR is based on a closed three-shaft recuperative Brayton cycle that uses helium as the working medium (gas or fluid). Chief advantages of this reactor are:

- ❖ It is inherently safe.
- ❖ It is surprisingly environmentally friendly.
- ❖ It boasts with great cost-effectiveness.

Figure 2-1 illustrates the main power system (MPS) of the PBMR.

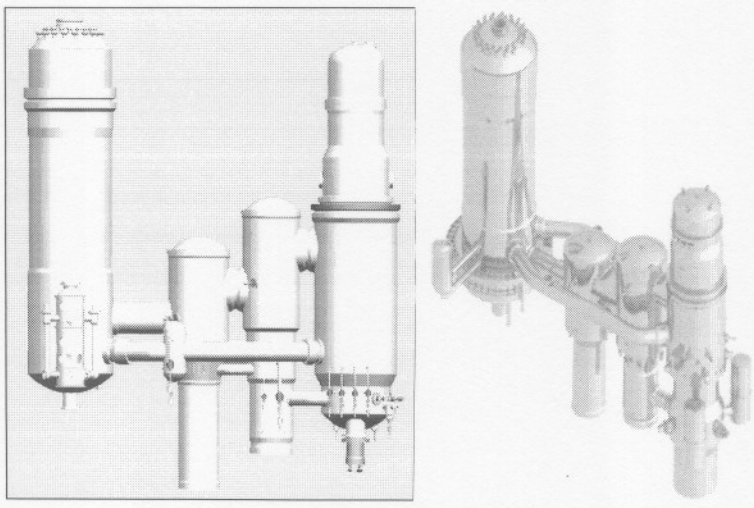


Figure 2-1: Solid model illustration of the MPS [23].

The innate problem of existing nuclear reactors is that they make use of a process that leads to the establishment of a radiation hazard. The PBMR is designed to ultimately realize a nuclear plant that distances itself from the dependency of a physical process causing a radiation hazard beyond the plant site boundary. The

estimated rating of a PBMR unit is approximately 150 MW of electrical power making the PBMR module the smallest standalone component of the PBMR power generation system. The module is capable of power generation in standalone mode, but the intention of ESKOM is to replace the Koeberg nuclear power station plant with ten of the newly developed PBMR units indicating that a unit is designed for versatile use in a power network [23].

The chemical and radiological inert characteristics of helium make it the prime candidate for use in the closed loop gas cycle of the PBMR plant and therefore eliminating the risks of nuclear contamination to the plant and the environment [24]. The helium transfers the heat produced by the nuclear fusion elements to the power turbine. Figure 2-2 is a schematic diagram of the Brayton cycle as implemented in the PBMR system layout. The Brayton cycle is the thermodynamic process where helium gas is heated in the reactor and circulates through turbines, compressors and heat exchangers. The induced gas flow in the helium cycle is used to generate electrical power.

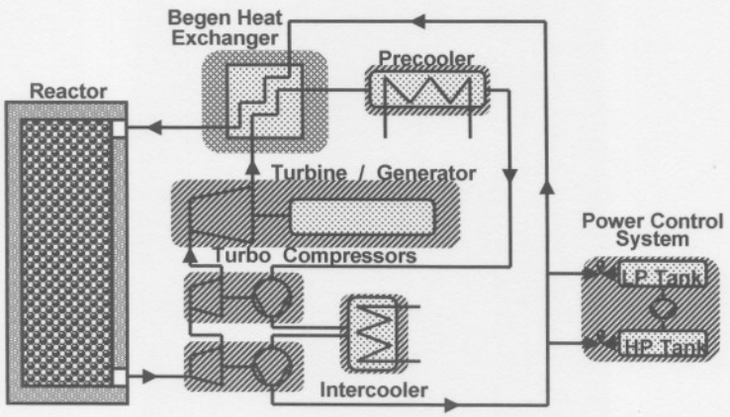


Figure 2-2: PBMR system layout and Brayton cycle [24].

As already said, a PBMR is a high-temperature helium-cooled reactor power plant using a direct cycle gas turbine. It is specifically call a pebble bed modular reactor because the design of the nuclear reactor dictates this naming of the plant. The reactor is of pebble bed design, meaning the fuel (coated uranium dioxide particles) in the nuclear process is contained in balls (or spheres) of graphite roughly the size of a cricket ball (60 mm diameter).

A graphite-lined silo of 10 metres high and 3.5 metres in diameter houses approximately 400 000 of these fuel pebbles. At the top of this reactor helium is introduced at about 500 °C and is gradually heated as it passes between the fuel pebbles, leaving the reactor at the bottom with a temperature of about 900 °C.

The design incorporates three turbines in the gas cycle. The first two turbines drive compressors while the third is exclusively exploited to drive the electrical power generator. At this stage the helium has cooled (after conversion of its energy) to around 600 °C and is passed through a recuperator where excess energy is released further cooling the helium to 140 °C. A precooler (water-cooled) optimizes the thermodynamics even more by lowering the helium temperature to 30 °C.

Finally the gas is repressurized by a turbo-compressor, flows to a regenerator heat-exchanger where it acquires residual energy and introduced back into the reactor.

Pneumatics store spent nuclear fuel pebbles in large storage vessels (tanks) situated at the base of the plant with enough storage capacity providing for storage of these spent balls right through the life of the plant. After shutdown of the plant the storage vessels must cope with an additional 40 to 50 years of effective storing of the spent fuel. An indication of the amount of fuel balls for a forty-year life cycle of a 100 MW PBMR plant is estimated at 2.5-million fuel balls [24].

2.3 Power Quality Overview

Although the idea of power quality (PQ) in utility networks primarily applies to the physical waveform of the power transmitted and received by the utility, it is important to note that waveform shape is not the only measure of PQ. Along with the concern regarding the shape of the waveforms (intimately related to the presence of harmonics), it is must be said there are a multitude of aspects describing PQ, such as electrical unbalance – the other chief concern.

As will be shown by later discussions, power quality concerns are of great importance for both utility and customers. There are a multitude of problems related to poor PQ. These range from device- and component failure, increased transmission and distribution (T&D) costs, limited capacity to deliver usable power, and many more mentionable problems all discussed, illustrated and proven in later sections in the study. One of the main problems in the event of poor PQ is the associated lack of service reliability offered by the utility. "Sensitive" customers may experience down-time and loss of revenue.

2.3.1 Electrical Unbalance and Asymmetrical Components

Asymmetrical components are electrical components in the supply that cause sequence components. An electric network is unbalanced when this occurs. Balanced networks are typically defined as three-phase networks having phase voltages and currents that are equal in magnitude for each of the three phases but are shifted exactly 120° in phase with respect to one another. Figure 2-3 illustrates the balanced condition phasor representation for a 380 V, 50 Hz network.

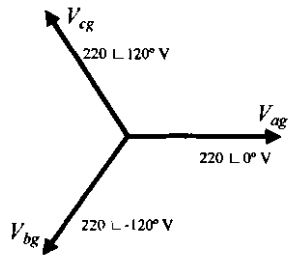


Figure 2-3: Balanced three-phase network.

For an unbalanced network these equal magnitude, 120° phase-shifted replicas of the phase voltages differ in magnitude and phase-shifts are not in equal 120° increments. These situations are the by-products of unbalanced loads in the electrical

network. Unbalanced loads are loads that require different voltage magnitudes and phase shifts for each phase they are connected to. Examples of unbalanced loads are arc furnaces, single-phase motors, single phase-transformers, electric railways, etc. These loads deform the balanced voltage supply and return an unbalanced condition to the electric network. Figure 2-4 illustrates the phasor representation of an unbalanced condition for a 380 V, 50 Hz network.

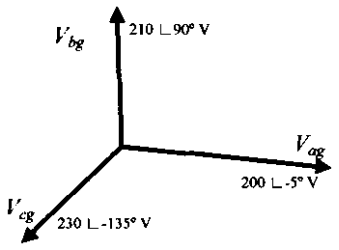


Figure 2-4: Unbalanced three-phase network.

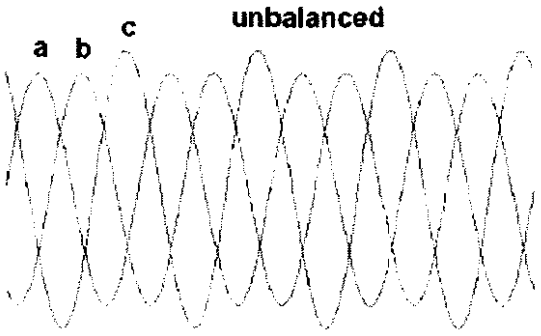


Figure 2-5: Unbalanced phase waveforms.

Unbalanced phase voltages and currents produce virtual components called sequence components [26]. There are three types of sequence components: Zero-sequence components, Positive-sequence components and Negative-sequence components. These sequence components are related to one another as well as to the phase components in the following manner:

$$\begin{bmatrix} V_{ag} \\ V_{bg} \\ V_{cg} \end{bmatrix} = \begin{bmatrix} 1 & 1 & 1 \\ 1 & a^2 & a \\ 1 & a & a^2 \end{bmatrix} \times \begin{bmatrix} V_0 \\ V_1 \\ V_2 \end{bmatrix} \text{ Voltage relation.} \quad (2.1)$$

$$\begin{bmatrix} I_a \\ I_b \\ I_c \end{bmatrix} = \begin{bmatrix} 1 & 1 & 1 \\ 1 & a^2 & a \\ 1 & a & a^2 \end{bmatrix} \times \begin{bmatrix} I_0 \\ I_1 \\ I_2 \end{bmatrix} \text{ Current relation.} \quad (2.2)$$

In (2.1) and (2.2) the number a is always $a = 1\angle 120°$ and where, V_{ag}, V_{bg} and V_{cg} are the respective a-, b- and c-phase voltages; V_0, V_1 and V_2 are the respective zero-, positive- and negative-sequence voltage components; I_a, I_b and I_c are the respective a-, b- and c-phase line currents; and I_0, I_1 and I_2 are the respective zero-, positive- and negative-sequence current components.

Inversely related with the symbol meanings as before:

$$\begin{bmatrix} V_0 \\ V_1 \\ V_2 \end{bmatrix} = \frac{1}{3} \times \begin{bmatrix} 1 & 1 & 1 \\ 1 & a & a^2 \\ 1 & a^2 & a \end{bmatrix} \times \begin{bmatrix} V_{ag} \\ V_{bg} \\ V_{cg} \end{bmatrix} \tag{2.3}$$

Equation (2.3) calculates the magnitude and the angle of V_0, V_1 and V_2. These are the zero sequence, positive sequence and negative sequence voltage components respectively. Equation (2.4) calculates the current equivalents for the magnitude and the angle of I_0, I_1 and I_2.

$$\begin{bmatrix} I_0 \\ I_1 \\ I_2 \end{bmatrix} = \frac{1}{3} \times \begin{bmatrix} 1 & 1 & 1 \\ 1 & a & a^2 \\ 1 & a^2 & a \end{bmatrix} \times \begin{bmatrix} I_a \\ I_b \\ I_c \end{bmatrix} \tag{2.4}$$

In this study unbalanced operating conditions are ignored. It is of utmost importance, however, to mention that for power systems that suffer poor power quality (PQ) due to the action of waveforms severely affected by the presence of harmonic distortion causing factors (discussed later), unbalanced operating conditions arise and is a common occurrence. In this study the scenarios are slightly subjected to harmonic distortion and the imbalance becomes negligible.

2.3.2 Harmonics

Alternating current (ac) power generation and transmission was adopted due to the increased transmission distances achieved and the ease of generating power.[✐] Maintenance requirements were also greatly reduced and the era of direct current (dc) transmission and distribution (T&D) came to an eventual end. However, with advances in semiconductor technology another problem for the use of ac power appeared – the problem of "electrical pollution".

Recently the dc option was revived due to the advantages it offers in eliminating the need for power factor correction, reduced construction and installation costs (provided the line is of suitable length) and many more benefits including the avoidance of creating an environment where harmonic components flourish. For now, unfortunately, the industry has to be content with the fact that harmonic pollution will always be present – a consequence of the established enduring nature of present practical power networks.

A harmonic is technically defined as "the sinusoidal component of a periodic wave or quantity having a frequency that is an integer multiple of the fundamental frequency" [27]. Waveforms that may be separated into individual harmonic components (or orders) are produced by electrical harmonic currents. Harmonics are said to be present when a current sine wave is not proportional to the voltage wave of the electrical system being investigated.

[✐] In South Africa the fundamental frequency for electric power generation, transmission and distribution is 50 Hz.

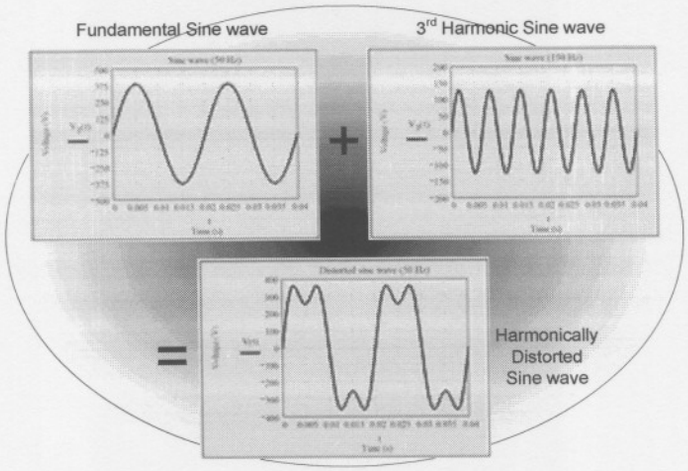


Figure 2-6: Distortion of the fundamental waveform by a harmonic waveform [27].

"Harmonic currents are continuous, integral whole number multiples of the fundamental frequency" (see [28]). The correct functioning of everyday electrical equipment and appliances require the power source to provide them with a "pure" supply of 50 Hz current, and while they will continue to operate if a tolerable measure of harmonic waveform distortion is present in the supply, it has been proven that the harmonic currents do work as they don't provide any usable power. These currents only congest the electrical system and reduce the system's capacity, even to the extent where they can lead to overloading of the system resulting in downtime, damages and financial loss.

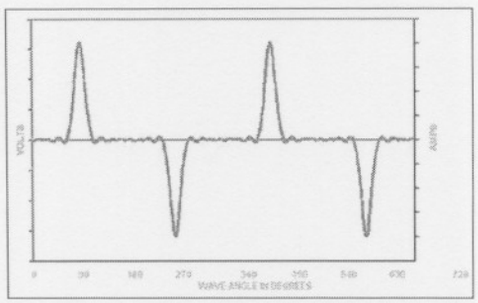


Figure 2-7: The waveforms of a single-phase two-pulse diode bridge converter [28].

A personal computer (PC) serves as an example of equipment that causes harmonic currents even though it uses 50 Hz current for power. The harmonics are caused by power electronics in the switched-mode power supply a PC draws its conditioned power from, much like the waveform in Figure 2-7. These harmonics caused by PCs flow back into the power network and, again, does no useful work. Each individual PC produces a small amount of harmonic current, but a large number of PCs from the same facility and coupled to the same common point (PCC) in an electrical system causes a "harmonic density". This can effectively overload an electrical system.

In recent times it has been a growing concern that electrical systems are not utilized in an efficient and effective manner. One of the major concerns being that harmonic currents are needlessly carried in the system from one point to another, taking up system capacity and lowering power delivery to some points in the system.

Lowered system capacity and power transmission capability is but one problem in modern electrical systems; other more immediate and troublesome products of harmonic "pollution" are overheated wires and transformers, increased energy costs, and system degradation and failure [28]. These all cause revenue losses and have far-reaching consequences on customers and utilities.

Table 2-1 is from [28] as well and clearly describes the results and causes of harmonics. The table was specifically chosen as the original authors succeeded in portraying the harmful factors associated with harmonic waveform distortion in a practical cause-and-effect manner. Most utilities have developed power quality (PQ) standards that specify limits for the "amount" of harmonic distortion that is allowed in an electric power system. One of these standards (NRS 048) relevant to this study will be presented in basic detail later on – detail found to be relevant to the study and necessary for its success.

Table 2-1: Results and causes of harmonics [28].

Symptom	Negative effects on the system
The neutral current exceeds any of the phase currents.	In a 3-phase, 4-wire system, neutral conductors can be severely affected by non-linear loads connected to 220V branch circuits. If the loads are single-phase, certain harmonics called triplens (multiples of the third harmonic: 3rd, 9th, 15th, etc.) add together in the neutral conductor, causing it to overload. The neutral is not protected by a circuit breaker.
Circuit breakers trip even though loads do not appear to be excessive.	Excessive harmonic currents reduce the amount of load a circuit breaker can support. Critical loads may trip off-line, resulting in catastrophic data and revenue loss.
Transformers, bus bars, wires and switchgear become hot.	System components may fail due to excess heat. Waste heat will increase air conditioning cost, as well.
System components emit noise (a buzzing sound).	System components can become magnetically resonant at harmonic frequencies. Noise is disruptive to facility personnel. Vibrations can cause mechanical damage.
Noise interferes with communications lines, and visible interference effects the operation of PC monitors.	Magnetic fields from high 3rd harmonic currents can cause interference with end-user electronic devices.
Triplens in the neutral conductor cause inductive interference, which can be heard on a phone line.	Telecommunications systems often give the first clue to a harmonics problem. Telecommunications cable is commonly run next to neutral conductors.

At this time it is thought appropriate to introduce the reader to the measure of this phenomenon. The following expression is a means to determine the "amount" the harmonic contents of the measured waveform has distorted it.

$$DF = \sqrt{\frac{\text{sum of squares of amplitudes of all harmonics}}{\text{square of amplitude of fundamental}}} \times 100\% \text{ or } THD = \frac{\sqrt{\sum_{h=2}^{\infty} A_h^2}}{A_1} \qquad (2.5)$$

where, *THD* defines both *Total Harmonic Voltage Distortion* (*VTHD*) and *Total Harmonic Current Distortion* (*ITHD*). The variables A_1 and A_h represent the *fundamental-* and *harmonic components* respectively of voltage and current.

2.3.2.1 Explaining Non-Sinusoidal Waveforms in Electrical Networks

An electrical power system (EPS) is an expansive, often complicated and intricate network of generation resources, power carrying lines, compensation equipment and loads. Each element, every piece of equipment and instrument of this network has impedance and subsequently the loads "see" the network as a combination of impedances through which power is fed. Before the advent of semi-conductor technology and the scientific leaps made in the field thereof, loads were mostly considered to be linear – that is a linear relation exists between the load current and its driving voltage [29] – with the exception of equipment such as transformers, rotating magnetic machinery and gas-discharge lamps. The exceptions (including that of semi-conductor technology) are known as non-linear loads as there is a non-linear relationship between the load current and the driving voltage.

Non-linear loads draw non-linear currents. In the case of semi-conductor equipment it means that they deform (specified by intentional design) the ideal current sine wave by way of switching the current through the semi-conductor power electronics. The current wave then loses in resemblance to that of the voltage wave.

Firstly ideal power transmission is presented and explained. Power is said to be ideally transmitted when a system has ideal power sources, i.e. ideal alternating current (ac) generators that have zero internal impedances and generate perfect sinusoidal waveforms regardless of the conditions of the loads. Also, the interconnecting elements and equipment exhibit zero impedance. Ideal power transmission further states that the optimum conditions for the best possible transmission of power is where the current and voltage are in-phase replicas of each other [29]. Finally, the system is consequently perfectly efficient and has no losses, but this is an utopical dream and can never practically be realized. Therefore, in this "electrical utopia" voltage distortion could never realize and non-sinusoidal current waves would have no effect – discussed later in full.

In contrast to ideal power transmission is practical power transmission. In practice only non-ideal (practical) generators exist and are made use of. Practical ac generators do have non-zero internal impedances and so do the interconnecting elements and equipment. With the use of non-linear loads in general, the ideal of "in-phase current and voltage replicas" is lost as non-linear currents start to flow through the network and do no work, as already stated in Section 2.3.2. Further compounding the problem is when these non-linear currents encounter the impedances of the power network. This leads to non-sinusoidal voltage drops caused by these non-linear currents flowing through the non-zero impedance. This is when harmonic voltage distortion manifests itself in a power network.

At this time the author proposes to introduce the term non-sinusoidal waveforms that refers to waveforms containing harmonic components, or harmonically distorted waveforms (harmonic distortion in general). Non-sinusoidal voltage waveforms are

"produced" at every point (node) in the power network where a non-sinusoidal (non-linear) current flows through an impedance. The problem is exacerbated when non-sinusoidal currents supply conventional linear loads as these loads exhibit frequency-dependent voltage drops of their own, even if they are considered to be non-distorting by nature [29].

The principal source of non-linear currents, harmonic current distortion or non-sinusoidal currents is semi-conductor power electronics technology. It is unthinkable in modern-day power networks to not have these devices performing their functions. They offer versatility, controllability and tailored solutions to almost all power supply and control problems encountered in a network. The drawback is that these devices rely on non-linear operation to facilitate increased control measures and thus an environment for harmonic (current) distortion to flourish is created. Semi-conductors have become the most popular and widespread tool of choice, therefore they are actively adding to increasing levels of distortion in networks.

In a sense non-sinusoidal waveforms can be thought of as "generated" when it comes to power sources subjected to the action of distorted waveforms. The generated perfect sinusoidal waveform deviates from this ideal of sinusoidality when non-linear currents are drawn from practical power sources. Thanks to the relatively small and almost negligible internal impedances of practical generators the influence on their terminal voltage is minute, but non-sinusoidality is still achieved. Harmonic currents propagate through the network as the distorted voltage waveform encounters generally large system impedances (inductive for the most part) leading to increased harmonic distortion levels.

This stage of the discussion obligates that an illustration is offered to practically illustrate the proliferation of harmonics in power networks. To present a whole detailed circuit drawing of a practical and realistic power system is pointless. It was decided to generously draw from the guidance of *Rens* in his doctoral writing. Figure 2-8 is a slightly revised version with minor alterations of an illustration developed by him [29].

The design and nature of cost-effective development of power networks call for optimum economic use of materials and resources. This leads to great responsibility placed on and reliability expected of these equipment. In similar fashion it follows that maximum performance is expected while the most possible customers are connected to a reliable power system. This is what Figure 2-8 aims to illustrate amongst others. The concept of a "*point of common coupling*" (PCC) is introduced and is perceived from the figure as a point in the system that feeds a multitude of loads or customers – i.e. a common point to which a number of different loads or customers are connected to in order to source them with power.

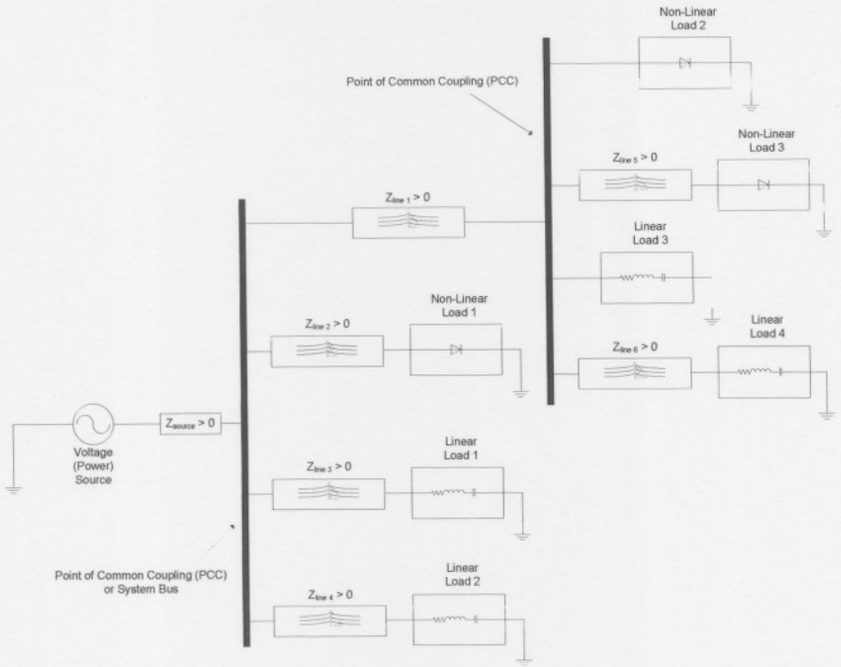


Figure 2-8: An example of a typical power system in practice with a source and loads [29].

In Figure 2-8 the voltage source represents the established power source belonging to the electric utility. The voltage source is connected through the generator's internal impedance to a system bus that could be seen as a PCC. The source generates sinusoidal waveforms (hardly ever realized in practice) and transmission lines transmit the voltage- and current waveforms through the network. In general, the transmission network has a low impedance as "seen" by the loads (or customers) connected to it.

Customers in close vicinity to one another, or of the same region, are generally connected to the same line feeders or generating power source, depending on which comes first. As already stated, these common connections are known as PCCs and are clearly indicated in Figure 2-8. Shown in the figure a PCC can either be near the source or at the end of a transmission line/feeder (or a series of them). It is primarily determined by the exact common point where a number of loads are connected. These loads can be of a linear or non-linear nature as indicated by Loads 1 through 7 and can either be directly coupled to the PCC or remotely via a transmission line (Loads 1 through 3).

Assessment of the non-linear loads, more specifically their associated detrimental effects on electrical waveforms (voltage- and current-), reveals that these non-sinusoidal load current waveforms add up to give the source current. In this manner the source current becomes distorted. Remembering that the impedance of lines in an electrical power network is a function of frequency (frequency-dependent), this leads to voltage drops in these lines across the frequency-dependent impedances (distinct orders of "harmonic voltage drops") and similarly for any impedance in the system. These harmonic order voltage drops are in turn superimposed onto the fundamental voltage waveform.

Thus every PCC now exhibits a non-sinusoidal (distorted) voltage waveform brought about by the distorted currents in the network and the action of the

frequency components of these currents in the network impedances. Since linear loads are frequently connected to the same PCC as non-linear loads they have to endure a non-sinusoidal supply and suffer in silence while bearing the associated harmful consequences of non-sinusoidal current waveforms. They have not caused the distortion nor agreed to it but, like many things in life, have to accept it.

Disregarding the negative effects (already well-versed) of harmonic "pollution" on the operation and effective life of electrical equipment, another concern calling for attention is the matter of metering. Conventional power measuring instruments and equipment are largely of electromechanical design and has proven to be grossly inaccurate (almost always at the expense of the paying customer) when measuring non-sinusoidal waveforms. This leads to increased expenditure and revenue losses for customers not responsible for harmonic "pollution" and distortion [30].

Since steady-state analysis is of paramount concern to this study no mention of the transient state of harmonic distortion will be made. It is deemed irrelevant for the outcomes and purposes of this writing, but it has to be said that since harmonic distortion manifests itself in varying levels in any power system, this manifestation is either steady-state, transient- or a combination of both. Another prerequisite of this study is that periodicity must be maintained by the non-sinusoidal waveforms; fortunately this is the usual case and is based on similar assumptions of *Rens* in his doctoral study on power quality (PQ) [29].

2.3.2.2 Equipment that causes Harmonic Distortion

Grady identifies three major categories of harmonic distortion sources [31]. Each of these categories is further divided in several classes, but the essence of every one remains true to its category. The main categories are classical non-linear loads, power electronic loads and "other non-linear loads". Each of these categories is presented in vital detail and brief explanations offered.

Classical non-linear loads are comprised of equipment associated with "linear" operation but due to design complications and operating extremes and measures exhibit a non-linear operating component. The main candidates are power transformers (especially the large ones), large rotating magnetic equipment (even electric machines and motors of any size), fluorescent lamps (gas discharge lamps with magnetic ballasts), and arc furnaces. The details of how they distort the waveforms are not important, but why this happens is a matter of interest. In magnetic equipment (transformers and machines) this phenomenon is observed as they are designed to operate beyond the knee defined by the magnetic material saturation curve employed in their core construction – cost reduction design purposes. In gas discharge lighting the lamp is ignited and extinguished in each half cycle [31]. After ignition the lamp has "negative resistive characteristics" and this contorts the waveform. Arc furnaces are actually non-periodic and are to be considered as transient loads that cause flicker; this is beyond the scope of the study.

The next category according to *Grady* is power electronic loads and these include line commutated converters, voltage-source converters and switched-mode power supplies. There is plenty that can be said about these kinds of equipment, but they all have one thing in common – semi-conductor power electronics. As briefly described

earlier, these are the main components responsible for the distortion of waveforms. This stems from their ability to quickly and efficiently switch a current flowing through them on or off. This switching has the greatest effect on the sinusoidal waveforms as it completely alters the waveform shape as a result. Line commutated converters are high-power (above 375 kW) AC/DC converters, voltage-source converters are for medium-power (below 375 kW) applications and switched-mode power supplies are low-power (up to approximately 5 kW) equipment.

The last category identified by *Grady* is "other non-linear loads". Cycloconverters (converters that alter the frequency, for instance 50 Hz, to another frequency, e.g. 60 Hz, or range of frequencies), static VAr compensators (supply of reactive power with a variable output) and motor power factor controllers are some of the multitude of examples grouped in this category. All of these have considerable effect on the shape of a waveform as they are designed with the intent of a maximum impact for energy-saving purposes through wave-shape manipulation.

2.3.2.3 The South African Power Quality Standard – NRS 048

The development of power quality (PQ) standards is still in its infancy throughout the world. This is partly due to the emergence of improved metering systems and the greater awareness of how poor PQ unjustly penalizes consumers. South Africa specially developed a unique set of PQ standards in 1996; called NRS 048, Electricity Supply – Quality of Supply.

From NRS 048 [32] the following was found regarding the acceptable limits for harmonic components in the electric supply. The compatibility levels for harmonic components on low-voltage (LV) and medium-voltage (MV) networks are given in Table 2-2 while the limits for high-voltage (HV) and extra high-voltage (EHV) networks are listed by Table 2-3. The total harmonic distortion (THD) of the supply voltage for LV and MV networks, including all harmonics up to the order 40, shall not exceed 8 %; and for HV and EHV networks the limit is 3 %.

Table 2-2: Compatibility levels for harmonic voltages in LV and MV networks [32].

1	2	3	4	5	6
Odd harmonics non-multiple of 3		***Odd harmonics multiple of 3***		***Even harmonics***	
Order (h)	*Harmonic Voltage (%)*	*Order (h)*	*Harmonic Voltage (%)*	*Order (h)*	*Harmonic Voltage (%)*
5	6	3	5	2	2
7	5	9	1,5	4	1
11	3.5	15	0,3	6	0,5
13	3	21	0,2	8	0,5
17	2	>21	0,2	10	0,5
19	1.5			12	0,2
23	1.5			>12	0,2
25	1.5				
>25	$0.2 + 1.3 \cdot \frac{25}{h}$				
Total harmonic distortion (THD) ≤ 8 %.					
NOTE — For each harmonic, the harmonic voltage distortion compatibility level is given as a percentage of the magnitude of the declared (fundamental frequency) voltage.					

The reader is once again reminded how total harmonic distortion is defined:

$$VTHD = \sqrt{\sum_{h=2}^{n} \frac{V_h^2}{V_1}} \tag{2.6}$$

where: *VTHD* is the total amount of Voltage Harmonic Distortion; V_h is the magnitude of the h[th] Voltage Harmonic component; V_1 is the magnitude of the Fundamental Voltage Harmonic component.

Equation (2.6) is explicitly defined as the calculated indication of the total harmonic voltage distortion and is of primary concern when consulting Table 2-2, Table 2-3 and Table 2-4. Last mentioned table (Table 2-4) is included for interest sake. The standard was reviewed in 1999 after it was decided to amend the standard of 1996 and a draft was published that contained Table 2-4. Essentially it reveals that LV and MV networks are grouped together and have a revised set of limits.

Table 2-3: Recommended limits for harmonic voltages in HV and EHV networks [32].

1	2	3	4	5	6
Odd harmonics non-multiple of 3		***Odd harmonics multiple of 3***		***Even harmonics***	
Order (h)	*Harmonic Voltage (%) HV - EHV*	*Order (h)*	*Harmonic Voltage (%) HV -EHV*	*Order (h)*	*Harmonic Voltage (%) HV - EHV*
5	2	3	2	2	1.5
7	2	9	1	4	1
11	1.5	15	0,3	6	0,5
13	1.5	21	0,2	8	0,4
17	1	>21	0,2	10	0,4
19	1			12	0,2
23	0.7			>12	0,2
25	0.7				
>25	$0.2 + 0.5 \cdot \frac{25}{h}$				
Total harmonic distortion (THD) ≤ 3 % in HV networks.					

For interest sake the limits for unbalanced supply conditions are also given. Similarly the following was found regarding the acceptable limits for unbalanced conditions in the electric supply. The compatibility level for unbalance on three-phase networks is 2%. On networks where there is a predominance of single-phase or two-phase customers, the assessed unbalance may be as much as 3 %.

$$VUB = \frac{V_n}{V_p} \times 100 \tag{2.7}$$

where *VUB* is the total amount of Voltage Unbalance; V_n is the magnitude of the Negative-phase Voltage component; V_p is the magnitude of the Positive-phase Voltage component.

Table 2-4: Limits for harmonic voltages in medium-voltage (MV) and HV networks [33].

1	2	3	4	5	6	7	8	9
Odd harmonics non-multiple of 3			***Odd harmonics multiple of 3***			***Even harmonics***		
Order (h)	*Harmonic Voltage (%) MV (and LV)*	*Harmonic Voltage (%) HV - EHV*	*Order (h)*	*Harmonic Voltage (%) MV (and LV)*	*Harmonic Voltage (%) HV - EHV*	*Order (h)*	*Harmonic Voltage (%) MV (and LV)*	*Harmonic Voltage (%) HV - EHV*
5	5	2	3	4	2	2	1.6	1.5
7	4	2	9	1.2	1	4	1	1
11	3	1.5	15	0.3	0.3	6	0.5	0.5
13	2.5	1.5	21	0.2	0.2	8	0.4	0.4
17	1.6	1	>21	0.2	0.2	10	0.4	0.4
19	1.2	1				12	0.2	0.2
23	1.2	0.7				>12	0.2	0.2
25	1.2	0.7						
>25	$0.2 + 0.5 \cdot \frac{25}{h}$	$0.2 + 0.5 \cdot \frac{25}{h}$						
Total harmonic distortion (THD) $\leq$ 6.5 % in MV networks.								
Total harmonic distortion (THD) $\leq$ 3 % in HV networks.								

2.3.3 Improving Grid Performance by connecting Distributed Resources

In this section a synthesis of the concepts discussed thus far is attempted. This follows from the author's own understanding of the fundamentals described up till now. A mental grasp of the preceding discussions leads to the following conclusions by way of logical reasoning:

- By lowering the impedance encountered by the transmitted power the resultant harmonic voltage drops & current distortions are reduced – this is achieved by connecting a power source closer to the responsible load sourcing the harmonic components to the grid.

- Connecting power sources instead of power factor correcting equipment (such as reactors – inductive and capacitive) is advantageous and avoids unwanted side-effects such as lowering of the resonant frequency of the system.

- A certain specified connected power source best caters for the various power specific requirements of arbitrary loads.

- Power sources could prevent propagation of distorted waveforms through the power network by "blocking the route" for them and isolating them to zones/regions in the network – preferably where they are caused.

- "Sensitive" loads could be provided with "undisturbed" power ("improved" PQ) by sourcing them with better located ("sited") power sources.

The reader is reminded of Figure 2-8. Inspection and logical reasoning affirms that the appropriate placement of a distributed generator/-resource (DG or DR) is as close as possible to either or both (all) of the problematic non-linear loads. The amount of DG would depend on a cost function, specifically tailored to determine the relevant ratios, and the individual capacity (power rating or capability) of each unit. Another approach would be to repeatedly examine the whole scenario (Figure

2-8 termed a scenario) if the option of a single sizable DG resource is used and this should reap varying benefits if applied at different points in the system; necessitating a cost function to measure the performance/impact of/on the system. Inspect Figure 2-9 with the proposed alterations.

The combination of the two source impedances lowers the overall source impedance seen by the load and effectively reduces the impedance that causes the harmonic component voltage drops. The DG source is also connected much closer (geographically) to the non-linear load and the need for long transmission lines that have high inherent impedance values is reversed. Of main concern is the capacity of the connected DG source – a high power rating capacity could be applied with much more effectiveness with the aid of active control measures. This results in an overall improvement of the power quality (PQ) in the network in varying degrees depending on the capacity of the DG source (and adopted control measures). As is shown in Figure 2-9, the connection can either be made at the point of common coupling (PCC) (or via a greatly shortened transmission line, or cable), or directly at the intended loads as shown in the middle part of Figure 2-9. This reduces line lengths even further. Separate DG units could also be connected, one to every load, depending on the rated size of both the load and DG.

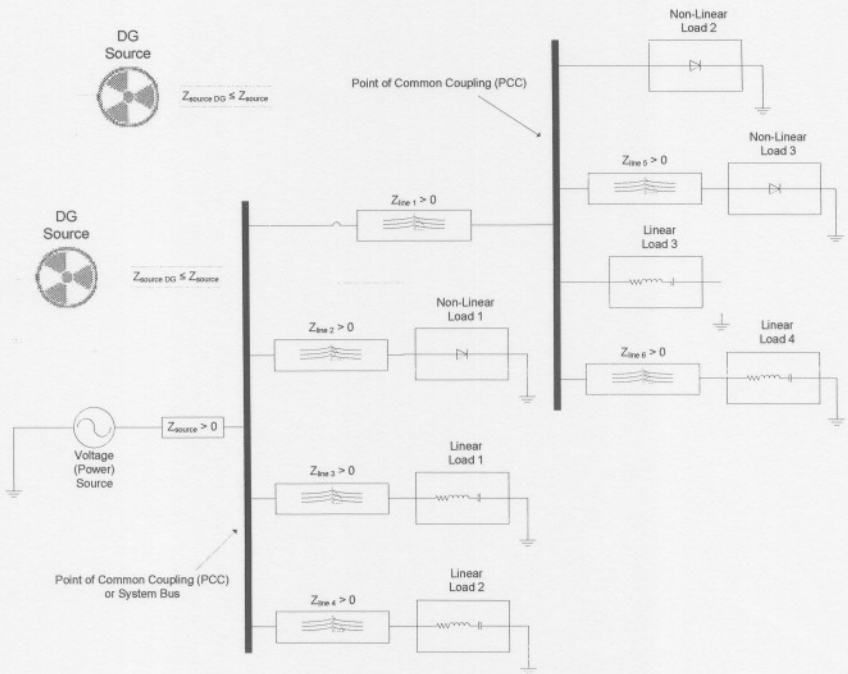


Figure 2-9: A suggestion for the use of DG in the example discussed in Section 2.3.2.1 [29].

2.3.4 Power Quality Issues in Distributed Generation

The most common symptoms associated with power quality (PQ) problems in systems that include DG are [34]:

- Harmonic distortion – The injection of currents having frequency components that are multiples of the fundamental frequency.
- Voltage imbalance – The grid voltage does not have identical voltage magnitude on each phase, and a 120° phase shift between each pair of phases.

- ❖ Voltage regulation – The upholding of the voltage within an acceptable range at the point of delivery to each customer.
- ❖ System losses – The active power losses in the whole power system (transformers, lines etc.)
- ❖ Flicker – The repetitive and rapid changes of voltage, which has the effect of causing unacceptable variations in light output and other adverse effects on power consumers and their equipment.
- ❖ Direct current injection – This can cause saturation and heating of transformers and motors. Can also cause these passive devices to produce unacceptable harmonic currents.

Power quality (PQ) refers to a wide spectrum of electromagnetic phenomena that describe the voltage and current at any given point in the system. The categorization of electromagnetic phenomena is given in Table 2-5. Key aspects of major relevance are discussed.

Table 2-5: PQ phenomena classification.

Categories		Duration	Voltage Magnitude
Transients	***Impulsive***	1 ns–>1 ms	
	Oscillatory	5 μs–50 ms	0–4 pu
Short duration variations	***Instantaneous sag***	0.5–30 cycles	0.1–0.9 pu
	Instantaneous swell	0.5–30 cycles	1.1–1.8 pu
	Momentary interruption	0.5 cycles–3 s	<0.1 pu
	Momentary sag	30 cycles–3 s	0.1–0.9 pu
	Momentary swell	30 cycles–3 s	1.1–1.4 pu
	Temporary interruption	3 s–1 min	<0.1 pu
	Temporary sag	3 s–1 min	0.1–0.9 pu
	Temporary swell	3 s–1 min	1.1–1.2 pu
Long duration variations	***Interruption sustained***	>1 min	0.0 pu
	Under-voltages	>1 min	0.8–0.9 pu
	Over-voltages	>1 min	1.1–1.2 pu
Voltage imbalance		steady state	0.5–2 %
Waveform distortion	***DC offset***	steady state	0–0.1 %
	Harmonics	steady state	0–20 %
	Inter-harmonics	steady state	0–2 %
	Notching	steady state	
	Noise	steady state	0–1 %
Voltage fluctuations	***Flicker***	intermittent	0.1–7 %
Power frequency variations		<10s	

Long Duration Voltage Variations

A variation of the rms-value of the voltage from nominal voltage for a time greater than 1 min. Long duration voltage variations can be either over-voltages or under-voltages. These variations are generally not the result of system faults, but are caused by load variations and switching [35].

Over-voltage

An over-voltage refers to a measured voltage having a value greater than the nominal voltage for a period greater than 1 min. Typical values are 1.1 to 1.2 pu [36]. Over-voltages can be the result of load switching, or variations in the reactive compensation on the system. Poor system voltage regulation capabilities or control

results in over-voltages. Incorrect tap settings on transformers can also result in system over-voltages. Figure 2-10 shows a typical over-voltage waveform.

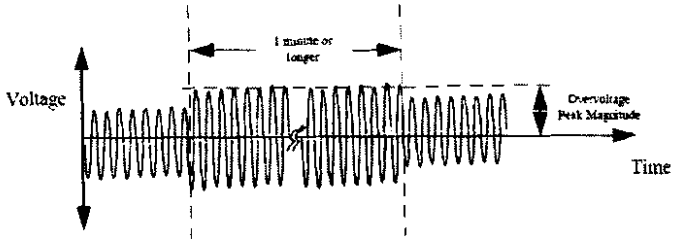


Figure 2-10: Typical over-voltage waveform [36].

Under-voltage

A measured voltage having a value less than the nominal voltage for a period of time greater than 1 min. Typical values are 0.8–0.9 pu [36]. Under-voltages are the result of the events which are the reverse of the events that cause over-voltages. Overloaded circuits also result in under-voltages.

Waveform Distortion

A waveform distortion can be classified as a steady state deviation from an ideal sine wave of power frequency characterized by the spectral content of the deviation.

Harmonics

Harmonics are sinusoidal voltages or currents having frequencies that are integer multiples of the frequency at which the supply system is designed to operate (termed the fundamental component) [36].

Harmonics combine with the fundamental voltage or current, and produce waveform distortion. Harmonic distortion exists due to the non-linear characteristics of devices and loads in the system. Non-linear devices can usually be modelled as current sources that inject harmonic currents into the power system. Voltage distortion results as these currents cause non-linear voltage drops across the system impedance. Harmonic currents result from the normal operation of non-linear devices on the power system. Figure 2-11 illustrates the waveform and harmonic spectrum for a typical adjustable speed drive input current.

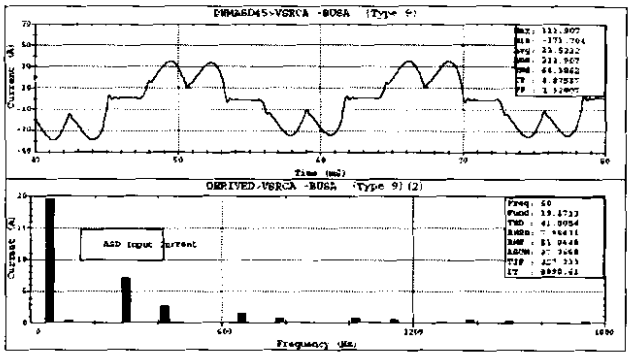


Figure 2-11: Variable speed drive input current waveform and harmonic spectrum [36].

Inter-harmonics

Inter-harmonics are voltages or currents having frequency components that are not integer multiples of the frequency at which the supply system is designed to operate [36]. They can appear as discrete frequencies or as a wide-band spectrum. Inter-harmonics can be found in networks of all voltage classes.

Notching

Notching is a periodic voltage disturbance caused by the normal operation of power electronics devices when current is commutated from one phase to another [36]. Voltage notching represents a special case that falls between transients and harmonic distortion. Since notching occurs continuously (steady state), it can be characterized through the harmonic spectrum of the affected voltage.

2.3.5 Power Quality and Distributed Generation

The objective of distribution system design is to supply customers at a voltage, which is within a prescribed, acceptable (or desired) range. Two voltage ranges are specified by ANSI (American National Standards Institute) [22]:

- Range A, covering normal operation – 0.95 pu–1.05 pu; and
- Range B, covering a wider range for infrequently occurring circumstances.

Normal variations in load, and DG operations, fall into the category covered by Range A. The service voltages in South Africa are to be between 209 V and 231 V, on a 220 V base. Distribution system voltage regulation design is based on relatively predictable daily and seasonal changes in loading. It can be assumed that loading on the various sections of a feeder follow more or less the same pattern over time.

Without DG, power flow is always unidirectional, and decreasing in real power (kW) magnitude with increasing distance from the substation. The addition of DG to a system can radically shift power flow patterns and make them unpredictable.

Net power flow can potentially reverse over a portion of the feeder or even over the entire feeder if DG production exceeds the load present at that specific time. These load flow variations can make it difficult to maintain adequate voltage regulation. Also, this unconventional load flow patterns can cause distribution system voltage regulation devices, such as step voltage regulators (SVR), load tap-changers, and switched capacitor banks to respond inappropriately.

Extensive case studies must be performed to assess the impact of DG on a distribution system and the distribution feeder's voltage profile. DG penetration can be increased in a system to observe the impact on the voltage regulation. DG penetration is defined as the ratio of the sum of all the DG output ratings on a feeder, divided by the base feeder peak load.

DG locations on the feeder must be evaluated for the following scenarios:

- distributed uniformly along the feeder

- ❖ lumped at the beginning of the feeder
- ❖ lumped at the middle of the feeder
- ❖ lumped at the end of the feeder.

2.4 Reliability, Cost and Planning – the antagonized Relationship

Reliability, cost and planning are intricately and intimately tied together and will be discussed shortly. As can be expected, cost and reliability are proportionally knitted together in their relationship – generally in terms of energy production, the more installed equipment costs, the more reliable it can be expected to be. It is with this in mind that planning has been altered to become known as value-based planning.

When referring to "reliability" in power networks, what is meant is the availability (continuity of service [2]) of electrical energy to the customer (consumer or load). A reliable power system is characterized by an uninterrupted supply of usable electrical power for an indefinite length of time (a permanent supply all the time). To achieve this utilities have to invest considerable financial amounts as well as time and effort (careful consideration) in planning the power network to realize the goal that is reliability.

Cost plays a major role in planning as the developer frequently has to decide which one of a multitude solutions (by and large this is the case) best suits the application and the effective management thereof. More often than not it boils down to high initial investment but savings in the long run; or lowered initial expenditure but increased running costs. Therefore, the planner has to take into consideration what solution not only satisfies the immediate requirements, but poses to be a sensible solution from an economic point of view for the future.

Planning is the final part that considers both reliability and cost concerns and is governed by the design specifications, type of solution developed, materials and processes required to realize the solution and a multitude of other influences and requirements that ultimately determine the final solution. All of these are discussed in greater detail in Appendix B and the reader is encouraged to study the individual influences of each as appended to the document.

2.5 Summary and Conclusion(s)

There exists a wide variety of technologies and this allows for the immediate and appropriate adaptable use of distributed generation (DG) to meet specific load demand and requirements. The technologies exhibit efficient and effective operation in general. The pebble bed modular reactor (PBMR) is a good representative substitute for most of the technologies and is suitable for use as the principal distributed generation power resource to study the effects of DG on power quality (PQ) in power networks.

Power quality (PQ) is of chief concern in existing power networks and the potential for improvement of the situation with the aid of DG is an eminent reality. PQ invariably influences system performance and must be considered if effective power transmission is the desired goal.

Value-based planning (VBP) is a useful technique and is intimately tied to the antagonized relationship between cost and reliability. An important element is to quantify how much the planner values effective and reliable service by analyzing the cost of improvement.

Chapter 3

Power System Scenarios

3.1 Introduction

In this chapter three scenarios are presented as well as the related calculations and assumptions that led to the establishment of the scenarios. For the purpose of this study it was decided to explore certain aspects of distributed generation (DG) and the related impacts regarding power quality (PQ) by simulation of the chosen scenarios with the aid of simulation software. The "impacts on PQ" being how much the various waveforms of the system are improved (if at all) – i.e. how well the waveforms are improved by removing the harmonic components that distort them.

It is assumed the reader is at familiar with the software used. Due to its universal recognition MATLAB® is used for the simulations. Simulink® SimPowerSystems blockset models are presented to the reader and the developed MATLAB-code for the m-files written in the study are provided on a supplemental documentation CD. The Simulink® modelling blocks and scenario models developed by the author during the study are appended in Appendix C.

The various values (line-, machine- and non-linear load calculations) were calculated using Mathcad® 2001 Professional. These worksheets are appended to the document in Appendix D and the reader can easily verify the calculations regarding each scenario.

3.2 Methods and Assumptions

All the calculations are based on the per-unit system. It is assumed the reader is familiar with the per-unit system and it will not be explained. The chosen base values are presented in Table 3-1. Additionally, the related equations and characteristic system values are provided. In the first column contains the chosen values defining some of the fundamental characteristics of the system(s), such as the thermal current limit [26] that defines limits for the amount of power certain transmission lines can safely cope with.

The second column contains the initial per-unit calculations that form the basis of the per-unit analysis of all the scenarios. These base values were chosen uniformly for all the scenarios to facilitate comparative evaluation of different scenarios.

The third column contains additional equations that assisted in improving each scenario to lend a realistic approach in the study of them. The first equation in the column is the well-known method to switch between per-unit systems where base values may differ, the second is to determine the thermal loading limit of the various lines in the scenario (each voltage level corresponding to a proportionally related power delivering capacity), and finally, the two equations at the end of the third column are basic rules for calculating reasonable values for both the snubber capacitance as well as the -resistance for the snubber circuit of a three-phase full-

bridge diode rectifier as used in the scenarios to introduce the reality of non-linear loads in the power system.

Table 3-1: Summary of the relevant mathematical equations.

Characteristic Scenario Values	Base Values	Additional Equations
Frequency; f = 50 Hz	$S_{base} = P_{base} = Q_{base} = 100$ MVA where S_{base} is base apparent power in VA; P_{base} is the base active power; Q_{base} is the base reactive power.	$Z_{p.u.new} = Z_{p.u.old}\left(\frac{V_{baseold}}{V_{basenew}}\right)^2\left(\frac{S_{basenew}}{S_{baseold}}\right)$ where $Z_{pu\ new}$ is the referred per-unit impedance after change of base; $Z_{pu\ old}$ is the initial per-unit impedance; $V_{base\ old}$ is the initial base voltage in V; $V_{base\ new}$ is the new base voltage in V; $S_{base\ old}$ is the initial base apparent power in VA; $S_{base\ new}$ is the new base apparent power in VA.
Sample Time; $T_s = 5\times10^{-5}$ s	$V_{baseLL} = \sqrt{3}\times V_{baseLN} = 275$ kV where $V_{base\ LL}$ is the base line-line voltage in V; $V_{base\ LN}$ is the base phase voltage in V.	$S_{thermal} = 3\left(\frac{V_{baseLL}}{\sqrt{3}}\right)I_{thermal}$ where $S_{thermal}$ is the thermal apparent power limit in VA; $V_{base\ LL}$ is the line-line voltage rating of the line in V; $I_{thermal}$ is the thermal current limit in A.
Thermal current limit of lines in the system; $I_{thermal} = 1000$ A	$I_{base} = \frac{S_{base}}{\sqrt{3}\times V_{baseLL}} \approx 209.946$ A where I_{base} is the base line current in A.	$C_s < \frac{P_n}{1000(2\cdot\pi\cdot f)V_n^2}$; $R_s > 2\frac{T_s}{C_s}$ where C_s is the snubber capacitance in F; P_n is the nominal power in W; f is the frequency in Hz; V_n is the nominal voltage in V; R_s is the snubber resistance in Ω; T_s is the sample time in seconds.
	$Z_{base} = R_{base} = X_{base} = \frac{V_{baseLL}^2}{S_{base}} \approx 756.25\ \Omega$ where Z_{base} is base impedance in Ω; R_{base} is the base resistance; X_{base} is the base reactance.	
	$Y_{base} = G_{base} = B_{base} = \frac{1}{Z_{base}} \approx 1.322\times10^{-3}$ where Y_{base} is base admittance in mho; G_{base} is the base conductance; B_{base} is the base susceptance.	

Assumptions made for the study of the scenarios are:

- The system and the effects of power quality (PQ) on it (its response to varying levels of PQ) can be investigated by means of a steady-state analysis therefore eliminating the need for protection equipment that clutters the simulation model and unnecessarily complicates the development thereof.
- ❖ Incoming lines (feeder lines) can be substituted and accurately modelled by synchronous generators. This was done to limit the pool of available power so as to realistically allow for the propagation of harmonic pollution through a power network.
- ❖ Three-phase transmission lines can realistically be modelled by three separate π section line models. The separate models are each connected to a separate

phase and therefore the system can be presented and investigated as a three-phase system while the trusted approach of single-phase analysis is still adopted and maintained.

- ❖ Harmonic pollution can be introduced to a power system by adding non-linear loads to it. The non-linear loads are connected in parallel with the existing loads to represent the non-linear load component of the load and it is assumed this is an accurate representation. The non-linear loads are chosen of such size that the Total Harmonic Distortion (*THD*) sufficiently exceeds the limit of 3 % as imposed by NRS 048 (Section 2.3.2.3) but not by an exaggerated margin. The author's judgement was regularly applied to determine this margin – as long as most of the load buses in the system exceeded 3 % *THD*. The distributed case of these non-linear loads include that an equal size of these loads are chosen. To ignore this entails choosing a unique amount of power for each non-linear load and formation of the scenario becomes too calculation intensive. A modelled non-linear load consists of a transformer supplying the necessary operating/nominal voltage (and of sufficient power rating) for the full-bridge diode rectifier that in turn feeds a purely resistive load – all these components require calculations that are clearly presented in the Mathcad® worksheet (Appendix D).
- ❖ Transformers are modelled without tap-changing control – a direct result of the first assumption regarding steady-state analysis.
- ❖ Generator control is ignored during analysis – once again; this is due to the steady-state analysis of the system(s).
- ❖ The PQ of a scenario can be improved significantly by adding generating equipment of lesser but sufficient size. This is done by adding modelled pebble bed modular reactors (PBMRs) at strategic points in the scenario designated for their attributes regarding improvement of PQ in the system. The improvement is measured by a developed cost function (Chapter 4) that returns an index gauging the performance of the improved system versus the cost of improvement (This is discussed in Chapter 5).

The reader is referred the calculations of each scenario as presented in Appendix D. This will aid in providing a clear indication of the reasoning (assumptions made) regarding the construction and the method of investigation of the scenarios. The worksheet is well commented with extensive notes explaining the necessary variables and their calculations. Studying the worksheet in its entirety will clearly define and illustrate the use of the calculations presented in Table 3-1.

3.3 The Scenarios and their Development

The third scenario was entirely provided by ESKOM (the national utility) and lends a much more realistic appeal to the study. The first and second scenarios are entirely fictional and were developed using the guidelines and ideologies of the scenario provided by ESKOM. Many of the given characteristic values (line model values, transformer ratings and impedance values, etc.) are repeatedly used between the respective scenarios. It was decided to do this as it ensures a realistic response from each scenario under investigation and the response is judged according to expected system performance.

More often than not the cumbersome task of compensating the transmission lines to maintain desirable voltage levels throughout the whole system was encountered, but this was usually solved by intuitive judgement and inspection of the system's response. The methods for the calculated amounts of compensation are not presented.

As with all power flow studies it follows that certain buses need to be identified and this is also the case in this study. For each scenario where an incoming line is substituted by an equivalent generator/source, certain bus types are chosen/defined. The bus type is determined depending on the information available for a bus. Some of the information for a bus is chosen by the researcher by means of an educated guess. Table 3-2 lists the bus types and their respective descriptions describing the various attributes/characteristics and inputs (or given/rated information) of each.

The scenarios after improvement are left for later discussion in Chapter 5. The placement of the pebble bed modular reactor(s) (PBMR(s)) is clearly illustrated and the amount of improvement as measured by the said cost function is discussed in detail. These scenarios are the "basic" (or "raw") systems that were developed/given for study and used to demonstrate the goal(s) of this study as stated earlier in this chapter; Sections 3.1 and 3.2.

Table 3-2: Power flow analysis bus types [35].

Bus Type	Description
Swing Bus	Only one swing bus can be defined for a system and this is the reference bus, i.e. where $V_{swing}\angle\delta_{swing}$ is known and is typically chosen as $1.0\angle 0°$ p.u.. This is the input data for the bus. During power flow analysis P_{swing} and Q_{swing} is calculated.
Load Bus	The inputs for this bus type are P_{load} and Q_{load}. V_{load} and δ_{load} are computed. Most buses are of this type.
Voltage-controlled Bus	$P_{control}$ and $V_{control}$ are the inputs. The computed unknowns are $Q_{control}$ and $\delta_{control}$. Examples of these buses are where generators, switched shunt capacitors, tap-changing transformers, or static-var systems are connected. Additional input data are the maximum- and minimum var limits ($Q_{Gcontrolmax}$ and $Q_{Gcontrolmin}$) that the respective equipment can supply.

3.3.1 The First Scenario

A common occurrence in a power system is that loads are distributed along a series of transmission lines forming a long line. For the purpose of this study it was decided to investigate the case where a series of medium-length transmission lines rated at 275 kV feed a series of loads at each bus. The incoming line that acts as the source for the scenario is modelled by a synchronous generator of sufficient rating (Table 3-3) and of which the characteristics were chosen such as to represent the substituted line as accurately as possible.

The first few loads are relatively small with two large loads at the end. The majority of the power drawn is situated at the end so as to fully load the series of transmission lines up to its end. Inspection of the system presented in Figure 3-1 reveals that a rather costly amount of reactive compensation is required to maintain preferred receiving-end voltage levels (± 1 pu).

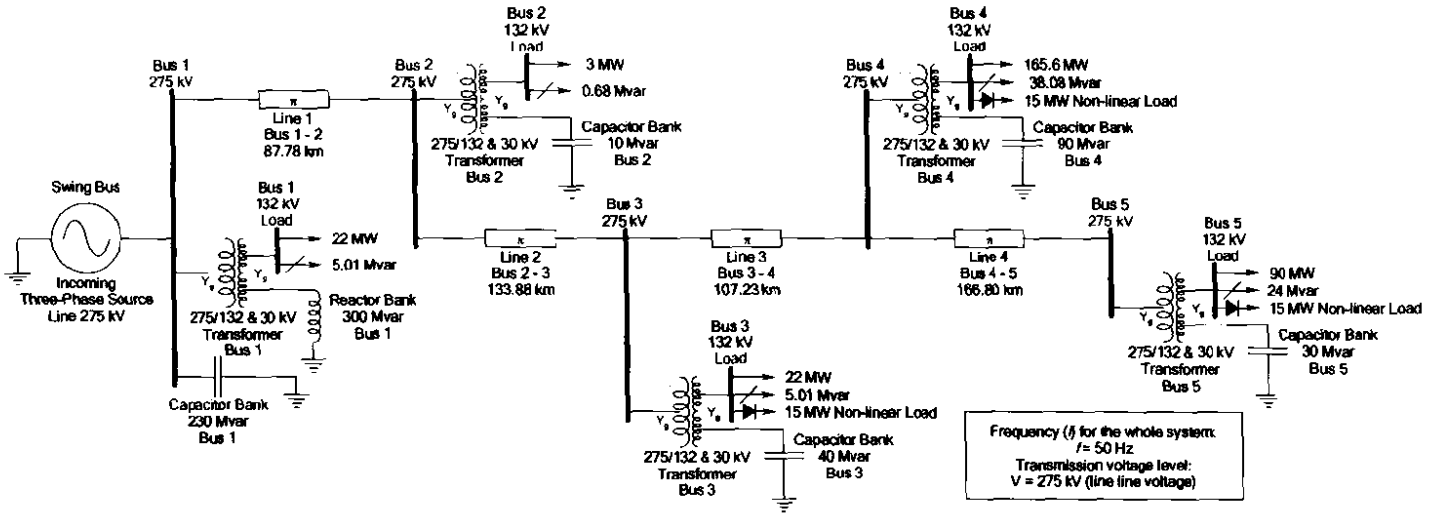


Figure 3-1: Scenario 1 consists of a series of medium-length lines with loads at intervals.

Table 3-3 presents the summarized data of the scenario. All the line-, transformer- and machine data as well as global system specifications are listed. The majority of the data originated from reliable sources (research material, ESKOM, experts in the field) or was carefully chosen under advisement from said authorities. Many of the characteristics of the system are calculated from this data as presented in Appendix D. Table 3-3 is the input data for the developed Simulink® models of each scenario. All the Simulink® models of the scenarios discussed here are appended in Appendix C.

Table 3-3: Detailed data summary of Scenario 1.

Machine Data[1]

Connected to Bus no. #	*Bus Type*	*Nominal Power* S_n (VA)	*Line-Line Voltage* V_n (V_{rms})	*Inertia* H (sec)	*Damping Factor* K_d (T_{pu}/ω_{pu})	*Pairs of Poles* $p()$	*Internal Impedance* (pu) *Resistance* R	*Reactance* X
1	Swing	1000×10^6	275×10^3	∞	0	1	0.007	2.185

All the machine impedances were calculated and the reader is referred to Appendix D where it is shown in the worksheet.

Line Data

Line no. #	*From Bus x to Bus y – x→y*	*Resistance* R (Ω/km)	*Inductance* L (H/km)	*Capacitance* C (F/km)	*Length* l (km)
1	1→2	6.22024×10^{-2}	1.01686×10^{-3}	1.15368×10^{-8}	87.78
2	2→3	6.19099×10^{-2}	1.01499×10^{-3}	1.15369×10^{-8}	133.88
3	3→4	6.19218×10^{-2}	1.01492×10^{-3}	1.15371×10^{-8}	107.23
4	4→5	6.18874×10^{-2}	1.02047×10^{-3}	1.14772×10^{-8}	166.80

All the line impedances were calculated and the reader is referred to Appendix D where it is shown in the worksheet.

All the listed values in this table are the required input data for the Simulink® model of Scenario 1. All the values are for a system operating at 50 Hertz.

Transformer Data

From Bus x to Bus y	*Nominal Power* S_n (VA)	*Primary Winding Impedances* (pu) R_1	L_1	*Secondary Winding Impedances* (pu) R_2	L_2	*Tertiary Winding Impedances* (pu) R_3	L_3
1→1 Load	400×10^6	0.002	0.08	0.002	0.08	0.002	0.08
2→2 Load	300×10^6	0.002	0.08	0.002	0.08	0.002	0.08
3→3 Load	300×10^6	0.002	0.08	0.002	0.08	0.002	0.08
4→4 Load	300×10^6	0.002	0.08	0.002	0.08	0.002	0.08
5→5 Load	300×10^6	0.002	0.08	0.002	0.08	0.002	0.08

The respective winding voltages of the transformers are clearly visible in Figure 3-1 and are therefore not listed in the table. The reactive compensation in the system is also clear.

3.3.2 The Second Scenario

In this scenario another common electric transmission system configuration is investigated. A load, such as a town or city, regularly has more than one incoming line/feeder. For this case it was decided to construct a scenario where three incoming lines supply a common load and the system has a Y-shaped look to it with the load situated at the point where the three lines meet (Figure 3-2).

The three respective lines are each independently connected to a source – a series of incoming lines, a bus, a substation, etc. – and these can be concluded to be infinite buses. Realising that a line is rated for a limited amount of power only (due to the line's thermal loading- and stability limit) and because protection equipment also limit the power transmitted, it follows that this cannot be an unlimited pool of power as an infinite bus suggests[2]. An infinite bus will also dampen or filter the effects of harmonic pollution and this is detrimental to the purposes of the study. This is then, once again, the reasons why generating machines are used to substitute the incoming lines and to represent these infinite buses.

[1] The machine data – in particular the inertia (H), damping factor (K_d) and the pairs of poles ($p()$) – were chosen as listed from available Simulink® demonstrations repeatedly showing that for substitution of transmission lines these values are valid/applicable. These values enable stable simulation of the scenarios. The machine models (per-unit Simplified Synchronous Machine(s) in this case) are dependent on their own per-unit system defined by base values supplied by the user.

[2] This is valid for Scenarios 1 and 3 as well.

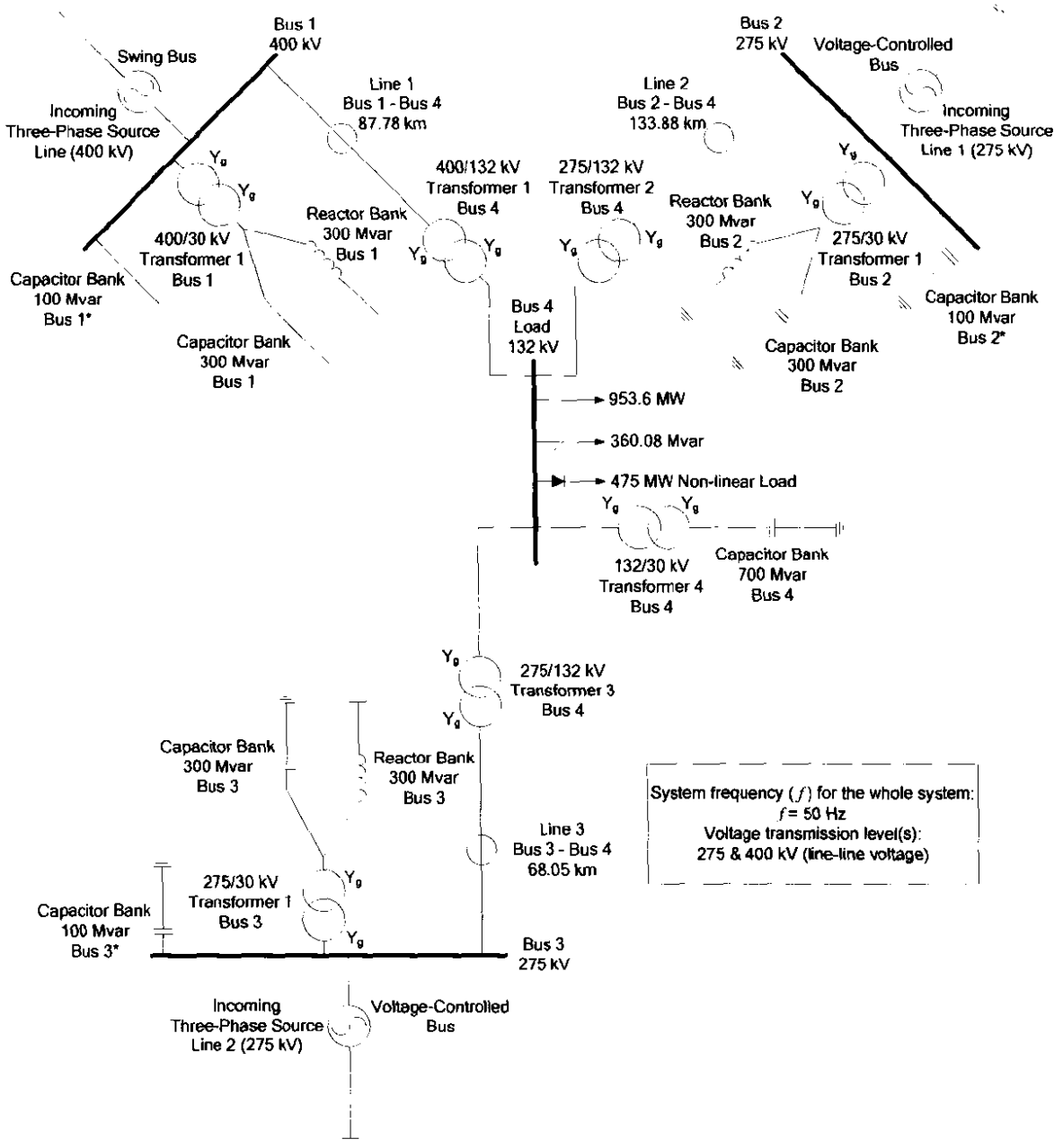


Figure 3-2: Scenario 2 is a system with transmission lines meeting at a common point.

Looking at the given line diagram, noticeable amounts of reactive compensation is connected to the system. This is mostly for the sake of stability when simulating the scenario in Simulink® and to allow for realistic impedance values to be used in the machine models to accurately represent the substituted lines.

A minor side-effect is that this reactive compensation equipment act as filters that filter out the harmonic components to a slight degree, but the total contribution is negligible and was ignored during the study. The large capacitor bank at the load bus is purely for line loadability and -regulation purposes. Again, Table 3-4 summarizes the relevant data of the system. The same comments, as mentioned earlier, apply.

Table 3-4: Detailed data summary of Scenario 2.

Machine Data

Connected to Bus no. #	*Bus Type*	*Nominal Power* S_n (VA)	*Line-Line Voltage* V_n (V_{rms})	*Inertia* H (sec)	*Damping Factor* K_d (T_{pu}/ω_{pu})	*Pairs of Poles* $p()$	*Internal Impedance* (pu) *Resistance* R	*Reactance* X
1	Swing	1000×10^6	400×10^3	∞	0	1	0.02	2.185
2	Voltage-controlled	750×10^6	275×10^3	∞	0	1	0.02	2.025
3	Voltage-controlled	750×10^6	275×10^3	∞	0	1	0.02	1.985

All the machine impedances were calculated and the reader is referred to Appendix D where it is shown in the worksheet.

Line Data

Line no. #	*From Bus x to Bus y – x→y*	*Resistance* R (Ω/km)	*Inductance* L (H/km)	*Capacitance* C (F/km)	*Length* l (km)
1	1→4	6.22024×10^{-2}	1.01686×10^{-3}	1.15368×10^{-8}	87.78
2	2→4	6.19099×10^{-2}	1.01499×10^{-3}	1.15369×10^{-8}	133.88
3	3→4	6.19003×10^{-2}	1.02055×10^{-3}	1.14773×10^{-8}	68.05

All the listed values in this table are the required input data for the Simulink® model of Scenario 2. All the values are for a system operating at 50 Hertz.

All the line impedances were calculated and the reader is referred to Appendix D where it is shown in the worksheet.

Transformer Data

Connected to Bus x or to Line y	*Nominal Power* S_n (VA)	*Primary Winding Impedances* (pu) R_1	L_1	*Secondary Winding Impedances* (pu) R_2	L_2	*Winding Line-Line Voltages* *Primary* V_1 (V_{rms})	*Secondary* V_2 (V_{rms})
Bus 1	400×10^6	0.002	0.08	0.002	0.08	400×10^3	30×10^3
Bus 2	400×10^6	0.002	0.08	0.002	0.08	275×10^3	30×10^3
Bus 3	400×10^6	0.002	0.08	0.002	0.08	275×10^3	30×10^3
Bus 4	800×10^6	0.002	0.08	0.002	0.08	132×10^3	30×10^3
Line 1 (end)	750×10^6	0.002	0.08	0.002	0.08	400×10^3	132×10^3
Line 2 (end)	500×10^6	0.002	0.08	0.002	0.08	275×10^3	132×10^3
Line 3 (end)	500×10^6	0.002	0.08	0.002	0.08	275×10^3	132×10^3

The respective winding voltages of the transformers are fairly visible in Figure 3-2, but the absent data is listed in the table for clarity sake. However, the reactive compensation in the system is clear from the figure.

3.3.3 The Third Scenario

At the start of this study it was advised to consult the local utility (ESKOM) to provide input on problematic scenarios, either in the existing electrical power system (EPS) or any hypothetical scenarios to their knowledge. The following scenario was provided and the extensive attention to detail indicates that this is a practical realistic scenario and exists. Input from ESKOM lends the study credibility and adds some purpose to the study as it illustrates a practical application of the outcomes for this study. The non-linear loads are the only detail not provided. This was added by the author using the same measures as for the preceding studies where non-linear loads are implemented.

This is the scenario that benchmarks the whole study's approach to solving the problem, namely, when harmonic pollution leads to poor power quality (PQ) in transmission networks. The proposed solution to this problem: to add power generating equipment of limited size (pebble bed modular reactor – PBMR) at carefully chosen points in the system while relying on the minimum amount of equipment – thus the improvement of the system is measured by a developed cost function (Chapter 4 & Chapter 5).

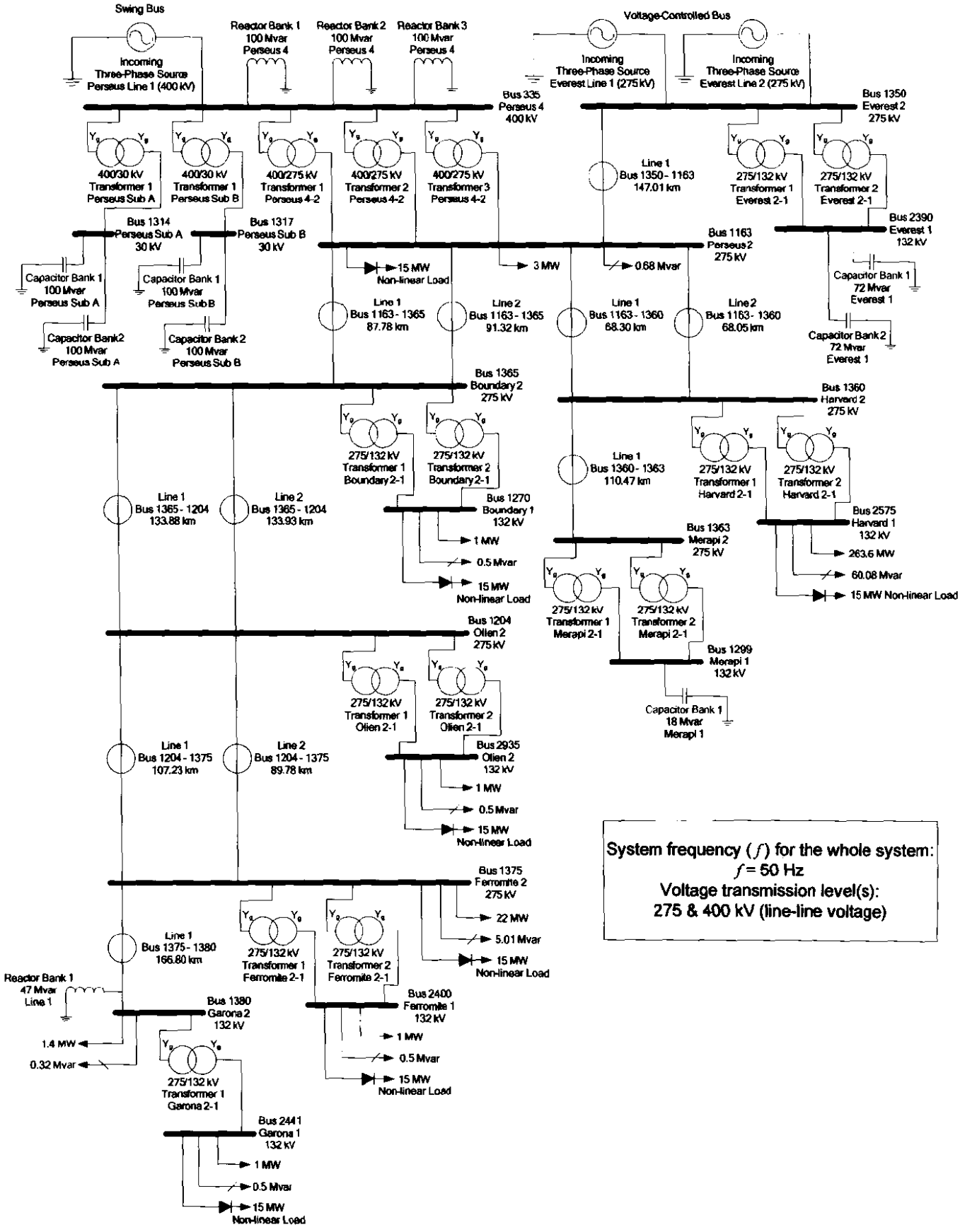


Figure 3-3: The transmission system as provided by ESKOM – Scenario 3.

Due to the size of the scenario and the amount of detail, comments about the scenario and its development are omitted. What can be said, though, is that the system is well-designed – line regulation is excellent and the minimum of reactive compensation equipment is necessary. A mentionable concern is the costly amount of lines that feed common buses, but the parallel lines do have advantages far above the advantages of adding compensation to improve line performances and power transmission capability. Unfortunately, construction of new transmission lines remains much more expensive. The technical data and specifications of the scenario are once more presented in the summarized version of Table 3-5.

Table 3-5: Detailed data summary of Scenario 3.

Machine Data

Connected to Bus no. #	*Bus Type*	*Nominal Power* S_n (VA)	*Line-Line Voltage* V_n (V_{rms})	*Inertia* H (sec)	*Damping Factor* K_d (T_{pu}/ω_{pu})	*Pairs of Poles* $p0$	*Internal Impedance* (pu) *Resistance* R	*Internal Impedance* (pu) *Reactance* X
335	Swing	1000×10^6	400×10^3	∞	0	1	0.02	15
1350	Voltage-controlled	500×10^6	275×10^3	∞	0	1	0.02	7.5
1350	Voltage-controlled	500×10^6	275×10^3	∞	0	1	0.02	7.5

All the machine impedances were calculated and the reader is referred to Appendix D where it is shown in the worksheet.

Line Data

Line no. #	*From Bus x to Bus y – x→y*	*Resistance* R (Ω/km)	*Inductance* L (H/km)	*Capacitance* C (F/km)	*Length* l (km)
1	1350→1163	6.20906×10^{-2}	1.03323×10^{-3}	1.13537×10^{-8}	147.01
1	1163→1360	6.21166×10^{-2}	1.01928×10^{-3}	1.14815×10^{-8}	68.30
2	1163→1360	6.19003×10^{-2}	1.02055×10^{-3}	1.14773×10^{-8}	68.05
1	1163→1365	6.22024×10^{-2}	1.01686×10^{-3}	1.15368×10^{-8}	87.78
2	1163→1365	6.21927×10^{-2}	1.01698×10^{-3}	1.15366×10^{-8}	91.32
1	1360→1363	6.22279×10^{-2}	1.01697×10^{-3}	1.15367×10^{-8}	110.47
1	1365→1204	6.19099×10^{-2}	1.01499×10^{-3}	1.15369×10^{-8}	133.88
2	1365→1204	6.18868×10^{-2}	1.02055×10^{-3}	1.14772×10^{-8}	133.93
1	1204→1375	6.19218×10^{-2}	1.01492×10^{-3}	1.15371×10^{-8}	107.23
2	1204→1375	6.23329×10^{-2}	9.91791×10^{-4}	1.16487×10^{-8}	89.78
1	1375→1380	6.18874×10^{-2}	1.02047×10^{-3}	1.14772×10^{-8}	166.80

All the line impedances were calculated and the reader is referred to Appendix D where it is shown in the worksheet.

All the listed values in this table are the required input data for the Simulink® model of Scenario 3. All the values are for a system operating at 50 Hertz.

Transformer Data

Transformer no. #	*From Bus x to Bus y*	*Nominal Power* S_n (VA)	*Primary Winding Impedances* (pu) R_1	*Primary Winding Impedances* (pu) L_1	*Secondary Winding Impedances* (pu) R_2	*Secondary Winding Impedances* (pu) L_2
1	1350→2390	500×10^6	0.002	0.08	0.002	0.08
2	1350→2390	500×10^6	0.002	0.08	0.002	0.08
1	335→1163	400×10^6	0.002	0.08	0.002	0.08
2	335→1163	400×10^6	0.002	0.08	0.002	0.08
3	335→1163	400×10^6	0.002	0.08	0.002	0.08
1	335→1314	300×10^6	0.002	0.08	0.002	0.08
1	335→1317	300×10^6	0.002	0.08	0.002	0.08
1	1360→2575	500×10^6	0.002	0.08	0.002	0.08
2	1360→2575	500×10^6	0.002	0.08	0.002	0.08
1	1365→1270	250×10^6	0.002	0.08	0.002	0.08
2	1365→1270	250×10^6	0.002	0.08	0.002	0.08
1	1363→1299	180×10^6	0.002	0.08	0.002	0.08
2	1363→1299	180×10^6	0.002	0.08	0.002	0.08
1	1204→2935	150×10^6	0.002	0.08	0.002	0.08
2	1204→2935	150×10^6	0.002	0.08	0.002	0.08
1	1375→2400	250×10^6	0.002	0.08	0.002	0.08
2	1375→2400	250×10^6	0.002	0.08	0.002	0.08
1	1380→2441	125×10^6	0.002	0.08	0.002	0.08

The respective winding voltages of the transformers are clearly visible in Figure 3-3 and are therefore not listed in the table. The reactive compensation in the system is also clear.

3.4 Results of the Scenarios

In this section the initial generated data of each simulated scenario is presented. The method of simulation is consistently applied to the scenarios. The simulation parameters also remain constant, refer to Table 3-6.

Table 3-6: Simulation parameters used for the simulations.

Simulation Parameters				
Variable Name		***Value (Simulation Input)***		
Frequency – f		f = 50 Hz		
Sample Time – T_s		$T_s = 5 \times 10^{-5}$ s		
Simulation Duration	Start Time	0.0	1 second	
	Stop Time	1.0		
Simulation Solver	Type	Variable-step	Discrete (no continuous states)	
	Maximum Step Size	Auto		

The first step is to initialize the machines that act as sources to the system. This is done by opening the PowerGUI. The model is discretized by supplying the sample time as listed by Table 3-6 in the designated input field. Next the "Load Flow and Machine Initialization" sub-routine is run to initialize the machines in the model. When the sub-routine has finished updating the machine "initial conditions" the simulation is run. When the simulation finishes the PowerGUI is once more opened. Now the user selects the "FFT Analysis" sub-routine, where the total harmonic distortion (*THD*) of both voltage- and current waveforms can be evaluated by selecting them in the "Structure" fields. Important to note is that a carefully chosen start time for the FFT analysis must be used – preferably when the whole system has reached steady-state operation – or else the harmonic components from the Fourier-analysis will not be accurate. The root-mean-square measurements (rms) of the three-phase waveforms (under the "Measurement Scopes" block of each scenario model) assist in determining when steady-state has been reached.

In general, the steady-state requirement is met after about 0.3 seconds of simulation and the chosen time instant for FFT-analysis is uniformly kept at 0.5 seconds. Other available measurements are the various waveforms at each measurement bus in the system also under the "Measurement Scopes" blocks of every scenario model. Another important requirement that begs mention is the terminal voltages (PowerGUI) of the generators. These need to be increased once non-linear loads are connected to maintain voltage levels throughout the transmission system.

Many of the scope blocks in the "Measurement Scopes" block of each model are set to write their generated measured data to the MATLAB-workspace where it is used (but not all of it) as the input for the "FFT Analysis" sub-routine of the PowerGUI. The rest of the data is used as input for the m-files (cost function) to measure the systems' performances. This pool of data is the measured power (active and reactive) of each bus, the voltage waveforms and the total harmonic voltage distortion (*THVD*).

Bearing in mind the appearance of the following output data set (measurement scopes); the specific output data for each scenario is presented in a tabulated format

under the relevant headings. Figure 3-4 is a typical pool of generated simulation data.

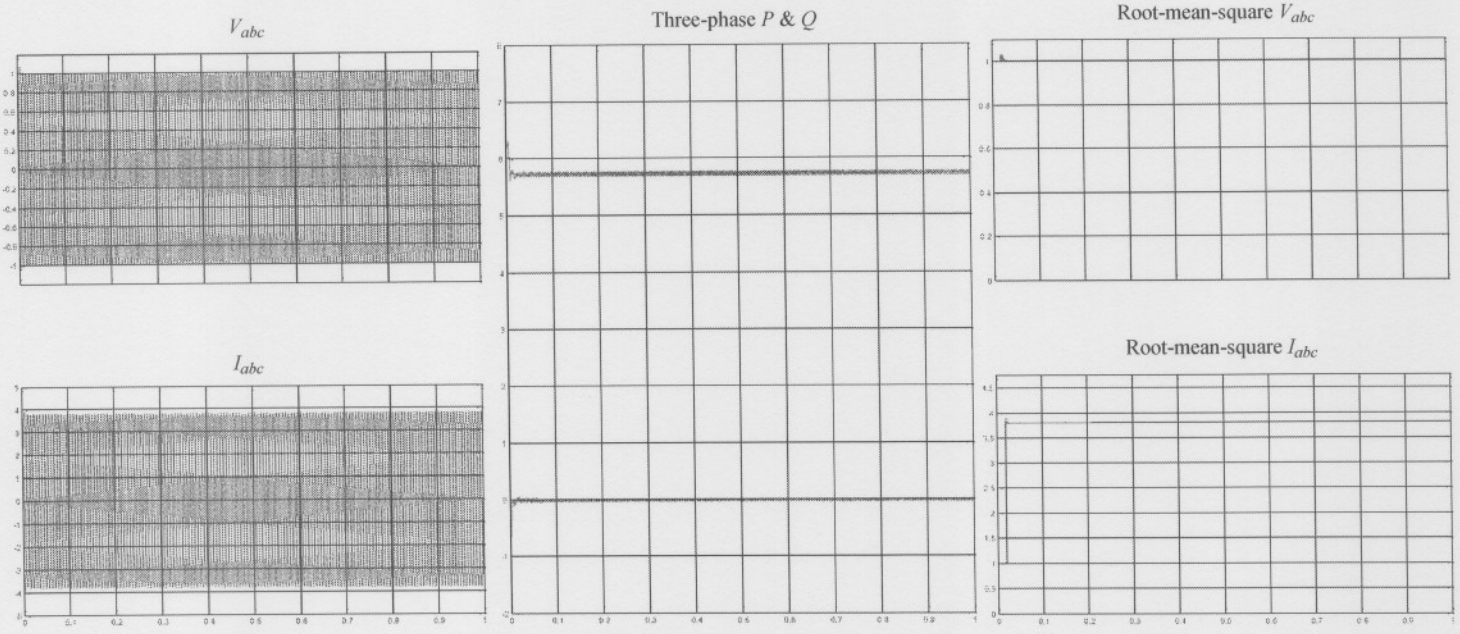


Figure 3-4: Typical measuements for a measurement bus.

On the left of Figure 3-4 is the measured simulated waveforms for each of the three phase-voltages – a-, b- and c-phase (top left); all three phase current waveforms are shown in the bottom left "scope". The vertical axis is the measured per-unit magnitude simulated and the horizontal axis is the simulation duration in seconds (the measurement plot time of the scopes).

In the middle of Figure 3-4 is the measured *instantaneous active power* (*P*) and the *-instantaneous reactive power* (*Q*). The instantaneous active power and -reactive power is given by (3.1)

$$\begin{aligned} p(t) &= v_a(t)i_a(t) + v_b(t)i_b(t) + v_c(t)i_c(t) \text{ and} \\ q(t) &= \frac{1}{\sqrt{3}}\left(v_{bc}(t)i_a(t) + v_{ca}(t)i_b(t) + v_{ab}(t)i_c(t)\right) \end{aligned} \tag{3.1}$$

where $p(t)$ is the instantaneous active power; $v_a(t)$ is the instantaneous a-phase voltage and $i_a(t)$ is the instantaneous a-phase line current (similarly for the remaining phases); $q(t)$ is the instantaneous reactive power; $v_{bc}(t)$ is the instantaneous line-line voltage (b- and c-phase) and $i_a(t)$ as already defined (again, similarly for the remaining phases).

It must be said that the active power in (3.1) remains true for harmonically distorted and unbalanced conditions, but the reactive power is only valid for balanced harmonic-free conditions. This measurement is ignored and is calculated with other proven methods (discussed and illustrated in Chapter 4).

In the right of Figure 3-4 is the measured root-mean-square (rms) magnitudes of both the phase-voltages and -currents. The axes are defined as before (waveform measurement).

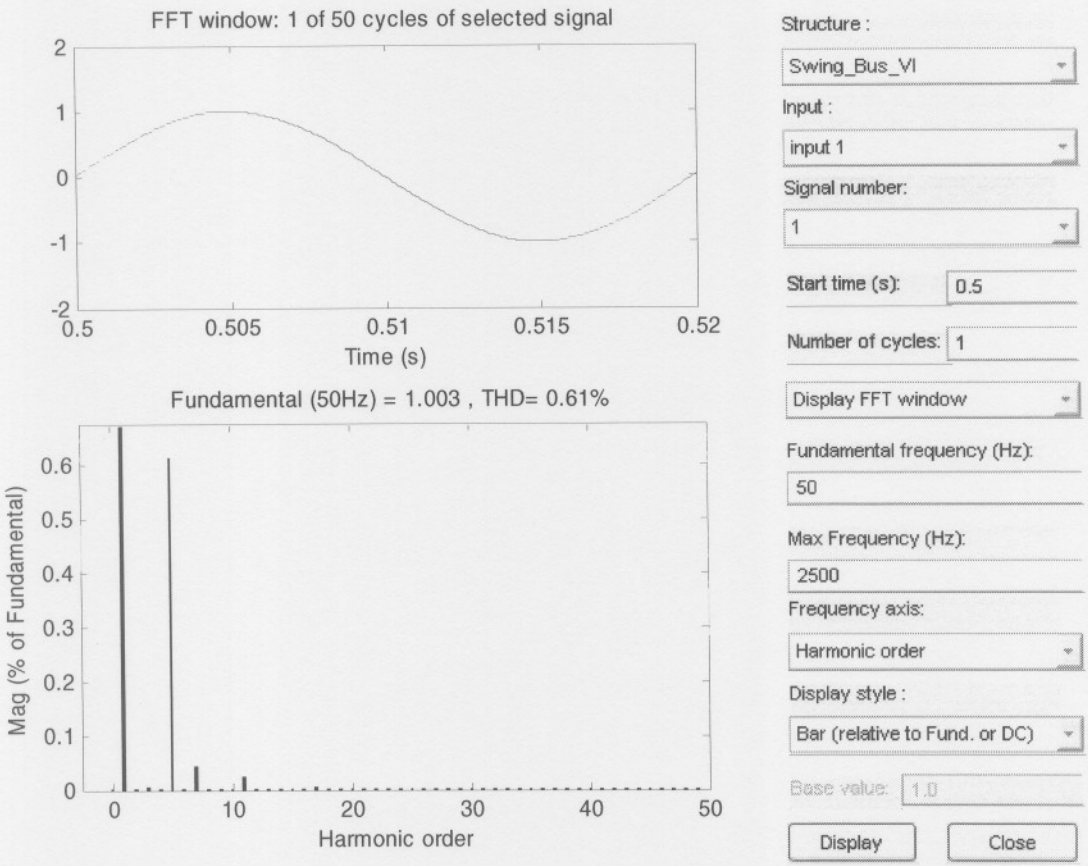


Figure 3-5: FFT-analysis of the a-phase voltage waveform in Figure 3-4.

Figure 3-5 demonstrates the appearance and functioning of the FFT-Analysis sub-routine of the PowerGUI. A snapshot of the a-phase voltage waveform (top plot in Figure 3-5) is taken after a period 0.5 seconds simulation. Steady-state has been reached by the system and the FFT-analysis of the generated waveform is considered to describe the expected normal operation of the scenario. The Fourier-spectrum is plotted in the bottom chart and the axes are clearly labelled.

3.4.1 The Results of Scenario 1

The results for Scenario 1 are listed in Table 3-7. This is the measured data (generated through simulation) of concern and is the basis for the need of improvement. In other words, this is the data representing the unimproved state of a so-called developed worst-case scenario. The single-phase analysis approach dictates that *phase A* is chosen as the reference phase to represent the measurements of the whole system. All the values listed are the per-unit measurements for *phase A* and all the systems/scenarios operate at phase balance, i.e. there are no (or negligibly minimal) unbalanced sequence components (Section 2.3.1).

Table 3-7: Summarized data results for Scenario 1.

Bus no #:	*Root-mean-square (rms) Phase Voltage – V* (pu)	*Root-mean-square (rms) Phase Current – I* (pu)	*Total Harmonic Voltage Distortion – THVD* (%)
1 (Swing)	1.003	3.808	0.61
1 (Load)	0.9473	0.2138	0.60
2	0.9986	3.586	0.65
2 (Load)	1.001	0.03078	0.79
3	1.004	3.454	2.10
3 (Load)	1.010	0.3752	3.99
4	1.009	2.952	0.73
4 (Load)	1.005	1.855	0.90
5	1.006	1.041	5.17
5 (Load)	0.9974	1.075	5.68

From the results it is seen that at Buses 3 Load, 5 and 5 Load the restrictions set by NRS 048 are not met. The scenario is in need of improvement and it shall be shown in Chapter 5 how this improvement is brought about. Another observation is that, fortunately for this case, the largest loads with non-linear components are situated at the end of the line and therefore there aren't any loads "further down" that will experience the intensified effects of the harmonic pollution caused at buses 4 and 5.

Usually the real case is large "polluting" loads early in the power network and the effects experienced by loads towards the end of the system is amplified by the characteristics of the transmission system resulting reaching harmfully exaggerated levels of harmonic pollution in the supply to these loads.

3.4.2 The Results of Scenario 2

The output for Scenario 2 is presented. Again the comments of the previous section (Scenario 1) are applicable.

Table 3-8: Summarized data results for Scenario 2.

Bus no #:	*Root-mean-square (rms) Phase Voltage – V* (pu)	*Root-mean-square (rms) Phase Current – I* (pu)	*Total Harmonic Voltage Distortion – THVD* (%)
1 (Swing)	1.004	6.302	4.17
2 (Voltage-controlled)	1.001	4.103	2.12
3 (Voltage-controlled)	1.010	3.996	2.92
4 (Load)	1.000	14.520	4.14

It is immediately evident that Buses 1 and 4 exceed the limits set by NRS 048. Also worth mentioning that the most power is drawn from the swing bus (Bus 1) and therefore this bus is subject to the largest version of the associated distorted current. This results in a greater measure of harmonic distortion (*ITHD*) in this bus than at the other two voltage-controlled buses (Buses 2 and 3). Furthermore, the machine at Bus 1 has the largest internal impedance, this impedance is directly responsible and accountable for the "generation" of harmonic components (section 2.3.2.1), and thus the larger impedance will result in the larger amount of total harmonic voltage distortion (*VTHD*).

3.4.3 The Results of Scenario 3

The results of Scenario 3 are limited to a short discussion aimed at the most important observations for this system. Once again the previous comments are kept in mind regarding the presented results.

Table 3-9: Summarized data results for Scenario 3.

Bus no #:	*Root-mean-square (rms) Phase Voltage – V* (pu)	*Root-mean-square (rms) Phase Current – I* (pu)	*Total Harmonic Voltage Distortion – THVD* (%)
335 (Swing)	0.9847	3.512	0.58
1350 (Voltage-controlled)	1.005	2.331	0.44
2390	1.028	1.481	0.46
1163 (Load)	0.9974	4.125	1.03
1314	1.102	2.204	0.27
1317	1.102	2.204	0.27
1360	0.9854	2.719	0.96
1365	1.017	1.482	2.08
2575 (Load)	0.9734	2.775	0.70
1363	1.001	0.1744	2.07
1270 (Load)	1.016	0.1611	1.49
1204	1.032	0.9487	3.23
1299	1.008	0.1815	2.11
2935 (Load)	1.030	0.1635	2.36
1375 (Load)	1.031	0.7376	3.39
2400 (Load)	1.030	0.1636	2.87
1380 (Load)	1.009	0.1762	3.83
2441 (Load)	1.004	0.1587	2.36

Not many of the buses exceed the limits imposed by NRS 048 and those that do exceed these limits aren't by much of a margin. Still, there is a wealth of information available to the observer of this system, as can be seen. The initial buses in the system reveal little influence subject to the harmonic pollution of the system, but further on in the transmission system the effects are more and more pronounced. Not wanting to coin the rule and state crudely that the worst measure of distortion must be expected at the end of the system, it does tend to be expected. As can be seen in this case the worst amount of pollution is found at buses that have unique attributes that allow for harmonics to flourish under those conditions; each bus has its own specific conditions that are liable for the influences caused by the harmonics present at the bus.

Buses 1204, 1375 and 1380 exhibit the largest distortion measures of the relevant waveforms, but they all lead to other buses that show lower measures of distortion. For this reason it has to be concluded that each bus is uniquely predisposed to the influences of harmonic components due to the measurable characteristics (impedances, etc.) of the bus which it inherits from connected equipment. In other words, it is concluded that a certain bus uniquely experiences the effects of non-sinusoidal (harmonically distorted) waveforms as a result of the inherent characteristics (mostly impedance) of equipment connected to the bus and the bus itself. This is valid for all three scenarios and for practical power systems in general (section 2.3.2.2).

3.5 Summary and Conclusions

The chosen method of modelling the developed scenarios proved to be effective and accurate. It was rather daunting at first to become accustomed and accomplished with the software applied in the method and study of the models, but once this was achieved the investigation was found to be succinct and comprehensive. The approach is realistic and scrutiny of the simulated results proves them as valid and accurate.

This part of the project was the most challenging: the time spent on data acquisition (which included correspondence with authorities that often led to extended periods of frustrated waiting for their reply); data preparation was extremely important - if the data was inaccurate the simulations were inconclusive; and finally, just getting the simulations to work (stable simulation) was a problem fraught with intuitive judgement, educated guesses, and repetitive adjustment of a multitude of variables (resulting in permutations numbering into the hundreds). Finally, the verification of the simulation models and generated data basically repeated this whole process.

It was found that the results coincide with what was expected and the conclusions drawn concur with the initial research of the study. These conclusions, or concurrences, are:

- The impedance of the source that feeds a non-linear load is proportionally responsible for the measure of the resulting harmonic distortion in the circuit that leads to the load, and further on after the selected load.
- There is no rule of thumb to determine the "weak spots" (points with the worst measure of harmonic pollution) in a system, unless there is an isolated dominant non-linear load connected at a singular point in the scenario. It can only be expected to fall within certain ranges and intuitive judgement is required to estimate these areas of concern in a scenario with distributed non-linear loads. Measurement of the system is the only true manner by which "weak spots" are determined.
- Reactive compensation equipment can act as attenuators/filters to harmonic equipment, but if not specifically designed for the purpose of filtering the compensation equipment could easily be damaged by harmonics present in the supply to such equipment.
- Poor power quality (PQ) exercises unnecessary strain on equipment in transmission networks (power transformer magnetic circuit saturation, overloading of lines, elevated voltage generation levels of generating equipment, etc.)
- The only true measure of usable power to a load/client is the fundamental component supplied to that load, but once harmonics are present, so much more unnecessary power is being supplied and could lead to damaging results for the load (if the load is susceptible and sensitive to such unfavourable conditions).

Chapter 4

Measuring Scenario Performance

4.1 Introduction

At the start of this study it was indicated that it is necessary to prove (or quantify) that a certain investigated scenario requires improvement. The improved scenario must, on the other hand, indicate no need for further improvement. A logical approach is to attempt to quantify this "amount of performance", before and after improvement. The only foreseeable method is to develop a cost function that measures this performance and gives the researcher a clear indication of the cost of the improvement, i.e. when there is enough improvement measures present in the scenario and further improvement would be unnecessary as it would only lead to negligible rise in performance and be cost-ineffective.

The aim of this chapter is then to guide the reader through and present the mathematics and reasoning related to the development of the said cost function. Finally the cost function is presented and the measurement variables (or indicators) are explained. A flowchart is also provided to illustrate the method (or procedure) of the cost function. The MATLAB® m-file(s) that calculates the mathematics is provided on the supplemental documentation CD and when studying the flowchart it is recommended that the reader inspects the code in the m-file as well.

Since the MATLAB® m-files are several lines of code and linked to a Microsoft® Excel spreadsheet (also of numerous worksheets): it would be senseless to present them in this document. All software related to the study is on the mentioned supplemental documentation CD.

4.2 The Mathematics: Sinusoidal & Non-sinusoidal Calculations

Firstly, it is important to note the following: since many readers are probably acquainted with the conventional (or "sinusoidal") mathematics regarding "harmonic-free" (*sinusoidal*) system analysis studies, it is only succinctly presented. The mathematical analysis of systems containing harmonic (*non-sinusoidal*) waveforms is in contrast with the conventional mathematics and is applied in this study. The calculations are done on a per-unit basis, unless stated otherwise, and the per-unit system is readily and easily applied in the mathematics of harmonically distorted waveforms. For interest sake, a concise and short comparison of the computational differences between the two mathematical theories is made in Appendix F. This is done by contrasting the results obtained by conventional mathematics with those with non-sinusoidal for one scenario.

4.2.1 Sinusoidal Mathematics

It is well known that power in single-phase ac circuits is easily extended to the three-phase system [35]. Now, for an arbitrary linear load system it follows that the *instantaneous voltage* and *-current* is given by (4.1)

$$v(t) = V_m \cos(\omega t + \theta_v)$$
$$i(t) = I_m \cos(\omega t + \theta_i) \tag{4.1}$$

The *instantaneous power* is the product of $v(t)$ and $i(t)$

$$p(t) = V_m I_m \cos(\omega t + \theta_v)\cos(\omega t + \theta_i) \tag{4.2}$$

Using the trigonometric identity

$$\cos A \cos B = \frac{1}{2}\cos(A - B) + \frac{1}{2}\cos(A + B) \tag{4.3}$$

for (4.2) results in

$$\begin{aligned} p(t) &= \frac{1}{2} V_m I_m [\cos(\theta_v - \theta_i) + \cos(2\omega t + \theta_v + \theta_i)] \\ &= \frac{1}{2} V_m I_m \{\cos(\theta_v - \theta_i) + \cos[2(\omega t + \theta_v) - (\theta_v - \theta_i)]\} \\ &= \frac{1}{2} V_m I_m [\cos(\theta_v - \theta_i) + \cos 2(\omega t + \theta_v)\cos(\theta_v - \theta_i) + \sin 2(\omega t + \theta_v)\sin(\theta_v - \theta_i)] \end{aligned} \tag{4.4}$$

The *root-mean-square* (rms) values of $v(t)$ and $i(t)$ are $|V| = V_m/\sqrt{2}$ and $|I| = I_m/\sqrt{2}$. Letting $\theta = (\theta_v - \theta_i)$, (4.4) reduces to, in terms of the rms values,

$$p(t) = |V||I|\cos\theta[1 + \cos 2(\omega t + \theta_v)] + |V||I|\sin\theta\sin 2(\omega t + \theta_v) \tag{4.5}$$

where θ is the *angle* between the voltage and the current, also known as the *impedance angle*. θ is positive when the load is inductive and it is said that the current lags the voltage, thus it is negative when the load is capacitive and the current then leads the voltage. Equation (4.5) consists of two parts – the terms containing the cosine waveforms and the terms made up of the sine waveforms. The first part (cosine) is the energy flow into the circuit dissipated in the pure resistance of the circuit. The second part (sine) is the energy borrowed and returned to the circuit and it oscillates between the inductive and capacitive parts of the circuit.

Now, consider the first part of (4.5)

$$p_R(t) = |V||I|\cos\theta + |V||I|\cos\theta\cos 2(\omega t + \theta_v) \tag{4.6}$$

The second term of (4.6), with a frequency twice that of the source, accounts for the sinusoidal variation in the absorption of power by the resistive portion of the load. The average value of this sinusoidal function is zero, therefore the *active* (or *real*) *power* delivered to the load is

$$P = |V||I|\cos\theta \tag{4.7}$$

The product of $|V|$ and $|I|$ is the *apparent power* and its unit is volt-ampere (VA) while $\cos\theta$ is known as the *power factor*. When the current lags the voltage, the power factor is considered lagging, and when the current leads the voltage, it is said to be a leading power factor.

The second part of (4.5)

$$p_X(t) = |V||I|\sin\theta\sin 2(\omega t + \theta_v) \tag{4.8}$$

pulsates at twice the frequency and has an average value of zero. This is power oscillating into and out of the load due to its reactive element (inductive, capacitive or a combination thereof). The amplitude of this pulsating power is termed *reactive power*

$$Q = |V||I|\sin\theta \tag{4.9}$$

and is measured in volt-ampere reactive (var). Inductive loads mean a positive Q and capacitive loads relate to a negative Q. Pure resistances result in a power factor of unity.

Finally, the *complex power* is defined from (4.7) and (4.9). Rewrite the instantaneous voltage and -current expressions in their complex rms phasor representations. $V = |V|\angle\theta_v$ and $I = |I|\angle\theta_i$, and consider Figure 4-1 and Figure 4-2.

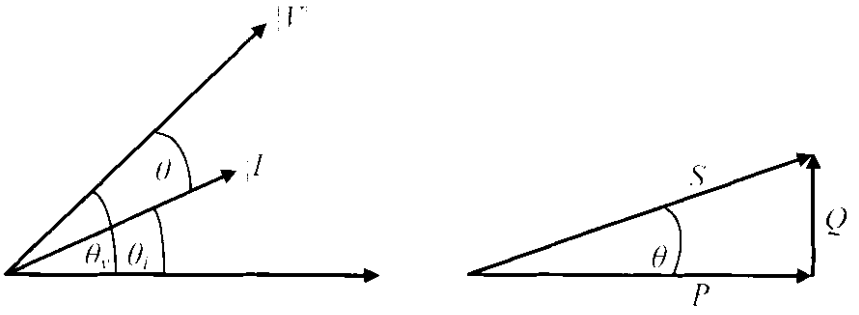


Figure 4-1: Phasor diagram and power triangle for a lagging power factor (inductive load).

The term VI^* results in

$$\begin{aligned} VI^* &= |V||I|\angle\theta_v - \theta_i = |V||I|\angle\theta \\ &= |V||I|\cos\theta + j|V||I|\sin\theta \end{aligned} \tag{4.10}$$

This is a complex quantity of which the real part is the average *active power*, P, and the imaginary part is the *reactive power*, Q. This complex power is the *apparent power*, S, given by $S = VI^* = P + jQ$ and the magnitude of S is $|S| = \sqrt{P^2 + Q^2}$ in VA (volt-amperes).

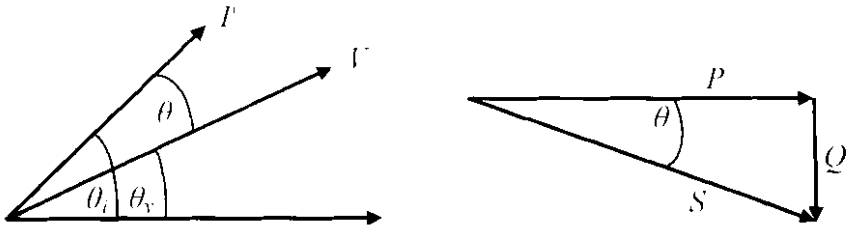


Figure 4-2: Phasor diagram and power triangle for a leading power factor (capacitive load).

Expanding (4.1) into (4.10) to include three-phase system studies crudely requires that the single-phase analysis presented above be done for each of the three separate phases of the three-phase system [26]. Adding the phase subscripts then results in the following set of equations (the *a*-subscript identifying *phase a*):

$$\begin{aligned} &v_a(t) = V_{a_m}\cos(\omega t + \theta_{v_a}),\ i_a(t) = I_{a_m}\cos(\omega t + \theta_{i_a}) \\ &P_a = |V_a||I_a|\cos\theta_a,\ Q_a = |V_a||I_a|\sin\theta_a, \text{ with } \theta_a = (\theta_{v_a} - \theta_{i_a}) \\ &S_a = V_a I_a^* = P_a + jQ_a \end{aligned} \tag{4.11}$$

similarly for the *b*- and *c*-phase.

It then follows that the *three-phase apparent power*, $S_{3\varphi}$, is the sum of the three separate phase quantities, in other words $S_{3\varphi} = S_a + S_b + S_c$. The *three-phase active power*, $P_{3\varphi}$, would then be given by (4.12)

$$\begin{aligned} P_{3\varphi} &= |V_a||I_a|\cos\theta_a + |V_b||I_b|\cos\theta_b + |V_c||I_c|\cos\theta_c \\ &= P_a + P_b + P_c \end{aligned} \tag{4.12}$$

and the *three-phase reactive power*, $Q_{3\varphi}$, is given by (4.13)

$$\begin{aligned} Q_{3\varphi} &= |V_a||I_a|\sin\theta_a + |V_b||I_b|\sin\theta_b + |V_c||I_c|\sin\theta_c \\ &= Q_a + Q_b + Q_c \end{aligned} \tag{4.13}$$

Thus, $S_{3\varphi} = \sqrt{P_{3\varphi}^2 + Q_{3\varphi}^2}$ VA, the magnitude of the three-phase apparent power. This set of equations is valid for systems with a measurable amount of unbalance, but for a balanced system, that is a system where all the phase quantities are equal in magnitude, they reduce to (4.14)

$$\left.\begin{aligned} P_{3\phi} &= 3|V_p||I_p|\cos\theta \\ Q_{3\phi} &= 3|V_p||I_p|\sin\theta \\ S_{3\phi} &= 3V_pI_p^* \end{aligned}\right\} \text{with } V_p \text{ and } I_p \text{ the phase voltage- and line current magnitudes}$$

$$\left.\begin{aligned} P_{3\phi} &= \sqrt{3}|V_L||I_L|\cos\theta \\ Q_{3\phi} &= \sqrt{3}|V_L||I_L|\sin\theta \\ S_{3\phi} &= \sqrt{3}V_LI_L^* \end{aligned}\right\} \text{with } V_L \text{ and } I_L \text{ the line voltage- and phase current magnitudes} \qquad (4.14)$$

$$S_{3\phi} = P_{3\phi} + jQ_{3\phi} \text{ and with } \theta = \theta_v - \theta_i$$

It should be perfectly clear that the mathematics presented above is only valid for "harmonic-free" waveforms. The mathematics pertaining to harmonically distorted waveforms is subsequently discussed. From here on "harmonic-free" waveforms are termed *sinusoidal waveforms* (or -voltage, -current, etc.) and harmonically distorted waveforms are hence known as *non-sinusoidal waveforms*.

In a sinusoidal system study the task of applying a power flow analysis (or load flow solution) to a system is frequently encountered. It is beyond the scope of this study to present the iterative techniques regarding power flow solutions. It would suffice to mention the prominent three techniques commonly in use, namely, the Gauss-Seidel method, Newton-Raphson- and Quasi-Newton-. These techniques operate accurately in sinusoidal systems, but since they were derived for sinusoidal systems using the equations for single-phase and balanced three-phase calculations as basis, they cannot readily be applied to non-sinusoidal systems. This phenomenon is comparatively illustrated in Appendix F.

4.2.2 Non-sinusoidal Mathematics

Due to the difficulties associated with graphically presenting the different harmonic orders that non-sinusoidal waveforms consist of, the reader is asked to excuse the absence of phasor representations as accompanying the discussions of the preceding section. This discussion is unfortunately presented in a purely mathematical manner. The following set of equations is a collection of practical definitions that equip the investigator with the necessary means to evaluate non-sinusoidal conditions and was published by an IEEE working group [38].

Suppose that non-sinusoidal time-dependent waveforms can be written as a function. It is then assumed that the phase voltage and line current signals for phase a is be given by (4.15)

$$\begin{aligned} v_a(t) &= V_{a0} + \sqrt{2}\sum_{h=0}^{\infty} V_{ah}\sin(h\omega t + \alpha_{ah}) \\ i_a(t) &= I_{a0} + \sqrt{2}\sum_{h=0}^{\infty} I_{ah}\sin(h\omega t + \beta_{ah}) \end{aligned} \qquad (4.15)$$

It accounts in similar fashion for phases b and c and with a positive symmetrical phase rotation these phase quantities will lag phase a by 120° and 240° respectively.

By rewriting these equations to suit the phase information for the remaining phases is defined in full.

For (4.15) it has to be explained what the variables mean, thus where:
$v_a(t)$ the instantaneous phase voltage for phase a;
$i_a(t)$ the instantaneous line current for phase a;
V_{a0} the average value for the phase voltage in phase a;
I_{a0} the average (or dc) value for the line current in phase a;
V_{ah} the rms value for the harmonic phase voltage component of order h in phase a;
I_{ah} the rms value for the harmonic line current component of order h in phase a;
α_{ah} the phase angle of the harmonic phase voltage component of order h in phase a;
β_{ah} the phase angle of the harmonic line current component of order h in phase a.

For rms magnitudes the equations are reduced to the following, while bearing in mind that the subscripts are relevantly altered to validate the expression(s) for the remaining phases.

$$\begin{aligned} V_a^2 &= V_{a1}^2 + \sum_{h=2}^{\infty} V_{ah}^2 = V_{a1}^2 + V_{aH}^2 \text{ with } V_{aH}^2 = \sum_{h=2}^{\infty} V_{ah}^2 \\ I_a^2 &= I_{a1}^2 + \sum_{h=2}^{\infty} I_{ah}^2 = I_{a1}^2 + I_{aH}^2 \text{ with } I_{aH}^2 = \sum_{h=2}^{\infty} I_{ah}^2 \end{aligned} \tag{4.16}$$

The *effective three-phase voltage*, V_e, and *-current*, I_e, is defined as

$$V_e = \sqrt{\frac{V_a^2 + V_b^2 + V_c^2}{3}} \text{ and } I_e = \sqrt{\frac{I_a^2 + I_b^2 + I_c^2}{3}} \tag{4.17}$$

or for phase-phase (or line-line) quantities

$$V_e = \sqrt{\frac{V_{ab}^2 + V_{bc}^2 + V_{ca}^2}{9}} \tag{4.18}$$

These quantities are an attempt to collectively describe the independent phase magnitudes as an average whole.

The respective (V_e and I_e) effective three-phase values can be separated into to uniquely describable parts

$$\begin{aligned} V_{e1} &= \sqrt{\frac{V_{a1}^2 + V_{b1}^2 + V_{c1}^2}{3}} \text{ and } V_{eH} = \sqrt{\frac{\sum_{h\neq 1}^{\infty}(V_{ah}^2 + V_{bh}^2 + V_{ch}^2)}{3}}, \text{ with } V_e = V_{e1} + V_{eH} \\ I_{e1} &= \sqrt{\frac{I_{a1}^2 + I_{b1}^2 + I_{c1}^2}{3}} \text{ and } I_{eH} = \sqrt{\frac{\sum_{h\neq 1}^{\infty}(I_{ah}^2 + I_{bh}^2 + I_{ch}^2)}{3}}, \text{ with } I_e = I_{e1} + I_{eH} \end{aligned} \tag{4.19}$$

where V_{e1} is the *effective three-phase fundamental harmonic voltage* component; I_{e1} is the *effective three-phase fundamental harmonic current* component; V_{eH} is the *effective three-phase harmonic voltage* component; I_{eH} is the *effective three-phase harmonic current* component.

The *three-phase effective apparent power*, S_e, is defined as

$$\begin{aligned} S_e^2 &= (V_e I_e)^2 = (V_{e1} I_{e1})^2 + (V_{e1} I_{eH})^2 + (V_{eH} I_{e1})^2 + (V_{eH} I_{eH})^2 \\ &= S_{e1}^2 + S_{eN}^2, \text{ with } S_{e1}^2 = (V_{e1} I_{e1})^2 \text{ and } S_{eN}^2 = (V_{e1} I_{eH})^2 + (V_{eH} I_{e1})^2 + (V_{eH} I_{eH})^2 \end{aligned} \quad (4.20)$$

where S_{e1} is coined the *effective fundamental apparent power*; and S_{eN} is the *effective non-fundamental apparent power* – with $V_{e1}I_{eH}$ the *current distortion power*; $V_{eH}I_{e1}$ the *voltage distortion power*; and $V_{eH}I_{eH}$ the *harmonic distortion power*.

At this point it is of utmost importance to note that, for power as defined by (4.20) in non-sinusoidal system analysis; the conventional (or sinusoidal) power triangle (Figure 4-1 and Figure 4-2) cannot remain valid and accurate for non-sinusoidal waveforms. Thus, $S = \sqrt{P^2 + Q^2}$ is not applicable. The continued discussion clarifies how this relationship needs to be altered for validity.

Consider the single-phase analysis of a non-linear (non-sinusoidal) system for a moment. Abandoning the phase- and three-phase effective subscripts to reduce the expressions to their single-phase rms equivalents, they become

$$\begin{aligned} V^2 &= V_1^2 + \sum_{h=2}^{\infty} V_h^2 = V_1^2 + V_H^2 \text{ with } V_H^2 = \sum_{h=2}^{\infty} V_h^2 \\ I^2 &= I_1^2 + \sum_{h=2}^{\infty} I_h^2 = I_1^2 + I_H^2 \text{ with } I_H^2 = \sum_{h=2}^{\infty} I_h^2 \\ S^2 &= (VI)^2 = (V_1 I_1)^2 + (V_1 I_H)^2 + (V_H I_1)^2 + (V_H I_H)^2 \\ &= S_1^2 + S_N^2, \text{ with } S_1^2 = (V_1 I_1)^2 \text{ and } S_N^2 = (V_1 I_H)^2 + (V_H I_1)^2 + (V_H I_H)^2 \end{aligned} \quad (4.21)$$

where V is the *rms voltage* magnitude; I is the *rms current* magnitude; V_1 is the *rms fundamental harmonic voltage* component; I_1 is the *rms fundamental harmonic current* component; V_H is the *rms harmonic voltage* component; I_H is the *rms harmonic current* component; S is the *apparent power*; S_1 is the *fundamental apparent power*; S_N is the *non-fundamental apparent power*.

The orthogonal relationship between the *real* (or *active*) *power* and the *imaginary* (or *reactive*) *power* holds true for higher order harmonic components in non-sinusoidal voltage- and current signals. A consequence of these higher order power quantities is that it can not be determined how they influence the *total reactive power* values. Thus, only the fundamental harmonic reactive power components can be accurately defined as a result. Subsequently the *fundamental active-* and *-reactive power* is related to the *fundamental apparent power*, thanks to their orthogonal relationship, by $S_1^2 = (V_1 I_1)^2 = P_1^2 + Q_1^2 = (V_1 I_1 \cos\theta_1)^2 + (V_1 I_1 \sin\theta_1)^2$ where θ_1 is the *phase angle difference* between α_1 and β_1, or $\alpha_1 - \beta_1$.

Another quantity comes into play at this stage, namely the *total single-phase non-active power*, N, given by (4.22)

$$N = \sqrt{S^2 - P^2} \tag{4.22}$$

It should be transparent by now that it is somewhat advantageous to examine the quantities in a non-sinusoidal study in terms of two independent parts, namely the fundamental- and harmonic part respectively. Now then, for active power it follows

$$\begin{aligned} &P^2 = P_1^2 + P_H{}^2 \\ &\text{with } P = \sum_{h=1}^{\infty} V_h I_h \cos\theta_h;\ \text{where } \theta_h = \alpha_h - \beta_h \\ &\text{and } P_1 = V_1 I_1 \cos\theta_1;\ \text{where } \theta_1 = \alpha_1 - \beta_1 \\ &\text{and } P_H = \sum_{h\neq 1}^{\infty} V_h I_h \cos\theta_h;\ \text{where } \theta_h = \alpha_h - \beta_h \end{aligned} \tag{4.23}$$

where P is the *total single-phase active power*; P_1 is the *fundamental single-phase active power*; P_H is the *total harmonic single-phase active power*.

Before expansion of the single-phase analysis discussion is made to include the three-phase case, it is worth mention of an introduced quantity at this point that is recognized in the single-phase system, but not in the three-phase system. This quantity is known as the *total harmonic single-phase apparent power*, S_H, and is defined to consist of the *total harmonic single-phase active power*, P_H, and the *total harmonic single-phase non-active power*, N_H

$$S_H{}^2 = P_H{}^2 + N_H{}^2 \tag{4.24}$$

With this the discussion of single-phase analysis is expanded to include the analysis of three-phase systems. Regarding the discussion of three-phase analysis, it's immediately important to note that only the *fundamental apparent power* (S_1) and the *non-fundamental apparent power* (S_N) are recognized in a three-phase non-sinusoidal power system, accordingly the following expression(s) are now explicitly termed for three-phase analysis

$$\begin{aligned} S_e{}^2 &= (V_e I_e)^2 = (V_{e1} I_{e1})^2 + (V_{e1} I_{eH})^2 + (V_{eH} I_{e1})^2 + (V_{eH} I_{eH})^2 \\ &= S_{e1}{}^2 + S_{eN}{}^2,\ \text{with } S_{e1}{}^2 = (V_{e1} I_{e1})^2 \text{ and } S_{eN}{}^2 = (V_{e1} I_{eH})^2 + (V_{eH} I_{e1})^2 + (V_{eH} I_{eH})^2 \end{aligned} \tag{4.25}$$

where S_{e1} is the *three-phase effective fundamental apparent power*; and S_{eN} is the *three-phase effective non-fundamental apparent power* – with $V_{e1}I_{eH}$ the *three-phase current distortion power*; $V_{eH}I_{e1}$ the *three-phase voltage distortion power*; and $V_{eH}I_{eH}$ the *three-phase harmonic distortion power*.

In order to quantify the "distortion amount" in three-phase power systems, the *equivalent total harmonic voltage distortion* factor and *equivalent total harmonic current distortion* factor is defined by (4.26)

$$VTHD_e = \frac{V_{eH}}{V_{e1}} \text{ and } ITHD_e = \frac{I_{eH}}{I_{e1}} \tag{4.26}$$

A novel application of the distortion factors is found when attempting to normalize the *non-fundamental apparent power* and is identified in this discussion as the true measure of harmonic pollution

$$\left(\frac{S_{eN}}{S_{e1}}\right)^2 = (ITHD_e)^2 + (VTHD_e)^2 + (ITHD_e VTHD_e)^2 \tag{4.27}$$

Since the unbalanced operating condition of a power system is beyond the scope of this study (the simulations were designed with a balanced operating condition in mind), the discussion of the mathematics accounting for this phenomenon is omitted. Although, it is interesting to mention that in a heavily distorted system, notable unbalanced operating conditions are inevitable, but as this study focuses on slightly distorted systems (bordering the limits set by NRS 048), this by-product is negligible.

Next the power factor is defined for both the *true apparent power factor* and the *displacement power factor*

$$PF = \frac{P_{3\phi}}{S_e} = \frac{P_{3\phi 1} + P_{3\phi H}}{S_e} \text{ and } DPF = \frac{P_{3\phi 1}}{S_{e1}} \tag{4.28}$$

Finally, as seen in (4.28), the concept of *effective power* values is dropped and the introduction of *true three-phase* quantities is made. This should not be confusing as it closely relates to the sinusoidal case, except that the sinusoidal case now accounts for more harmonic orders than only the fundamental. Equation (4.28) contains the *total three-phase active power*, $P_{3\phi}$, which is a combination of the *total three-phase fundamental active power*, $P_{3\phi 1}$, and the *total three-phase harmonic active power*, $P_{3\phi H}$

$$\begin{aligned}
&P_{3\phi} = \sum_{h=0}^{\infty} P_{3\phi h} = P_{3\phi 1} + \sum_{h\neq 1}^{\infty} P_{3\phi h} = P_{3\phi 1} + P_{3\phi H} \\
&P_{3\phi 1} = P_{a1} + P_{b1} + P_{c1} = V_{a1}I_{a1}\cos(\alpha_{a1} - \beta_{a1}) + V_{a1}I_{b1}\cos(\alpha_{b1} - \beta_{b1}) + V_{c1}I_{c1}\cos(\alpha_{c1} - \beta_{c1}) \\
&P_{3\phi H} = P_{aH} + P_{bH} + P_{cH} = \sum_{h\neq 1}^{\infty} V_{ah}I_{ah}\cos(\alpha_{ah} - \beta_{ah}) + \sum_{h\neq 1}^{\infty} V_{bh}I_{bh}\cos(\alpha_{bh} - \beta_{bh}) + \sum_{h\neq 1}^{\infty} V_{ch}I_{ch}\cos(\alpha_{ch} - \beta_{ch})
\end{aligned} \tag{4.29}$$

Ultimately, the *total three-phase reactive power*, $Q_{3\phi}$, can only be defined for the fundamental three-phase quantities

$$Q_{3\phi 1} = Q_{a1} + Q_{b1} + Q_{c1} = V_{a1}I_{a1}\sin(\alpha_{a1} - \beta_{a1}) + V_{a1}I_{b1}\sin(\alpha_{b1} - \beta_{b1}) + V_{c1}I_{c1}\sin(\alpha_{c1} - \beta_{c1}) \tag{4.30}$$

where the definitions of the variables are analogous to the combined meanings of the sinusoidal definitions and the newly introduced definitions for the active power in non-sinusoidal applications.

A quantitative measure for the "amount" of harmonic pollution is by application of (4.27). A value of zero will indicate no harmonic pollution, as this index S_{eN}/S_{el} increases; it is attributed to increasing harmonic pollution. The components of this index indicate the cause; as the effective voltage- and current harmonic distortion factors are the only key components of the index. The index S_{eN}/S_{el} fully deserves the name *harmonic pollution indicator*, and it will be employed as such in the cost function. This is done under advisement from the literature source [38].

Intimately associated with the outcomes of this study is the need to accurately determine the power flow analysis of a scenario. No attempt is made to derive such a method, as this is far beyond the scope of the study. What was found is that the only accurate and measurable way to determine the power flow solution is through simulation with a simulation software package (MATLAB® Simulink® SimPowerSystems blockset) that is capable of accurately simulating power systems with non-linear loads (non-sinusoidal power systems).

4.3 The Cost Function

As the research and literature study progressed, certain prominent variables (or indicators) came to the fore and after careful consideration a select few were chosen to ultimately act with paramount influence in the cost function. The exact mathematical interdependencies of these variables are painstaking; thus, a concise flowchart is given to illustrate these relationships in Figure 4-3.

The mathematical calculation flowchart of Figure 4-3 depicts a calculation process repeatedly applied to every bus (and transmission line where applicable) in the developed power system of each respective scenario. After this "pool of data" is calculated for every bus (and line) in the scenario, the variables of concern (identified by the shaded "clouds" in Figure 4-3) are applied in the cost function as will be illustrated by Figure 4-4.

While negotiating the numerous pitfalls of the "non-sinusoidal mathematics" discussed above, it was discovered that it is rarely defined in a clear manner whether the quantity of concern is a complex value or an absolute magnitude. It is decided that the phase information is neglected in the application of the mathematics, except for where the complex values are readily available.

As already mentioned, the "clouds" in Figure 4-3 are the variables that are ultimately applied in the cost function. As can be seen these variables are tied into a rather complicated network of equations, expressions and measurements, but they remain central to the purpose of quantifying how well the scenario being investigated performs. These three variables (or variable groups), are the key factors that precisely describes the overall effectiveness, efficiency and quality of power in the general scenario.

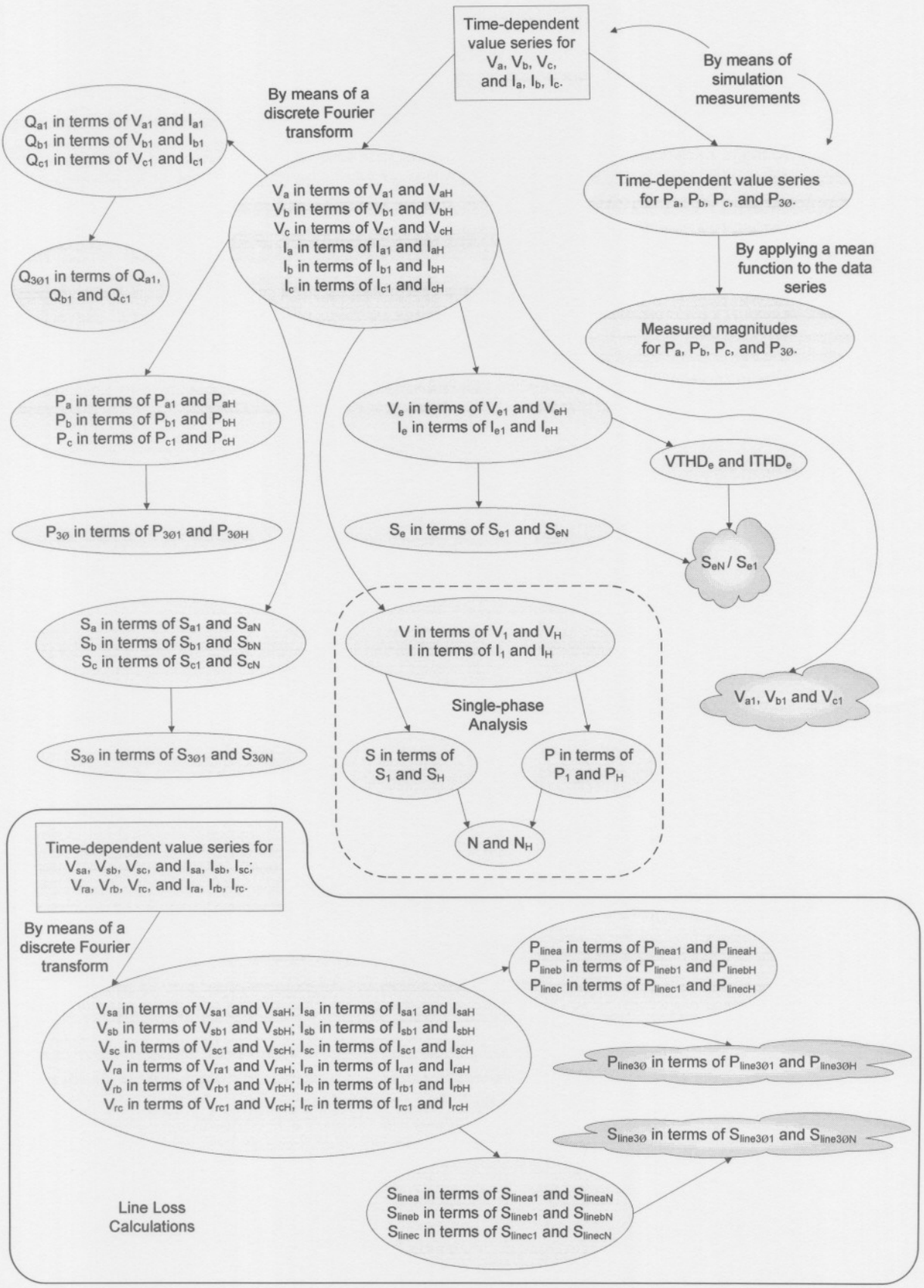


Figure 4-3: Mathematical calculation flowchart depicting the variable interrelationships.

The next point of discussion is how these selected few variables are used. The cost function must provide an indication (index) of the performance of a scenario. This index is required before it is attempted to improve the scenario. After such improvement is implemented the index delivers an indication of the amount of improvement. The function should also be used as an optimization parameter, in other words, the indicator must reveal the point where the optimum solution has been reached and where further improvement would only lead to unnecessary expenses.

Suppose that a PBMR unit costs 1 billion Rand. It would appear logical to measure the "amount of improvement" in terms of this cost – more units implemented means more billions of Rand spent. A practical improvisation is to quantify the "cost of improvement" as a ratio of the "amount of improvement", or alternatively

$$\text{Cost Function} = \frac{\text{Cost of PBMR installed}}{\text{Performance measure improvement}}.$$

Given that utilities measure the fundamental voltage phase components (V_{a1}, V_{b1} and V_{c1}), it's ensured that the correct amount of power is delivered to the consumers and enables the consumers' equipment to function as intended. Thus, the first part of this performance indicator is a measure of how well the scenario's voltage regulation is. This is a simplified single index that considers all the scenario buses. The nominal phase voltage magnitude for any bus is usually 1 pu. An exception is made for varying load conditions; this means that there is a "permitted range" that determines acceptable voltage levels ranges from 0.95 pu to 1.05 pu. A root-mean-square indicator is proposed and would ensure the best representation.

$$Index_V = \sqrt{\frac{\sum_{i=1}^{n} |V_{i_{e1}} - 1|^2}{n}} \tag{4.31}$$

where $Index_V$ is the *voltage regulation indicator*; V_{ie1} is the *effective three-phase fundamental voltage magnitude* for bus i; and n is the *number of buses*.

The second part of the performance indicator is generated from the normalized indicator, S_{eN}/S_{e1}, calculated for all measured scenario buses. This is a comprehensive index that considers not only the amount of voltage harmonic distortion, but the current harmonic distortion as well. It is similar to the voltage indicator, as it also relies on the rms-principle.

$$Index_{THD} = \sqrt{\frac{\sum_{i=1}^{n} \left(\frac{S_{i_{eN}}}{S_{i_{e1}}} \right)^2}{n}} \tag{4.32}$$

where $Index_{THD}$ is the *harmonic distortion indicator*; S_{ieN} / S_{ie1} is the *harmonic pollution indicator* for bus i; and n is the *number of buses*.

The third, and last, indicator is a measure of the efficiency of the transmission system. This indicator is the rms-normalized *per-unit active power line losses* collectively representing the transmission lines of the scenario.

$$Index_{Ploss} = \sqrt{\frac{\sum_{i=1}^{l} P_{loss_i}^{\ 2}}{l}} \tag{4.33}$$

where $Index_{Ploss}$ is the *line loss indicator*; $P_{loss\,i}$ is the *per-unit three-phase active power loss* for line i; and l is the *number of transmission lines*.

Now that these three indices are defined, how are they put together? Mathematically the performance index looks as follows and it is noted that the index is 1 for a lossless, sinusoidal, perfectly regulated power system. Anything less than 1 is a reduction in performance.

$$Index_{performance} = \left[1 - \left(Index_{V} + Index_{THD}\right)\right] - \left[\frac{\left(Index_{V} + Index_{THD}\right)}{\left(Index_{V} + Index_{THD}\right)} * Index_{Ploss}\right] \tag{4.34}$$

where $Index_{performance}$ is the *performance indicator*; $Index_V$ is the *voltage indicator*; $Index_{THD}$ is the *harmonic distortion indicator*; and $Index_{Ploss}$ is the *line loss indicator*.

The next question is how is optimization applied? Well, as mentioned, the improvement of the scenario comes at a cost – the cost of a PBMR unit at a R1 billion price tag. One proposed method of improvement is to strategically place the PBMR unit(s) in the scenario. This prevents (or at least postpones) the unnecessary expenditure of buying more units.

The solution determines that a unit is installed at a specific point in the scenario where it has largest advantageous influence; after repeatedly investigating the placements in the scenario (through simulation). For this method the placement causing the largest increase in the performance index is the optimal configuration, and since placement is of paramount concern the cost of the unit(s) is ignored. Then

$Index_{performance_{optimum}} = \max(Index_{i_{performance}})$; for $1,\ldots,i,\ldots,n$ with n the number of permutations. (4.35)

where $Index_{performance\ optimum}$ is the *optimum performance indicator*; $Index_{i\ performance}$ is the *performance indicator* for placement permutation i; n is the *number of placement permutations*.

The second proposed method is to increase the amount of units coupled with a strategic placement plan. The amount of these units required to cause a cost-efficient result is determined by the ratio of the cost of the installed units and the "amount of improvement" (amount increase in the performance indicator). Finally, once the ratio reaches an inefficient cost per improvement value the scenario is considered optimized for the previous solution before inefficiency is reached. Thus,

$$Index_{ratio_{optimum}} = \min\left[\frac{Units_{DG} * Cost_{DG}}{\max(Index_{i_{performance}})}\right]; \quad (4.36)$$

for $1,\ldots,i,\ldots,n$ with n the number of placement permutations

where $Index_{ratio\ optimum}$ is the *optimum ratio indicator* for amount of DG per "amount of improvement"; $Units_{DG}$ is the *number of DG units*; $Cost_{DG}$ is the *cost of a DG unit*; $Index_{i\ performance}$ is the *performance indicator* for placement permutation i; n is the *number of placement permutations*.

The following flowchart demonstrates how the cost function operates.

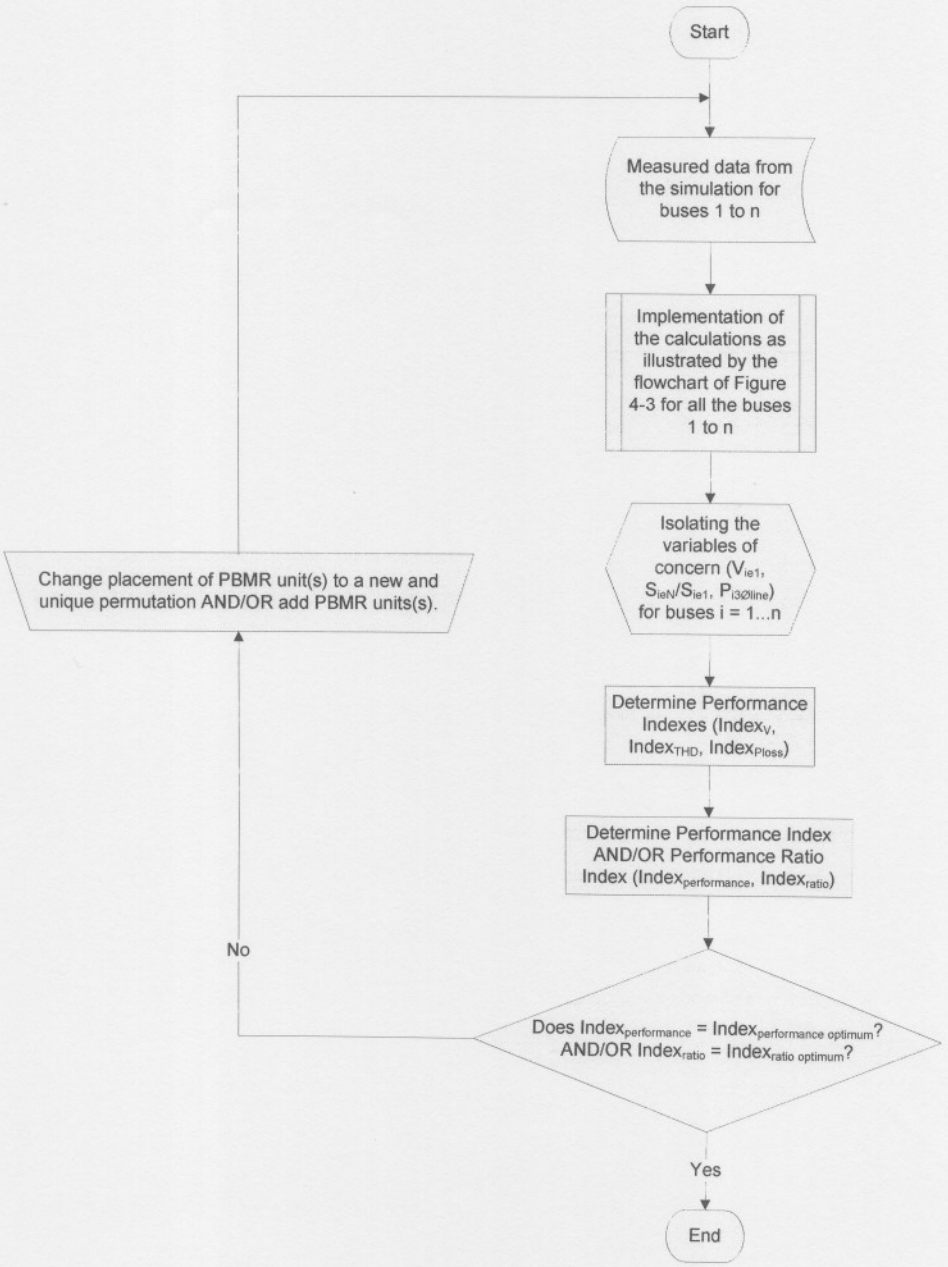


Figure 4-4: Cost function flowchart.

4.4 Testing and Verification of the Cost Function

An ideal scenario, with a performance index of unity, is a theoretical possibility. Such a scenario exhibits zero line (system) losses, has no disturbances of power quality (PQ) caused by the presence of harmonically distorted waveforms, and has perfect voltage regulation. This is never achieved in practice. The ideal use of such a scenario (achieved in the theoretical realm of simulation where endless possibilities exist) is to verify and test the developed cost function in this document.

The three individual indices are separately adjusted and the performance index is tested whether it accurately relates the adjustment of the individual variable. Meanwhile, the other two indices are kept constant – preferably as close as possible to zero. The best simulation scenario available for this idyllic use is the un-altered scenario from ESKOM (Appendix C and Appendix E). This scenario is almost entirely free of non-sinusoidal waveforms (those that do exist are negligibly small). No illustrations are given here; the relevant figures are available in Appendix C.

In the un-altered (harmonic-free) state the voltage regulation index is easily tested. The generating voltages are adjusted to intentionally drive the voltage levels to new steady-state values and the *voltage regulation indicator* is calculated (while the system is maintained so as not to change the *harmonic distortion-* and *line loss indicator*). The newly calculated value for the adjusted state is used to determine the new *performance index* after which a comparison of the two states (initial and altered) is made. The initial voltage settings of the three established generators are set to approximately increase the overall system voltage by 20%. Figure 4-5 illustrates the response of the performance index and it is shown that it accurately relays the breach of the permitted voltage regulation range (0.95 – 1.05 pu) for the system. The *voltage regulation indicator* has a new value of 0.174554; the accepted maximum overall value of deviation for this indicator being 0.05. Poor voltage regulation is confirmed. The *performance indicator* experiences a related decrease from 0.940397 to 0.824580.

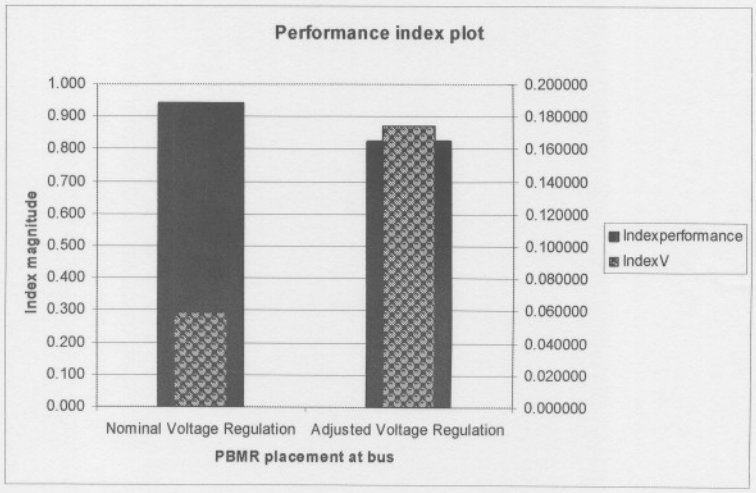


Figure 4-5: *Voltage regulation indicator* influence on the *performance indicator*.

In a similar fashion the *harmonic distortion indicator* is deliberately adjusted by the addition of a moderate non-linear load (rated at 50 MW – see Appendix D

Scenario 3 calculation worksheet). The previously calculated indicator is compared with the new one and so are the performance indices. The *voltage regulation-* and *line loss indicator* are kept constant (or as "unchanged" as permitted by the simulation). The practicality of maintaining the ignored indicators at constant levels is a near-impossible objective at the expense of many exhaustive efforts. Figure 4-6 shows the increase of the *harmonic distortion indicator* from 0.001080 to 0.207421. This is clearly reflected by the response of the performance indicator – a drop from 0.940397 to 0.741314. This is an accurate response and gives a true indication of the scenario's performance related to harmonic polluting factors.

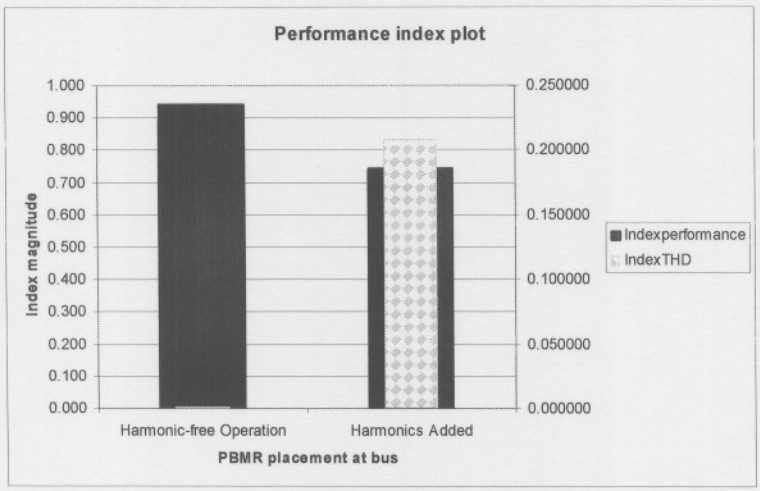


Figure 4-6: *Harmonic distortion indicator* influence on the *performance indicator*.

The *line loss indicator* can be modified by means of two adjustments – the line impedance characteristics can be changed, or the power flow through the line is varied. Both impart problems to the test simulation: the first method is unrealistic as practical power transmission lines are unable to change their properties inherited from their construction; the requirement to maintain constant *voltage regulation-* and harmonic distortion indicators is overly complicated by the second method.

The second method is attempted and negligible change in the other two indicators is assumed and considered. The power demands of the loads at Buses 1299 and 2441 (see Appendix C Project_Scenario_Ideal simulation model diagram) is greatly increased. This causes increased power flow in all the transmission lines in the scenario leading to increased losses. A harmonic-free, ideally voltage regulated system is maintained.

From Figure 4-7 it is straightforwardly perceived that the line losses have increased – the line loss indicator was 1.7022E-08 was and has risen to 2.6456E-08 (almost doubled). Unfortunately the variance in the performance indicator is not so easily seen – it is best described in actual calculated quantities. It was 0.9403969004 and has decreased to 0.9403968909. The change is very minimal and this is due to the small magnitude nature of the normalized calculated *line losses*. This is not of major concern and would suffice to recommend that a different normalization method is applied.

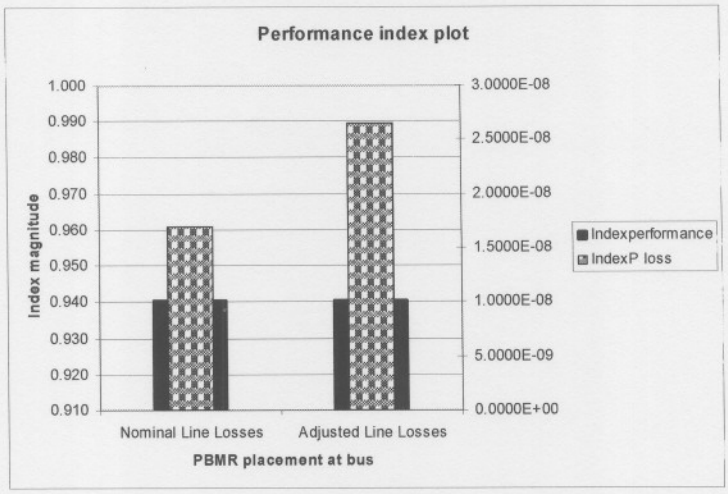


Figure 4-7: *Line loss indicator* influence on the *performance indicator*.

4.5 Summary

The cost function development was a task of lesser complications than the model development of Chapter 3. Still, it required a careful understanding and a firm grasp of the mathematical concepts related to the detailed functioning of the various structural dimensions of the cost function. Once the mathematics is understood it is clear (from the related literature) exactly which variables enjoy principal priority. Utilizing these variables in a unique manner allows for a comprehensive, concise and accurate mathematical description and method that quantifies the performance of a scenario and caters for the optimization thereof.

The chosen variables forming the basis of the cost function are carefully chosen under advisement from the literature – the referenced sources ([26], [35], [38], and [39]) all clearly illustrate the importance of these variables. *Glover et al.* and *Saadat* both ascribe considerable concern to voltage regulation in power networks ($Index_V$); the IEEE working group on non-sinusoidal conditions identifies S_{eN}/S_{e1} as the true measure of harmonic pollution; and *Caldon et al.* used line losses as basis to optimize a distributed generation network by means of reactive power control.

The cost function has a sound logical structure and positively indicates performance; 1 or relatively close to 1 (depending on the per-unit magnitudes of the line loss index, $Index_{Ploss}$) indicates optimized efficiency, little or no harmonic pollution ($Index_{THD} \approx 0$) is present and voltage regulation is ideal ($Index_V \approx 0$). Small values (<<1) indicate poor performance and a need for system improvement.

The cost function accurately describes and quantifies a scenario's performance and is readily applied as a basis for optimization. This is shown in section 4.4 describing the testing and evaluation of the cost function. It cannot, however, be suggested as the only measure of system performance as it was specifically tailored to meet the requirements of this study. The goal is to improve the performance of a power scenario while investigating the effects of distributed generation (DG) on the power quality (PQ) in electrical power systems.

Chapter 5

Simulation Results and Scenario Performance Improvement

5.1 Introduction

The reader has witnessed how to develop power system scenarios, concluded that the presence of non-sinusoidal components in these scenarios' electrical power flow entails special mathematics to accurately analyze the power flow, and finally, a suggested measure of each scenario's performance was presented. In this chapter the results of both the non-sinusoidal mathematics analysis, and the cost function measuring the scenario performances, are presented.

The first two scenarios are used to demonstrate an optimization process using the developed cost function (various indices and performance index) to establish optimum strategic placement of distributed generation (DG) resources, such as pebble bed modular reactors (PBMRs), in the respective scenarios. The last scenario (Scenario 3) is only intuitively optimized (solved) as the scope of the study does not include an optimization process.

As will be shown, the problem of optimizing a scenario's performance is a rather complex problem and an optimum solution can only be attained with the use of some sort of automated computer-aided design (CAD), e.g. using a genetic algorithm. The process involves repetitive placement of DG units for all possible placement permutations, repeatedly testing the various cost function indices (*voltage regulation-*, *harmonic distortion-* and *line loss indicator*) for compliancy to accepted index measures, and finally, finding the best *performance index* for the scenario and the associated placement permutation responsible for the performance. Another part of this optimization process is adding a DG unit(s) and once again repeating the placement permutation inspection, until acceptable performance is achieved.

The aim of this study was not to develop the mentioned CAD design above. The purpose was to study different power system scenarios, add distributed generation (DG) resources (PBMRs), and study the effects thereof on the power quality of the system/scenario. Attempting to quantify these "effects" the cost function was developed and suggested to be used as a measure for the optimization of such scenarios. These results are now presented.

5.2 Generated Simulation Results Data Structure

For verification purposes the data structure of the results obtained from the study is shortly presented. It is trivial to present all the available results in full, but all the data resources are available on the supplemental documentation CD.

Due to the relatively small system structure of Scenario 2 (Figure 3-2), the related results for Scenario 2 are presented to present the different groups of analyzed data that ultimately culminate in the group of data that completely describes the performance of a scenario.

The "raw" data (simulation measurements) is not presented due to the complicated and exceedingly lengthy nature of the measurement data files. The first group of tabulated processed data is the non-sinusoidal mathematical analysis of each bus and line for a given scenario.

Table 5-1: Selected calculated and measured results for the Swing Bus of Scenario 2.

Steady-state Analysis Results from MATLAB® using the power_analyze function (voltage and current).

	V_a	V_b	V_c	I_a	I_b	I_c	V_{ab}	V_{bc}	V_{ca}	I_{ab}	I_{bc}	I_{ca}
Magnitude (rms pu)	1.35	1.35	1.35	7.29722	7.29722	7.29722	1.35	1.35	1.35	7.29722	7.29722	7.29722
Angle (deg)	5.639E-06	-120	120	28.1637	-91.8363	148.164	30	-90	150	58.1637	-61.8363	178.164

Steady-state Simulation Results from MATLAB® Simulink using the developed model (voltage and current).

	V_a	V_b	V_c	I_a	I_b	I_c	V_{ab}	V_{bc}	V_{ca}	I_{ab}	I_{bc}	I_{ca}
Magnitude (rms pu)	1.003	1.00371	1.00359	6.30255	6.30205	6.30201	1.73969	1.73982	1.73993	10.9162	10.9154	10.9161
Angle (deg)	1.301E-02	-119.986	120.052	NaN	NaN	NaN	NaN	NaN	NaN	NaN	NaN	NaN
Fundamental Magnitude (pu)	1.0036	1.00355	1.0037	6.30249	6.30208	6.30205	1.73818	1.73835	1.73843	10.916	10.9152	10.916
Fundamental Angle (deg)	0	-119.992	120.006	NaN	NaN	NaN	NaN	NaN	NaN	NaN	NaN	NaN
Total Harmonic Distortion (%)	4.1688	4.14062	4.12823	0.525111	0.522585	0.522106	NaN	NaN	NaN	NaN	NaN	NaN

Steady-state Simulation Scope Readouts from the developed model (voltage, current, active- and reactive power).

	V_a	V_b	V_c	I_a	I_b	I_c	$P_{3\Phi}$	$Q_{3\Phi}$	$P_{3\Phi}$ (MW)	$Q_{3\Phi}$ (Mvar)
Measured Magnitude (rms pu)	1.00446	1.00439	1.00448	6.30253	6.30221	6.30217	9.31966	-1.775350	931.966	-177.535

Steady-state Single-phase Simulation Results from the model (voltage, current, apparent- and active power).

	V	V_1	V_H	I	I_1	I_H	S	S_1	S_N	P	P_1	P_H
Magnitude (rms pu & pu)	1.003003	1.003604	3.59E-02	6.302543	6.302491	0.02873204	3.16073918	3.16260014	0.112625	3.10664	3.10664	6.0362E-05
Angle (deg)	NaN	0	NaN	NaN	10.7944	NaN	NaN	-10.7944	NaN	NaN	NaN	NaN

Steady-state Single-phase Simulation Results from the model (non-active power), continued...

	S_H	N	N_H
Magnitude (pu)	5.158E-04	1.921E+00	5.192E-04

Steady-state Effective Three-phase Simulation Results from the model (voltage, current, apparent power and harmonic pollution indicator).

	V_e (Phase)	I_e (Line)	V_e (Line)	I_e (Phase)	V_{e1}	V_{eH}	I_{e1}	I_{eH}	S_e	S_{e1}	S_{eN}	S_{eN} / S_{e1}
Magnitude (rms pu)	1.00343	6.3022	1.00448	6.30229	1.0036	0.035901	6.30249	0.028732	3.16074	3.1626	0.112625	0.036062
Total Harmonic Distortion (%)	3.57718	0.455883	NaN	NaN	NaN	NaN	NaN	NaN	NaN	NaN	NaN	3.60615

Steady-state Three-phase Results from the model (fundamental voltage, -current, fundamental reactive power, true apparent- and displacement power factor).

	V_{a1}	V_{b1}	V_{c1}	I_{a1}	I_{b1}	I_{c1}	$Q_{3\Phi1}$	Q_{a1}	Q_{b1}	Q_{c1}	PF	DPF
Fundamental Magnitude (pu)	1.003604	1.003554	1.003700	6.302491	6.302072	6.302044	-1.776070	-0.592307	-0.591673	-0.592085	0.942937	0.982322

Steady-state Three-phase Simulation Results from the model (active power), continued...

	$P_{3\Phi}$	$P_{3\Phi1}$	$P_{3\Phi H}$	P_{a1}	P_{b1}	P_{c1}	P_{aH}	P_{bH}	P_{cH}
Magnitude (pu)	9.31998	9.3198	0.00017793	3.10664	3.10639	3.10677	6.0362E-05	5.9636E-05	5.7929E-05

Steady-state Three-phase Simulation Results from the model (apparent power), continued...

	$S_{3\Phi}$	$S_{3\Phi1}$	$S_{3\Phi N}$	S_{a1}	S_{b1}	S_{c1}	S_{aN}	S_{bN}	S_{cN}
Magnitude (pu)	9.88399	9.487523	0.396468	3.16260014	3.16223588	3.16268628	0.132886	0.131977	0.131605

Table 5-2: Calculated and measured results for Line 1 in Scenario 2.

Sending-end values from simulation measurements of the developed model (voltage and current).

	V_{sa}	V_{sb}	V_{sc}	I_{sa}	I_{sb}	I_{sc}
Magnitude (rms pu)	1.003004	1.003708	1.003588	6.186712	6.185062	6.185397
	V_{sa1}	V_{sb1}	V_{sc1}	I_{sa1}	I_{sb1}	I_{sc1}
Fundamental magnitude (pu)	1.003605	1.003556	1.003698	6.185689	6.185502	6.185483
	V_{saH}	V_{sbH}	V_{scH}	I_{saH}	I_{sbH}	I_{scH}
Harmonic magnitude (pu)	0.035901	0.019216	0.040030	0.112549	0.089164	0.111594

Receiving-end values from simulation measurements of the developed model (voltage and current).

	V_{ra}	V_{rb}	V_{rc}	I_{ra}	I_{rb}	I_{rc}
Magnitude (rms pu)	0.986592	0.987628	0.987168	6.164811	6.164665	6.164701
	V_{ra1}	V_{rb1}	V_{rc1}	I_{ra1}	I_{rb1}	I_{rc1}
Fundamental magnitude (pu)	0.987239	0.987165	0.987295	6.163817	6.163810	6.163880
	V_{raH}	V_{rbH}	V_{rcH}	I_{raH}	I_{rbH}	I_{rcH}
Harmonic magnitude (pu)	0.038130	0.033068	0.035486	0.143228	0.135235	0.137366

Calculated line loss measurements from the developed model (apparent-, active- and non-active power).

	$S_{s\,3\Phi}$	$S_{s\,3\Phi}$	$S_{line\,3\Phi}$	$P_{line\,3\Phi}$	$N_{line\,3\Phi}$
Magnitude (pu)	6.206957	6.106111	0.684039	0.1573	0.665707

The data of Table 5-1 and Table 5-2 are obtained by the following process: first the simulation of Scenario 2 is run in MATLAB® Simulink® obtaining the necessary simulated measurements (generated "raw" data). Next the measured data is analyzed and processed by a developed MATLAB® m-file written by the author. The associated m-file of each scenario computes the non-sinusoidal mathematics and the outputs of this m-file are 21×12 and 7×6 matrices that closely resemble Table 5-1 and Table 5-2. The output matrices of the m-file are used in Microsoft® Excel to improve the readability of the calculated and measured data and to produce graphs that plot the performance indices.

Table 5-1 and Table 5-2 are only for one bus and one line each, thus the "bigger" the scenario, the more of these tables are created, and every one of these tables are necessary to calculate the final performance values and to optimize the scenario, as is demonstrated by Table 5-3 comparatively summarizing a scenario (Scenario 2).

Table 5-3: Comparative summary of selected results for Scenario 2.

Bus name	Comparative bus data, line data and calculated cost function index values.								
	Three-phase effective value analysis (voltage, current and Total Harmonic Distortion)								
Swing bus	$V_{s\emptyset}$ (pu)	V_{s1} (pu)	$V_{s\emptyset H}$ (pu)	$I_{s\emptyset}$ (pu)	I_{s1} (pu)	$I_{s\emptyset H}$ (pu)	$VTHD_{s\emptyset}$ (%)	$ITHD_{s\emptyset}$ (%)	$S_{s\emptyset N}$ / S_{s1}
	1.003430	1.003600	0.035901	6.302200	6.302490	0.028732	3.577180	0.455883	0.036062
	Three-phase power analysis (apparent, active and reactive power)								
	$S_{3\emptyset}$ (MVA)	$S_{3\emptyset 1}$ (MVA)	$S_{3\emptyset N}$ (MVA)	$P_{3\emptyset}$ (MW)	$P_{3\emptyset 1}$ (MW)	$P_{3\emptyset H}$ (MW)	$Q_{3\emptyset 1}$ (Mvar)	PF	DPF
	988.3990	948.7523	39.646800	931.9980	931.9800	0.017793	-177.607000	0.942937	0.982322
Bus 2 Voltage-controlled	$V_{r\emptyset}$ (pu)	V_{r1} (pu)	$V_{r\emptyset H}$ (pu)	$I_{r\emptyset}$ (pu)	I_{r1} (pu)	$I_{r\emptyset H}$ (pu)	$VTHD_{r\emptyset}$ (%)	$ITHD_{r\emptyset}$ (%)	$S_{r\emptyset N}$ / S_{r1}
	1.000920	1.000930	0.020265	4.102820	4.102990	0.015047	2.024610	0.366738	0.020576
	$S_{3\emptyset}$ (MVA)	$S_{3\emptyset 1}$ (MVA)	$S_{3\emptyset N}$ (MVA)	$P_{3\emptyset}$ (MW)	$P_{3\emptyset 1}$ (MW)	$P_{3\emptyset H}$ (MW)	$Q_{3\emptyset 1}$ (Mvar)	PF	DPF
	629.2540	615.9926	13.261000	595.3310	595.3270	0.003760	-158.217000	0.946090	0.966451
Bus 3 Voltage-controlled	$V_{r\emptyset}$ (pu)	V_{r1} (pu)	$V_{r\emptyset H}$ (pu)	$I_{r\emptyset}$ (pu)	I_{r1} (pu)	$I_{r\emptyset H}$ (pu)	$VTHD_{r\emptyset}$ (%)	$ITHD_{r\emptyset}$ (%)	$S_{r\emptyset N}$ / S_{r1}
	1.009470	1.009600	0.025291	3.995640	3.995840	0.016834	2.505060	0.421289	0.025403
	$S_{3\emptyset}$ (MVA)	$S_{3\emptyset 1}$ (MVA)	$S_{3\emptyset N}$ (MVA)	$P_{3\emptyset}$ (MW)	$P_{3\emptyset 1}$ (MW)	$P_{3\emptyset H}$ (MW)	$Q_{3\emptyset 1}$ (Mvar)	PF	DPF
	623.0540	605.0788	17.975600	588.2710	588.2630	0.007570	-141.658000	0.944172	0.972209
Bus 4 Load	$V_{l\emptyset}$ (pu)	V_{l1} (pu)	$V_{l\emptyset H}$ (pu)	$I_{l\emptyset}$ (pu)	I_{l1} (pu)	$I_{l\emptyset H}$ (pu)	$VTHD_{l\emptyset}$ (%)	$ITHD_{l\emptyset}$ (%)	$S_{l\emptyset N}$ / S_{l1}
	1.000280	1.000320	0.037300	14.523900	14.521500	0.622782	3.728770	4.288690	0.056853
	$S_{3\emptyset}$ (MVA)	$S_{3\emptyset 1}$ (MVA)	$S_{3\emptyset N}$ (MVA)	$P_{3\emptyset}$ (MW)	$P_{3\emptyset 1}$ (MW)	$P_{3\emptyset H}$ (MW)	$Q_{3\emptyset 1}$ (Mvar)	PF	DPF
	2315.4900	2178.8652	136.625000	2034.6100	2034.6600	-0.049647	779.495000	0.878695	0.933816
	Calculated from the measured data obtained from the Simulink model simulation.								
	Sending-end rms voltage and current								
	Voltage (rms)			Current (rms)			Calculated three-phase power line loss.		
Line 1	$V_{s\emptyset}$ (pu)	$V_{s\emptyset 1}$ (pu)	$V_{s\emptyset H}$ (pu)	$I_{s\emptyset}$ (pu)	$I_{s\emptyset 1}$ (pu)	$I_{s\emptyset H}$ (pu)	$S_{line3\emptyset}$ (MVA)	$P_{line3\emptyset}$ (MW)	$N_{line3\emptyset}$
	1.003004	1.003605	0.035901	6.186712	6.185689	0.112549	68.40388	15.73000	66.57070
	Receiving-end rms voltage and current								
	Voltage (rms)			Current (rms)					
	$V_{r\emptyset}$ (pu)	$V_{r\emptyset 1}$ (pu)	$V_{r\emptyset H}$ (pu)	$I_{r\emptyset}$ (pu)	$I_{r\emptyset 1}$ (pu)	$I_{r\emptyset H}$ (pu)			
	0.986592	0.987239	0.038130	6.164811	6.163817	0.143226			
Line 2	$V_{s\emptyset}$ (pu)	$V_{s\emptyset 1}$ (pu)	$V_{s\emptyset H}$ (pu)	$I_{s\emptyset}$ (pu)	$I_{s\emptyset 1}$ (pu)	$I_{s\emptyset H}$ (pu)	$S_{line3\emptyset}$ (MVA)	$P_{line3\emptyset}$ (MW)	$N_{line3\emptyset}$
	1.000724	1.000933	0.020265	3.958270	3.957733	0.065443	89.79414	21.12100	87.27480
	$V_{r\emptyset}$ (pu)	$V_{r\emptyset 1}$ (pu)	$V_{r\emptyset H}$ (pu)	$I_{r\emptyset}$ (pu)	$I_{r\emptyset 1}$ (pu)	$I_{r\emptyset H}$ (pu)			
	0.976141	0.976346	0.028601	3.927721	3.927909	0.050213			
Line 3	$V_{s\emptyset}$ (pu)	$V_{s\emptyset 1}$ (pu)	$V_{s\emptyset H}$ (pu)	$I_{s\emptyset}$ (pu)	$I_{s\emptyset 1}$ (pu)	$I_{s\emptyset H}$ (pu)	$S_{line3\emptyset}$ (MVA)	$P_{line3\emptyset}$ (MW)	$N_{line3\emptyset}$
	1.009301	1.009602	0.025291	3.878025	3.877254	0.077457	44.19513	9.40463	43.18290
	$V_{r\emptyset}$ (pu)	$V_{r\emptyset 1}$ (pu)	$V_{r\emptyset H}$ (pu)	$I_{r\emptyset}$ (pu)	$I_{r\emptyset 1}$ (pu)	$I_{r\emptyset H}$ (pu)			
	0.989177	0.989671	0.032116	3.875115	3.874532	0.072195			
	Calculated index measures for the scenario.								
	$Index_{performance}$	$Index_V$	$Index_{THD}$	$Index_{P\,loss}$					
	0.957429	0.005150	0.037421	1.6145E-07					

Now that the reader is familiar with how the generated resulting data is structured and treated, the discussion for each scenario is continued. The reader is referred to the Nomenclature (Table 0-1) and Chapter 4 if any of the meanings of the variables in the tables presented here are unclear, but great care has been taken to present the variables with their respective meanings and source information in the tables.

It is also worth mentioning that the results in Table 5-1, Table 5-2 and Table 5-3 are for no connected DG units to the scenario. The results listed in these tables undergo considerable change when a DG unit is connected at a point (usually a bus) in the scenario. The DGs are connected to a scenario at a suitable bus as this conforms to the interconnection standards as presented by [10] and [11]. This does not, however, rule out the possibility of e.g. connection of a unit at a strategically viable point along a transmission line. The only reason connection to a line is not presented in the study, is because this results in placement permutations numbering into hundreds and is far beyond the scope of the study, but it can be accomplished by an artificial intelligent tool employing the measures presented earlier.

5.3 Scenario 1 Results

It seems logical to first comparatively present the bus- and line information for Scenario 1 (system structure given in Figure 3-1) with no DG units present, followed by the same calculated results for a certain selected DG placement permutation to demonstrate the influences/effects of DG (PBMR) connection to a system. Finally, a chronological presentation of the performance index for each placement permutation is presented and graphically illustrated with an accompanying graph plot to demonstrate the suggested use of the performance measures for optimization of the scenario, and ultimately, a suggested optimum solution is described and discussed.

Table 5-4.1 and Table 5-4.2 are summarized comparisons of the measured and calculated results for Scenario 1 with no PBMR connected. As can be seen from the resulting data, the scenario exhibits fairly good *voltage regulation* and as a consequence of the Swing Bus being the only power source, the series of lines is fully loaded for the length of it, subsequently causing relatively higher *line losses*. The impedance path for each non-linear load is resultantly higher and the propagated effects of the polluting loads are experienced in a greater degree. The large linear load connected at Bus 4 Load does, however, diminish the effects of the non-linear portion of the load connected at that bus. Unfortunately, it still leads to intensified *harmonic pollution* levels at Buses 3, 3 Load, 5 and 5 Load, which also have their own non-linear load portions to cope with.

The compensation equipment in the scenario (capacitor- and reactor banks) alleviate these negative effects to a degree, but this can only be described as an advantageous side-effect of minor filtering and ultimately the pollution reaches levels where the filtering effect of the compensating equipment is neglected. The *voltage regulation* of the system rapidly drops to unacceptable levels with the rise of non-sinusoidal power drawn associated with the addition of non-linear loads. *Line losses* also increase abruptly due to the related *harmonic active power* that accompanies the presence of non-sinusoidal waveforms. The scenario exhibits unacceptable voltage distortion levels at Buses 3, 3 Load, 5 and 5 Load.

Table 5-4.1: Summarized results for all the buses Scenario 1.

Bus name	Comparative bus data, line data and calculated cost function index values.								
Swing Bus	*Three-phase effective value analysis (voltage, current and Total Harmonic Distortion)*								
	V_e (pu)	V_{e1} (pu)	V_{eH} (pu)	I_e (pu)	I_{e1} (pu)	I_{eH} (pu)	$VTHD_e$ (%)	$ITHD_e$ (%)	S_{eN}/S_{e1}
	1.003310	1.003320	0.006123	3.807810	3.807770	0.005602	0.610230	0.147121	0.006277
	Three-phase power analysis (apparent-, active and reactive power)								
	$S_{3\Phi}$ (MVA)	$S_{3\Phi1}$ (MVA)	$S_{3\Phi N}$ (MVA)	$P_{3\Phi}$ (MW)	$P_{3\Phi1}$ (MW)	$P_{3\Phi H}$ (MW)	$Q_{3\Phi1}$ (Mvar)	PF	DPF
	576.6790	573.0631	3.615590	573.0620	573.0610	0.000399	-1.555550	0.993727	0.999996
Bus 1 Load	V_e (pu)	V_{e1} (pu)	V_{eH} (pu)	I_e (pu)	I_{e1} (pu)	I_{eH} (pu)	$VTHD_e$ (%)	$ITHD_e$ (%)	S_{eN}/S_{e1}
	0.947334	0.947341	0.005666	0.213749	0.213751	0.000865	0.598047	0.404551	0.007220
	$S_{3\Phi}$ (MVA)	$S_{3\Phi1}$ (MVA)	$S_{3\Phi N}$ (MVA)	$P_{3\Phi}$ (MW)	$P_{3\Phi1}$ (MW)	$P_{3\Phi H}$ (MW)	$Q_{3\Phi1}$ (Mvar)	PF	DPF
	30.5942	30.3738	0.220358	29.6160	29.6155	0.000489	6.744410	0.968029	0.975036
Bus 2	V_e (pu)	V_{e1} (pu)	V_{eH} (pu)	I_e (pu)	I_{e1} (pu)	I_{eH} (pu)	$VTHD_e$ (%)	$ITHD_e$ (%)	S_{eN}/S_{e1}
	0.998603	0.998609	0.005524	3.585920	3.585890	0.061115	0.553196	1.704310	0.017919
	$S_{3\Phi}$ (MVA)	$S_{3\Phi1}$ (MVA)	$S_{3\Phi N}$ (MVA)	$P_{3\Phi}$ (MW)	$P_{3\Phi1}$ (MW)	$P_{3\Phi H}$ (MW)	$Q_{3\Phi1}$ (Mvar)	PF	DPF
	547.0090	537.1362	9.872320	527.1720	527.1770	-0.004755	-102.955000	0.963737	0.981458
Bus 2 Load	V_e (pu)	V_{e1} (pu)	V_{eH} (pu)	I_e (pu)	I_{e1} (pu)	I_{eH} (pu)	$VTHD_e$ (%)	$ITHD_e$ (%)	S_{eN}/S_{e1}
	1.000710	1.000720	0.004763	0.030783	0.030783	0.000123	0.475948	0.399622	0.006215
	$S_{3\Phi}$ (MVA)	$S_{3\Phi1}$ (MVA)	$S_{3\Phi N}$ (MVA)	$P_{3\Phi}$ (MW)	$P_{3\Phi1}$ (MW)	$P_{3\Phi H}$ (MW)	$Q_{3\Phi1}$ (Mvar)	PF	DPF
	4.6632	4.6207	0.042457	4.5065	4.5064	0.000099	1.021470	0.966401	0.975259
Bus 3	V_e (pu)	V_{e1} (pu)	V_{eH} (pu)	I_e (pu)	I_{e1} (pu)	I_{eH} (pu)	$VTHD_e$ (%)	$ITHD_e$ (%)	S_{eN}/S_{e1}
	1.004330	1.004340	0.020518	3.454490	3.454460	0.033488	2.042940	0.969426	0.022614
	$S_{3\Phi}$ (MVA)	$S_{3\Phi1}$ (MVA)	$S_{3\Phi N}$ (MVA)	$P_{3\Phi}$ (MW)	$P_{3\Phi1}$ (MW)	$P_{3\Phi H}$ (MW)	$Q_{3\Phi1}$ (Mvar)	PF	DPF
	532.5080	520.4175	12.090000	501.6650	501.6740	-0.009591	-138.411000	0.942080	0.963984
Bus 3 Load	V_e (pu)	V_{e1} (pu)	V_{eH} (pu)	I_e (pu)	I_{e1} (pu)	I_{eH} (pu)	$VTHD_e$ (%)	$ITHD_e$ (%)	S_{eN}/S_{e1}
	1.009940	1.009950	0.040000	0.375432	0.375232	0.023605	3.960600	6.290730	0.074379
	$S_{3\Phi}$ (MVA)	$S_{3\Phi1}$ (MVA)	$S_{3\Phi N}$ (MVA)	$P_{3\Phi}$ (MW)	$P_{3\Phi1}$ (MW)	$P_{3\Phi H}$ (MW)	$Q_{3\Phi1}$ (Mvar)	PF	DPF
	62.0342	56.8393	5.194830	55.3431	55.4098	-0.066712	12.667500	0.892139	0.974850
Bus 4	V_e (pu)	V_{e1} (pu)	V_{eH} (pu)	I_e (pu)	I_{e1} (pu)	I_{eH} (pu)	$VTHD_e$ (%)	$ITHD_e$ (%)	S_{eN}/S_{e1}
	1.008580	1.008580	0.006170	2.952070	2.952000	0.102356	0.611706	3.467340	0.035210
	$S_{3\Phi}$ (MVA)	$S_{3\Phi1}$ (MVA)	$S_{3\Phi N}$ (MVA)	$P_{3\Phi}$ (MW)	$P_{3\Phi1}$ (MW)	$P_{3\Phi H}$ (MW)	$Q_{3\Phi1}$ (Mvar)	PF	DPF
	462.4820	446.6079	15.873600	433.5950	433.5560	0.038697	-107.181000	0.937540	0.970775
Bus 4 Load	V_e (pu)	V_{e1} (pu)	V_{eH} (pu)	I_e (pu)	I_{e1} (pu)	I_{eH} (pu)	$VTHD_e$ (%)	$ITHD_e$ (%)	S_{eN}/S_{e1}
	1.004520	1.004520	0.007635	1.855070	1.855090	0.039167	0.760025	2.111300	0.022440
	$S_{3\Phi}$ (MVA)	$S_{3\Phi1}$ (MVA)	$S_{3\Phi N}$ (MVA)	$P_{3\Phi}$ (MW)	$P_{3\Phi1}$ (MW)	$P_{3\Phi H}$ (MW)	$Q_{3\Phi1}$ (Mvar)	PF	DPF
	286.6510	279.5218	7.129540	272.5750	272.5320	0.043240	62.118800	0.950895	0.974994
Bus 5	V_e (pu)	V_{e1} (pu)	V_{eH} (pu)	I_e (pu)	I_{e1} (pu)	I_{eH} (pu)	$VTHD_e$ (%)	$ITHD_e$ (%)	S_{eN}/S_{e1}
	1.006310	1.006310	0.051800	1.040590	1.040560	0.076350	5.147500	7.337380	0.089709
	$S_{3\Phi}$ (MVA)	$S_{3\Phi1}$ (MVA)	$S_{3\Phi N}$ (MVA)	$P_{3\Phi}$ (MW)	$P_{3\Phi1}$ (MW)	$P_{3\Phi H}$ (MW)	$Q_{3\Phi1}$ (Mvar)	PF	DPF
	171.2910	157.0721	14.219300	156.9940	157.0390	-0.044468	3.226380	0.916534	0.999789
Bus 5 Load	V_e (pu)	V_{e1} (pu)	V_{eH} (pu)	I_e (pu)	I_{e1} (pu)	I_{eH} (pu)	$VTHD_e$ (%)	$ITHD_e$ (%)	S_{eN}/S_{e1}
	0.997355	0.997357	0.056499	1.074420	1.074520	0.043192	5.664860	4.019670	0.069498
	$S_{3\Phi}$ (MVA)	$S_{3\Phi1}$ (MVA)	$S_{3\Phi N}$ (MVA)	$P_{3\Phi}$ (MW)	$P_{3\Phi1}$ (MW)	$P_{3\Phi H}$ (MW)	$Q_{3\Phi1}$ (Mvar)	PF	DPF
	172.0840	160.7546	11.329700	155.8460	155.8960	-0.050096	39.223600	0.905637	0.969776

Table 5-4.2: Summarized results for all the lines of Scenario 1 and performance index.

Line 1	*Calculated from the measured data obtained from the Simulink® model simulation.*						*Calculated three-phase power line loss.*		
	Sending-end rms voltage and current								
	Voltage (rms)			*Current (rms)*					
	$V_{s\,a}$ (pu)	$V_{s\,at}$ (pu)	$V_{s\,ah}$ (pu)	$I_{s\,a}$ (pu)	$I_{s\,at}$ (pu)	$I_{s\,ah}$ (pu)	$S_{line3\emptyset}$ (MVA)	$P_{line3\emptyset}$ (MW)	$N_{line3\emptyset}$
	1.003302	1.003320	0.006123	3.624005	3.623648	0.060777	49.35669	11.02230	48.11020
	Receiving-end rms voltage and current								
	Voltage (rms)			*Current (rms)*					
	$V_{r\,a}$ (pu)	$V_{r\,at}$ (pu)	$V_{r\,ah}$ (pu)	$I_{r\,a}$ (pu)	$I_{r\,at}$ (pu)	$I_{r\,ah}$ (pu)			
	0.998599	0.998612	0.005524	3.586301	3.585885	0.061115			
Line 2	$V_{s\,a}$ (pu)	$V_{s\,at}$ (pu)	$V_{s\,ah}$ (pu)	$I_{s\,a}$ (pu)	$I_{s\,at}$ (pu)	$I_{s\,ah}$ (pu)	$S_{line3\emptyset}$ (MVA)	$P_{line3\emptyset}$ (MW)	$N_{line3\emptyset}$
	0.998599	0.998612	0.005524	3.534941	3.534550	0.057833	71.05713	17.07570	68.97490
	$V_{r\,a}$ (pu)	$V_{r\,at}$ (pu)	$V_{r\,ah}$ (pu)	$I_{r\,a}$ (pu)	$I_{r\,at}$ (pu)	$I_{r\,ah}$ (pu)			
	1.004126	1.004335	0.020518	3.454610	3.454460	0.033488			
Line 3	$V_{s\,a}$ (pu)	$V_{s\,at}$ (pu)	$V_{s\,ah}$ (pu)	$I_{s\,a}$ (pu)	$I_{s\,at}$ (pu)	$I_{s\,ah}$ (pu)	$S_{line3\emptyset}$ (MVA)	$P_{line3\emptyset}$ (MW)	$N_{line3\emptyset}$
	1.004126	1.004335	0.020518	3.018583	3.017271	0.089117	41.47531	9.84955	40.28880
	$V_{r\,a}$ (pu)	$V_{r\,at}$ (pu)	$V_{r\,ah}$ (pu)	$I_{r\,a}$ (pu)	$I_{r\,at}$ (pu)	$I_{r\,ah}$ (pu)			
	1.008602	1.008583	0.006170	2.953756	2.952001	0.102356			
Line 4	$V_{s\,a}$ (pu)	$V_{s\,at}$ (pu)	$V_{s\,ah}$ (pu)	$I_{s\,a}$ (pu)	$I_{s\,at}$ (pu)	$I_{s\,ah}$ (pu)	$S_{line3\emptyset}$ (MVA)	$P_{line3\emptyset}$ (MW)	$N_{line3\emptyset}$
	1.008602	1.008583	0.006170	1.113126	1.112591	0.139994	8.45725	3.26474	7.80170
	$V_{r\,a}$ (pu)	$V_{r\,at}$ (pu)	$V_{r\,ah}$ (pu)	$I_{r\,a}$ (pu)	$I_{r\,at}$ (pu)	$I_{r\,ah}$ (pu)			
	1.007139	1.006307	0.051800	1.038387	1.040557	0.076350			
Performance	*Calculated index measures for the scenario.*								
	$Index_{performance}$	$Index_V$	$Index_{THD}$	$Index_{P\,loss}$					
	0.936598	0.017450	0.045952	1.1410E-07					

The same tabulated group of results is presented in Table 5-5.1 and Table 5-5.2 for placement of a DG unit at Bus 3 Load. It is immediately evident that voltage regulation is improved, harmonic pollution is reduced, and line losses are considerably less. This specific placement also happens to be the optimum placement solution for a DG unit delivering full capacity to the scenario. It goes without saying that performance levels can be improved significantly by applying basic control to these DG units connected to the system. The control of these units is beyond the scope of this study and the steady-state operation of the unit at some chosen level of generation (usually "fully on", i.e. all available active power capacity) is considered to be sufficient.

Table 5-5.1: Summarized bus results for Scenario 1 with DG connected to Bus 3 Load.

Bus name	Comparative bus data, line data and calculated cost function index values.								
Swing Bus	*Three-phase effective value analysis (voltage, current and Total Harmonic Distortion)*								
	V_e (pu)	V_{e1} (pu)	V_{eH} (pu)	I_e (pu)	I_{e1} (pu)	I_{eH} (pu)	$VTHD_e$ (%)	$ITHD_e$ (%)	S_{eN}/S_{e1}
	0.997610	0.997612	0.001824	2.018210	2.018220	0.001677	0.182789	0.083086	0.002008
	Three-phase power analysis (apparent, active and reactive power)								
	S_{3e} (MVA)	S_{3e1} (MVA)	S_{3eN} (MVA)	P_{3e} (MW)	P_{3e1} (MW)	P_{3eH} (MW)	Q_{3e1} (Mvar)	PF	DPF
	302.6400	302.0079	0.631561	300.1700	300.1690	0.000038	-33.276400	0.991837	0.993911
Bus 1 Load	V_e (pu)	V_{e1} (pu)	V_{eH} (pu)	I_e (pu)	I_{e1} (pu)	I_{eH} (pu)	$VTHD_e$ (%)	$ITHD_e$ (%)	S_{eN}/S_{e1}
	0.941950	0.941951	0.001687	0.212534	0.212535	0.000259	0.179147	0.121695	0.002166
	S_{3e} (MVA)	S_{3e1} (MVA)	S_{3eN} (MVA)	P_{3e} (MW)	P_{3e1} (MW)	P_{3eH} (MW)	Q_{3e1} (Mvar)	PF	DPF
	30.0971	30.0295	0.067600	29.2799	29.2798	0.000046	6.667950	0.972848	0.975036
Bus 2	V_e (pu)	V_{e1} (pu)	V_{eH} (pu)	I_e (pu)	I_{e1} (pu)	I_{eH} (pu)	$VTHD_e$ (%)	$ITHD_e$ (%)	S_{eN}/S_{e1}
	1.006870	1.006870	0.002608	1.834180	1.834190	0.017992	0.259012	0.980902	0.010145
	S_{3e} (MVA)	S_{3e1} (MVA)	S_{3eN} (MVA)	P_{3e} (MW)	P_{3e1} (MW)	P_{3eH} (MW)	Q_{3e1} (Mvar)	PF	DPF
	280.0790	277.0166	3.062510	264.9350	264.9360	-0.000506	-80.914100	0.945931	0.956390
Bus 2 Load	V_e (pu)	V_{e1} (pu)	V_{eH} (pu)	I_e (pu)	I_{e1} (pu)	I_{eH} (pu)	$VTHD_e$ (%)	$ITHD_e$ (%)	S_{eN}/S_{e1}
	1.009000	1.009000	0.004375	0.031038	0.031038	0.000058	0.433604	0.188368	0.004728
	S_{3e} (MVA)	S_{3e1} (MVA)	S_{3eN} (MVA)	P_{3e} (MW)	P_{3e1} (MW)	P_{3eH} (MW)	Q_{3e1} (Mvar)	PF	DPF
	4.7231	4.6976	0.025498	4.5814	4.5813	0.000023	1.038460	0.969999	0.975259
Bus 3	V_e (pu)	V_{e1} (pu)	V_{eH} (pu)	I_e (pu)	I_{e1} (pu)	I_{eH} (pu)	$VTHD_e$ (%)	$ITHD_e$ (%)	S_{eN}/S_{e1}
	1.007870	1.007870	0.006443	1.701270	1.701280	0.010358	0.639278	0.608811	0.008828
	S_{3e} (MVA)	S_{3e1} (MVA)	S_{3eN} (MVA)	P_{3e} (MW)	P_{3e1} (MW)	P_{3eH} (MW)	Q_{3e1} (Mvar)	PF	DPF
	259.6950	257.1986	2.496000	254.5050	254.5060	-0.001112	-37.118900	0.980016	0.989531
Bus 3 Load	V_e (pu)	V_{e1} (pu)	V_{eH} (pu)	I_e (pu)	I_{e1} (pu)	I_{eH} (pu)	$VTHD_e$ (%)	$ITHD_e$ (%)	S_{eN}/S_{e1}
	0.982128	0.982130	0.011197	1.482280	1.482270	0.017301	1.140060	1.167160	0.016316
	S_{3e} (MVA)	S_{3e1} (MVA)	S_{3eN} (MVA)	P_{3e} (MW)	P_{3e1} (MW)	P_{3eH} (MW)	Q_{3e1} (Mvar)	PF	DPF
	222.4630	218.3625	4.100600	-194.9270	-194.9450	0.017778	98.380100	-0.876223	-0.892759
Bus 4	V_e (pu)	V_{e1} (pu)	V_{eH} (pu)	I_e (pu)	I_{e1} (pu)	I_{eH} (pu)	$VTHD_e$ (%)	$ITHD_e$ (%)	S_{eN}/S_{e1}
	1.012030	1.012040	0.004481	2.960330	2.960380	0.030295	0.442790	1.023360	0.011151
	S_{3e} (MVA)	S_{3e1} (MVA)	S_{3eN} (MVA)	P_{3e} (MW)	P_{3e1} (MW)	P_{3eH} (MW)	Q_{3e1} (Mvar)	PF	DPF
	455.1620	449.3939	5.768020	436.3220	436.3420	-0.020708	-107.520000	0.958607	0.970957
Bus 4 Load	V_e (pu)	V_{e1} (pu)	V_{eH} (pu)	I_e (pu)	I_{e1} (pu)	I_{eH} (pu)	$VTHD_e$ (%)	$ITHD_e$ (%)	S_{eN}/S_{e1}
	1.007910	1.007910	0.007735	1.861120	1.861180	0.033215	0.767471	1.784600	0.019427
	S_{3e} (MVA)	S_{3e1} (MVA)	S_{3eN} (MVA)	P_{3e} (MW)	P_{3e1} (MW)	P_{3eH} (MW)	Q_{3e1} (Mvar)	PF	DPF
	287.6480	281.3791	6.268710	274.3420	274.3080	0.033810	62.684100	0.953742	0.974870
Bus 5	V_e (pu)	V_{e1} (pu)	V_{eH} (pu)	I_e (pu)	I_{e1} (pu)	I_{eH} (pu)	$VTHD_e$ (%)	$ITHD_e$ (%)	S_{eN}/S_{e1}
	1.009640	1.009630	0.039178	1.043720	1.043710	0.055601	3.880430	5.327230	0.065939
	S_{3e} (MVA)	S_{3e1} (MVA)	S_{3eN} (MVA)	P_{3e} (MW)	P_{3e1} (MW)	P_{3eH} (MW)	Q_{3e1} (Mvar)	PF	DPF
	168.6920	158.0653	10.627200	157.9490	158.0260	-0.076263	3.526670	0.936317	0.999751
Bus 5 Load	V_e (pu)	V_{e1} (pu)	V_{eH} (pu)	I_e (pu)	I_{e1} (pu)	I_{eH} (pu)	$VTHD_e$ (%)	$ITHD_e$ (%)	S_{eN}/S_{e1}
	1.000560	1.000560	0.042201	1.078310	1.078290	0.033786	4.217740	3.133290	0.052559
	S_{3e} (MVA)	S_{3e1} (MVA)	S_{3eN} (MVA)	P_{3e} (MW)	P_{3e1} (MW)	P_{3eH} (MW)	Q_{3e1} (Mvar)	PF	DPF
	170.8910	161.8348	9.056160	156.7960	156.8750	-0.079491	39.758600	0.917518	0.969353

Table 5-5.2: Summarized line results for Scenario 1 with DG connected to Bus 3 Load.

	Calculated from the measured data obtained from the Simulink® model simulation.						Calculated three-phase power line loss.		
	Sending-end rms voltage and current.								
	Voltage (rms)			Current (rms)					
Line 1	$V_{s\,a}$ (pu)	$V_{s\,a1}$ (pu)	$V_{s\,alt}$ (pu)	$I_{s\,a}$ (pu)	$I_{s\,a1}$ (pu)	$I_{s\,alt}$ (pu)	$S_{line3\emptyset}$ (MVA)	$P_{line3\emptyset}$ (MW)	$N_{line3\emptyset}$
	0.997612	0.997612	0.001824	1.910774	1.910824	0.018363	13.50159	3.37060	13.07410
	Receiving-end rms voltage and current								
	Voltage (rms)			Current (rms)					
	$V_{r\,a}$ (pu)	$V_{r\,a1}$ (pu)	$V_{r\,alt}$ (pu)	$I_{r\,a}$ (pu)	$I_{r\,a1}$ (pu)	$I_{r\,alt}$ (pu)			
	1.006875	1.006875	0.002608	1.834155	1.834187	0.017992			
	$V_{s\,a}$ (pu)	$V_{s\,a1}$ (pu)	$V_{s\,alt}$ (pu)	$I_{s\,a}$ (pu)	$I_{s\,a1}$ (pu)	$I_{s\,alt}$ (pu)	$S_{line3\emptyset}$ (MVA)	$P_{line3\emptyset}$ (MW)	$N_{line3\emptyset}$
Line 2	1.006875	1.006875	0.002608	1.775096	1.775120	0.017411	17.67723	5.12799	16.91710
	$V_{r\,a}$ (pu)	$V_{r\,a1}$ (pu)	$V_{r\,alt}$ (pu)	$I_{r\,a}$ (pu)	$I_{r\,a1}$ (pu)	$I_{r\,alt}$ (pu)			
	1.007865	1.007869	0.006443	1.701291	1.701285	0.010358			
	$V_{s\,a}$ (pu)	$V_{s\,a1}$ (pu)	$V_{s\,alt}$ (pu)	$I_{s\,a}$ (pu)	$I_{s\,a1}$ (pu)	$I_{s\,alt}$ (pu)	$S_{line3\emptyset}$ (MVA)	$P_{line3\emptyset}$ (MW)	$N_{line3\emptyset}$
Line 3	1.007865	1.007869	0.006443	3.025550	3.025683	0.028288	41.70306	9.90708	40.50920
	$V_{r\,a}$ (pu)	$V_{r\,a1}$ (pu)	$V_{r\,alt}$ (pu)	$I_{r\,a}$ (pu)	$I_{r\,a1}$ (pu)	$I_{r\,alt}$ (pu)			
	1.012027	1.012038	0.004481	2.960232	2.960376	0.030295			
	$V_{s\,a}$ (pu)	$V_{s\,a1}$ (pu)	$V_{s\,alt}$ (pu)	$I_{s\,a}$ (pu)	$I_{s\,a1}$ (pu)	$I_{s\,alt}$ (pu)	$S_{line3\emptyset}$ (MVA)	$P_{line3\emptyset}$ (MW)	$N_{line3\emptyset}$
Line 4	1.012027	1.012038	0.004481	1.111154	1.115292	0.104032	8.49727	3.28145	7.83809
	$V_{r\,a}$ (pu)	$V_{r\,a1}$ (pu)	$V_{r\,alt}$ (pu)	$I_{r\,a}$ (pu)	$I_{r\,a1}$ (pu)	$I_{r\,alt}$ (pu)			
	1.010389	1.009635	0.039178	1.042494	1.043709	0.055601			
	Calculated index measures for the scenario.								
Performance	$Index_{performance}$	$Index_V$	$Index_{THD}$	$Index_{P\,loss}$					
	0.951098	0.020458	0.028443	6.0534E-08					

Another effect is the improvement of the overall power factor for the scenario. It's apparent by now that where non-sinusoidal waveforms are present, power factor correction becomes complicated practice. The additional equipment employed to improve the power factor lead to other serious undesired side-effects, such as lowering of the system resonant frequency and eventually resonance manifests and causes major concern. The harmonic components present could be within this resonant range, causing resonance associated problems usually ending with equipment failure. By adding generators (DG) instead of traditional power factor correcting equipment (capacitor- and reactor banks), the consequence of the lowered resonant frequency is eliminated.

The following discussion is an attempt to motivate and identify the effects of DG placement in a scenario at different points in the system. In Table 5-6 the calculated performance indices (*performance-*, *voltage regulation-*, *harmonic distortion-* and *line loss indicator*) are presented in a chronological manner for a DG unit placement for the succession of buses in Scenario 1. It also illustrates an optimum solution using two units placed as shown in Figure 5-2 where the two nuclear symbols represent the DG units. Figure 5-1 is a chronological plot of calculated performance indices for a sequential placement of DG units.

Table 5-6: Calculated performance indices for all possible DG placement permutations.

Performance index as calculated for every placement permutation				
Placement at Bus #	*Calculated index measures for the scenario*			
	$Index_{performance}$	$Index_{V}$	$Index_{THD}$	$Index_{P\ loss}$
No PBMR	0.936598	0.017450	0.045952	1.1410E-07
Swing Bus	0.936558	0.018920	0.044522	1.1616E-07
Bus 1 Load	0.941606	0.013144	0.045249	1.1506E-07
Bus 2	0.938238	0.015297	0.046465	1.0110E-07
Bus 2 Load	0.933718	0.019080	0.047201	1.0378E-07
Bus 3	0.938804	0.020138	0.041058	5.9948E-08
Bus 3 Load	0.951098	0.020458	0.028443	6.0534E-08
Bus 4	0.924905	0.021490	0.053605	3.0851E-08
Bus 4 Load	0.914399	0.028058	0.057542	2.9878E-08
Bus 5	0.909310	0.028354	0.062336	3.5330E-08
Bus 5 Load	0.895162	0.044867	0.059972	4.0799E-08
Solution	0.953205	0.027517	0.019277	2.5509E-08

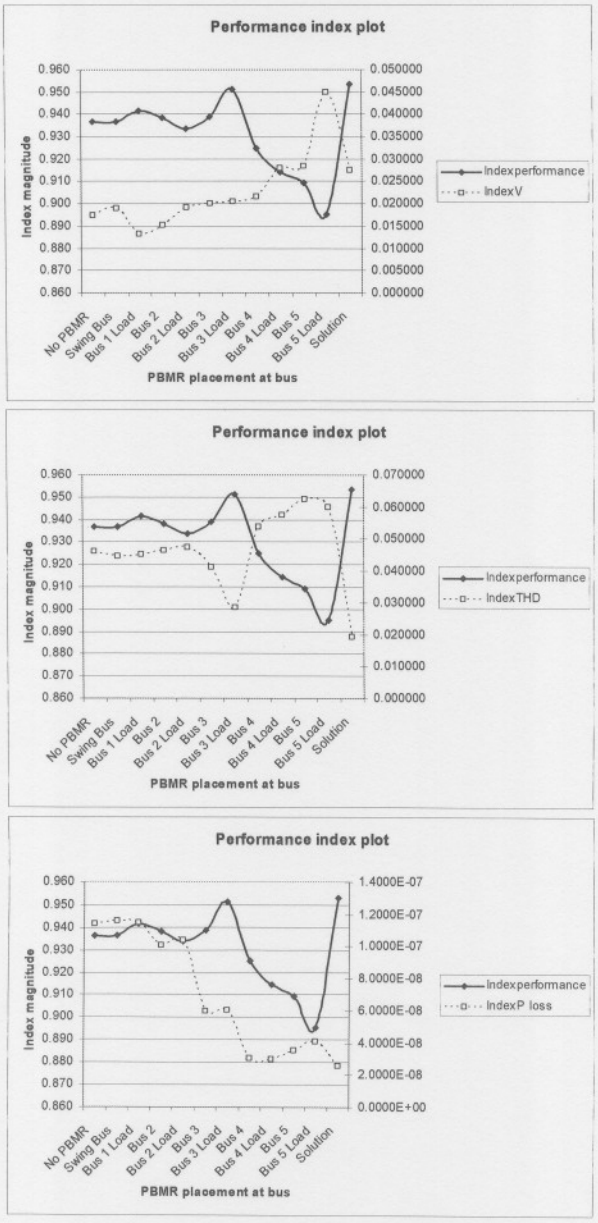


Figure 5-1: Performance index plot for placement of a DG unit at the labelled bus.

Bus 3 Load clearly delivers the best overall scenario performance when a DG unit is connected to it (for the case of single unit placement). Voltage regulation is improved; harmonic distortion levels are at their lowest and line losses drop suitably (see Figure 5-1). Unacceptable voltage distortion levels remain at Bus 5 and 5 Load and do not meet the NRS 048 requirements (section 2.3.2.3). The line compensating equipment require adjustment to operate satisfactorily for the "new" system, but the discussion of this adjustment process is ignored because the study is based on steady-state analysis and real power systems use static-var systems to adjust the regulation automatically.

Considering that the aim of the optimization process should be that all buses in the scenario meet the requirements set by NRS 048, placement of a single DG unit at Bus 3 Load cannot be the optimum solution. In fact, adding a unit at Bus 5 Load should reduce the harmonic distortion levels and ensure compliance to the NRS 048 standard. This is presented as a suggested optimum solution for Scenario 1. The two nuclear symbols in Figure 5-2 represent the DG units for optimum placement and improvement of Scenario 1 (Figure 3-1). This solution ensures that all buses meet the NRS 048 standard requirements and as can be seen from Table 5-6 and Figure 5-1 it achieves the best performance indices. The performance index is the highest for this solution; the other indicators (*voltage regulation-*, *harmonic distortion-* and *line loss-*) are at their lowest.

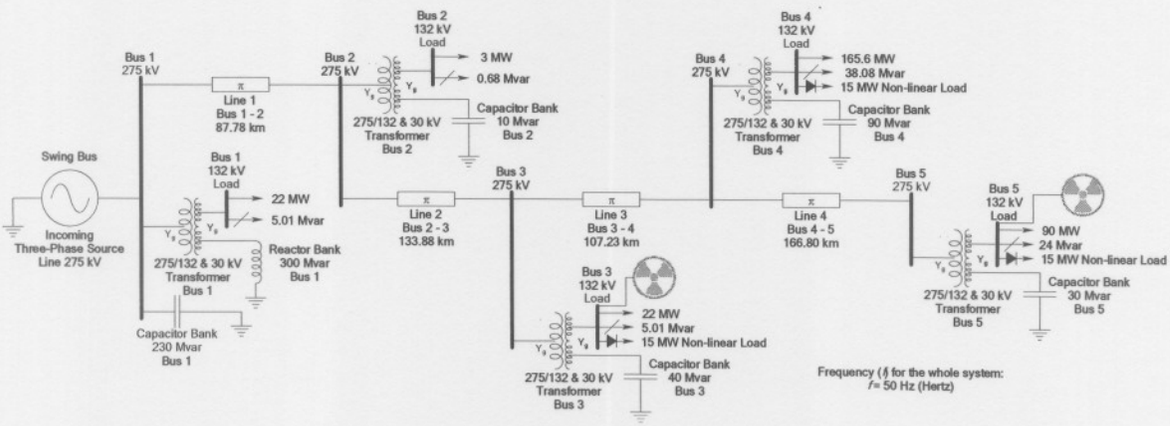


Figure 5-2: Suggested placement of the DG units resulting in an optimum solution.

In general, the effects experienced by a scenario with the addition of DG (PBMRs), is summarized as follows:

Some placements (connection points) of the units delivered better performance than others (Bus 3 Load connection) because the impedance paths leading to the connected sources act as passive filters with elements comprised of the system's characteristic equipment. System performance for Scenario 1, generally improves in all three aspects (all three indicators show a downward trend) as the DG is connected towards the end of the line. This is a consequence of the rated demand at the end-point of the line; the majority of large loads with non-linear components connect at the mid- to end-sections of the line.

Another reason is that the source impedance of the non-linear loads is greatly reduced with the addition of the DG unit and the non-sinusoidal waveforms act upon much less of an impedance and cannot result in augmented harmonic distortion influences. The DG unit isolates the non-linear load's non-sinusoidal waveforms and these waveforms are prevented from spreading through the rest of the transmission network. Connection of additional DGs culminates in a mutually contributed effect of the reasons/motivations discussed here.

Bearing in mind that a PBMR has a price tag in the region of a billion Rand, and that construction of new transmission lines can cost as much as 5 billion rand (depending on the power rating of the line), it has to be considered which of the two available options the system analyzer should use. The fact remains that generating equipment continue to offer many more advantages than additional power transmission lines and therefore generating should enjoy priority if price is not an issue. This is the argument for an economical approach mentioned in section 2.4 with the discussion of planning considerations.

A purely cost-based analysis of the improvement of the scenario reveals that with no PBMR present the performance indicator was 0.936598. The best placement solution (connection at Bus 3 Load) lifted the performance to 0.951098. This was an investment of 1 billion rand to bring about an improvement margin of 0.0145, or stated otherwise, 1 billion rand per 0.0145 improvement margin. This is the economical implications of improving a scenario. For the suggested optimum solution the cost-improvement ratio is much less (2 billion per 0.016607, or 1 billion per 0.0083053) than the best placement solution, but given that for this solution all the buses adhere to the NRS 048 standard requirements it is then certainly a necessary investment if the standard is to be respected as the governing body.

5.4 Scenario 2 Results

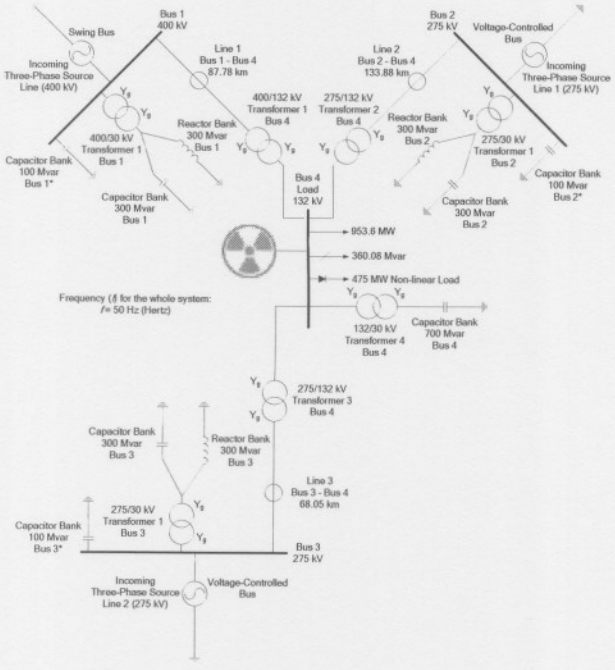


Figure 5-3: DG placement solution for Scenario 2.

The results of Scenario 2 were already presented in section 5.2 and will not be repeated. The suggested DG placement is briefly illustrated, the associated effects demonstrated and the solution is concisely discussed. Figure 5-3 illustrates the optimum placement solution for Scenario 2. The structure of Scenario 2 is such that placement of generating equipment at other buses in the system (Swing Bus and Buses 2 and 3) would only add capacity at those buses but provide very little room for the already mentioned harmonic reducing effects to exercise maximum influence – impedance paths are minimally influenced, filtering is attenuated and the polluting harmonic components aren't isolated.

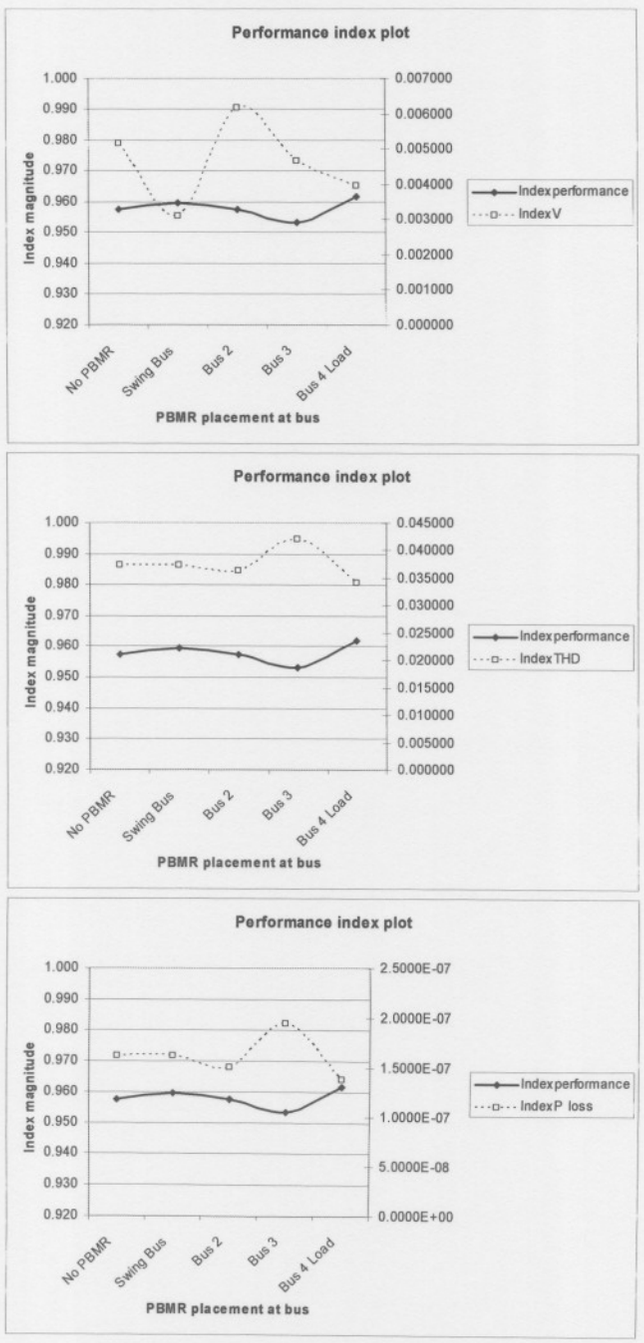


Figure 5-4: Performance index plot for Scenario 2.

Since placement is of concern, the technical detail of Scenario 2 is of lesser concern, but the reader is referred to Figure 3-2 if the system specifications are of interest and cannot be obtained from Figure 5-3. The consequence of the different DG placement options available is graphically illustrated by Figure 5-4 and given by Table 5-7.

Table 5-7: Calculated performance indices for different DG placements in Scenario 2.

Performance Index as calculated for every placement permutation				
Placement at Bus #	Calculated index parameters for the scenario			
	$Index_{performance}$	$Index_V$	$Index_{THD}$	$Index_{P\ loss}$
No PBMR	0.957429	0.005150	0.037421	1.6145E-07
Swing Bus	0.959613	0.003093	0.037294	1.6230E-07
Bus 2	0.957415	0.006177	0.036408	1.4948E-07
Bus 3	0.953309	0.004658	0.042033	1.9436E-07
Bus 4 Load	0.961751	0.003965	0.034284	1.3752E-07

Due to the sheer magnitudes of the power flow values present in Scenario 2, the effect of a mere 150 MW generating capacity DG unit is dwarfed in comparison, but it is noticed in the improved performance of the scenario for each of the placements. It is recommended that either the generating capacity of the modular unit be increased, or that more units are connected to Bus 4 Load to bring about the eventual desired improvement margins for Scenario 2. The completely solved situation for Scenario 2 is not discussed; the final solution would involve continued connection of generating units at Bus 4 Load until the voltage distortion limits of NRS 048 are satisfied and the performance margins become cost-effective. There exists a universal direct proportional relationship between the three indicators – if any one of them increase a rise of roughly the same degree in the others are observed for most cases.

In this scenario, improvement of the waveforms in the system is based purely on the isolation principle described in the discussion of Scenario 1's results. The non-sinusoidal waveforms are prevented (or retarded) from flowing back through the entire network to the sources and thus have a reduced effect. Voltage regulation by means of line compensating equipment remains a practice that should be altered once generation is added to the system, but given that most utilities usually employ static-var systems this is done automatically in reality.

The tabulated results for connection of a single DG unit at Bus 4 Load are given in Table 5-8 for thoroughness' sake. Shortly, the power factor deteriorates overall for the scenario, but this is due to the immense ratings of the line compensating equipment present in the system. Since less active power flows through the lines when it is locally generated at the load requiring it, the reactive powers in the transmission network stored or delivered by the compensating equipment accordingly alters the power factor of the bus it is connected to. Line losses are considerably less and this promotes the attenuation effect of the system on harmonic components. Stability of so many generators could be a problem but stability is a far beyond the scope of this study.

Filtering techniques could be applied to filter harmonics out of the system's waveforms and active- and passive filtering techniques are two proven and reliable options when filtering is considered. These options are exceptionally expensive and are only employed by the most sensitive of clients who require very high power quality standards. Filtering is rarely applied due to the enormous cost thereof.

Table 5-8: Results for Scenario 2 with a DG unit connected to Bus 4 Load.

Bus name	Comparative bus data, line data and calculated cost function index values.								
Swing Bus	Three-phase effective value analysis (voltage, current and Total Harmonic Distortion)								
	V_s (pu)	V_{s1} (pu)	V_{sH} (pu)	I_s (pu)	I_{s1} (pu)	I_{sH} (pu)	$VTHD_s$ (%)	$ITHD_s$ (%)	S_{sN} / S_{s1}
	1.004930	1.004910	0.030624	3.774380	3.774290	0.024258	3.047470	0.642724	0.031146
	Three-phase power analysis (apparent-, active and reactive power)								
	$S_{3\phi}$ (MVA)	$S_{3\phi1}$ (MVA)	$S_{3\phi N}$ (MVA)	$P_{3\phi}$ (MW)	$P_{3\phi1}$ (MW)	$P_{3\phi H}$ (MW)	$Q_{3\phi1}$ (Mvar)	PF	DPF
	591.5890	568.9114	22.677100	525.5720	525.5550	0.016389	-217.835000	0.888407	0.923791
Bus 2 Voltage-controlled	V_s (pu)	V_{s1} (pu)	V_{sH} (pu)	I_s (pu)	I_{s1} (pu)	I_{sH} (pu)	$VTHD_s$ (%)	$ITHD_s$ (%)	S_{sN} / S_{s1}
	1.002590	1.002530	0.018693	4.084980	4.084860	0.013801	1.864610	0.337853	0.018950
	$S_{3\phi}$ (MVA)	$S_{3\phi1}$ (MVA)	$S_{3\phi N}$ (MVA)	$P_{3\phi}$ (MW)	$P_{3\phi1}$ (MW)	$P_{3\phi H}$ (MW)	$Q_{3\phi1}$ (Mvar)	PF	DPF
	626.4510	614.3312	12.119300	592.8550	592.8520	0.003034	-161.026000	0.946372	0.965037
Bus 3 Voltage-controlled	V_s (pu)	V_{s1} (pu)	V_{sH} (pu)	I_s (pu)	I_{s1} (pu)	I_{sH} (pu)	$VTHD_s$ (%)	$ITHD_s$ (%)	S_{sN} / S_{s1}
	1.005090	1.005050	0.019431	4.108840	4.108700	0.013005	1.933370	0.316511	0.019591
	$S_{3\phi}$ (MVA)	$S_{3\phi1}$ (MVA)	$S_{3\phi N}$ (MVA)	$P_{3\phi}$ (MW)	$P_{3\phi1}$ (MW)	$P_{3\phi H}$ (MW)	$Q_{3\phi1}$ (Mvar)	PF	DPF
	636.7720	619.3987	17.373600	599.6880	599.6810	0.006999	-155.040000	0.941762	0.968166
Bus 4 Load	V_s (pu)	V_{s1} (pu)	V_{sH} (pu)	I_s (pu)	I_{s1} (pu)	I_{sH} (pu)	$VTHD_s$ (%)	$ITHD_s$ (%)	S_{sN} / S_{s1}
	1.002630	1.002620	0.032500	12.439000	12.436800	0.547195	3.241550	4.399810	0.054668
	$S_{3\phi}$ (MVA)	$S_{3\phi1}$ (MVA)	$S_{3\phi N}$ (MVA)	$P_{3\phi}$ (MW)	$P_{3\phi1}$ (MW)	$P_{3\phi H}$ (MW)	$Q_{3\phi1}$ (Mvar)	PF	DPF
	1988.3000	1870.3808	117.915000	1652.0900	1652.1200	-0.031595	876.826000	0.830907	0.883307
Line 1	Calculated from the measured data obtained from the Simulink® model simulation.						Calculated three-phase power line loss.		
	Sending-end rms voltage and current								
	Voltage (rms)			Current (rms)					
	$V_{s\phi}$ (pu)	$V_{s\phi1}$ (pu)	$V_{s\phiH}$ (pu)	$I_{s\phi}$ (pu)	$I_{s\phi1}$ (pu)	$I_{s\phiH}$ (pu)	$S_{line3\phi}$ (MVA)	$P_{line3\phi}$ (MW)	$N_{line3\phi}$
	1.004630	1.004913	0.030624	3.508418	3.507389	0.097338	21.86873	5.74251	21.10130
	Receiving-end rms voltage and current								
	Voltage (rms)			Current (rms)					
	$V_{r\phi}$ (pu)	$V_{r\phi1}$ (pu)	$V_{r\phiH}$ (pu)	$I_{r\phi}$ (pu)	$I_{r\phi1}$ (pu)	$I_{r\phiH}$ (pu)			
	0.997797	0.998336	0.033072	3.463252	3.463546	0.137762			
Line 2	$V_{s\phi}$ (pu)	$V_{s\phi1}$ (pu)	$V_{s\phiH}$ (pu)	$I_{s\phi}$ (pu)	$I_{s\phi1}$ (pu)	$I_{s\phiH}$ (pu)	$S_{line3\phi}$ (MVA)	$P_{line3\phi}$ (MW)	$N_{line3\phi}$
	1.002374	1.002530	0.018693	3.935220	3.934746	0.063299	88.73211	20.92430	86.22970
	$V_{r\phi}$ (pu)	$V_{r\phi1}$ (pu)	$V_{r\phiH}$ (pu)	$I_{r\phi}$ (pu)	$I_{r\phi1}$ (pu)	$I_{r\phiH}$ (pu)			
	0.978024	0.978695	0.036877	3.904202	3.903866	0.051132			
Line 3	$V_{s\phi}$ (pu)	$V_{s\phi1}$ (pu)	$V_{s\phiH}$ (pu)	$I_{s\phi}$ (pu)	$I_{s\phi1}$ (pu)	$I_{s\phiH}$ (pu)	$S_{line3\phi}$ (MVA)	$P_{line3\phi}$ (MW)	$N_{line3\phi}$
	1.004995	1.005054	0.019431	3.970246	3.969892	0.058615	46.35997	9.82738	45.30640
	$V_{r\phi}$ (pu)	$V_{r\phi1}$ (pu)	$V_{r\phiH}$ (pu)	$I_{r\phi}$ (pu)	$I_{r\phi1}$ (pu)	$I_{r\phiH}$ (pu)			
	0.987528	0.987798	0.023278	3.962141	3.962150	0.056770			
Performance	Calculated index measures for the scenario								
	$Index_{performance}$	$Index_V$	$Index_{THD}$	$Index_{P\,loss}$					
	0.961751	0.003965	0.034284	1.3752E-07					

5.5 Scenario 3 Results

This is the largest scenario investigated during the study. Due to steady-state analysis the compensation equipment present in the system was once again assumed to be active and was simulated as such. The compensation was not adjusted with the addition of PBMRs and therefore the voltage regulation differs moderately between placement permutations.

No placement permutations were investigated as the system is so large and intuitive placement of DGs was decided in and attempt to resolve the experienced power quality (PQ) problems in the system. This is also an attempt to demonstrate how the system should be assessed and the how performance measures can be applied to assist in determining a predicted optimum solution for the system.

The initial scenario has the following characteristics, to mention a prominent few. The summarized data results in Table 5-9 (parts 1-5) is given to assist the discussion. The voltage regulation is relatively good and as a consequence of the generous use of parallel transmission lines ensures voltage regulation remains at acceptable levels under widely varied load conditions. The parallel lines unfortunately make it difficult to accurately predict where the worst PQ conditions exist. However, these parallel lines contribute greatly to maintaining line losses at a minimum throughout the system.

The loads also differ greatly in size and the largest linear load (Bus 2575 Harvard 1) is rated at ±265 MW and ±70 Mvar. The smallest linear loads are 1 MW and 0.5 Mvar and therefore experience the worst effects associated with distorted waveforms. The non-linear loads are kept uniform for the study – this was already motivated and discussed in section 3.2.

The power factors calculated for the system varies considerably from bus to bus and this is attributed to the wide variety of loads connected to a bus – either solely compensating equipment or prevailing non-linear loads.

Table 5-9.1: Summarized bus data results for the initial condition of Scenario 3.

Bus name	Comparative bus data, line data and calculated cost function index values.								
Swing Bus	Three-phase effective value analysis (voltage, current and Total Harmonic Distortion)								
	V_e (pu)	V_{e1} (pu)	V_{eH} (pu)	I_e (pu)	I_{e1} (pu)	I_{eH} (pu)	$VTHD_e$ (%)	$ITHD_e$ (%)	S_{eN}/S_{e1}
	0.984718	0.984712	0.004390	3.511530	3.511540	0.000651	0.445841	0.018526	0.004462
	Three-phase power analysis (apparent, active and reactive power)								
	$S_{3\Phi}$ (MVA)	$S_{3\Phi 1}$ (MVA)	$S_{3\Phi N}$ (MVA)	$P_{3\Phi}$ (MW)	$P_{3\Phi 1}$ (MW)	$P_{3\Phi H}$ (MW)	$Q_{3\Phi 1}$ (Mvar)	PF	DPF
	521.7120	518.6780	3.033480	378.3370	378.3370	0.000047	-354.807000	0.725184	0.729425
Bus 1350 Voltage-controlled	V_e (pu)	V_{e1} (pu)	V_{eH} (pu)	I_e (pu)	I_{e1} (pu)	I_{eH} (pu)	$VTHD_e$ (%)	$ITHD_e$ (%)	S_{eN}/S_{e1}
	1.004840	1.004840	0.003368	2.331200	2.331210	0.000462	0.335158	0.019837	0.003357
	$S_{3\Phi}$ (MVA)	$S_{3\Phi 1}$ (MVA)	$S_{3\Phi N}$ (MVA)	$P_{3\Phi}$ (MW)	$P_{3\Phi 1}$ (MW)	$P_{3\Phi H}$ (MW)	$Q_{3\Phi 1}$ (Mvar)	PF	DPF
	352.9490	351.3727	1.576660	231.0990	231.0990	0.000056	-264.681000	0.654766	0.657704
Bus 2390	V_e (pu)	V_{e1} (pu)	V_{eH} (pu)	I_e (pu)	I_{e1} (pu)	I_{eH} (pu)	$VTHD_e$ (%)	$ITHD_e$ (%)	S_{eN}/S_{e1}
	1.028370	1.028370	0.004677	1.480930	1.480880	0.030822	0.454843	2.081300	0.021305
	$S_{3\Phi}$ (MVA)	$S_{3\Phi 1}$ (MVA)	$S_{3\Phi N}$ (MVA)	$P_{3\Phi}$ (MW)	$P_{3\Phi 1}$ (MW)	$P_{3\Phi H}$ (MW)	$Q_{3\Phi 1}$ (Mvar)	PF	DPF
	234.2870	228.4360	5.850980	-0.0005	-0.0005	0.000003	-228.436000	-0.000002	-0.000002

Table 5-9.2: Summarized bus data results for the initial condition of Scenario 3, continued.

Bus 1163	V_e (pu)	V_{e1} (pu)	V_{eH} (pu)	I_e (pu)	I_{e1} (pu)	I_{eH} (pu)	$VTHD_e$ (%)	$ITHD_e$ (%)	S_{eN}/S_{e1}
	0.997424	0.997415	0.008403	4.124990	4.124960	0.088567	0.842475	2.147100	0.023065
	$S_{3\Phi}$ (MVA)	$S_{3\Phi1}$ (MVA)	$S_{3\Phi N}$ (MVA)	$P_{3\Phi}$ (MW)	$P_{3\Phi1}$ (MW)	$P_{3\Phi H}$ (MW)	$Q_{3\Phi1}$ (Mvar)	PF	DPF
	632.0490	617.1515	14.897100	594.2860	594.2890	-0.003107	-166.423000	0.940253	0.962955
Bus 1314	V_e (pu)	V_{e1} (pu)	V_{eH} (pu)	I_e (pu)	I_{e1} (pu)	I_{eH} (pu)	$VTHD_e$ (%)	$ITHD_e$ (%)	S_{eN}/S_{e1}
	1.102100	1.102100	0.002957	2.204250	2.204240	0.029471	0.268266	1.337010	0.013637
	$S_{3\Phi}$ (MVA)	$S_{3\Phi1}$ (MVA)	$S_{3\Phi N}$ (MVA)	$P_{3\Phi}$ (MW)	$P_{3\Phi1}$ (MW)	$P_{3\Phi H}$ (MW)	$Q_{3\Phi1}$ (Mvar)	PF	DPF
	369.4460	364.3960	5.049630	0.0000	0.0000	0.000000	-364.396000	0.000000	0.000000
Bus 1317	V_e (pu)	V_{e1} (pu)	V_{eH} (pu)	I_e (pu)	I_{e1} (pu)	I_{eH} (pu)	$VTHD_e$ (%)	$ITHD_e$ (%)	S_{eN}/S_{e1}
	1.102100	1.102100	0.002957	2.204250	2.204240	0.029471	0.268266	1.337010	0.013637
	$S_{3\Phi}$ (MVA)	$S_{3\Phi1}$ (MVA)	$S_{3\Phi N}$ (MVA)	$P_{3\Phi}$ (MW)	$P_{3\Phi1}$ (MW)	$P_{3\Phi H}$ (MW)	$Q_{3\Phi1}$ (Mvar)	PF	DPF
	369.4460	364.3960	5.049630	0.0000	0.0000	0.000000	-364.396000	0.000000	0.000000
Bus 1360	V_e (pu)	V_{e1} (pu)	V_{eH} (pu)	I_e (pu)	I_{e1} (pu)	I_{eH} (pu)	$VTHD_e$ (%)	$ITHD_e$ (%)	S_{eN}/S_{e1}
	0.985410	0.985405	0.008678	2.718790	2.718830	0.020602	0.880648	0.757768	0.011618
	$S_{3\Phi}$ (MVA)	$S_{3\Phi1}$ (MVA)	$S_{3\Phi N}$ (MVA)	$P_{3\Phi}$ (MW)	$P_{3\Phi1}$ (MW)	$P_{3\Phi H}$ (MW)	$Q_{3\Phi1}$ (Mvar)	PF	DPF
	407.0380	401.8769	5.161630	399.8150	399.8080	0.007044	40.726400	0.982253	0.994852
Bus 1365	V_e (pu)	V_{e1} (pu)	V_{eH} (pu)	I_e (pu)	I_{e1} (pu)	I_{eH} (pu)	$VTHD_e$ (%)	$ITHD_e$ (%)	S_{eN}/S_{e1}
	1.017200	1.017180	0.019756	1.482090	1.482130	0.088491	1.942240	5.970510	0.062796
	$S_{3\Phi}$ (MVA)	$S_{3\Phi1}$ (MVA)	$S_{3\Phi N}$ (MVA)	$P_{3\Phi}$ (MW)	$P_{3\Phi1}$ (MW)	$P_{3\Phi H}$ (MW)	$Q_{3\Phi1}$ (Mvar)	PF	DPF
	240.8820	226.1410	14.741400	163.7130	163.7490	-0.035238	-155.968000	0.679641	0.724100
Bus 2575	V_e (pu)	V_{e1} (pu)	V_{eH} (pu)	I_e (pu)	I_{e1} (pu)	I_{eH} (pu)	$VTHD_e$ (%)	$ITHD_e$ (%)	S_{eN}/S_{e1}
	0.973420	0.973415	0.004980	2.775260	2.775250	0.039880	0.511622	1.436980	0.015254
	$S_{3\Phi}$ (MVA)	$S_{3\Phi1}$ (MVA)	$S_{3\Phi N}$ (MVA)	$P_{3\Phi}$ (MW)	$P_{3\Phi1}$ (MW)	$P_{3\Phi H}$ (MW)	$Q_{3\Phi1}$ (Mvar)	PF	DPF
	412.1580	405.2247	6.933960	395.2310	395.2270	0.004661	89.457500	0.958931	0.975328
Bus 1363	V_e (pu)	V_{e1} (pu)	V_{eH} (pu)	I_e (pu)	I_{e1} (pu)	I_{eH} (pu)	$VTHD_e$ (%)	$ITHD_e$ (%)	S_{eN}/S_{e1}
	1.000560	1.000510	0.010400	0.175454	0.174438	0.016985	1.039450	9.736820	0.097927
	$S_{3\Phi}$ (MVA)	$S_{3\Phi1}$ (MVA)	$S_{3\Phi N}$ (MVA)	$P_{3\Phi}$ (MW)	$P_{3\Phi1}$ (MW)	$P_{3\Phi H}$ (MW)	$Q_{3\Phi1}$ (Mvar)	PF	DPF
	30.7144	26.1792	4.535210	1.0952	1.0947	0.000511	-26.156300	0.035659	0.041817
Bus 1270	V_e (pu)	V_{e1} (pu)	V_{eH} (pu)	I_e (pu)	I_{e1} (pu)	I_{eH} (pu)	$VTHD_e$ (%)	$ITHD_e$ (%)	S_{eN}/S_{e1}
	1.015810	1.015810	0.014107	0.161218	0.161114	0.035755	1.388760	22.192700	0.222382
	$S_{3\Phi}$ (MVA)	$S_{3\Phi1}$ (MVA)	$S_{3\Phi N}$ (MVA)	$P_{3\Phi}$ (MW)	$P_{3\Phi1}$ (MW)	$P_{3\Phi H}$ (MW)	$Q_{3\Phi1}$ (Mvar)	PF	DPF
	30.4834	24.5538	5.929630	24.0422	24.0227	0.019459	5.079150	0.788697	0.978371
Bus 1204	V_e (pu)	V_{e1} (pu)	V_{eH} (pu)	I_e (pu)	I_{e1} (pu)	I_{eH} (pu)	$VTHD_e$ (%)	$ITHD_e$ (%)	S_{eN}/S_{e1}
	1.032270	1.032240	0.032113	0.948688	0.948692	0.026687	3.111030	2.813040	0.041952
	$S_{3\Phi}$ (MVA)	$S_{3\Phi1}$ (MVA)	$S_{3\Phi N}$ (MVA)	$P_{3\Phi}$ (MW)	$P_{3\Phi1}$ (MW)	$P_{3\Phi H}$ (MW)	$Q_{3\Phi1}$ (Mvar)	PF	DPF
	154.3130	146.8939	7.419130	137.0490	137.1110	-0.061999	-52.710500	0.888123	0.933401
Bus 1299	V_e (pu)	V_{e1} (pu)	V_{eH} (pu)	I_e (pu)	I_{e1} (pu)	I_{eH} (pu)	$VTHD_e$ (%)	$ITHD_e$ (%)	S_{eN}/S_{e1}
	1.008430	1.008410	0.018542	0.182392	0.181519	0.016862	1.838730	9.289380	0.094712
	$S_{3\Phi}$ (MVA)	$S_{3\Phi1}$ (MVA)	$S_{3\Phi N}$ (MVA)	$P_{3\Phi}$ (MW)	$P_{3\Phi1}$ (MW)	$P_{3\Phi H}$ (MW)	$Q_{3\Phi1}$ (Mvar)	PF	DPF
	32.0345	27.4570	4.577420	-0.0001	-0.0001	-0.000003	-27.457000	-0.000002	-0.000002
Bus 2935	V_e (pu)	V_{e1} (pu)	V_{eH} (pu)	I_e (pu)	I_{e1} (pu)	I_{eH} (pu)	$VTHD_e$ (%)	$ITHD_e$ (%)	S_{eN}/S_{e1}
	1.030120	1.030110	0.022254	0.163385	0.163482	0.035155	2.160330	21.503700	0.216170
	$S_{3\Phi}$ (MVA)	$S_{3\Phi1}$ (MVA)	$S_{3\Phi N}$ (MVA)	$P_{3\Phi}$ (MW)	$P_{3\Phi1}$ (MW)	$P_{3\Phi H}$ (MW)	$Q_{3\Phi1}$ (Mvar)	PF	DPF
	31.3177	25.2624	6.055350	24.7743	24.7739	0.000450	4.943940	0.791064	0.980663
Bus 1375	V_e (pu)	V_{e1} (pu)	V_{eH} (pu)	I_e (pu)	I_{e1} (pu)	I_{eH} (pu)	$VTHD_e$ (%)	$ITHD_e$ (%)	S_{eN}/S_{e1}
	1.031510	1.031500	0.034229	0.737283	0.737586	0.033786	3.318360	4.580670	0.056584
	$S_{3\Phi}$ (MVA)	$S_{3\Phi1}$ (MVA)	$S_{3\Phi N}$ (MVA)	$P_{3\Phi}$ (MW)	$P_{3\Phi1}$ (MW)	$P_{3\Phi H}$ (MW)	$Q_{3\Phi1}$ (Mvar)	PF	DPF
	121.3410	114.1225	7.218650	110.9940	111.0580	-0.064109	26.269200	0.914726	0.973147

Table 5-9.3: Summarized bus data results for the initial condition of Scenario 3, continued.

Bus 2400	V_{ϕ} (pu)	$V_{\phi 1}$ (pu)	$V_{\phi H}$ (pu)	I_{ϕ} (pu)	$I_{\phi 1}$ (pu)	$I_{\phi H}$ (pu)	$VTHD_{\phi}$ (%)	$ITHD_{\phi}$ (%)	$S_{\phi N}$ / $S_{\phi 1}$
	1.030200	1.030180	0.028564	0.163378	0.163599	0.034929	2.772750	21.350300	0.215378
	$S_{3\phi}$ (MVA)	$S_{3\phi 1}$ (MVA)	$S_{3\phi N}$ (MVA)	$P_{3\phi}$ (MW)	$P_{3\phi 1}$ (MW)	$P_{3\phi H}$ (MW)	$Q_{3\phi 1}$ (Mvar)	PF	DPF
	31.3786	25.2734	6.105110	24.7960	24.8082	-0.012206	4.826780	0.790223	0.981594
Bus 1380	V_{ϕ} (pu)	$V_{\phi 1}$ (pu)	$V_{\phi H}$ (pu)	I_{ϕ} (pu)	$I_{\phi 1}$ (pu)	$I_{\phi H}$ (pu)	$VTHD_{\phi}$ (%)	$ITHD_{\phi}$ (%)	$S_{\phi N}$ / $S_{\phi 1}$
	1.009120	1.009150	0.036732	0.176004	0.176223	0.033034	3.639930	18.745600	0.191079
	$S_{3\phi}$ (MVA)	$S_{3\phi 1}$ (MVA)	$S_{3\phi N}$ (MVA)	$P_{3\phi}$ (MW)	$P_{3\phi 1}$ (MW)	$P_{3\phi H}$ (MW)	$Q_{3\phi 1}$ (Mvar)	PF	DPF
	32.3726	26.6775	5.695120	25.9057	25.9774	-0.071697	6.071690	0.800234	0.973756
Bus 2441	V_{ϕ} (pu)	$V_{\phi 1}$ (pu)	$V_{\phi H}$ (pu)	I_{ϕ} (pu)	$I_{\phi 1}$ (pu)	$I_{\phi H}$ (pu)	$VTHD_{\phi}$ (%)	$ITHD_{\phi}$ (%)	$S_{\phi N}$ / $S_{\phi 1}$
	1.004300	1.004290	0.018793	0.158483	0.158737	0.032929	1.871290	20.744600	0.208324
	$S_{3\phi}$ (MVA)	$S_{3\phi 1}$ (MVA)	$S_{3\phi N}$ (MVA)	$P_{3\phi}$ (MW)	$P_{3\phi 1}$ (MW)	$P_{3\phi H}$ (MW)	$Q_{3\phi 1}$ (Mvar)	PF	DPF
	29.4968	23.9149	5.581980	23.3725	23.4465	-0.073999	4.709810	0.792373	0.980415

Table 5-9.4: Summarized line data results for the initial condition of Scenario 3.

Line 1 Bus 1350 to 1163	*Calculated from the measured data obtained from the Simulink® model simulation.*						*Calculated three-phase power line loss.*		
	Sending-end rms voltage and current								
	Voltage (rms)			*Current (rms)*					
	$V_{s\phi}$ (pu)	$V_{s\phi 1}$ (pu)	$V_{s\phi H}$ (pu)	$I_{s\phi}$ (pu)	$I_{s\phi 1}$ (pu)	$I_{s\phi H}$ (pu)	$S_{line3\phi}$ (MVA)	$P_{line3\phi}$ (MW)	$N_{line3\phi}$
	1.004844	1.004838	0.003368	1.540329	1.540402	0.030100	14.92928	4.66659	14.18120
	Receiving-end rms voltage and current								
	Voltage (rms)			*Current (rms)*					
	$V_{r\phi}$ (pu)	$V_{r\phi 1}$ (pu)	$V_{r\phi H}$ (pu)	$I_{r\phi}$ (pu)	$I_{r\phi 1}$ (pu)	$I_{r\phi H}$ (pu)			
	0.997410	0.997418	0.008403	1.496175	1.496121	0.022218			
Line 1 Bus 1163 to 1360	$V_{s\phi}$ (pu)	$V_{s\phi 1}$ (pu)	$V_{s\phi H}$ (pu)	$I_{s\phi}$ (pu)	$I_{s\phi 1}$ (pu)	$I_{s\phi H}$ (pu)	$S_{line3\phi}$ (MVA)	$P_{line3\phi}$ (MW)	$N_{line3\phi}$
	0.997410	0.997418	0.008403	1.355526	1.355559	0.010126	5.41714	1.06836	5.31074
	$V_{r\phi}$ (pu)	$V_{r\phi 1}$ (pu)	$V_{r\phi H}$ (pu)	$I_{r\phi}$ (pu)	$I_{r\phi 1}$ (pu)	$I_{r\phi H}$ (pu)			
	0.985393	0.985408	0.008678	1.357620	1.357653	0.010288			
Line 2 Bus 1163 to 1360	$V_{s\phi}$ (pu)	$V_{s\phi 1}$ (pu)	$V_{s\phi H}$ (pu)	$I_{s\phi}$ (pu)	$I_{s\phi 1}$ (pu)	$I_{s\phi H}$ (pu)	$S_{line3\phi}$ (MVA)	$P_{line3\phi}$ (MW)	$N_{line3\phi}$
	0.997410	0.997418	0.008403	1.359045	1.359078	0.010152	5.43119	1.06619	5.32551
	$V_{r\phi}$ (pu)	$V_{r\phi 1}$ (pu)	$V_{r\phi H}$ (pu)	$I_{r\phi}$ (pu)	$I_{r\phi 1}$ (pu)	$I_{r\phi H}$ (pu)			
	0.985393	0.985408	0.008678	1.361146	1.361180	0.010314			
Line 1 Bus 1163 to 1365	$V_{s\phi}$ (pu)	$V_{s\phi 1}$ (pu)	$V_{s\phi H}$ (pu)	$I_{s\phi}$ (pu)	$I_{s\phi 1}$ (pu)	$I_{s\phi H}$ (pu)	$S_{line3\phi}$ (MVA)	$P_{line3\phi}$ (MW)	$N_{line3\phi}$
	0.997410	0.997418	0.008403	0.939773	0.941807	0.062885	3.01484	0.82326	2.90026
	$V_{r\phi}$ (pu)	$V_{r\phi 1}$ (pu)	$V_{r\phi H}$ (pu)	$I_{r\phi}$ (pu)	$I_{r\phi 1}$ (pu)	$I_{r\phi H}$ (pu)			
	1.017114	1.017181	0.019756	0.758111	0.759122	0.045574			
Line 2 Bus 1163 to 1365	$V_{s\phi}$ (pu)	$V_{s\phi 1}$ (pu)	$V_{s\phi H}$ (pu)	$I_{s\phi}$ (pu)	$I_{s\phi 1}$ (pu)	$I_{s\phi H}$ (pu)	$S_{line3\phi}$ (MVA)	$P_{line3\phi}$ (MW)	$N_{line3\phi}$
	0.997410	0.997418	0.008403	0.910962	0.912940	0.060874	2.92244	0.81532	2.80640
	$V_{r\phi}$ (pu)	$V_{r\phi 1}$ (pu)	$V_{r\phi H}$ (pu)	$I_{r\phi}$ (pu)	$I_{r\phi 1}$ (pu)	$I_{r\phi H}$ (pu)			
	1.017114	1.017181	0.019756	0.722109	0.723027	0.042917			
Line 1 Bus 1360 to 1363	$V_{s\phi}$ (pu)	$V_{s\phi 1}$ (pu)	$V_{s\phi H}$ (pu)	$I_{s\phi}$ (pu)	$I_{s\phi 1}$ (pu)	$I_{s\phi H}$ (pu)	$S_{line3\phi}$ (MVA)	$P_{line3\phi}$ (MW)	$N_{line3\phi}$
	0.985393	0.985408	0.008678	0.475068	0.475351	0.033190	0.73816	0.14901	0.72297
	$V_{r\phi}$ (pu)	$V_{r\phi 1}$ (pu)	$V_{r\phi H}$ (pu)	$I_{r\phi}$ (pu)	$I_{r\phi 1}$ (pu)	$I_{r\phi H}$ (pu)			
	1.000534	1.000509	0.010400	0.175173	0.174438	0.016985			
Line 1 Bus 1365 to 1204	$V_{s\phi}$ (pu)	$V_{s\phi 1}$ (pu)	$V_{s\phi H}$ (pu)	$I_{s\phi}$ (pu)	$I_{s\phi 1}$ (pu)	$I_{s\phi H}$ (pu)	$S_{line3\phi}$ (MVA)	$P_{line3\phi}$ (MW)	$N_{line3\phi}$
	1.017114	1.017181	0.019756	0.699162	0.701543	0.061818	2.29824	0.90274	2.11352
	$V_{r\phi}$ (pu)	$V_{r\phi 1}$ (pu)	$V_{r\phi H}$ (pu)	$I_{r\phi}$ (pu)	$I_{r\phi 1}$ (pu)	$I_{r\phi H}$ (pu)			
	1.031959	1.032237	0.032113	0.475671	0.475611	0.013401			

Table 5-9.5: Summarized line- and performance data for initial conditions of Scenario 3.

Line 2 Bus 1365 to 1204	$V_{s\,a}$ (pu)	$V_{s\,a1}$ (pu)	$V_{s\,alt}$ (pu)	$I_{s\,a}$ (pu)	$I_{s\,a1}$ (pu)	$I_{s\,alt}$ (pu)	$S_{line3\emptyset}$ (MVA)	$P_{line3\emptyset}$ (MW)	$N_{line3\emptyset}$
	1.017114	1.017181	0.019756	0.695227	0.697594	0.061477	2.28530	0.89614	2.10227
	$V_{r\,a}$ (pu)	$V_{r\,a1}$ (pu)	$V_{r\,alt}$ (pu)	$I_{r\,a}$ (pu)	$I_{r\,a1}$ (pu)	$I_{r\,alt}$ (pu)			
	1.031959	1.032237	0.032113	0.473141	0.473081	0.013286			
Line 1 Bus 1204 to 1375	$V_{s\,a}$ (pu)	$V_{s\,a1}$ (pu)	$V_{s\,alt}$ (pu)	$I_{s\,a}$ (pu)	$I_{s\,a1}$ (pu)	$I_{s\,alt}$ (pu)	$S_{line3\emptyset}$ (MVA)	$P_{line3\emptyset}$ (MW)	$N_{line3\emptyset}$
	1.031959	1.032237	0.032113	0.378464	0.378697	0.033006	0.56900	0.32168	0.46935
	$V_{r\,a}$ (pu)	$V_{r\,a1}$ (pu)	$V_{r\,alt}$ (pu)	$I_{r\,a}$ (pu)	$I_{r\,a1}$ (pu)	$I_{r\,alt}$ (pu)			
	1.031129	1.031493	0.034229	0.339714	0.339518	0.018360			
Line 2 Bus 1204 to 1375	$V_{s\,a}$ (pu)	$V_{s\,a1}$ (pu)	$V_{s\,alt}$ (pu)	$I_{s\,a}$ (pu)	$I_{s\,a1}$ (pu)	$I_{s\,alt}$ (pu)	$S_{line3\emptyset}$ (MVA)	$P_{line3\emptyset}$ (MW)	$N_{line3\emptyset}$
	1.031959	1.032237	0.032113	0.436141	0.435987	0.031314	0.65517	0.31049	0.57693
	$V_{r\,a}$ (pu)	$V_{r\,a1}$ (pu)	$V_{r\,alt}$ (pu)	$I_{r\,a}$ (pu)	$I_{r\,a1}$ (pu)	$I_{r\,alt}$ (pu)			
	1.031129	1.031493	0.034229	0.399763	0.399897	0.016061			
Line 1 Bus 1375 to 1360	$V_{s\,a}$ (pu)	$V_{s\,a1}$ (pu)	$V_{s\,alt}$ (pu)	$I_{s\,a}$ (pu)	$I_{s\,a1}$ (pu)	$I_{s\,alt}$ (pu)	$S_{line3\emptyset}$ (MVA)	$P_{line3\emptyset}$ (MW)	$N_{line3\emptyset}$
	1.031129	1.031493	0.034229	0.182740	0.176661	0.047284	0.42274	0.34056	0.25046
	$V_{r\,a}$ (pu)	$V_{r\,a1}$ (pu)	$V_{r\,alt}$ (pu)	$I_{r\,a}$ (pu)	$I_{r\,a1}$ (pu)	$I_{r\,alt}$ (pu)			
	1.008610	1.009150	0.036732	0.542765	0.542254	0.036212			
Performance	Calculated index measures for the scenario.								
	$Index_{performance}$	$Index_V$	$Index_{THD}$	$Index_{P\,loss}$					
	0.842729	0.039019	0.118252	1.5769E-08					

The reasoning related to the intuitive and predicative solving for improved performance and optimization of the system relies on the influences mentioned in both discussions pertaining to Scenarios 1 and 2. These influential factors are assumed to uphold for points exhibiting similar in action in Scenario 3 as for points in Scenario 1 and 2 where these influences could be adjudicated as the major contributing reasons.

At Buses 1163 and 1365 (Figure 3-3) the possibility to isolate and prevent the harmonic components from affecting the rest of the network is identified as all of the non-linear loads are somehow connected to these two buses. Connection of a single DG unit at each of these buses (Figure 5-6) resulted in an immediate and noticeable improvement in the performance of the scenario, but since no active control measures are applied the improvement is brought about in a rather crude fashion.

Some buses exhibit deteriorated PQ levels (increased distortion levels) while others show improved PQ. The scenario can be improved much more effectively by employing more DG units at better investigated/identified points in the system, but the general idea should be clear by now. The solution is an attempt at applying predictive solving of the scenario. The tabulated results for the suggested solution are omitted as they are very similar to the initial results (Table 5-9 parts 1-5). The performance graph is graphically presented (as a bar plot) in Table 5-10 and Figure 5-5.

Table 5-10: Performance index information for initial- and suggested conditions.

Performance index as calculated for every placement permutation				
Placement at Bus #	Calculated index measures for the scenario			
	$Index_{performance}$	$Index_V$	$Index_{THD}$	$Index_{P\,loss}$
No PBMR	0.842729	0.039019	0.118252	1.5769E-08
Suggested Solution	0.849052	0.037040	0.113908	1.6692E-08

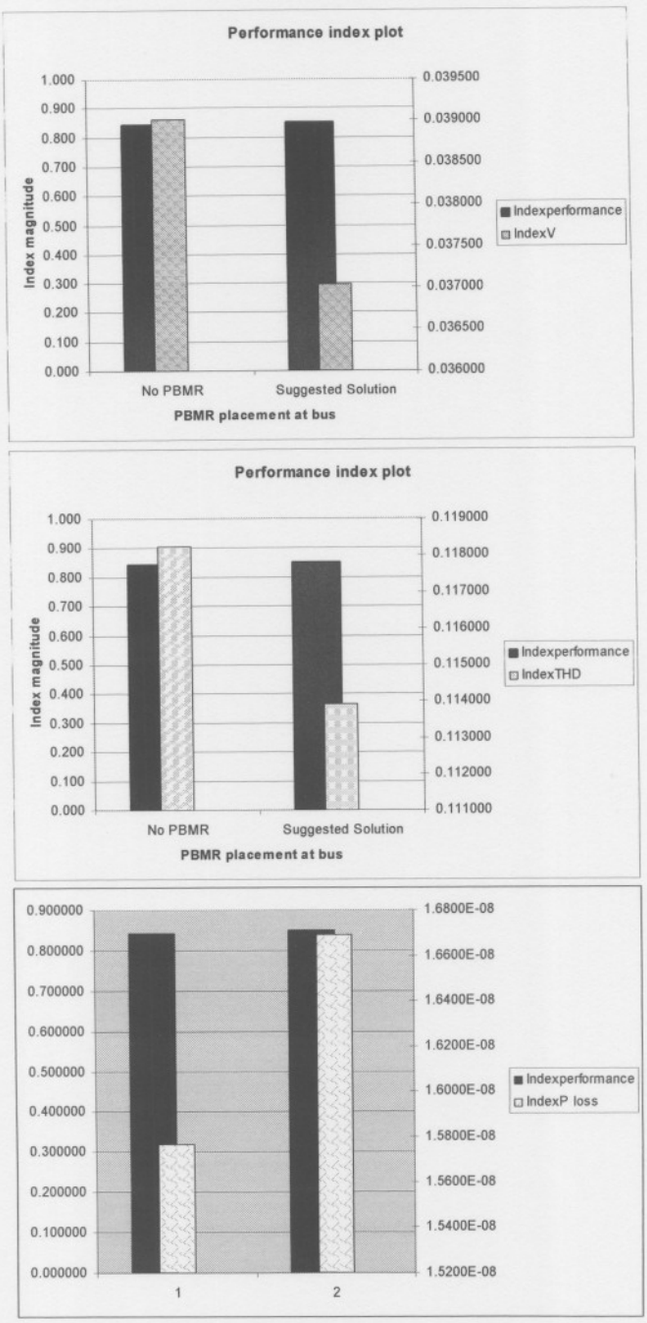


Figure 5-5: Bar plots of the performances for the two conditions of Scenario 3.

The *performance indicator* is higher for the suggested solution; therefore the related *voltage regulation-* and *harmonic distortion indicators* are lower as is expected for improved performance. Unexpectedly, the *line loss indicator* has risen but it is suspected that the lack of control for the connected DG units can be responsible for this phenomenon. A much better solution is possible and would easily be determined with the aid of a developed CAD design aimed at identifying optimum solutions.

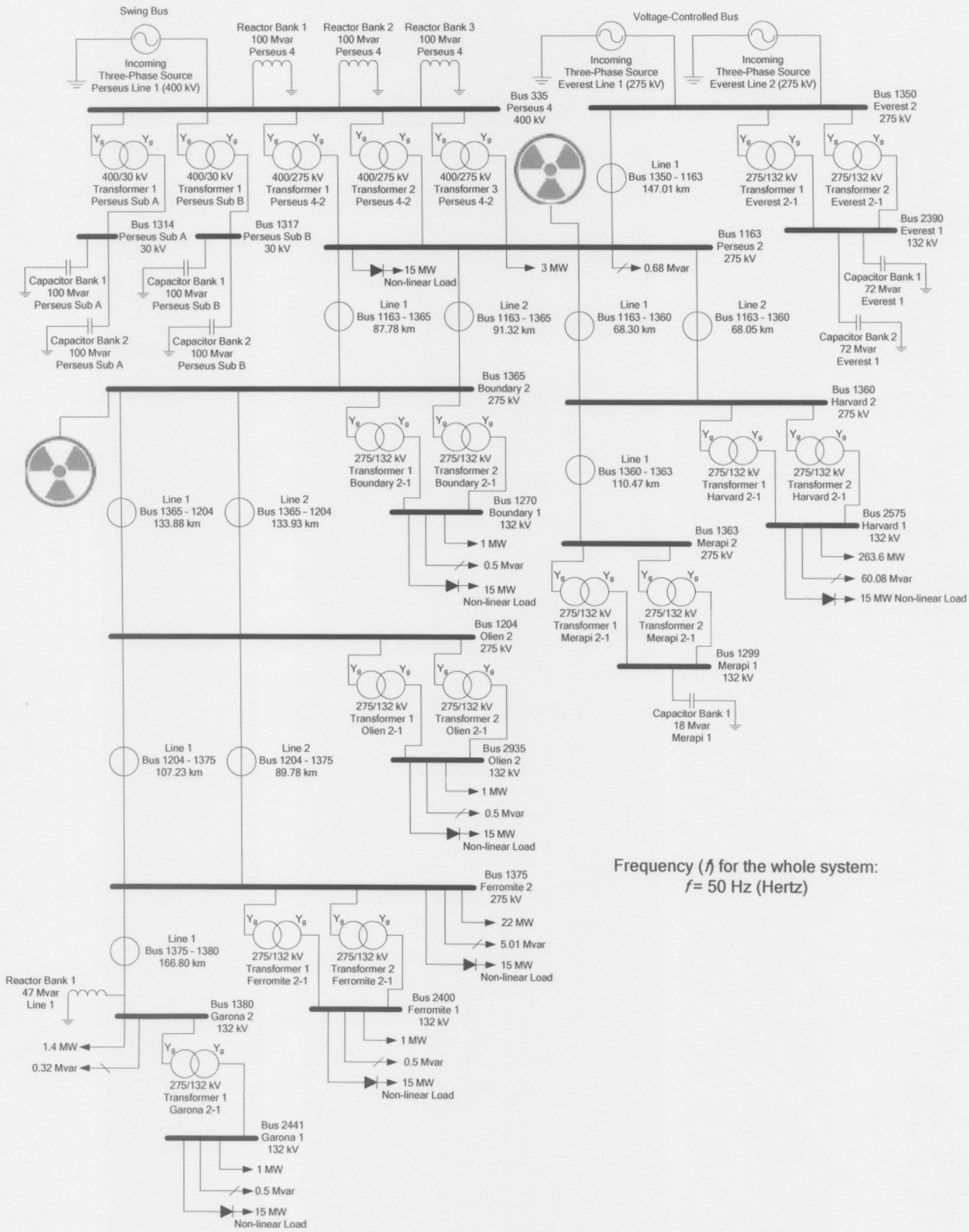


Figure 5-6: DG placement for the suggested solution for Scenario 3.

5.6 Summary and Conclusions

The developed scenarios showed evidence of reacting to the applied improvement and the measures by which the performance of a scenario was adjusted after connection of additional power generating equipment (DG or PBMRs) was entirely unique for every situation investigated. The attempts at improving the performance of a scenario based on the developed measures of Chapter 4 proved to be effective and useful. The measures can be adjusted to provide clear indications and the discussion of the recommendations for the adjustments of the measures is left for Chapter 6.

The distinct possibility of total system improvement exists proves very effective. The effects of distributed generation (DG) in a power system with poor power quality (PQ) is found to be beneficial for most of the concerned and relevant factors – such as voltage regulation, system efficiency (system- and line losses), diminished distortion levels and improved power factors for the connected loads.

In conclusion, the developed performance indicators (*performance-*, *voltage regulation-* and *harmonic distortion indicator*) were accurate, although they were slightly too normalized, and could effectively be applied in studies where the intended improvement investigated in this study is a desired practice. Computer aided software designs will undoubtedly augment the processes described and developed in the study and ultimately provide much more efficient, effective and accurate solutions.

Optimization techniques require study, but this is not part of the aims for this study. Reactive compensation equipment of DG scenarios also begs consideration as this equipment needs adjustment, due to slightly modified operating conditions, to effectively operate in conjunction with implemented DG.

Chapter 6

Overview, Conclusions and Recommendations

6.1 Introduction

In this final chapter the entire study is succinctly summarized, conclusions are drawn and recommendations for improvements to and further work for the study is made. This chapter is the author's own perspective of the details of the study and should not be seen as a field expert's point of view. All the technical detail and foundation for the study is clearly and accurately supported by the research and literature studied during the course of the investigation. The research proved true and accurate and the guidelines used to define the study parameters (such as NRS 048) were proven to be realistic, ideal and practical.

6.2 Overview

In short, the study was an investigation into the effects of distributed generation (DG) on the power quality (PQ) of power networks. The following effects were observed and include those before and after the addition of DG (by means of PBMR). All the effects are supported by the literature study:

6.2.1 Waveform distortion (harmonic distortion):

The effects are listed in a short cause-effect manner. The knowledge earlier introduced should provide the reader with necessary comprehension of the concepts explained. This is what the study "boiled down to".

Harmonic distortion is the result of *non-sinusoidal waveforms*, which are produced by *non-linear loads*, that flow back to the power source and dissipates in the source impedance where it is then "generated" in a sense and fed back into the network. In this manner harmonic distortion manifests itself in a power network (Sections 2.3.2.1 and 2.3.2.2). *Voltage distortion* showed a general reduction for most cases where a PBMR (or DG) was connected at a certain point to the system. *Current distortion* showed the same tendency. The amount the measured waveform shape improved (both voltage and current) widely varied for different placements of the DG, i.e. every point of connection influenced the whole scenario (or power network) in a unique way.

The absence of generator control for the incorporated DG consequently had a worsened level of *waveform distortion* in a few isolated instances. *Voltage-* and *current distortion* are uniquely influenced by unique non-linear loads and in some cases *voltage distortion* is at acceptable levels while *current distortion* is substantial. The waveform never regained its true fundamental shape, but in an optimized solution the resemblance of the fundamental waveform was greatly restored for all the points of concern (proved by measurement at all the buses).

The individual harmonic components generally obeyed the identified characteristic harmonic behaviour of generic power electronic converters (diode

bridge) as is identified by [37]. The individual harmonic limits as set by NRS 048 were rarely exceeded once optimized improvement was applied, but the possibility calls for the study to inspect every individual component and possibly apply filtering (active or passive) where necessary if the perpetrating harmonic component persists in the optimized solution. *Voltage regulation* in the system was severely affected by the presence of non-sinusoidal waveforms.

6.2.2 Voltage regulation (generated- and transmitted voltage levels):

The *fundamental voltage magnitude* drops dramatically if non-linear loads are connected to the system and the generating equipment have to compensate radically to correct the associated drop; utilities measure the *fundamental magnitude* and use this as a control variable.

The *root-mean-square* (*rms*) *voltage* (and *current*) *magnitude* is unpredictably influenced when applied to non-sinusoidal waveforms; i.e. the harmonic order and the magnitude of each individual order determine the calculated *rms* value of the *voltage* (and *current*). The *rms magnitude* could differ considerably from the *fundamental magnitude* in some cases – depending on the amount of *harmonic distortion*. The network generally responds as if it is heavily loaded when non-linear loads of smallish to moderate size (rating) are connected; thus *line compensation* also requires adjustment to accommodate the loads and correct the *line regulation*.

Once DG was connected at specific points towards the end of the network the *voltage regulation* was improved significantly. *Line regulation* is improved and depending on the generated output of the DG unit line compensating equipment requires minor adjustments. In fact, DG can support the *voltage-* and *line regulation* of the scenario, or power network, if active control is applied to the generator.

6.2.3 System efficiency – line losses (and transformers, etc.):

The distorted (non-sinusoidal) waveforms produce higher system losses due to the *active harmonic power* component that is dissipated when a non-sinusoidal waveform enters an impedance. The power system is made up of a network of these impedances and *active harmonic power* is dissipated in every one of these impedances. *Non-active power* (and *harmonic non-active power*), encompassing the *fundamental reactive power*, "constipates" the system capacity and the conductors of the power network experience reduced transmitted *active power* capacities.

The conductors experience "skin effect" under non-sinusoidal conditions, i.e. the higher frequency harmonic components "crowd" in the "outer shell" on the perimeter of the conductors and the current density is increased. The *skin depth* is therefore proportionally affected by the measured level of *harmonic distortion*.

With the addition of DG all of the above observed effects are reduced and *system losses* drop noticeably. Furthermore, the *power flow* of the system is altered and since less power is drawn from the initial power sources (power demand is reduced) the *active power losses* in the system is accordingly reduced.

6.2.4 More observations (power flow, *power factor*, reliability, etc.):

During the study comparisons between conventional power flow analysis techniques (Gauss-Seidel- and Newton-Raphson iterative power flow solution techniques) and the simulation results for the respective scenarios were made. It was repeatedly proven that not only was the voltage- and power magnitudes grossly inaccurate in some instances, but the phase information were inaccurate (up to 5 degrees in some cases at a certain point in the scenario).

The *power factor* usually improved and reached desired levels at most buses (depending on the nature of the connected equipment); the load buses experienced an improved power factor. *System reliability* is immensely improved with the addition of DG due to the increased delivered active power capacity and the inherent operational stable quality of the employed DG.

The effects listed above associated with DG have proven to be beneficial in all instances. Other advantages of DG include: the generating capacity of the power network is increased and since this is of major concern for South Africa (in 2003 it was announced that peak demand capacity could be insufficient as early as 2007) this is a major advantage; the power network becomes deregulated and the economic impacts are numerous and fruitful in a multi-organizational system; the power system exhibits a much more reliable performance and the utility will suffer much less financial loss due to outages and downtime as will the clients; and finally, the power system structure is strengthened in the most convenient way for future development and becomes less prone to sabotage or unforeseen reliability problems.

6.3 Conclusions

The conclusions drawn after careful assessment of the study are the following divided into two groups: the conclusions that remain universally valid and account for both the cases where distributed generation (DG) is applied or not applied; and the conclusions that motivate why these universal effects are affected by DG. With and without the use of DG the following remain valid, but the degree of influence these effects enjoy is greatly reduced once DG is applied:

Harmonically distorted waveforms (*non-sinusoidal waveforms*) are directly responsible for increased strain on power systems and the connected equipment. This is attributable to increased *generation voltage levels*, reduction of system *power transmission capacity*, increased *line compensation* levels, etc. Measured *power factors* are adversely affected and system capacity is reduced. This is a consequence of the presence of harmonic active power and non-active power (see equation (4.28) in Section 4.2.2).

Non-sinusoidal waveforms directly contribute to a drop in system efficiency. *Line losses* increase and in general so do all system losses accordingly increase. *Non-active power* (and *harmonic active power*), a consequence of *non-sinusoidal waveforms*, reduces the *active power* delivering capacity for a given generating condition and due to the inevitable adjustment of the generation control variables to meet demand, *system losses* once again increase.

Voltage regulation is unavoidably and undesirably affected by *non-sinusoidal waveforms*. Total *root-mean-square* (*rms*) magnitudes differ considerably from *fundamental* magnitudes and as a result the fundamental magnitude at a point may lie in the "acceptable range" (0.95 pu to 1.05 pu) while the total rms magnitude might be well out of this acceptable range; resulting in other unwanted problems such as undesired equipment operation or failure.

With DG applied the listed conclusions above still hold true, but their effects are significantly reduced. These are conclusions drawn as to why these effects are reduced:

Non-sinusoidal waveform sources can be isolated. In other words, with the addition of a appropriately rated DG unit(s) (PBMR(s)) at the site of the *non-linear load* (source where the *non-sinusoidal waveform* is produced and the *fundamental sinusoidal waveform's* distortion takes place) the non-sinusoidal waveform is prevented to some extent or hindered from flowing back to the rest of the power network (where harmonic distortion flourishes once it encounters source impedances, or any impedance for that matter, for it to manifest itself).

The system's impedance elements (largely inductive for power transformers, capacitive and inductive for transmission lines, and either exclusively capacitive or inductive for compensating equipment) could act as passive filtering equipment (provided that they are sufficiently underrated to cope with the extra strain) in some instances and for certain DG placements/siting in the scenario/power network.

A reduction in the source impedance, as seen by a specific non-linear load of concern, also contributes to the attenuated propagation effect of harmonic distortion in the rest of the power network. This is closely related to the first conclusion listed in this paragraph.

With regards to the assumptions made at the commencement of this study, they all proved to be true and valid as well as accurate. The effects of DG on the PQ of power systems are beneficial and the negative consequences associated with poor PQ can effectively be remedied and lessened to ultimately provide satisfactory system performance. The performance of a system can be quantified and the measure is appropriately adopted in the practice of optimization.

The guidelines fashioned from the results of the study and the observed effects of DG are presented. These guidelines are aimed at providing insight into the strategic placement of distributed resources. The proposed guidelines are:

- If a customer experiences PQ problems the situation can be considerably improved by connection of a suitably rated "pure" (unpolluted) power source at the site of the customer, but the rest of the power network is minimally influenced.

- If PQ and scenario performance improvement for the entire scenario is desired, the distributed resource(s) should be connected at strategic points in the system – points where it is predicted within reason and after careful

consideration that the disturbing (or polluting) load can be "isolated" and hindered (hopefully even prevented) from influencing the rest of the network.

- ❖ Some points of DG connection exhibit a global system affect by means of attenuating the waveform distortion through the rest of the network. This is a consequence of either coincidental formation of passive filtering paths on the network, and or due to the lowered source impedance to non-linear loads.

With these guidelines it is feasible practice to utilize DG to improve PQ in power networks. However, the performance improvement remains subject to the ratings of the DG, the amount of DG, the type of distributed resource and the measure of the initial system performance. Applying the guidelines in a cost-effective manner remains a relative optimization practice and is subject to the desired targets set by the optimizer.

6.4 Recommendations

Despite the substantial work done to effectively study the effects of distributed generation (DG) on the power quality (PQ) in power networks there remains a considerable amount of improvements to the study. These improvements include alterations, adjustments and modifications to the existing study as well as suggestions for further work in the study.

6.4.1 The Study at Present

Not much can be said, except that the developed cost function could be adjusted. It is suggested that some sort of rule-based normalization of the various indices (*voltage regulation-*, *harmonic distortion-* and *line loss indicator*) is adopted. The current normalized nature inhibits a true reflection of the PQ situation at an individual bus. If for instance, most buses display acceptable distortion levels, but a single bus exceeds the limits by a sizable margin, this singular bus's contribution to the overall *harmonic distortion indicator* for the whole scenario is diminished and the overall appearance of the system is that of acceptable waveform performance. The same holds true for the *voltage regulation indicator* in a similar fashion. As for the individual harmonic components, they should receive more attention during the study to ensure they comply with the NRS 048 limits for individual harmonic components.

Regarding the *line loss indicator*, the per-unit magnitudes of the respective line losses are employed to deliver a normalized value for the system's line losses. This per-unit basis should be adjusted to deliver larger values. As can be seen the present use of the per-unit values results in a rather insignificantly small value. It is suggested that the line loss be converted to a percentage margin of the difference between line loss for sinusoidal operation and line loss for non-sinusoidal operation.

Lastly, the rule-based approach of the two identified indicators allows for an artificial intelligent (AI) computer-aided design (CAD) that could effectively calculate more truthful indicators if, for instance, fuzzy logic techniques are applied. The CAD software could also be used for future development as will be discussed shortly.

6.4.2 Future Work

Suggestions for future work include, amongst others, the generation control possibility of the distributed resources as a promising improvement. With control the performance improvement margin can increase significantly. The control can also be of a rule-based artificial intelligent nature further maximizing the potential of the DG system.

The cost function algorithm and flow chart can easily be altered to accommodate a rule-based approach and a fully automated AI computer design will undoubtedly provide the best results when an optimal solution is desired. The program will be an effective tool providing accurate predictions for how a system will respond to improvement.

Filtering techniques in conjunction with distributed resources is another major consideration. This will unquestionably ensure the best performance for any power system scenario and depending on the type of distributed resource introduced to assist in system performance improvement, the financial cost and economic implication of the filtering technique design solution could be kept at a minimum.

Appendix

Appendix A Remaining Distributed Generation Technologies

A.1 Fuel Cell Powered Distributed Generators

Fuel cells provide a significant different approach to the production of electrical power from fossil fuel. A fuel cell is likened to a chemical battery and in essence can be called as such because of the fundamental similarities of their operation – they both produce direct current by using an electrochemical process.

Direct current (dc) is produced in a fuel cell in a chemical catalyst driven process where hydrogen is oxidized in the presence of oxygen or air [2]. The hydrogen can also be extracted from a fossil fuel containing this element. A fuel cell is an extremely reliable and favourable source of energy as it does not have any moving parts (only the minor auxiliary systems may require moving parts).

Furthermore, other advantageous characteristics include: they are silent, environmentally friendly as they produce little or no pollutants when operated correctly, and fuel efficiencies of these devices far exceed the most advanced classical power generating systems (reciprocating- and gas turbine plants) [2].

Save for the aforementioned advantages, fuel cells do have one major disadvantage: cost. They are extremely costly devices to build and maintain and this stems from their operating and design fundamentals. These inherent design characteristics and consequences are themselves also nuisances.

Fuel cells produce high-current, low-voltage (± 1 to 2 Volts) dc power requiring a DC/AC converter with either a separate or incorporated power filtering system to enable reliable and effective ac power. Due to their complex design techniques and the chemical nature of the operating principles of operation they are also dependent on highly specialized personnel for correct installation, proper operation and maintenance.

The operation of a fuel cell has to start by first identifying that, to the best knowledge of the author, there are five types of fuel cells: phosphoric acid -, alkaline -, molten carbonate -, solid oxide -, and proton-exchange membrane fuel cells. With disregard to the fuel cell type, it basically operates on the principle of directly converting chemical energy to electrical energy, much like a battery but with the distinction of continuously being "recharged" (or "re-powered") by a process of chemical replacement involving fuel and air [2].

The foundation of the operating principles of a fuel cell is laid by the ample supply of hydrogen-containing fossil fuel. In a fuel cell the hydrogen is attained/extracted from a fossil fuel and oxidized with oxygen obtained from air. The oxidization is a controlled catalyst-aided chemical process that combines the hydrogen and oxygen under monitored conditions.

The chemical product of this process is H_20 (water) but since the oxidation is likened to combustion the water is actually steam. This steam is vented (exhausted) through auxiliary systems and used to perform additional useful work (co-generation), this added advantage depends on the type of fuel cell. This outlet, termed exhaust, is on the whole pure steam (virtually pollutant-free) and commonly exceeds temperatures of ±538 °C [2].

The other salient product is an electrical charge, produced by the oxidation of the hydrogen in the presence of an electrolyte. This charge drives a direct current flow from the anode to the cathode of the fuel cell and is the most integral energy product as it is intended for, and capable of, direct application as electrical power. The voltage level of a fuel cell is greatly influenced by the type of electrolyte.

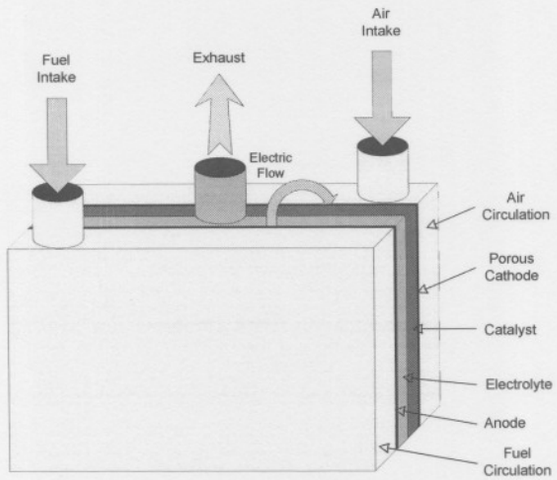


Figure A-1: Illustration of the elements of a fuel cell [2].

This oxidization can only be equated to combustion because, as for combustion there would be 'n visible open flame, oxidation has no flame but, instead, is a continuous process of combining the hydrogen and oxygen a single molecule at a time. This is the key reason why fuel cells are so incredibly efficient and exhibit emission-free operation. The catalyst promotes and controls the oxidation and allows for molecular control of the whole process by chemical means. It is almost a pure process and therefore the factors that contribute to the formation of present day pollutants are close to extinct in fuel cells.

Application of the electrical energy produced in a fuel is complicated due to certain constraining factors – the low voltage (< 2 Volts) of a fuel cell, and the dc nature of the electrical charge of a fuel cell. Current, in contrast to the voltage produced, is not a limiting factor for a fuel cell and the physical dimensions of the construction thereof is the only influential factor concerning a fuel cell's current delivering capacity – the plate size determines the active area of the anode-electrolyte-cathode surfaces, larger area in contact with these active agents, larger current produced [2].

The application of a fuel cell's electrical power is however easily accommodated owing to the development of power electronic-driven DC/AC converters (or inverter – inverts dc to ac). Luckily the dc power of a fuel cell is continuous and smooth and

this has the advantage that it simplifies the design and the job of the DC/AC converters to produce optimum ac power.

A.2 Renewable Resource Distributed Generators

In essence the strict and classical meaning of distributed generation (DG) is easily catered for by renewable power generation resources. These power sources are small, modular and rely on geographically suitable sites, whereas these sites are frequently found to be of convenience to both the established grid and the new DG resource.

The definition of DG revolves around the application of power generating resources that are modular, small and can be sited at various favourable points in the power system. Another asset is that this kind of equipment can expediently connect to the lower voltage level parts of the electrical power grid – the area where the presence of DG is considered necessary [2].

The freely available trait of the energy (or fuel) applied in renewable power generation resources is an exceptional advantage as in modern times the fossil fuel reserves are on an increasing decline and in rising demand. This is also a non-nuclear option and found to be the desired solution for most parties involved in eco-conscious power industry development. Some of these solutions/options do however produce pollutants but the majority are considered to be environmentally friendly with little or no ecological impacts.

The energy is free and widely available, even in the case of the various trash and biomass burners. The completely free energy sources include solar-, wind- and low-head hydropower production. In some instances a renewable energy source (replenishable) can be established, either through cultivation – growing the fuel to be used – or by storage of the various renewable energy sources – in certain stored energy systems, but this is presented under its own heading later on.

The major types of renewable energy resources are derived from a multitude either in use today or being developed. As mentioned before these include: solar – thermal and photovoltaic; wind; low-head hydro; and the various trash and biomass "burners" [2]. Avoiding the bulky discussion of each of these types it would be adequate to briefly mention each one of these and their operating basics.

The most well-known of these types is electrical power production by solar energy means due to the flexibility and ease of applicability it offers. The most common of the solar energy types is the photovoltaic application of the sun's solar energy to directly produce electricity, but another uncommon method is by harnessing the sun's thermal solar energy to drive classical thermodynamic systems that subsequently produce electricity. The last method is termed "*solar thermal power generation*" and the first is known as "*photovoltaic generation*". Both of these deserve a brief discussion.

The energy costs nothing but unfortunately the designer/engineer is burdened with the problem of somehow catering for the schedule and daily cycle of the sun (the cycle being a chief restriction in design and duty cycle of such systems/plants).

The sun is the sole source of solar power which is only available during daytime. Fortunately the predictability of the sun's schedule and cycle offers ways of circumventing this problem and makes it a much more reliable source of power than wind generation, even on days with overcast conditions [2].

A.2.1 Solar Thermal Power Generation

Solar thermal power generation relies on the surplus thermal energy component obtained from the sun's dividend of solar energy. This is suitably viewed as a simple conversion chain or sequence expression, namely **Solar Thermal Power Generation: Light → Heat → Power** [2]. This is achieved by using systems employing mirrors that reflect and concentrate sunlight producing intense heat energy at a certain specified point in the electric power producing plant. At this point the heat energy acts much like heat sources in conventional mechanical-to-electric conversion processes and performs useful work as dictated by thermodynamic principles (Figure A-2).

These systems offer the assurance that the electrical energy produced is analogous to that of traditional steam-turbine power plants and thanks to these identical electrical output characteristics allow them to be considered as proven and free of risk(s). The spin-off of this is that adequate knowledge and understanding of the technology involved already exists ensuring thorough maintenance and conscientious operating thereof. The mechanical conversion methods include the anomaly of the Stirling cycle reciprocating engine illustrated in Figure A-3 and explained later on.

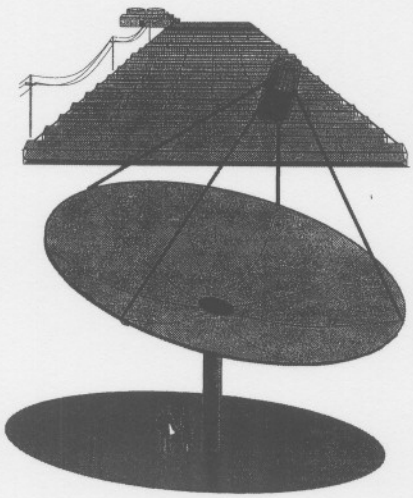


Figure A-2: Two types of solar thermal power, trough- and parabolic mirror [2].

As already can be seen from the preceding paragraphs, much of the interest revolves around, as well as much of the operation relies on, the mirror types employed in solar thermal systems – either stored thermal energy or directly/actively applied thermal energy systems. The mirrors are responsible for the process of solar concentration – the method(s) by which solar energy is concentrated and the usable thermal effect thereof collectively amplified.

This is accomplished by either of the following, and hence also termed types of mirrors: actively aimed flat mirrors – known as heliostats; aimed or static mirrors with parabolic cross-sections in one dimension – trough mirrors; aimed or static mirrors with parabolic cross-sections in two dimensions – parabolic mirrors. The static mirrors of the last two types heavily rely on well thought-out placement fixtures as to maximize the solar concentration during the daily cycle, whereas those with either one-dimensional- or two-dimensional tracking offer increased or optimum solar concentration levels throughout the day respectively. In any case however, placement remains of main concern as the location of the mirrors have to offer reliable sunlight measures ensuring optimum operation of the adopted energy system [2].

What is the measure of this energy from the sun? Well, unfortunately the amount of energy from the sun is not strictly constant as it is influenced by a multitude of disturbing factors. Firstly, the unit for the amount of energy radiated by the sun and absorbed by the earth is called the "*solar constant*" and is defined to be the amount of solar power flux that passes through the mean earth orbit [25]. Presently the accepted value is 1367 W/m^2. Earth-based instruments will record lower values of solar power flux because of atmospheric attenuation and typically the recorded value is somewhere in the range of 1000 W/m^2 at sea level.

Insolation is another term regularly encountered when working with solar dependent energy systems. Insolation is defined as solar radiation on the earth's surface. The problem with this term is that it is frequently confused with *insulation* – the preventing of conduction of heat, electricity, etc. Recently the term has generally been replaced by "*solar irradiance*" because of the confusion caused by the correspondence of the previous terms. Solar irradiance is more specifically defined as the amount of solar energy that arrives at a specific area of a surface during a specific time interval (radiant flux density) and is typically measured in units of W/m^2 [25].

As can be seen from the definition of the solar constant, solar energy can either be reflected (i.e. the same amount of energy for an area is "passed on" via reflection of a mirror to another area of same size – heliostats or flat mirror types) or concentrated on a single line or a single point (with the aid of parabolic cross-sectional mirrors – trough- or parabolic mirrors). The measure of amplification of solar energy by using mirrors is called "*suns*" and is defined as a unit which multiplies the amount of energy the earth can receive from the sun [25]. This value is typically applied in the solar concentrator community to provide an indication of how well the mirror type concentrates the solar energy it reflects onto a specified point or line. Note that this unit is not precisely defined; it usually is less than the solar constant.

Heliostats individually achieve little as they incidentally reflect the same energy received from the sun onto another area/point and essentially little or no concentration of solar energy takes place (±1 sun); therefore considered as non-concentrating by nature. When collectively utilized in a "heliostat field" they offer vast concentration levels of solar energy from a large area to a much smaller area. This concentrated solar energy is readily applicable for driving thermodynamic systems and ultimately generating electricity.

Trough mirrors concentrate solar energy on a line formed by the focal point along the length of the trough. This is thanks to the parabolic cross-section in one dimension of the mirror. A pipe carrying a fluid heated by solar concentration runs along this concentrated line of solar energy. Concentrations of 10–50 suns are typically achieved by trough mirrors [2].

The highest possible practical concentration of solar energy is achieved by parabolic mirrors and range from 2 500–4 000 suns [2]. These are mirrors with parabolic cross-sections in two dimensions enabling these high insolation levels to be reached. The heat generated by these mirrors can drive a Stirling-cycle engine-generator mounted at the focal point or heat fluids producing steam that drive turbine-generators.

Up till now it has been mentioned on occasion that solar thermal power generation can either be directly applied or stored for later use. The latter case is termed "*solar thermal energy storage (STES) power generation*" and it differs marginally from solar thermal power generation. Both systems consist of the same basic parts, with the exception of a *heavily insulated storage tank* which is solely employed by the STES system. The storage tank equips the system with the ability to provide energy production in periods where solar energy is unavailable (at night or heavily overcast conditions). The basic parts are:

- Mirrors (a field in the case of heliostats and trough mirrors)
- Central receiver (or *solar receiver* – situated on top of a central tower in the focal point of the mirror field). It can either be a Stirling-cycle engine (parabolic mirror) or an array of pipes containing an *operating fluid* that is heated here and pumped to the electric power conversion machinery.
- Operating fluid (an *oil* or *liquid salt* depending on the temperatures achieved by the mirror concentrators – oils for temperatures ranging up to 400 °C and molten salts for temperatures above 540 °C). Any solar thermal energy system has a *limited energy storage capability* thanks to the thermal retaining characteristics of these operating fluids in combination with the insulation of the pipes transporting the fluid to the various parts of the system. This allows the system to "ride through" short periods of decreased solar irradiance. The exception is the STES system that incorporates a thermal storage tank or vessel to increase its thermal storage capability adequately; equipping it with the necessary means to provide for energy production for longer periods (night time or heavily overcast conditions).
- Heat exchanger, steam generator, turbine generator, power system interchange control (essentially identical parts and technology as used for steam turbine power plants).

The Stirling-cycle engine is a rather unique and interesting technological phenomenon. This engine is driven by an external heat source in contrast to conventional internal combustion engines. Air is the operating fluid used in Stirling engines. Figure A-3 conceptually illustrates the simplified cycle of this type of engine. It is of outright importance that the reader immediately comprehends that the operation of these engines relies on three very vital principles: compression of air causes it to heat up and expansion of air cools it down; air is compressible and solids

(mechanical parts) are not; and finally, an especially large flywheel provides the necessary "stored energy" (momentum) to complete each operation cycle.

The Stirling-cycle engine offers one of the few "direct methods" by which the concentrated solar energy can be readily converted to electrical energy. These engines need a fairly high level of insolation concentration and therefore are usually almost exclusively used in conjunction with parabolic mirror type systems.

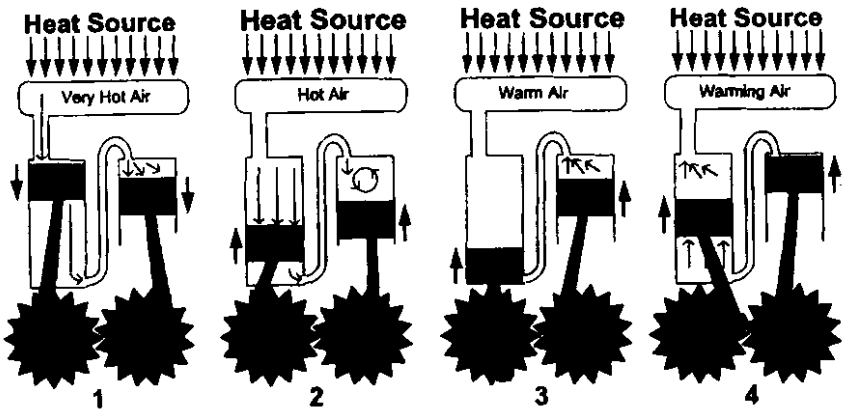


Figure A-3: The Stirling cycle illustrated here with a "single cylinder" Stirling engine [2].

A.2.2 Solar Photovoltaic Power Generation

Solar photovoltaic (PV) electricity generation wholly relies on the available light energy from the sun. Various types of "solar cells" have been developed to harness the solar light energy from sunlight. All of these do however employ the same principles of construction and function. Thanks to the development of the multitude of available modern-day semiconductor technologies and the knowledge base that evolved around them; certain known characteristic responses of these technologies are effectively utilized to directly produce electrical energy.

As indistinctly mentioned before, solar cells are semi-conductor devices. These semiconductor devices consist of flat p-n junction diodes. The diodes are purposely designed to be flat as to effectively guarantee that as large an area as possible is exposed to solar light (or more commonly sunlight). The p-n junction is located as close as possible to the surface of each diode's outer construction. A p-n junction is a certain "seam" obtained when two different types of semi-conductor material types are joined. These two types are the p-type and n-type substances respectively.

In more detail, the most common semi-conductor material used in solar cells is silicon. The p-type silicon is formed when a certain amount of a doping agent is added to the pure silicon to free up electrons and form "holes" in the silicon structure. The n-type silicon is obtained from adding another doping agent to the pure silicon to create an excess of free electrons in the silicon material's crystal structure. Once these two treated silicon "types" are correctly and effectively joined a semi-conductor diode device has been "built".

In solar cells the exposure of this junction to sunlight causes the free electrons in the n-type material to flow through the "latent" junction region between the n- and p-type materials towards the "holes" in the p-type material and in this manner a driving current is established that can supply external electric loads. The exposure of the p-n junction to sunlight results in photons hitting the free electrons and placing them in an increased energy state that send them searching for "holes" to attach to due to the energy they acquired from the photons, thus leading to the driving current.

A single solar cell constructed in this manner and less than a square centimetre in size produces dc electric power (usually less than a watt) at low voltage (typically ± 0.5 V) [2]. As can be seen from these values the power needs of various electrical equipment connected to a "solar cell" source warrants the cells to be connected in an array of some sort, as these power requirements are rarely if ever met by a single solar cell. Connecting the cells in series ("stacked") raises the output voltage and parallel connections increase the output current, much like the arrays formed with normal batteries.

The typical construction of a solar cell is shown in Figure A-4. Silicon is easily damaged and consequently a metal backing plate and a glass cover is provided to provide an increased measure of strength in the construction of the cells as well as protect the cells harmful natural elements. A metallic film or fine metal screen mesh is placed on the "negative side" of the p-n junction to act as current collector and provide electrical connection for the circuit between this metallic film and the metal backing plate (substrate).

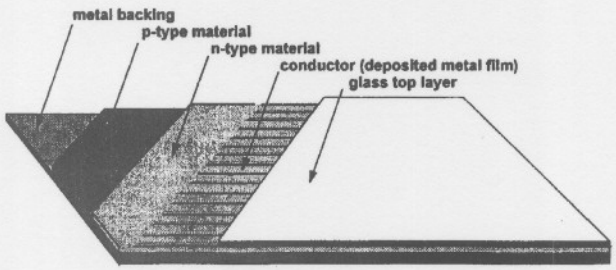


Figure A-4: Structure of a typical PV cell [2].

The produced potential (approximately 0.5 V) is across the p-n junction, i.e. from top to bottom, and the current (and accordingly the power) are in direct proportion to the designed/exposed surface area and the amount of sunlight. Because these cells are usually no less than ½ square centimetre or more than one square foot (± 0.093 m^2) while maintaining an output potential of around 0.5 volt regardless of the size of the cell, they are "stacked" effectively adding up their voltages setting up a more useful potential [2].

This leads to standardized panels manufactured by a manufacturer that provides convenient voltage levels ranging from 3–24 volts and with the series arrays parallel connected in such a manner that the power rating is defined by the output current and voltage. These panels can be grouped in any array to satisfy the customer's power requirements. The final stage is a DC/AC converter to cater for ac equipment.

A major drawback of solar cells is that although their efficiencies are considered acceptable (in the range of 5–15 % taking into account that the energy is completely free), their *effectiveness* is quite low. The aforementioned potential- and power values indicate that the costly solar cells have a poor area-to-power ratio for conventional load purposes (a household for instance). They are however the ideal power solution of choice for remote and rural loads as they are pollutant-free, virtually running cost free and easily sited.

A.2.3 Other Renewable Generation Resources

By now the means and methods of either mechanically or electronically converting the various generated energy types (electrical-, kinetic-, chemical-, etc.) have been well-conversed. It is therefore suggested that no further explanation(s) need be made of this part of each technology. As a result it simplifies further discussions of the topic to the point where it suffices to present the remaining renewable generation resources in a few key words while ignoring the operation intricacies.

The first of these remaining other renewable generation resources is wind power generation. The kinetic energy of the wind is used to turn a windmill (or wind turbine). Once again, as with solar energy, the energy is free and the technology non-polluting. It has the major advantage that it offers a viable source of energy available for a full 24-hour daily period, but unfortunately wind is unpredictable and contrary to the promising abundance of it often proves unreliable. As with solar technologies they are extremely expensive while they also offer little energy storage solutions and their environmental impacts exceed that of solar power.

In short, a variety of generators are used to convert the rotating mechanical power to electricity of which the synchronous generator is the least popular as they require a constant rotational speed to generate and maintain the correct line frequency and wind will definitely not offer the desired speed by itself. As a result either of the following generator types is used to overcome the challenge of constantly varying wind speed: *inductive generation*, *DC generation*, generations aided by a *variable-speed ac drive*.

Next we have low-head hydro power production. Low-head refers to the small difference between the high- and low water levels from one side to the other of the water turbine. The viability of low-head hydro (opposite being conventional hydro power production using a substantial head) is dictated by the suitability of a site in a river offering sufficient flow or head. This ultimately guarantees if the power generating turbine will have enough energy to turn and generate electricity [2].

Biomass and trash burning is another unique power production option and offers solutions to waste disposal while producing usable energy. The resultant ash produced by the burning of the waste (unwanted foliage and organic waste, trash or even crops grown and harvested specifically for this purpose – biomass power plant) unfortunately still requires waste management of its own, but land fills seem to be the best solution. Once again, the fuel is free but this option leads to considerable pollution levels.

Geothermal promises to be another of the few sources of free energy relatively easily applied for generation purposes. These power plants are once again constructed where these geothermal sites exist and that seems to be its only concern along with high initial cost. The "measure" of geothermal activity also determines the eventual output of the power plant and the viability of it has to be considered in this regard.

Tidal power is one of the most recent of these technologies and attempts to harness the energy of the ocean's waves and or varying high- and low tides. Generation using the ocean's waves is still experimental at this stage but tidal power using the cycle of tides is much like low-head hydro, except that it usually only operates for "outgoing cycles" of the tides. Water is stored in large reservoirs during high tide and released to flow through the power turbine at low tide.

A.3 Distributed Generation and Energy Storage

The main purpose of energy storage is to assist distributed generation (DG) resources. Only in a few isolated and highly sophisticated instances are they intended to operate in stand-alone mode as backup for the main energy sourcing options. This last option will not be discussed here and brief mention of it would do.

The assistance energy storage systems lends DG is further divided in three separate descriptions. Energy storage can aid in stabilizing the electrical power grid as seen by the DG unit allowing for the unit to maintain a constant and stable output under fluctuating load conditions. If well-specified and adequate amounts of energy storage are installed, it can momentarily replace the DG for periods where the DG is unavailable (maintenance or "fuel-related" issues). The last instance where DG benefits from energy storage is where non-dispatchable DG is augmented by energy storage to operate as a dispatchable resource giving it the ability to exhibit a tolerable level of fluctuating output. These beneficial features are listed in Table A-1 along with the foremost distinguishing characteristics of each.

Table A-1: The three major applications of energy storage with DG [2].

Planning Aspect	Reason why energy storage is being applied in conjunction with DG system		
	Energy Stabilization	***Ride-Through***	***Dispatchability***
Reason	Shave needle peaks in the non-coincident load curve, due to large appliances, etc.	Provide energy to serve load during periods when DG output is unavailable.	Provide energy stored to stabilize DG availability to meet various schedules.
Benefit	Lowers peak DG capacity needed. Improves voltage regulation.	Service from PV, etc. can now be maintained during night time, etc.	DG owner can now bid and sell power contracts for arbitrary schedules.
Storage	Must be enough to "shave" appliance peaks and meet their short-term needs.	Dictated by load during "DG unavailable" times Usually ½ day's energy.	Must be enough to transform the DG schedule into the desired sales schedule.
Peak	Relatively great: all the energy stored must be released in just a few minutes.	Relatively small, only one eighth to tenth of stored energy.	Requires more than for ride-through but much less, relatively, than for energy stability.
Method	Based on detailed assessment of daily load curve, on a minute-to-minute basis.	Based on hourly analysis of load needs over a year and DG availability stats.	Based on hourly analysis of desired schedules, DG availability stats, business cases.
Design	Typically high-energy, low-storage design with enough capacity to avoid deep cycle.	Must achieve size balance between storage size and DG.	Must achieve an overall balance among DG unit size, storage size, and total cost.

Briefly, the major groups of electrical energy storage are chemical-, electrical- and physical storage [2]. These groups can further be grouped into two main approaches, namely energy stored as electrical energy (e.g. batteries) or other types of physical energy storage (thermal-, momentum-, etc.) from which it can be quickly and effectively converted to electrical energy on demand.

The first most popular, logical and simplest means of electrical energy storage is provided by batteries – the storage and conversion of chemical energy to electrical energy. The nature of battery design, construction and operation is common knowledge and there is no need to repeat it here. The direct current (dc) output of batteries only requires a decent DC/AC converter to allow for widespread use in alternating current (ac) systems.

To the author's knowledge two technologies exist that store electrical energy as electrical energy. The first – and by far the most sophisticated, scientific and modern solution (still very much in experimental development) – is the superconducting magnetic energy storage (SMES) system. The second is capacitors that can be compared to batteries. Both these systems store power at very high density and can release it almost instantaneously.

These two technologies, although related in their shared goal of storing electrical energy, have vastly different approaches when it comes to the fundamentals of retaining that energy. For an SMES the electrical energy is stored as a constantly rotating zero-voltage current in a superconducting coil, while for a capacitor it stores energy as a voltage potential (a charge) between to "plates" that has no current flow under storage conditions. The similarity of both however is that they store power as dc and is easily converted to ac power when needed.

The previously discussed solar thermal energy storage (STES) system is an example of physical energy storage means. Other examples include compressed air- and spinning flywheel systems. The stored-to-electrical energy conversion methods of these systems are far more complicated than those of battery or electrical energy storage technologies. They have a lot of auxiliary systems that are responsible for converting the energy, as well as storing the energy. For instance, compressor pumps and motors respectively for the compressed air- and spinning flywheel systems to "build up" the energy reserve and the thermal-to-electricity generator of the STES system.

Appendix B Reliability, Cost and Planning continued

B.1 Power System Reliability

Important to immediately note is that of all the reliability definitions given in Table B-1, "*interruption*" and "*outage*" are of principal concern. These two terms are frequently used either jointly or interchangeably, but they have vastly dissimilar meanings. Outage refers to general equipment failure (or incorrect operating equipment, e.g. superfluous breaker trips) of the power supply system or part thereof. Interruption, on the other hand, is a termination of supply (or service) to one or more customers [2]. In other words, outages almost always are the cause of interruptions, but this does not hold true for the reverse case.

Table B-1: Reliability terms and definitions [2].

Characteristic	Explanation
Availability	The fraction of the time that service is available. The (steady-state) probability that power will be available.
Duration	The total elapsed time of an interruption or outage.
Failure Rate	The average number of failures of a component or unit of the system in a given time (usually a year).
Failure Probability	The probability that a unit or system will be in a "failure mode" at a time selected at random.
Frequency	How often interruptions or outages, as the case may be, occur.
Interruption	A cessation of service to one or more customers, whether power was being used at that moment or not.
Mean Time Between Failures (MTBF)	The average or expected time a unit of equipment is in service between failures.
Mean Time To Repair (MTTR)	The average or expected time to repair an "outaged" component or unit of the system, once failed.
Outage	The unavailability of part of the power supply system, whether due to unexpected or planned circumstances.
Forced Outage	The outage due to unexpected and unscheduled event (usually a failure or impending failure).
Scheduled Outage	An outage that was planned and scheduled in advance (usually maintenance).
Reliability	The fraction of time that a unit of equipment or portion of the system is capable of performing the required function. The (steady state) probability that it will be in service in a condition where it can function as required.
Reporting Period	The period of time over which reliability, interruption, and outage statistics have been gathered or computed.
Restoration	Return of electric service after an interruption, because of repair of the outage causing the interruption, or because of re-switching of the supply source, or the starting of an alternate DG source.
Restoration Time	The time required to restore service to an interrupted customer or portion of the system.
Service	Supply of electric power in sufficient amount and quality to satisfy customer demand.

The distributed generation (DG) planner has quite a lot of freedom when it comes to the planning of reliable exploitation of DG resources. DG offers adaptability, ease of implementation and control, and cost-effective means of augmenting existing power systems. All of these serve to make DG the preferred method of improving system reliability. The planner only has to take into consideration how much the investor is prepared to spend and what the goals (or outcomes) of the design are in terms of reliability – i.e. back-up power or power quality (PQ) improvement, to name a few. Cost is the major concern in such planning and development schemes.

B.2 Planning- and Development Cost

Any development of sorts costs money. The planner, engineer, developer or designer has to be content with this fact. Any major project or development invariably consists of a "variety of costs" – also termed "types of cost" [2]. The various elements of the cost of a major development (such as establishing/introducing DG in a region or part of the power network) include purchases, labour, initial resources, construction and materials, operating costs, etc. and all of these have a single common base – money in whichever currency is preferred.

Once the absolute financial value of a certain solution has been determined the process of choosing the best solution to meet the design specifications is largely based upon finding the cheapest one while meeting the majority of requirements to a satisfactory degree as agreed between developer and investor. A holistic approach is adopted in most cases where cost-effective development is the goal, but in some cases (such as sensitive ecosystems) some impacts of the development cannot be converted to a cost base. This circumstance influences planning in a whole other complex way.

The following common types of cost have been identified [2]:

Initial cost – the investment made to acquire the base equipment, facility or resource(s); i.e. all the equipment and instruments that eventually erects and makes up the power generating facility.

Continuing costs – the operating costs incurred during running of the facility for its lifetime, such as fuel for the plant, maintenance, personnel expenses, etc.

Fixed costs – these costs remain constant regardless of the power solution (DG) opted for or any permutation adopted in the planning analysis thereof.

B.3 Cost versus Reliability

As a rule the more costly and expensive distributed generation (DG) solutions tend to be the more reliable, except for a select few technologies involving experimental and scientific approaches where greater significance is accredited to certain other concerns (e.g. power delivering speed, efficiency, etc.). As a result it has to be weighed whether the customer (DG investor, planner, developer, designer, and so on) wants a cheap solution, or a reliable one.

Together with reliability comes power quality (PQ) and the more reliable DG solutions are almost always the ones that offer superior PQ. Thus, from these three prerequisites of reliability, cost and power quality an imaginary "value cube" is drawn showing the three established dimensions of power provision – quantity, quality and cost (Figure B-1) [2].

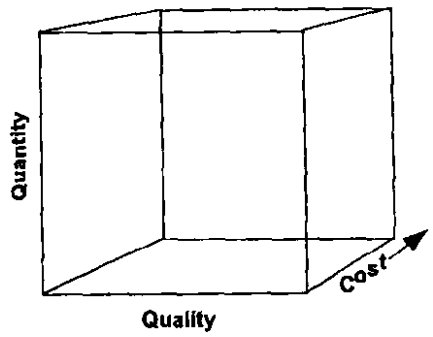


Figure B-1: The three dimensions of the DG "value cube": quantity, quality, and cost [2].

B.4 Value-Based Planning

Value-based planning (VBP) is when both the cost of the DG supplier, or the utility, to provide the power and the cost suffered by the consumer, or customer, due to the level of reliability offered (or lack thereof) by these power authorities are compared to determine a minimum target point where both the parties are satisfied. In other words, a consumer could be needlessly charged for reliability offered by a power providing authority if this particular customer has no need for reliability levels of this order.

DG offers unique solutions for unique customers. This is what makes it such a versatile, adaptable and easily applied technology. The problem in the past was that utilities had to offer a single level of reliability and PQ to a variety of customers. With DG each consumer has the freedom to specify its own specific power needs (in terms of cost, reliability and PQ) tailored to suit them individually. VBP is graphically illustrated in Figure B-2.

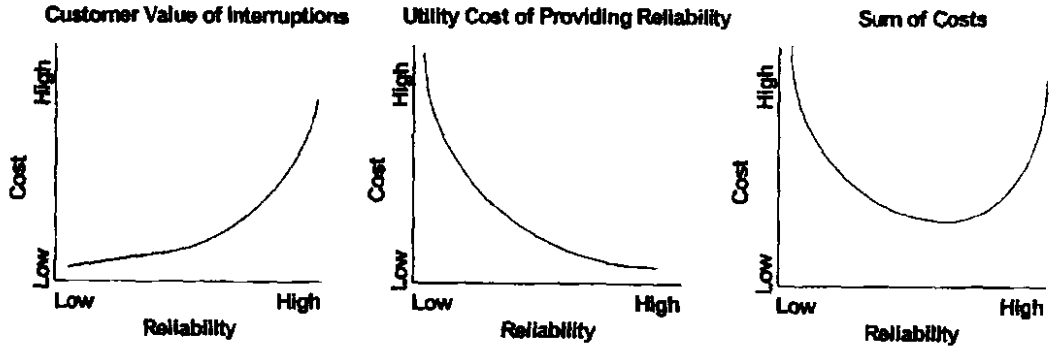
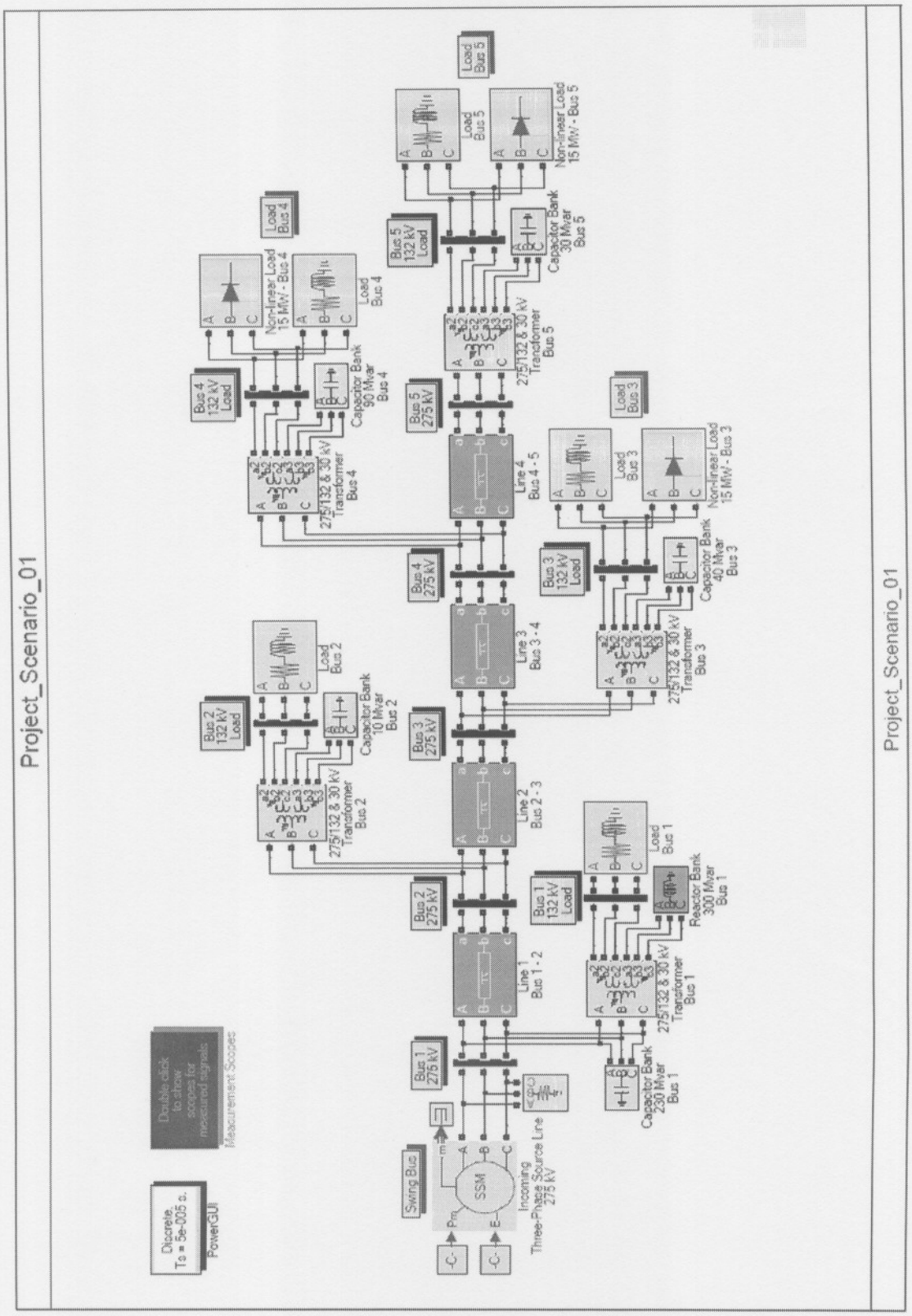
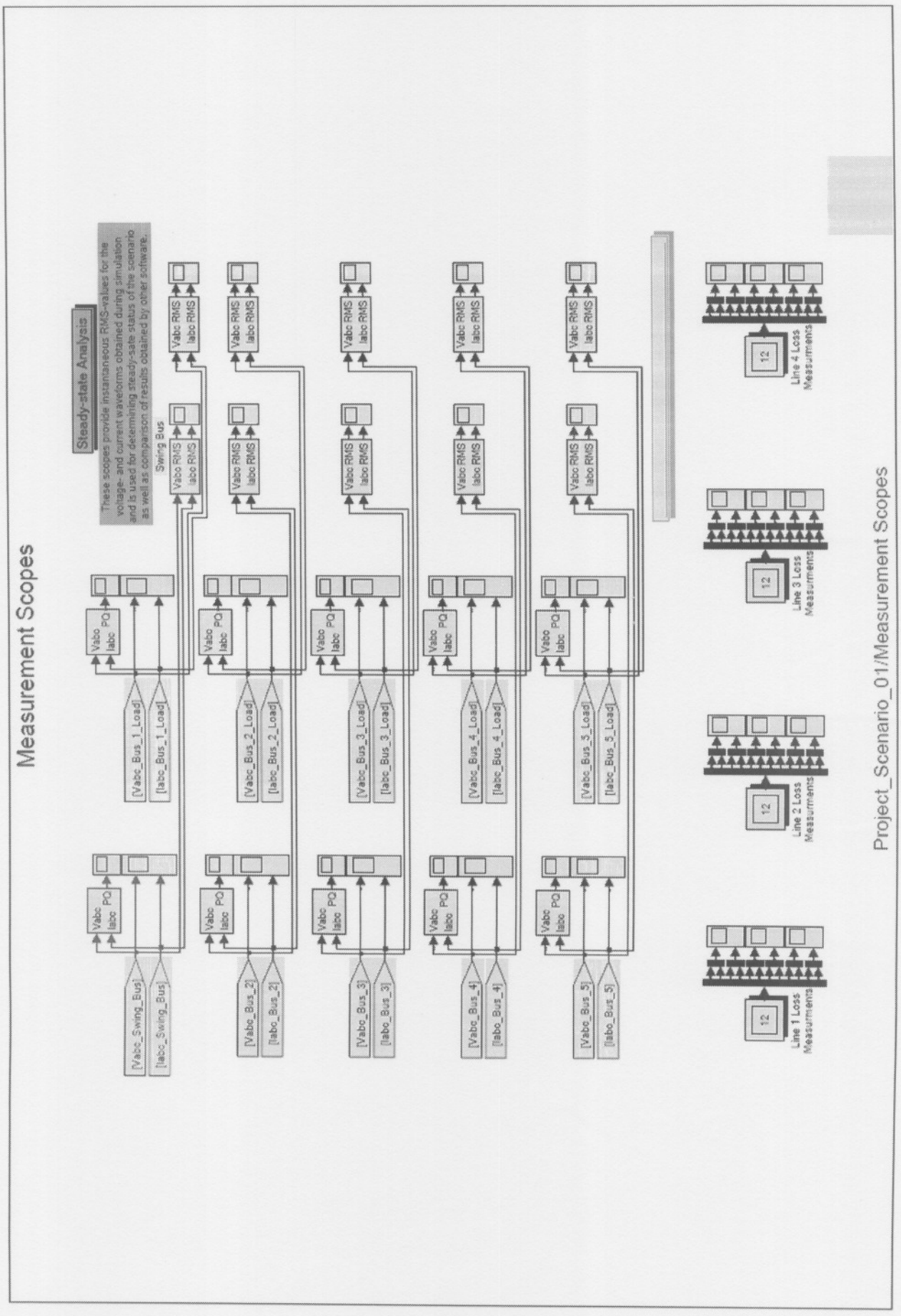


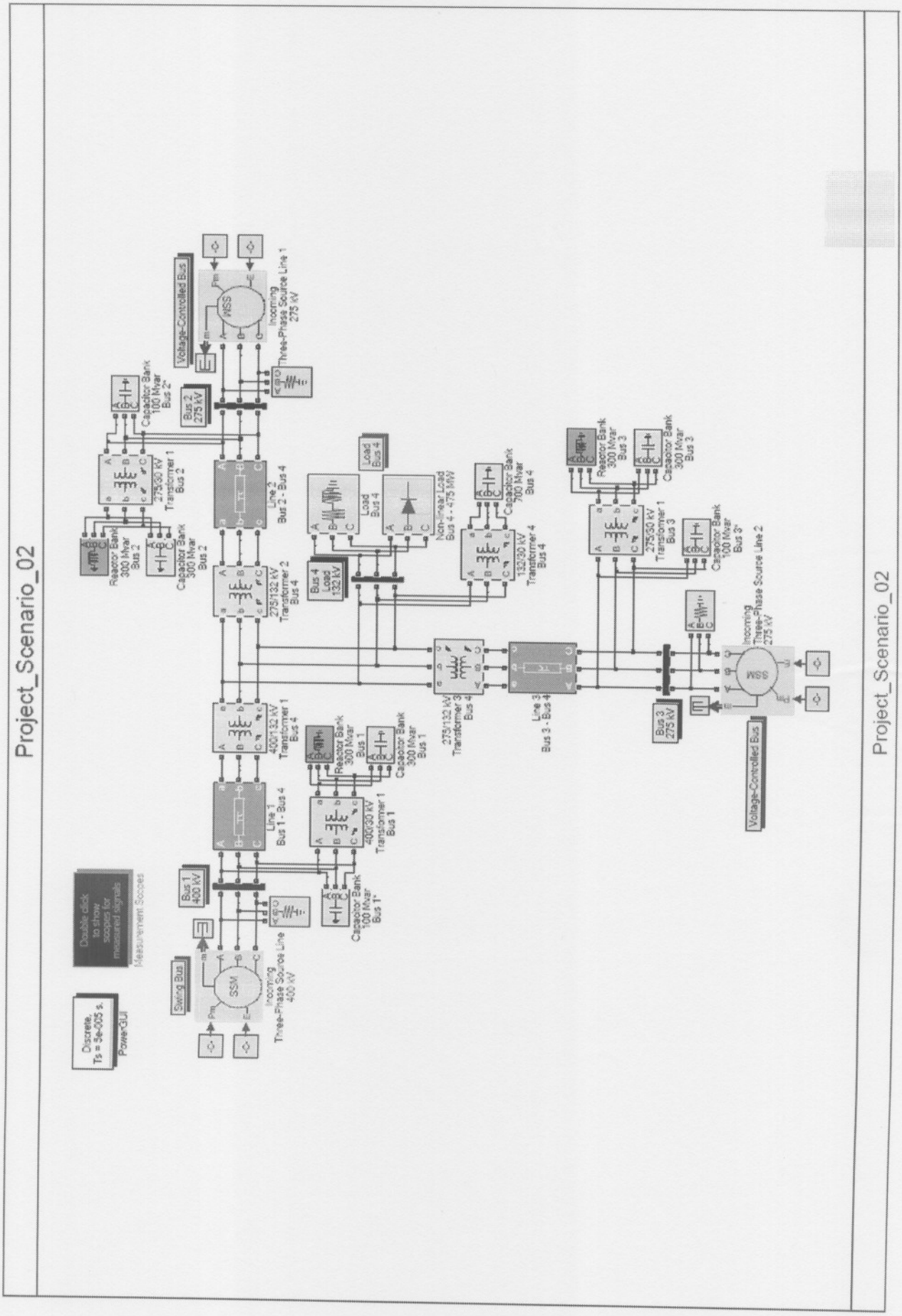
Figure B-2: Value-based planning involving cost to the utility and the consumer [2].

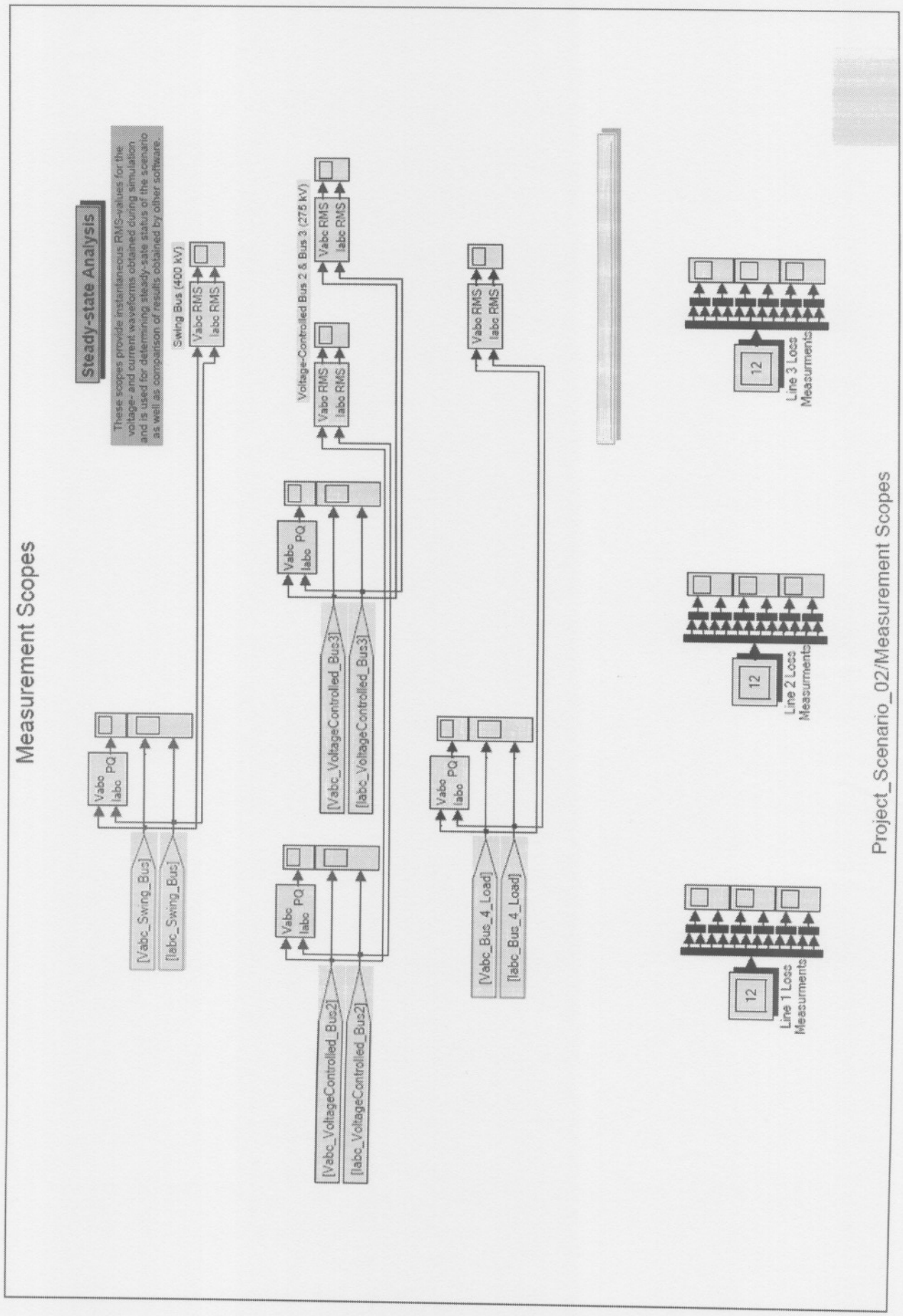
Appendix C Developed MATLAB® Simulink® models

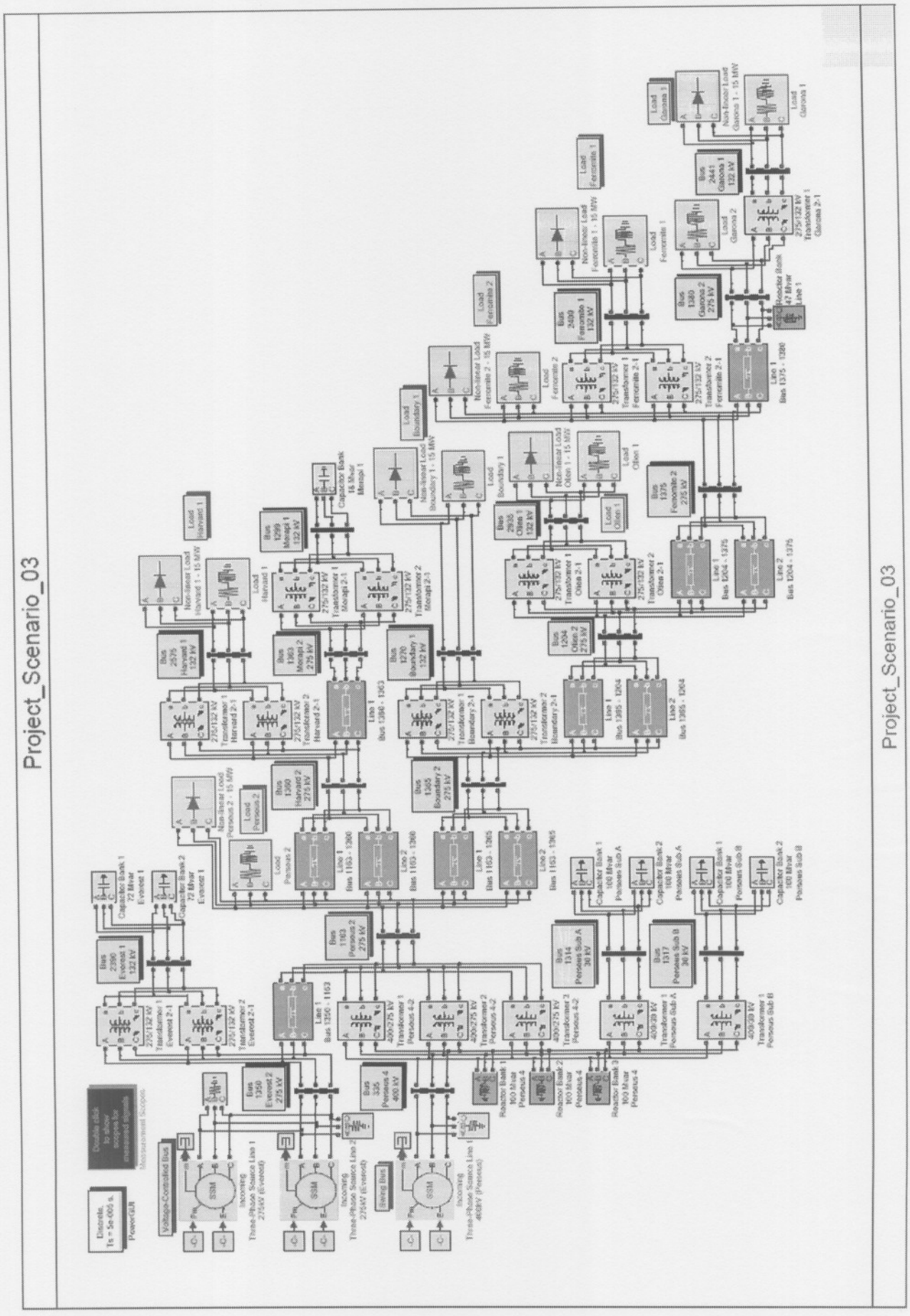
C.1 Power System Scenarios

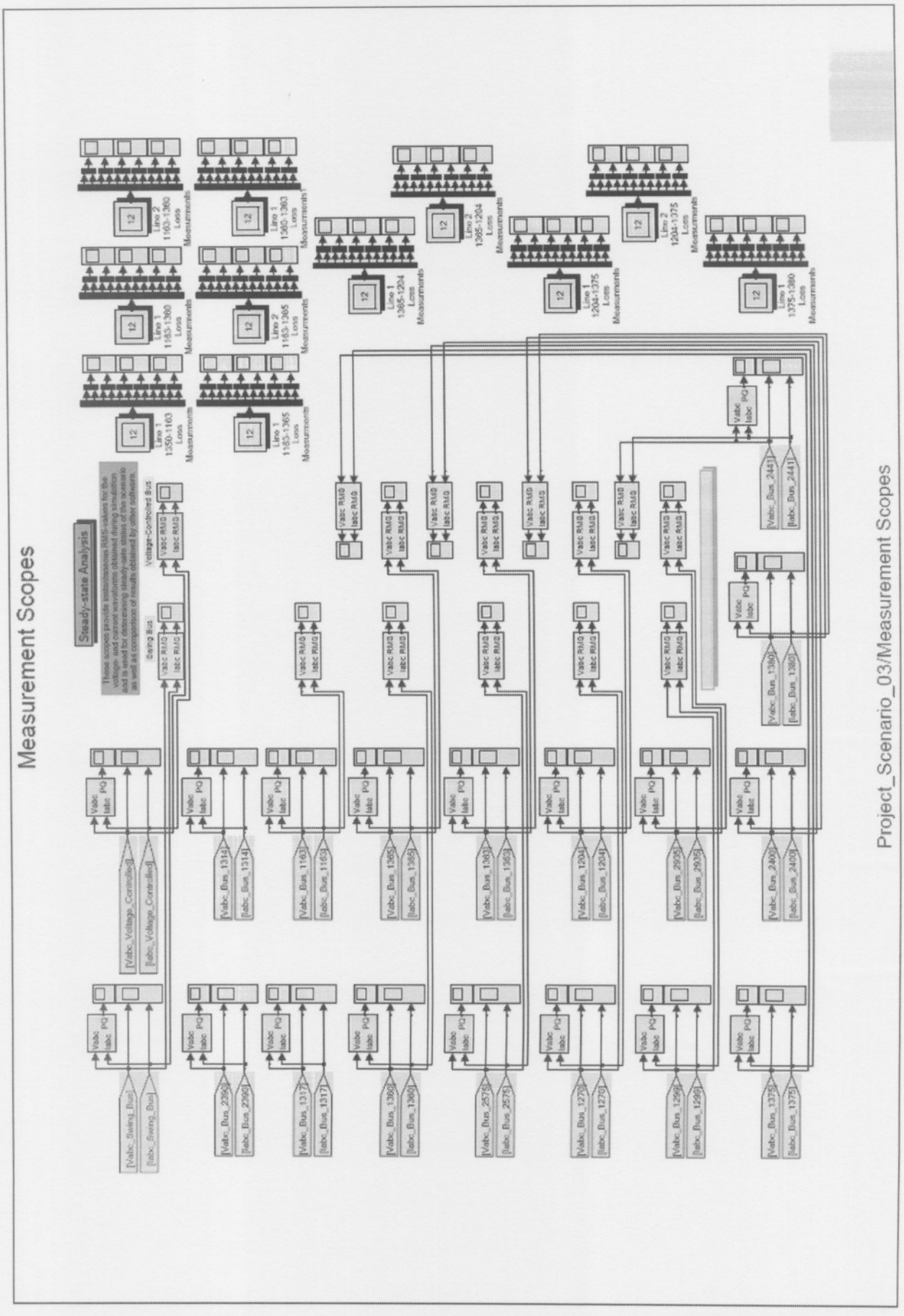


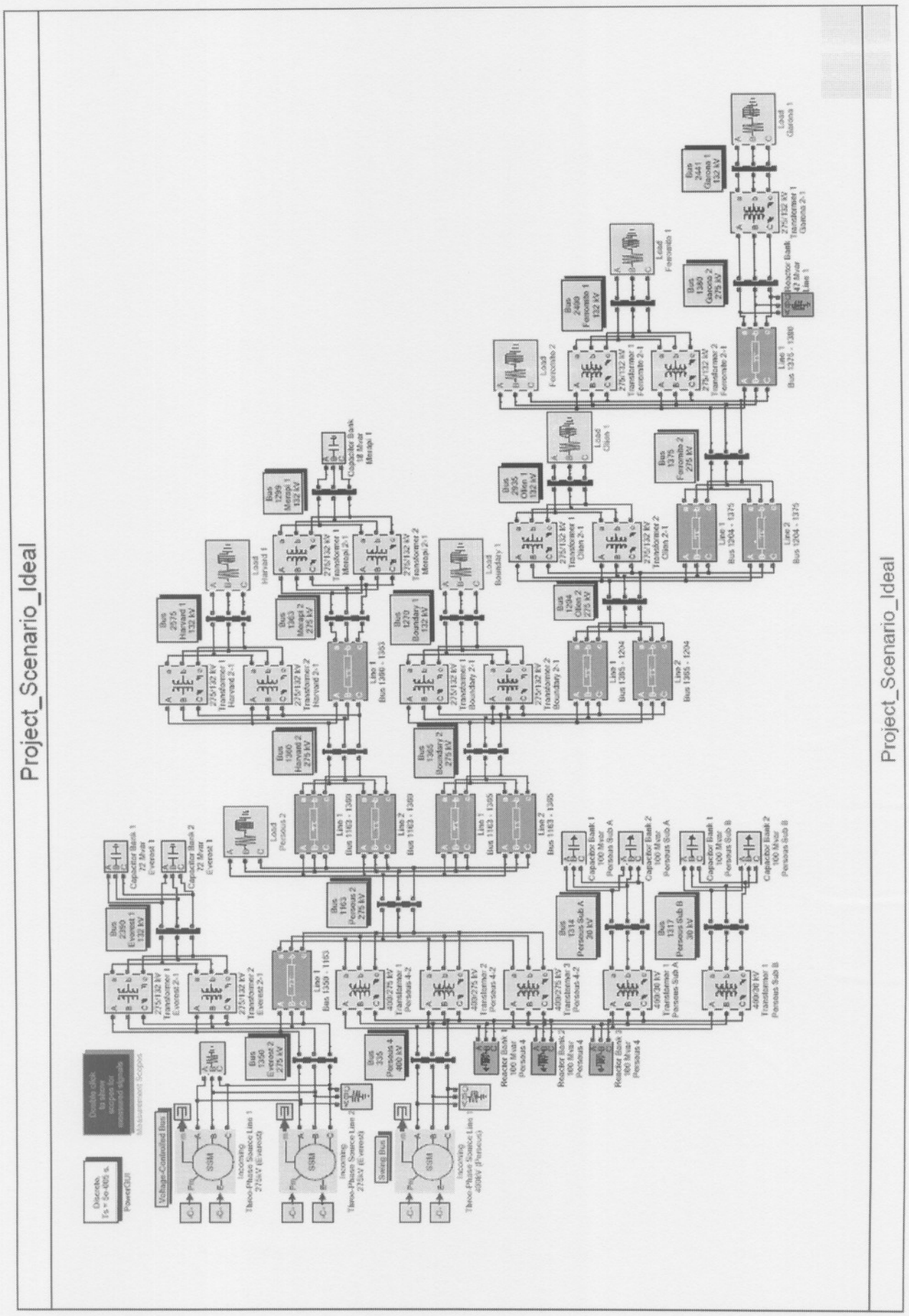

Measurement Scopes
Steady-state Analysis
These scopes provide instantaneous RMS-values for the voltage- and current waveforms obtained during simulation and is used for determining steady-sate status of the scenario as well as comparison of results obtained by other software.
Swing Bus
Vabc RMS
Iabc RMS
Vabc PQ
Iabc
[Vabc_Swing_Bus]
[Iabc_Swing_Bus]
[Vabc_Bus_1_Load]
[Iabc_Bus_1_Load]
[Vabc_Bus_2]
[Iabc_Bus_2]
[Vabc_Bus_2_Load]
[Iabc_Bus_2_Load]
[Vabc_Bus_3]
[Iabc_Bus_3]
[Vabc_Bus_3_Load]
[Iabc_Bus_3_Load]
[Vabc_Bus_4]
[Iabc_Bus_4]
[Vabc_Bus_4_Load]
[Iabc_Bus_4_Load]
[Vabc_Bus_5]
[Iabc_Bus_5]
[Vabc_Bus_5_Load]
[Iabc_Bus_5_Load]
12
Line 1 Loss Measurments
Line 2 Loss Measurments
Line 3 Loss Measurments
Line 4 Loss Measurments
Project_Scenario_01/Measurement Scopes

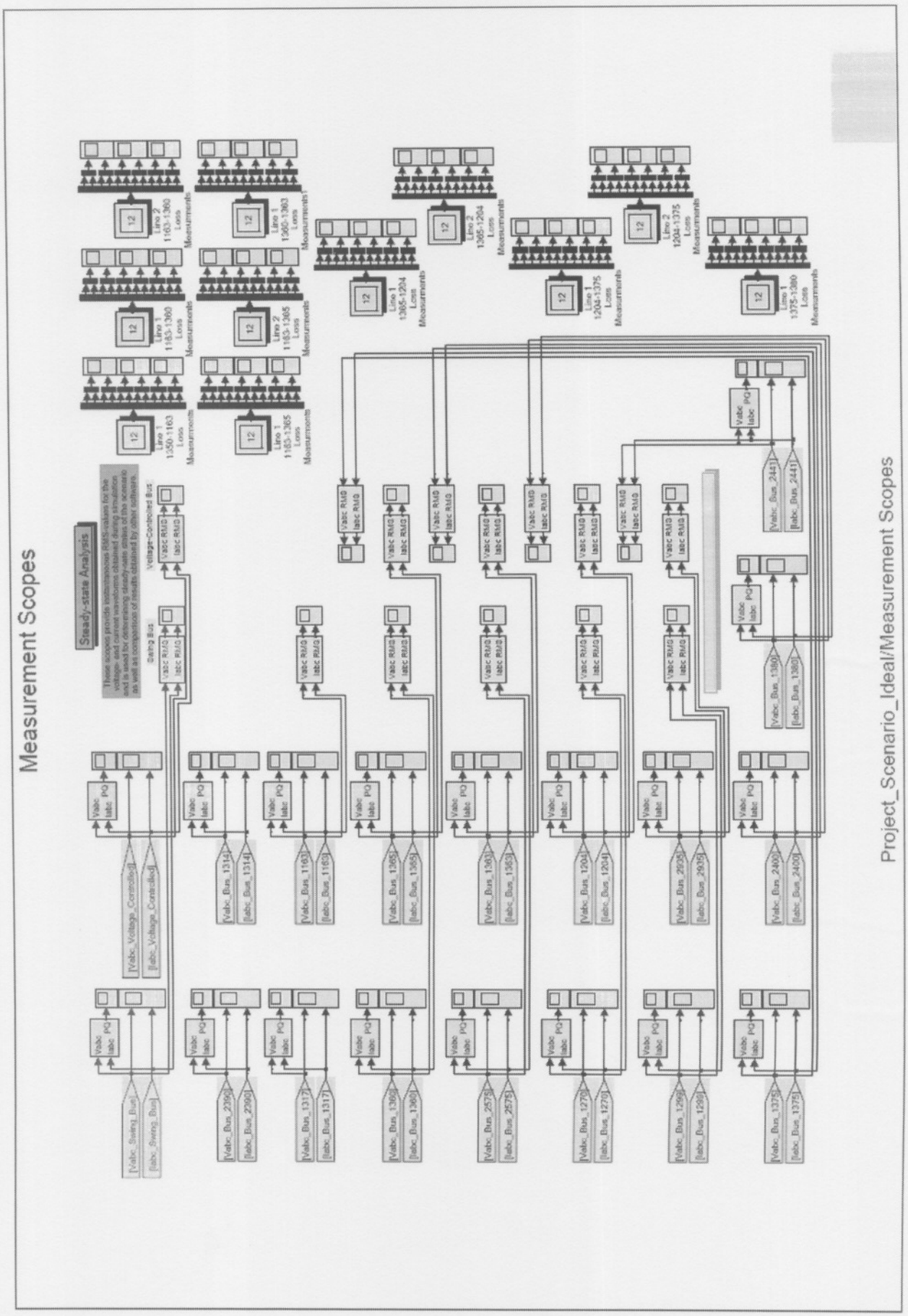

Project_Scenario_02
Project_Scenario_02
Discrete,
Ts = 3e-005 s.
powergui
Double click
to show
scopes for
measured signals
Measurement Scopes
Swing Bus
SSM
Incoming
Three-Phase Source Line
400 kV
Bus 1
400 kV
Line 1
Bus 1 - Bus 4
400/132 kV
Transformer 1
Bus 4
400/30 kV
Transformer 1
Bus 1
Capacitor Bank
100 Mvar
Bus 1*
Reactor Bank
300 Mvar
Bus 1
Capacitor Bank
300 Mvar
Bus 1
Voltage-Controlled Bus
WSS
Incoming
Three-Phase Source Line 1
275 kV
Bus 2
275 kV
Capacitor Bank
100 Mvar
Bus 2*
275/30 kV
Transformer 1
Bus 2
Reactor Bank
300 Mvar
Bus 2
Capacitor Bank
300 Mvar
Bus 2
Line 2
Bus 2 - Bus 4
275/132 kV
Transformer 2
Bus 4
Bus 4
Load
132 kV
Load
Bus 4
Load
Bus 4*
Non-linear Load
Bus 4 - 475 MW
132/30 kV
Transformer 4
Bus 4
Capacitor Bank
700 Mvar
Bus 4
275/132 kV
Transformer 3
Bus 4
Line 3
Bus 3 - Bus 4
Reactor Bank
300 Mvar
Bus 3
Capacitor Bank
300 Mvar
Bus 3
275/30 kV
Transformer 1
Bus 3
Capacitor Bank
100 Mvar
Bus 3*
Bus 3
275 kV
Incoming
Three-Phase Source Line 2
275 kV
WSS
Voltage-Controlled Bus


Measurement Scopes
Steady-state Analysis
These scopes provide instantaneous RMS-values for the voltage- and current waveforms obtained during simulation and is used for determining steady-sate status of the scenario as well as comparison of results obtained by other software.
Swing Bus (400 kV)
Vabc RMS
Iabc RMS
Vabc PQ
Iabc
[Vabc_Swing_Bus]
[Iabc_Swing_Bus]
Voltage-Controlled Bus 2 & Bus 3 (275 kV)
[Vabc_VoltageControlled_Bus3]
[Iabc_VoltageControlled_Bus3]
[Vabc_VoltageControlled_Bus2]
[Iabc_VoltageControlled_Bus2]
[Vabc_Bus_4_Load]
[Iabc_Bus_4_Load]
12
Line 3 Loss Measurments
Line 2 Loss Measurments
Line 1 Loss Measurments
Project_Scenario_02/Measurement Scopes

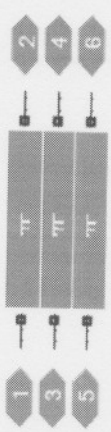
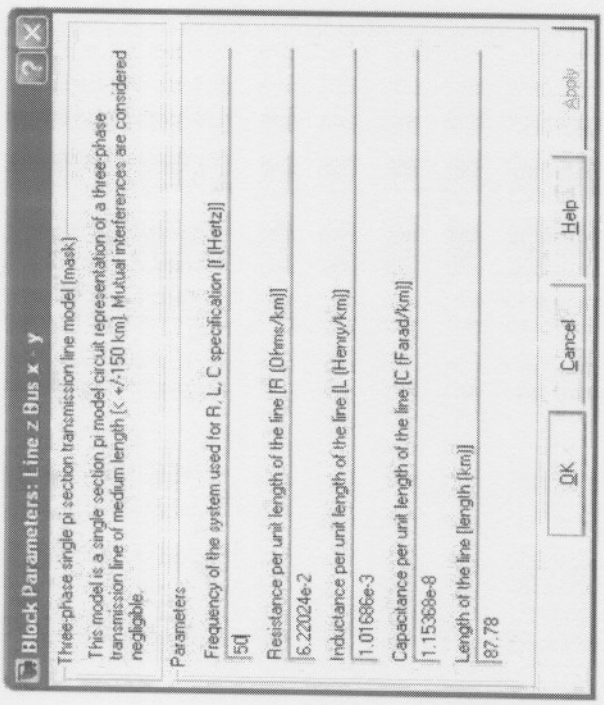
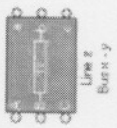

Project_Scenario_03
Project_Scenario_03


Measurement Scopes
Project_Scenario_03/Measurement Scopes
Steady-state Analysis
These scopes provide instantaneous RMS-values for the voltage and current waveforms obtained during simulation and is used for observing steady-state behaviour of the circuit as well as comparison of results obtained by other software.
Swing Bus
Voltage-Controlled Bus
Vabc RMS
Iabc RMS
Vabc PQ
Iabc
[Vabc_Swing_Bus]
[Iabc_Swing_Bus]
[Vabc_Voltage_Controlled]
[Iabc_Voltage_Controlled]
[Vabc_Bus_1314]
[Iabc_Bus_1314]
[Vabc_Bus_2390]
[Iabc_Bus_2390]
[Vabc_Bus_1163]
[Iabc_Bus_1163]
[Vabc_Bus_1317]
[Iabc_Bus_1317]
[Vabc_Bus_1365]
[Iabc_Bus_1365]
[Vabc_Bus_1360]
[Iabc_Bus_1360]
[Vabc_Bus_1383]
[Iabc_Bus_1383]
[Vabc_Bus_2575]
[Iabc_Bus_2575]
[Vabc_Bus_1204]
[Iabc_Bus_1204]
[Vabc_Bus_1270]
[Iabc_Bus_1270]
[Vabc_Bus_2935]
[Iabc_Bus_2935]
[Vabc_Bus_1299]
[Iabc_Bus_1299]
[Vabc_Bus_2400]
[Iabc_Bus_2400]
[Vabc_Bus_1375]
[Iabc_Bus_1375]
[Vabc_Bus_2441]
[Iabc_Bus_2441]
[Vabc_Bus_1380]
[Iabc_Bus_1380]
Line 1 1350-1163 Loss Measurements
Line 2 1163-1360 Loss Measurements
Line 1 1163-1365 Loss Measurements
Line 2 1365-1363 Loss Measurements
Line 1 1365-1204 Loss Measurements
Line 2 1365-1204 Loss Measurements
Line 1 1204-1375 Loss Measurements
Line 2 1204-1375 Loss Measurements
Line 1 1375-1380 Loss Measurements


Project_Scenario_Ideal
Project_Scenario_Ideal


Measurement Scopes
Project_Scenario_Ideal/Measurement Scopes
Steady-state Analysis
These scopes provide instantaneous RMS values for the voltage and current waveforms obtained during simulation and is used for determining steady-state states of the scenario as well as comparison of results obtained by other software.
Voltage-Controlled Bus
Swing Bus
Vabc RMS
Iabc RMS
Vabc PQ
Iabc
Line 1 1163-1360 Loss Measurements
Line 2 1163-1360 Loss Measurements
Line 1 1360-1363 Loss Measurements
Line 2 1360-1363 Loss Measurements
Line 1 1360-1204 Loss Measurements
Line 2 1360-1204 Loss Measurements
Line 1 1204-1375 Loss Measurements
Line 2 1204-1375 Loss Measurements
Line 1 1375-1380 Loss Measurements
Line 1 1150-1163 Loss Measurements
Line 1 1163-1365 Loss Measurements
Line 2 1163-1365 Loss Measurements
[Vabc_Voltage_Controlled]
[Iabc_Voltage_Controlled]
[Vabc_Swing_Bus]
[Iabc_Swing_Bus]
[Vabc_Bus_1314]
[Iabc_Bus_1314]
[Vabc_Bus_2390]
[Iabc_Bus_2390]
[Vabc_Bus_1163]
[Iabc_Bus_1163]
[Vabc_Bus_1317]
[Iabc_Bus_1317]
[Vabc_Bus_1365]
[Iabc_Bus_1365]
[Vabc_Bus_1360]
[Iabc_Bus_1360]
[Vabc_Bus_2573]
[Iabc_Bus_2573]
[Vabc_Bus_1204]
[Iabc_Bus_1204]
[Vabc_Bus_1279]
[Iabc_Bus_1279]
[Vabc_Bus_2935]
[Iabc_Bus_2935]
[Vabc_Bus_1298]
[Iabc_Bus_1298]
[Vabc_Bus_2400]
[Iabc_Bus_2400]
[Vabc_Bus_1375]
[Iabc_Bus_1375]
[Vabc_Bus_2441]
[Iabc_Bus_2441]
[Vabc_Bus_1380]
[Iabc_Bus_1380]

C.2 Developed MATLAB® Simulink® Modelling Blocks

Line z Bus x - y	Block Input Dialogue	Block Model Icon
		

Three-Fase Instantaneous RMS Measurement

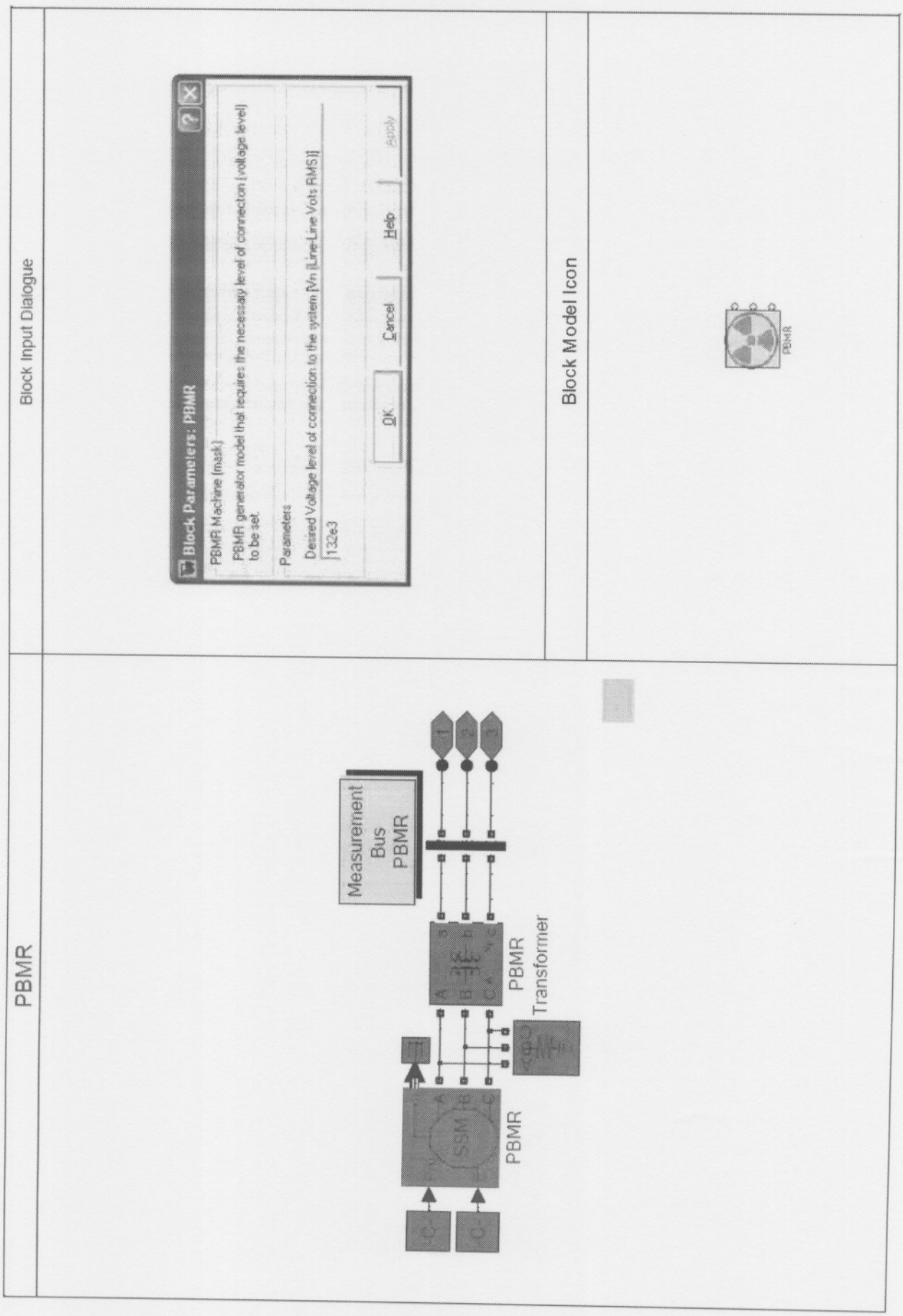
Block Input Dialogue

Block Model Icon

Non-linear Load

Block Input Dialogue

Block Model Icon


PBMR
Block Input Dialogue
Block Parameters: PBMR
PBMR Machine (mask)
PBMR generator model that requires the necessary level of connection (voltage level) to be set.
Parameters
Desired Voltage level of connection to the system [Vn (Line-Line Volts RMS)]
132e3
OK
Cancel
Help
Apply
Block Model Icon
PBMR
Measurement Bus PBMR
PBMR Transformer
PBMR

Appendix D Mathcad® 2001 Worksheets

Base Value Calculations:

The chosen base values for calculation of the relevant parameters of the model(s):

$S_{base} := 100 \cdot 10^6$ $f := 50$ $f = 50\,s\,Hz$ $T_s := 5 \cdot 10^{-5}$ $T_s = 5 \times 10^{-5}\,Hz\,s$

$V_{base} := 275 \cdot 10^3$ $I_{base} := \frac{S_{base}}{\sqrt{3} \cdot V_{base}}$ $I_{base} = 209.946\,\frac{1}{A}\,A$

$Z_{base} := \frac{V_{base}^2}{S_{base}}$ $Z_{base} = 756.25\,S\,\Omega$

$Y_{base} := \frac{1}{Z_{base}}$ $Y_{base} = 1.322 \times 10^{-3}\,\Omega\,mho$

Power flow initialization calculations:

{Test for violation of 1000 A limit of line currents}

$I_{thermal} := 1000$ $V_{n_400} := 400 \cdot 10^3$ $V_{n_275} := 275 \cdot 10^3$ $V_{n_132} := 132 \cdot 10^3$

$S_{thermal_400} := 3\left(\frac{V_{n_400}}{\sqrt{3}}\right) \cdot I_{thermal}$ $S_{thermal_400} = 692.82 \times 10^6$ $I_{base_400} := \frac{S_{base}}{\sqrt{3} \cdot V_{n_400}}$

$\therefore S_{thermal_400} := 690 \cdot 10^6$

$S_{thermal_275} := 3\left(\frac{V_{n_275}}{\sqrt{3}}\right) \cdot I_{thermal}$ $S_{thermal_275} = 476.314 \times 10^6$ $I_{base_275} := \frac{S_{base}}{\sqrt{3} \cdot V_{n_275}}$

$\therefore S_{thermal_275} := 475 \cdot 10^6$

$S_{thermal_132} := 3\left(\frac{V_{n_132}}{\sqrt{3}}\right) \cdot I_{thermal}$ $S_{thermal_132} = 228.631 \times 10^6$ $I_{base_132} := \frac{S_{base}}{\sqrt{3} \cdot V_{n_132}}$

$\therefore S_{thermal_132} := 225 \cdot 10^6$

$I_{thermal_pu_400} := \frac{I_{thermal}}{I_{base_400}}$ $I_{thermal_pu_400} = 6.928$

$I_{thermal_pu_275} := \frac{I_{thermal}}{I_{base_275}}$ $I_{thermal_pu_275} = 4.763$

$I_{thermal_pu_132} := \frac{I_{thermal}}{I_{base_132}}$ $I_{thermal_pu_132} = 2.286$

Scenario 1:

Line Parameter Calculations:

The following scenario is completely fictional, but the same ideology was used as for the scenario provided by ESKOM. Many of the values are from this scenario for realism's sake.
The following is true for every Line that is investigated in order to determine the line parameters:
Line *x*; with *x* specifying the line number.
Bus *y* to *z*; with *y* and *z* specifying the bus numbers from (*y*) to (*z*) for the line between them.
$Length_x$; the length of Line *x* in km with *x* as defined earlier.
R_x; with *R* the line resistance in per unit and *x* as defined earlier.
X_x; with *X* the line reactance in per unit and *x* as defined earlier.
B_x; with *B* the line susceptance in per unit and *x* as defined earlier.

Line 1; Bus 1 to 2:

$Length_1 := 87.78 \quad R_1 := 0.00722 \; X_1 := 0.03708 \; B_1 := 0.24060 \; 0.5B_1 = 0.1203$

$$R_{1real_km} := \frac{R_1 \cdot Z_{base}}{Length_1} \quad R_{1real_km} = 6.22024 \times 10^{-2}$$

$$X_{1real_km} := \frac{X_1 \cdot Z_{base}}{Length_1} \quad X_{1real_km} = 3.19455 \times 10^{-1} \quad L_1 := \frac{X_{1real_km}}{2 \cdot \pi \cdot f} \quad L_1 = 1.01686 \times 10^{-3}$$

$$B_{1real_km} := \frac{B_1 \cdot Y_{base}}{Length_1} \quad B_{1real_km} = 3.62439 \times 10^{-6} \quad C_1 := \frac{B_{1real_km}}{2 \cdot \pi \cdot f} \quad C_1 = 1.15368 \times 10^{-8}$$

Line 2; Bus 2 to 3:

$Length_2 := 133.88 \; R_2 := 0.01096 \; X_2 := 0.05645 \; B_2 := 0.36696 \; 0.5B_2 = 0.18348$

$$R_{2real_km} := \frac{R_2 \cdot Z_{base}}{Length_2} \quad R_{2real_km} = 6.19099 \times 10^{-2}$$

$$X_{2real_km} := \frac{X_2 \cdot Z_{base}}{Length_2} \quad X_{2real_km} = 3.1887 \times 10^{-1} \quad L_2 := \frac{X_{2real_km}}{2 \cdot \pi \cdot f} \quad L_2 = 1.01499 \times 10^{-3}$$

$$B_{2real_km} := \frac{B_2 \cdot Y_{base}}{Length_2} \quad B_{2real_km} = 3.62441 \times 10^{-6} \quad C_2 := \frac{B_{2real_km}}{2 \cdot \pi \cdot f} \quad C_2 = 1.15369 \times 10^{-8}$$

Line 3; Bus 3 to 4:

$Length_3 := 107.23 \; R_3 := 0.00878 \; X_3 := 0.04521 \; B_3 := 0.29392 \; 0.5B_3 = 0.14696$

$$R_{3real_km} := \frac{R_3 \cdot Z_{base}}{Length_3} \quad R_{3real_km} = 6.19218 \times 10^{-2}$$

$$X_{3real_km} := \frac{X_3 \cdot Z_{base}}{Length_3} \quad X_{3real_km} = 3.18848 \times 10^{-1} \quad L_3 := \frac{X_{3real_km}}{2 \cdot \pi \cdot f} \quad L_3 = 1.01492 \times 10^{-3}$$

$$B_{3real_km} := \frac{B_3 \cdot Y_{base}}{Length_3} \quad B_{3real_km} = 3.62449 \times 10^{-6} \quad C_3 := \frac{B_{3real_km}}{2 \cdot \pi \cdot f} \quad C_3 = 1.15371 \times 10^{-8}$$

Line 4; Bus 4 to 5:

$Length_4 := 166.80\ R_4 := 0.01365 X_4 := 0.07071 B_4 := 0.4548305 B_4 = 0.227415$

$$R_{4real_km} := \frac{R_4 \cdot Z_{base}}{Length_4} \quad R_{4real_km} = 6.18874 \times 10^{-2}$$

$$X_{4real_km} := \frac{X_4 \cdot Z_{base}}{Length_4} \quad X_{4real_km} = 3.2059 \times 10^{-1} \qquad L_4 := \frac{X_{4real_km}}{2 \cdot \pi \cdot f} \quad L_4 = 1.02047 \times 10^{-3}$$

$$B_{4real_km} := \frac{B_4 \cdot Y_{base}}{Length_4} \quad B_{4real_km} = 3.60568 \times 10^{-6} \qquad C_4 := \frac{B_{4real_km}}{2 \cdot \pi \cdot f} \quad C_4 = 1.14772 \times 10^{-8}$$

Machine equivalents for incoming line substitution calculations:

The values of the relevant constants describing the mathematical and theoretical machine models were chosen with the following in mind: Stability of the entire system; Substitution of chosen supply transmission lines by machines to cater for realistic power quality consequences and creating a limited power pool for the sources of the scenario. The values were chosen under advisement from: the study leader, experts in the field, the research material, available data sheets (PBMR), and Simulink examples in MATLAB.

Machine constants:

Swing Bus: $H_{Swing} := \infty \quad K_{d_Swing} := 0 \quad p_{Swing} := 1 \quad R_{Swing} := 0.007 \qquad L_{Swing} := 0.0526$

$$S_{base_Swing} := 1000 \cdot 10^6 \qquad V_{base_Swing} := 275 \cdot 10^3 \qquad X_{Swing} := 2 \cdot \pi \cdot f \cdot L_{Swing} \quad X_{Swing} = 16.525$$

$$Z_{base_Swing} := \frac{V_{base_Swing}^2}{S_{base_Swing}} \quad Z_{base_Swing} = 75.625\,S\Omega \qquad X_{pu_old_Swing} := \frac{X_{Swing}}{Z_{base_Swing}}$$

$$X_{pu_new_Swing} := X_{pu_old_Swing} \left(\frac{V_{base}}{V_{base_Swing}} \right)^2 \cdot \left(\frac{S_{base_Swing}}{S_{base}} \right) \quad X_{pu_new_Swing} = 2.185$$

PBMR: $H_{PBMR} := \infty \quad K_{d_PBMR} := 0 \quad p_{PBMR} := 1 \quad R_{PBMR} := 0.001 \quad L_{PBMR} := 0.18$

$$S_{base_PBMR} := 150 \cdot 10^6 \quad V_{base_PBMR} := 15 \cdot 10^3 \quad X_{PBMR} := 2 \cdot \pi \cdot f \cdot L_{PBMR} \quad X_{PBMR} = 56.549$$

$$Z_{base_PBMR} := \frac{V_{base_PBMR}^2}{S_{base_PBMR}} \quad Z_{base_PBMR} = 1.5\,S\Omega \qquad X_{pu_old_PBMR} := \frac{X_{PBMR}}{Z_{base_PBMR}}$$

$$X_{pu_new_PBMR} := X_{pu_old_PBMR} \left(\frac{V_{base_PBMR}}{V_{base}} \right)^2 \cdot \left(\frac{S_{base}}{S_{base_PBMR}} \right) \quad X_{pu_new_PBMR} = 0.075$$

Non-linear load calculations:

The scenario is supposedly part of the South African grid, therefore it has to meet the South African power quality standards, namely the NRS048 Power Quality Standards document. This standard/guideline states that for High-Voltage (HV) & Extra High-Voltage (EHV) networks the Total Harmonic Distortion (THD) should not exceed 3%:

$\therefore$ THD $\leq$ 3%

Bearing the above limit in mind the calculations that determine the size of the non-linear loads that introduce the harmonic components to the scenario were chosen such that these limits could be met after establishment of PBMR in the scenario aimed at improvement of Quality of Supply (QoS). Furthermore, NRS048 has a summarized table stating that there are limits for each harmonic order subject to the above rule mentioned earlier. The table is provided in the project report in the section that discusses the various power quality standards.

Distributed non-linear load calculations:

These loads are connected at the load buses in the system and gives the scenario a much more realistic appearance as the real case most usually is a distributed case of small non-linear loads.

{Test for violation of 1000 A limit of line currents} $V_n := 11 \cdot 10^3$

$$S_{thermal} := 3\left(\frac{V_n}{\sqrt{3}}\right) \cdot I_{thermal} \quad S_{thermal} = 19.053 \times 10^6 \quad \therefore S_{thermal} := 15 \cdot 10^6 \quad P_n := 15 \cdot 10^6$$

$3 \cdot 15 = 45$ {3 load buses available in the network and each drawing 15 MW amounting to 45 MW}

Values for Snubber Capacitances and -Resistances respectively:

$$C_S := \frac{P_n}{1000 \cdot (2 \cdot \pi \cdot f) \cdot V_n^2} \quad C_S < C_S \quad C_S = 3.946 \times 10^{-7} \quad \therefore C_S := 3.5 \cdot 10^{-7} \quad C_S = 350 \times 10^{-9} \frac{kg\,m^2}{s^4\,A^2} F$$

$$R_S := \frac{2 \cdot T_s}{C_S} \quad R_S > R_s \quad R_s = 285.714 \quad \therefore R_S := 300 \quad R_S = 300 \times 10^0 S\Omega$$

Value for the DC Resistance amounting to the required load drawn:

$$E_d := \frac{3 \cdot \sqrt{2}}{\pi} \cdot V_n \quad E_d = 14.855 \times 10^3 \frac{s^3 A}{kg\,m^2} V$$

$$R_{DC_Load} := \frac{E_d^2}{P_n} \quad R_{DC_Load} = 14.712\,S\Omega$$

Scenario 2:

Line Parameter Calculations:

The following scenario is completely fictional, but the same ideology was used as for the scenario provided by ESKOM. Many of the values are from this scenario for realism's sake.
The following is true for every Line that is investigated in order to determine the line parameters:
Line *x*; with *x* specifying the line number.
Bus *y* to *z*; with *y* and *z* specifying the bus numbers from (*y*) to (*z*) for the line between them.
$Length_x$; the length of Line *x* in km with *x* as defined earlier.
R_x; with *R* the line resistance in per unit and *x* as defined earlier.
X_x; with *X* the line reactance in per unit and *x* as defined earlier.
B_x; with *B* the line susceptance in per unit and *x* as defined earlier.

Line 1; Bus 1 to 4:

$Length_1 := 87.78 \quad R_1 := 0.00722 X_1 := 0.03708 B_1 := 0.24060\ 0.5B_1 = 0.1203$

$$R_{1real_km} := \frac{R_1 \cdot Z_{base}}{Length_1} \quad R_{1real_km} = 6.22024 \times 10^{-2}$$

$$X_{1real_km} := \frac{X_1 \cdot Z_{base}}{Length_1} \quad X_{1real_km} = 3.19455 \times 10^{-1} \quad L_1 := \frac{X_{1real_km}}{2 \cdot \pi \cdot f} \quad L_1 = 1.01686 \times 10^{-3}$$

$$B_{1real_km} := \frac{B_1 \cdot Y_{base}}{Length_1} \quad B_{1real_km} = 3.62439 \times 10^{-6} \quad C_1 := \frac{B_{1real_km}}{2 \cdot \pi \cdot f} \quad C_1 = 1.15368 \times 10^{-8}$$

Line 2; Bus 2 to 4:

$Length_2 := 133.88 \ R_2 := 0.01096 X_2 := 0.05645 B_2 := 0.36696\ 0.5B_2 = 0.18348$

$$R_{2real_km} := \frac{R_2 \cdot Z_{base}}{Length_2} \quad R_{2real_km} = 6.19099 \times 10^{-2}$$

$$X_{2real_km} := \frac{X_2 \cdot Z_{base}}{Length_2} \quad X_{2real_km} = 3.1887 \times 10^{-1} \quad L_2 := \frac{X_{2real_km}}{2 \cdot \pi \cdot f} \quad L_2 = 1.01499 \times 10^{-3}$$

$$B_{2real_km} := \frac{B_2 \cdot Y_{base}}{Length_2} \quad B_{2real_km} = 3.62441 \times 10^{-6} \quad C_2 := \frac{B_{2real_km}}{2 \cdot \pi \cdot f} \quad C_2 = 1.15369 \times 10^{-8}$$

Line 3; Bus 3 to 4:

$Length_3 := 68.05 \quad R_3 := 0.00557 X_3 := 0.02885 B_3 := 0.018556\ 0.5B_3 = 9.278 \times 10^{-3}$

$$R_{3real_km} := \frac{R_3 \cdot Z_{base}}{Length_3} \quad R_{3real_km} = 6.19003 \times 10^{-2}$$

$$X_{3real_km} := \frac{X_3 \cdot Z_{base}}{Length_3} \quad X_{3real_km} = 3.20614 \times 10^{-1} \quad L_3 := \frac{X_{3real_km}}{2 \cdot \pi \cdot f} \quad L_3 = 1.02055 \times 10^{-3}$$

$$B_{3real_km} := \frac{B_3 \cdot Y_{base}}{Length_3} \quad B_{3real_km} = 3.60571 \times 10^{-7} \quad C_3 := \frac{B_{3real_km}}{2 \cdot \pi \cdot f} \quad C_3 = 1.14773 \times 10^{-9}$$

Machine equivalents for incoming line substitution calculations:

Machine constants:

Swing Bus: $H_{Swing} := \infty$ $K_{d_Swing} := 0$ $p_{Swing} := 1$ $R_{Swing} := 0.02$ $L_{Swing} := 0.2354$

$S_{base_Swing} := 1000 \cdot 10^6$ $V_{base_Swing} := 400 \cdot 10^3$ $X_{Swing} := 2 \cdot \pi \cdot f \cdot L_{Swing}$ $X_{Swing} = 73.953$

$$Z_{base_Swing} := \frac{V_{base_Swing}^2}{S_{base_Swing}} \quad Z_{base_Swing} = 160\,S\Omega \quad X_{pu_old_Swing} := \frac{X_{Swing}}{Z_{base_Swing}}$$

$$X_{pu_new_Swing} := X_{pu_old_Swing} \cdot \left(\frac{V_{base}}{V_{base_Swing}}\right)^2 \cdot \left(\frac{S_{base_Swing}}{S_{base}}\right) \quad X_{pu_new_Swing} = 2.185$$

Voltage-Controlled Bus(es): $H_{VCtl} := \infty$ $K_{d_VCtl} := 0$ $p_{VCtl} := 1$ $R_{VCtl} := 0.02$ $L_{VCtl_1} := 0.08665$

$S_{base_VCtl} := 750 \cdot 10^6$ $V_{base_VCtl} := 275 \cdot 10^3$ $X_{VCtl_1} := 2 \cdot \pi \cdot f \cdot L_{VCtl_}$ $X_{VCtl_1} = 27.222$

$$Z_{base_VCtl} := \frac{V_{base_VCtl}^2}{S_{base_VCtl}} \quad Z_{base_VCtl} = 100.833\,S\Omega \quad X_{pu_old_VCtl_1} := \frac{X_{VCtl_1}}{Z_{base_VCtl}}$$

$$X_{pu_new_VCtl_1} := X_{pu_old_VCtl_1} \cdot \left(\frac{V_{base}}{V_{base_VCtl}}\right)^2 \cdot \left(\frac{S_{base_VCtl}}{S_{base}}\right) \quad X_{pu_new_VCtl_1} = 2.025$$

$L_{VCtl_2} := 0.0849$ $X_{VCtl_2} := 2 \cdot \pi \cdot f \cdot L_{VCtl_}$ $X_{VCtl_2} = 26.688$ $X_{pu_old_VCtl_2} := \frac{X_{VCtl_2}}{Z_{base_VCtl}}$

$$X_{pu_new_VCtl_2} := X_{pu_old_VCtl_2} \cdot \left(\frac{V_{base}}{V_{base_VCtl}}\right)^2 \cdot \left(\frac{S_{base_VCtl}}{S_{base}}\right) \quad X_{pu_new_VCtl_2} = 1.985$$

PBMR: $H_{PBMR} := \infty$ $K_{d_PBMR} := 0$ $p_{PBMR} := 1$ $R_{PBMR} := 0.001$ $L_{PBMR} := 0.18$

$S_{base_PBMR} := 150 \cdot 10^6$ $V_{base_PBMR} := 15 \cdot 10^3$ $X_{PBMR} := 2 \cdot \pi \cdot f \cdot L_{PBMR}$ $X_{PBMR} = 56.549$

$$Z_{base_PBMR} := \frac{V_{base_PBMR}^2}{S_{base_PBMR}} \quad Z_{base_PBMR} = 1.5\,S\Omega \quad X_{pu_old_PBMR} := \frac{X_{PBMR}}{Z_{base_PBMR}}$$

$$X_{pu_new_PBMR} := X_{pu_old_PBMR} \cdot \left(\frac{V_{base_PBMR}}{V_{base}}\right)^2 \cdot \left(\frac{S_{base}}{S_{base_PBMR}}\right) \quad X_{pu_new_PBMR} = 0.075$$

Non-linear load calculations:

The scenario is supposedly part of the South African grid, therefore it has to meet the South African power quality standards, namely the NRS048 Power Quality Standards document. This standard/guideline states that for High-Voltage (HV) & Extra High-Voltage (EHV) networks the Total Harmonic Distortion (THD) should not exceed 3%:

$\therefore$ THD $\leq 3\%$

Bearing the above limit in mind the calculations that determine the size of the non-linear loads that introduce the harmonic components to the scenario were chosen such that these limits could be met after establishment of PBMR in the scenario aimed at improvement of Quality of Supply (QoS). Furthermore, NRS048 has a summarized table stating that there are limits for each harmonic order subject to the above rule mentioned earlier. The table is provided in the project report in the section that discusses the various power quality standards.

Non-linear load at Bus 4:

This load is connected at the load bus in the system and accounts for the non-linear load portion of the existing load. This gives the scenario a much more realistic appearance as the real case most usually is a conventional load containing a sum of small non-linear loads.

{Test for violation of 1000 A limit of line currents} $V_n := 275 \cdot 10^3$

$$S_{thermal} := 3\left(\frac{V_n}{\sqrt{3}}\right) \cdot I_{thermal} \quad S_{thermal} = 476.314 \times 10^6 \quad \therefore S_{thermal} := 475 \cdot 10^6 \quad P_n := 475 \cdot 10^6$$

Values for Snubber Capacitance and -Resistance respectively:

$$C_s := \frac{P_n}{1000 \cdot (2 \cdot \pi \cdot f) \cdot V_n^2} \quad C_S < C_s \quad C_s = 1.999 \times 10^{-8} \quad \therefore C_S := 1.5 \cdot 10^{-8} \quad C_S = 15 \times 10^{-9} \frac{kg\,m^2}{s^4 A^2} F$$

$$R_s := \frac{2 \cdot T_s}{C_S} \quad R_S > R_s \quad R_s = 6.667 \times 10^3 \quad \therefore R_S := 7 \cdot 10^3 \quad R_S = 7 \times 10^3 \, S\Omega$$

Value for the DC Resistance amounting to the required load drawn:

$$E_d := \frac{3 \cdot \sqrt{2}}{\pi} \cdot V_n \quad E_d = 371.38 \times 10^3 \frac{s^3 A}{kg\,m^2} V$$

$$R_{DC_Load} := \frac{E_d^2}{P_n} \quad R_{DC_Load} = 290.365 \, S\Omega$$

Scenario 3:

Line Parameter Calculations:

All of the following information regarding the line parameters and the structure of the scenariowas kindly provided by ESKOM.
The following is true for every Line that is investigated in order to determine the line parameters:
Line *x*; with *x* specifying the line number.
Bus *y* to *z*; with *y* and *z* specifying the bus numbers from (*y*) to (*z*) for the line between them.
$Length_x$; the length of Line *x* in km with *x* as defined earlier.
R_x; with *R* the line resistance in per unit and*x* as defined earlier.
X_x; with *X* the line reactance in per unit and*x* as defined earlier.
B_x; with *B* the line susceptance in per unit and*x* as defined earlier.

Line 1; Bus 1163 to 1350:

$Length_1 := 147.01 \quad R_1 := 0.01207 \quad X_1 := 0.06310 \quad B_1 := 0.396550.5B_1 = 0.198275$

$$R_{1real_km} := \frac{R_1 \cdot Z_{base}}{Length_1} \quad R_{1real_km} = 6.20906 \times 10^{-2}$$

$$X_{1real_km} := \frac{X_1 \cdot Z_{base}}{Length_1} \quad X_{1real_km} = 3.246 \times 10^{-1} \qquad L_1 := \frac{X_{1real_km}}{2 \cdot \pi \cdot f} \quad L_1 = 1.03323 \times 10^{-3}$$

$$B_{1real_km} := \frac{B_1 \cdot Y_{base}}{Length_1} \quad B_{1real_km} = 3.56686 \times 10^{-6} \qquad C_1 := \frac{B_{1real_km}}{2 \cdot \pi \cdot f} \quad C_1 = 1.13537 \times 10^{-8}$$

Line 2; Bus 1163 to 1360:

$Length_2 := 68.30 \quad R_2 := 0.00561 \quad X_2 := 0.02892 \quad B_2 := 0.018631 \quad 0.5B_2 = 9.3155 \times 10^{-3}$

$$R_{2real_km} := \frac{R_2 \cdot Z_{base}}{Length_2} \quad R_{2real_km} = 6.21166 \times 10^{-2}$$

$$X_{2real_km} := \frac{X_2 \cdot Z_{base}}{Length_2} \quad X_{2real_km} = 3.20216 \times 10^{-1} \qquad L_2 := \frac{X_{2real_km}}{2 \cdot \pi \cdot f} \quad L_2 = 1.01928 \times 10^{-3}$$

$$B_{2real_km} := \frac{B_2 \cdot Y_{base}}{Length_2} \quad B_{2real_km} = 3.60703 \times 10^{-7} \qquad C_2 := \frac{B_{2real_km}}{2 \cdot \pi \cdot f} \quad C_2 = 1.14815 \times 10^{-9}$$

Line 3; Bus 1163 to 1360:

$Length_3 := 68.05 \quad R_3 := 0.00557 \quad X_3 := 0.02885 \quad B_3 := 0.018556 \quad 0.5B_3 = 9.278 \times 10^{-3}$

$$R_{3real_km} := \frac{R_3 \cdot Z_{base}}{Length_3} \quad R_{3real_km} = 6.19003 \times 10^{-2}$$

$$X_{3real_km} := \frac{X_3 \cdot Z_{base}}{Length_3} \quad X_{3real_km} = 3.20614 \times 10^{-1} \qquad L_3 := \frac{X_{3real_km}}{2 \cdot \pi \cdot f} \quad L_3 = 1.02055 \times 10^{-3}$$

$$B_{3real_km} := \frac{B_3 \cdot Y_{base}}{Length_3} \quad B_{3real_km} = 3.60571 \times 10^{-7} \qquad C_3 := \frac{B_{3real_km}}{2 \cdot \pi \cdot f} \quad C_3 = 1.14773 \times 10^{-9}$$

Line 4; Bus 1163 to 1365:

$Length_4 := 87.78 \quad R_4 := 0.00722 \; X_4 := 0.03708 \; B_4 := 0.24060 \; 0.5B_4 = 0.1203$

$$R_{4real_km} := \frac{R_4 \cdot Z_{base}}{Length_4} \quad R_{4real_km} = 6.22024 \times 10^{-2}$$

$$X_{4real_km} := \frac{X_4 \cdot Z_{base}}{Length_4} \quad X_{4real_km} = 3.19455 \times 10^{-1} \qquad L_4 := \frac{X_{4real_km}}{2 \cdot \pi \cdot f} \quad L_4 = 1.01686 \times 10^{-3}$$

$$B_{4real_km} := \frac{B_4 \cdot Y_{base}}{Length_4} \quad B_{4real_km} = 3.62439 \times 10^{-6} \qquad C_4 := \frac{B_{4real_km}}{2 \cdot \pi \cdot f} \quad C_4 = 1.15368 \times 10^{-8}$$

Line 5; Bus 1163 to 1365:

$Length_5 := 91.32 \quad R_5 := 0.00751 \; X_5 := 0.03858 \; B_5 := 0.25030 \; 0.5B_5 = 0.12515$

$$R_{5real_km} := \frac{R_5 \cdot Z_{base}}{Length_5} \quad R_{5real_km} = 6.21927 \times 10^{-2}$$

$$X_{5real_km} := \frac{X_5 \cdot Z_{base}}{Length_5} \quad X_{5real_km} = 3.19493 \times 10^{-1} \qquad L_5 := \frac{X_{5real_km}}{2 \cdot \pi \cdot f} \quad L_5 = 1.01698 \times 10^{-3}$$

$$B_{5real_km} := \frac{B_5 \cdot Y_{base}}{Length_5} \quad B_{5real_km} = 3.62435 \times 10^{-6} \qquad C_5 := \frac{B_{5real_km}}{2 \cdot \pi \cdot f} \quad C_5 = 1.15366 \times 10^{-8}$$

Line 6; Bus 1204 to 1365:

$Length_6 := 133.88 \quad R_6 := 0.01096 \; X_6 := 0.05645 \; B_6 := 0.36696 \; 0.5B_6 = 0.18348$

$$R_{6real_km} := \frac{R_6 \cdot Z_{base}}{Length_6} \quad R_{6real_km} = 6.19099 \times 10^{-2}$$

$$X_{6real_km} := \frac{X_6 \cdot Z_{base}}{Length_6} \quad X_{6real_km} = 3.1887 \times 10^{-1} \qquad L_6 := \frac{X_{6real_km}}{2 \cdot \pi \cdot f} \quad L_6 = 1.01499 \times 10^{-3}$$

$$B_{6real_km} := \frac{B_6 \cdot Y_{base}}{Length_6} \quad B_{6real_km} = 3.62441 \times 10^{-6} \qquad C_6 := \frac{B_{6real_km}}{2 \cdot \pi \cdot f} \quad C_6 = 1.15369 \times 10^{-8}$$

Line 7; Bus 1204 to 1365:

$Length_7 := 133.93 \quad R_7 := 0.01096 \; X_7 := 0.05678 \; B_7 := 0.36520 \; 0.5B_7 = 0.1826$

$$R_{7real_km} := \frac{R_7 \cdot Z_{base}}{Length_7} \quad R_{7real_km} = 6.18868 \times 10^{-2}$$

$$X_{7real_km} := \frac{X_7 \cdot Z_{base}}{Length_7} \quad X_{7real_km} = 3.20614 \times 10^{-1} \qquad L_7 := \frac{X_{7real_km}}{2 \cdot \pi \cdot f} \quad L_7 = 1.02055 \times 10^{-3}$$

$$B_{7real_km} := \frac{B_7 \cdot Y_{base}}{Length_7} \quad B_{7real_km} = 3.60568 \times 10^{-6} \qquad C_7 := \frac{B_{7real_km}}{2 \cdot \pi \cdot f} \quad C_7 = 1.14772 \times 10^{-8}$$

Line 8; Bus 1204 to 1375:

$Length_8 := 107.23 \quad R_8 := 0.00878 \quad X_8 := 0.04521 \quad B_8 := 0.29392 \quad 0.5B_8 = 0.14696$

$$R_{8real_km} := \frac{R_8 \cdot Z_{base}}{Length_8} \quad R_{8real_km} = 6.19218 \times 10^{-2}$$

$$X_{8real_km} := \frac{X_8 \cdot Z_{base}}{Length_8} \quad X_{8real_km} = 3.18848 \times 10^{-1} \qquad L_8 := \frac{X_{8real_km}}{2 \cdot \pi \cdot f} \quad L_8 = 1.01492 \times 10^{-3}$$

$$B_{8real_km} := \frac{B_8 \cdot Y_{base}}{Length_8} \quad B_{8real_km} = 3.62449 \times 10^{-6} \qquad C_8 := \frac{B_{8real_km}}{2 \cdot \pi \cdot f} \quad C_8 = 1.15371 \times 10^{-8}$$

Line 9; Bus 1204 to 1375:

$Length_9 := 89.78 \quad R_9 := 0.00740 \quad X_9 := 0.03699 \quad B_9 := 0.24847 \quad 0.5B_9 = 0.124235$

$$R_{9real_km} := \frac{R_9 \cdot Z_{base}}{Length_9} \quad R_{9real_km} = 6.23329 \times 10^{-2}$$

$$X_{9real_km} := \frac{X_9 \cdot Z_{base}}{Length_9} \quad X_{9real_km} = 3.1158 \times 10^{-1} \qquad L_9 := \frac{X_{9real_km}}{2 \cdot \pi \cdot f} \quad L_9 = 9.91791 \times 10^{-4}$$

$$B_{9real_km} := \frac{B_9 \cdot Y_{base}}{Length_9} \quad B_{9real_km} = 3.65956 \times 10^{-6} \qquad C_9 := \frac{B_{9real_km}}{2 \cdot \pi \cdot f} \quad C_9 = 1.16487 \times 10^{-8}$$

Line 10; Bus 1360 to 1363:

$Length_{10} := 110.47 \quad R_{10} := 0.00909 \quad X_{10} := 0.04667 \quad B_{10} := 0.30279 \quad 0.5B_{10} = 0.151395$

$$R_{10real_km} := \frac{R_{10} \cdot Z_{base}}{Length_{10}} \quad R_{10real_km} = 6.22279 \times 10^{-2}$$

$$X_{10real_km} := \frac{X_{10} \cdot Z_{base}}{Length_{10}} \quad X_{10real_km} = 3.19491 \times 10^{-1} \qquad L_{10} := \frac{X_{10real_km}}{2 \cdot \pi \cdot f} \quad L_{10} = 1.01697 \times 10^{-3}$$

$$B_{10real_km} := \frac{B_{10} \cdot Y_{base}}{Length_{10}} \quad B_{10real_km} = 3.62436 \times 10^{-6} \qquad C_{10} := \frac{B_{10real_km}}{2 \cdot \pi \cdot f} \quad C_{10} = 1.15367 \times 10^{-8}$$

Line 11; Bus 1375 to 1380:

$Length_{11} := 166.80 \quad R_{11} := 0.01365 \quad X_{11} := 0.07071 \quad B_{11} := 0.45483 \quad 0.5B_{11} = 0.227415 \quad GI_{pu} := 0.47000$

$$R_{11real_km} := \frac{R_{11} \cdot Z_{base}}{Length_{11}} \quad R_{11real_km} = 6.18874 \times 10^{-2}$$

$$X_{11real_km} := \frac{X_{11} \cdot Z_{base}}{Length_{11}} \quad X_{11real_km} = 3.2059 \times 10^{-1} \qquad L_{11} := \frac{X_{11real_km}}{2 \cdot \pi \cdot f} \quad L_{11} = 1.02047 \times 10^{-3}$$

$$B_{11real_km} := \frac{B_{11} \cdot Y_{base}}{Length_{11}} \quad B_{11real_km} = 3.60568 \times 10^{-6} \qquad C_{11} := \frac{B_{11real_km}}{2 \cdot \pi \cdot f} \quad C_{11} = 1.14772 \times 10^{-8}$$

$GI_{real} := GI_{pu} \cdot S_{base} \qquad GI_{real} = 47 \times 10^{6}$

Machine equivalents for incoming line substitution calculations:

The values of the relevant constants describing the mathematical and theoretical machine models were chosen with the following in mind: Stability of the entire system; Substitution of chosen supply transmission lines by machines to cater for realistic power quality consequences and creating a limited power pool for the sources of the scenario. The values were chosen under advisement from: the study leader, experts in the field, the research material, available data sheets (PBMR), and Simulink examples in MATLAB.

Machine constants:

Swing Bus: $H_{Swing} := \infty \quad K_{d_Swing} := 0 \quad p_{Swing} := 1 \quad R_{Swing} := 0.02 \quad L_{Swing} := 1.61625$

$S_{base_Swing} := 1000 \cdot 10^6 \quad V_{base_Swing} := 400 \cdot 10^3 \quad X_{Swing} := 2 \cdot \pi \cdot f \cdot L_{Swing} \quad X_{Swing} = 507.76$

$$Z_{base_Swing} := \frac{V_{base_Swing}^2}{S_{base_Swing}} \quad Z_{base_Swing} = 160\,S\Omega \quad X_{pu_old_Swing} := \frac{X_{Swing}}{Z_{base_Swing}}$$

$$X_{pu_new_Swing} := X_{pu_old_Swing}\left(\frac{V_{base}}{V_{base_Swing}}\right)^2 \cdot \left(\frac{S_{base_Swing}}{S_{base}}\right) \quad X_{pu_new_Swing} = 15$$

Voltage-Controlled Bus: $H_{VCtl} := \infty \quad K_{d_VCtl} := 0 \quad p_{VCtl} := 1 \quad R_{VCtl} := 0.02 \quad L_{VCtl} := 0.7222$

$S_{base_VCtl} := 500 \cdot 10^6 \quad V_{base_VCtl} := 275 \cdot 10^3 \quad X_{VCtl} := 2 \cdot \pi \cdot f \cdot L_{VCtl} \quad X_{VCtl} = 226.886$

$$Z_{base_VCtl} := \frac{V_{base_VCtl}^2}{S_{base_VCtl}} \quad Z_{base_VCtl} = 151.25\,S\Omega \quad X_{pu_old_VCtl} := \frac{X_{VCtl}}{Z_{base_VCtl}}$$

$$X_{pu_new_VCtl} := X_{pu_old_VCtl}\left(\frac{V_{base}}{V_{base_VCtl}}\right)^2 \cdot \left(\frac{S_{base_VCtl}}{S_{base}}\right) \quad X_{pu_new_VCtl} = 7.5$$

PBMR: $H_{PBMR} := \infty \quad K_{d_PBMR} := 0 \quad p_{PBMR} := 1 \quad R_{PBMR} := 0.001 \quad L_{PBMR} := 0.18$

$S_{base_PBMR} := 150 \cdot 10^6 \quad V_{base_PBMR} := 15 \cdot 10^3 \quad X_{PBMR} := 2 \cdot \pi \cdot f \cdot L_{PBMR} \quad X_{PBMR} = 56.549$

$$Z_{base_PBMR} := \frac{V_{base_PBMR}^2}{S_{base_PBMR}} \quad Z_{base_PBMR} = 1.5\,S\Omega \quad X_{pu_old_PBMR} := \frac{X_{PBMR}}{Z_{base_PBMR}}$$

$$X_{pu_new_PBMR} := X_{pu_old_PBMR}\left(\frac{V_{base_PBMR}}{V_{base}}\right)^2 \cdot \left(\frac{S_{base}}{S_{base_PBMR}}\right) \quad X_{pu_new_PBMR} = 0.075$$

Non-linear load calculations:

The scenario is part of the South African grid, therefore it has to meet the South African power quality standards, namely the NRS048 Power Quality Standards document. This standard/guideline states that for High-Voltage (HV) & Extra High-Voltage (EHV) networks the Total Harmonic Distortion (THD) should not exceed 3%:

$\therefore$ THD $\leq$ 3%

Bearing the above limit in mind the calculations that determine the size of the non-linear loads that introduce the harmonic components to the scenario were chosen such that these limits could be met after establishment of PBMR in the scenario aimed at improvement of Quality of Supply (QoS). Furthermore, NRS048 has a summarized table stating that there are limits for each harmonic order subject to the above rule mentioned earlier. The table is provided in the project report in the section that discusses the various power quality standards.

Non-linear load at Harvard 1 (Bus 2575):

{Test for violation of 1000 A limit of line currents} $V_n := 32 \cdot 10^3$

$S_{thermal} := 3\left(\frac{V_n}{\sqrt{3}}\right) \cdot I_{thermal}$ $S_{thermal} = 55.426 \times 10^6 \frac{s^3}{kg\,m^2} W$ $\therefore S_{thermal} := 50 \cdot 10^6$ $P_n := 50 \cdot 10^6$

Values for Snubber Capacitances and -Resistances respectively:

$C_s := \frac{P_n}{1000 \cdot (2 \cdot \pi \cdot f) \cdot V_n^2}$ $C_S < C_s$ $C_s = 1.554 \times 10^{-7}$ $\therefore C_S := 1.5 \cdot 10^{-7}$ $C_S = 150 \times 10^{-9} \frac{kg\,m^2}{s^4 A^2} F$

$R_s := \frac{2 \cdot T_s}{C_S}$ $R_S > R_s$ $R_s = 666.667$ $\therefore R_S := 700$ $R_S = 700 \times 10^0 S\Omega$

Value for the DC Resistance amounting to the required load drawn:

$E_d := \frac{3}{\pi} \cdot \sqrt{2} \cdot V_n$ $E_d = 43.215 \times 10^3 \frac{s^3 A}{kg\,m^2} V$

$R_{Harvard_1} := \frac{E_d^2}{P_n}$ $R_{Harvard_1} = 37.351\ S\Omega$

Distributed non-linear load calculations:

These loads are connected at the smaller buses in the system and gives the scenario a much more realistic appearance as the real case most usually is a distributed case of small non-linear loads.

{Test for violation of 1000 A limit of line currents} $V_n := 11 \cdot 10^3$

$S_{thermal} := 3\left(\frac{V_n}{\sqrt{3}}\right) \cdot I_{thermal}$ $S_{thermal} = 19.053 \times 10^6$ $\therefore S_{thermal} := 15 \cdot 10^6$ $P_n := 15 \cdot 10^6$

$7 \cdot 15 = 105$ {7 load buses available in the network and each drawing 15 MW amounting to 105 MW}

Values for Snubber Capacitances and -Resistances respectively:

$C_s := \frac{P_n}{1000 \cdot (2 \cdot \pi \cdot f) \cdot V_n^2}$ $C_S < C_s$ $C_s = 3.946 \times 10^{-7}$ $\therefore C_S := 3.5 \cdot 10^{-7}$ $C_S = 350 \times 10^{-9} \frac{kg\,m^2}{s^4 A^2} F$

$R_s := \frac{2 \cdot T_s}{C_S}$ $R_S > R_s$ $R_s = 285.714$ $\therefore R_S := 300$ $R_S = 300 \times 10^0 S\Omega$

Value for the DC Resistance amounting to the required load drawn:

$E_d := \frac{3 \cdot \sqrt{2}}{\pi} \cdot V_n$ $E_d = 14.855 \times 10^3 \frac{s^3 A}{kg\,m^2} V$

$R_{DC_Load} := \frac{E_d^2}{P_n}$ $R_{DC_Load} = 14.712\,S\Omega$

Appendix E Data provided by ESKOM for Scenario 3

```
BUS DATA
   I, 'BUS NAME', BASKV,
  335,'PERSS4  ', 400
 1163,'PERSS7  ', 275
 1204,'OLIEN2  ', 275
 1270,'BNDRY1  ', 132
 1299,'MERAP1  ', 132
 1314,'PERSS 5A',  30
 1317,'PERSS 5B',  30
 1350,'EVRST2  ', 275
 1360,'HARVR2  ', 275
 1363,'MERAP2  ', 275
 1365,'BNDRY2  ', 275
 1375,'FERRM2  ', 275
 1380,'GARN2   ', 275
 2390,'EVRST1  ', 132
 2400,'FERRM1  ', 132
 2441,'GARN1   ', 132
 2575,'HARVR1  ', 132
 2935,'OLIEN1  ', 132
0 / END OF BUS DATA, BEGIN LOAD DATA

 LOAD DATA
 I,       P,       Q,
 1163    3.000,   0.680
 1375   22.000,   5.010
 1380    1.400,   0.320
 1575  263.600,  60.080
0 / END OF LOAD DATA, BEGIN BRANCH DATA

 NON-TRANSFORMER BRANCH DATA
 I,     J,  CKT,      R,         X,         B,      RATEA,   RATEB,         GI,       LEN,
 1163, 1350,'1 ',   0.01207,   0.06312,   0.39655,  478.20,  628.70,      0.00000,   147.01
 1163, 1360,'1 ',   0.00561,   0.02940,   0.18031,  478.20,  628.70,      0.00000,    68.30
 1163, 1360,'2 ',   0.00557,   0.02885,   0.18556,  478.20,  628.70,      0.00000,    68.05
 1163, 1365,'1 ',   0.00722,   0.03709,   0.24060,  478.20,  628.70,      0.00000,    87.78
 1163, 1365,'2 ',   0.00751,   0.03855,   0.25039,  478.20,  628.70,      0.00000,    91.32
 1204, 1365,'1 ',   0.01096,   0.05645,   0.36696,  478.20,  628.70,      0.00000,   133.88
 1204, 1365,'2 ',   0.01096,   0.05678,   0.36570,  478.20,  628.70,      0.00000,   133.93
 1204, 1375,'1 ',   0.00878,   0.04521,   0.29330,  478.20,  628.70,      0.00000,   107.23
 1204, 1375,'2 ',   0.00740,   0.03699,   0.24847,  227.70,  299.60,      0.00000,    89.39
 1360, 1363,'1 ',   0.00909,   0.04667,   0.30279,  478.20,  628.70,      0.00000,   110.47
 1375, 1380,'1 ',   0.01365,   0.07071,   0.45483,  478.20,  628.70,     -0.47000,   166.80
0 / END OF BRANCH DATA, BEGIN TRANSFORMER DATA

 TRANSFORMER DATA
  I,     J,  CKT, LINE X, MVA BASE, RATEA,    RATEB,     VMAX,     VMIN,     NUMBER TAPS
  335, 1163, 1, 0.00393,   100.00  400.00,   480.00,   1.05000, 1.00000,   17,
  335, 1163, 2, 0.00395,   100.00  400.00,   480.00,   1.05000, 1.00000,   17,
  335, 1163, 3, 0.02650,   100.00  400.00,   480.00,   1.05000, 1.00000,   17,
  335, 1314, 1, 0.01000,   100.00  300.00,   360.00,   1.05000, 1.00000,    9,
  335, 1317, 1, 0.01000,   100.00  300.00,   360.00,   1.05000, 1.00000,    9,
 1204, 2935, 1, 0.06200,   100.00  180.00,   180.00,   1.05000, 1.00000,   17,
 1204, 2935, 2, 0.06200,   100.00  180.00,   180.00,   1.05000, 1.00000,   17,
 1365, 1270, 1, 0.04680,   100.00  250.00,   300.00,   1.05000, 1.00000,   17,
 1365, 1270, 2, 0.04770,   100.00  250.00,   300.00,   1.05000, 1.00000,   17,
 1363, 1299, 1, 0.05677,   100.00  180.00,   216.00,   1.05000, 1.00000,   13,
 1363, 1299, 2, 0.05684,   100.00  180.00,   216.00,   1.05000, 1.00000,   13,
 1350, 2390, 1, 0.02500,   100.00  500.00,   600.00,   1.05000, 1.00000,   17,
 1350, 2390, 2, 0.02500,   100.00  500.00,   600.00,   1.05000, 1.00000,   17,
 1360, 2575, 1, 0.02360,   100.00  500.00,   600.00,   1.05000, 1.00000,   17,
 1360, 2575, 2, 0.02340,   100.00  500.00,   600.00,   1.05000, 1.00000,   17,
 1375, 2400, 1, 0.04640,   100.00  250.00,   300.00,   1.05000, 1.00000,   17,
 1375, 2400, 2, 0.04720,   100.00  250.00,   300.00,   1.05000, 1.00000,   17,
 1380, 2441, 1, 0.09760,   100.00  125.00,   150.00,   1.05000, 1.00000,   17,
0 / END OF TRANSFORMER DATA, BEGIN SWITCHED SHUNT DATA

 SWITCHED SHUNT DATA
 I,    VSWHI,   VSWLO,    BINIT,  N1,   B1
  335,1.05000,1.00000, -100.00,  3,-100.00
 1299,1.05000,1.00000,    0.00,  1,   18.00
 1314,1.05000,1.00000,    0.00,  2,  100.00
 1317,1.05000,1.00000,    0.00,  2,  100.00
 2390,1.05000,1.00000,   72.00,  2,   72.00
```

Appendix F Comparing Load Flow Analysis and Simulation Results

Regardless of how accurate the estimates of the initial values for the iterative techniques were, the iterative analysis could not accurately determine the load flow solutions for Scenario 1 (for slight to moderate levels of harmonic distortion – 3-5% *THD*). The calculated errors exceeded the scientifically acceptable margin of 5% as is applicable for this kind of studies.

Power Flow Solution by Newton-Raphson Method
Maximum Power Mismatch = 7.52751e-008
No. of Iterations = 5

Bus No.	Voltage Mag.	Angle Degree	Load MW	Load Mvar	Generation MW	Generation Mvar	Injected Mvar
1	1.073	0.000	0.000	0.000	590.521	-138.102	230.000
2	1.047	-10.605	0.000	0.000	0.000	0.000	0.000
3	1.031	-26.896	0.000	0.000	0.000	0.000	0.000
4	1.016	-38.194	0.000	0.000	0.000	0.000	0.000
5	1.039	-44.759	0.000	0.000	0.000	0.000	0.000
6	1.067	-1.179	29.616	6.744	0.000	0.000	0.000
7	1.046	-10.793	4.506	1.021	0.000	0.000	0.000
8	1.019	-29.299	55.343	12.805	0.000	0.000	0.000
9	0.930	-51.457	272.575	62.100	0.000	0.000	0.000
10	0.997	-51.627	155.845	38.896	0.000	0.000	0.000
11	1.013	0.080	0.000	0.000	0.000	224.224	-300.000
12	1.087	-10.661	0.000	0.000	0.000	45.074	10.000
13	1.121	-27.022	0.000	0.000	0.000	86.984	40.000
14	1.126	-38.348	0.000	0.000	0.000	63.728	90.000
15	1.122	-44.874	0.000	0.000	0.000	87.171	30.000
Total			517.885	121.566	590.521	369.079	100.000

Line Flow and Losses

--Line-- from	to	Power at bus & line flow MW	Mvar	MVA	--Line loss-- MW	Mvar	Transformer tap
1		590.521	91.898	597.629			
	2	560.776	4.252	560.793	19.751	74.415	
	6	29.632	7.392	30.540	0.016	0.648	
	11	0.112	80.254	80.254	0.112	4.478	
2		0.000	0.000	0.000			
	1	-541.025	70.164	545.556	19.751	74.415	
	3	536.467	-18.180	536.775	28.796	108.723	
	7	4.507	1.037	4.625	0.000	0.016	
	12	0.051	-53.021	53.021	0.051	2.053	
3		0.000	0.000	0.000			
	2	-507.671	126.903	523.292	28.796	108.723	
	4	452.009	-25.470	452.726	16.891	56.183	
	8	55.405	15.292	57.477	0.062	2.487	
	13	0.256	-116.725	116.725	0.256	10.259	
4		0.000	0.000	0.000			
	3	-435.118	81.653	442.713	16.891	56.183	
	5	160.362	-77.254	178.001	3.781	-28.453	
	9	274.383	134.406	305.533	1.808	72.305	
	14	0.373	-138.805	138.806	0.373	14.923	
5		0.000	0.000	0.000			
	4	-156.582	48.801	164.010	3.781	-28.453	
	10	156.364	59.653	167.356	0.519	20.757	
	15	0.218	-108.454	108.454	0.218	8.717	
6		-29.616	-6.744	30.374			
	1	-29.616	-6.744	30.374	0.016	0.648	
7		-4.506	-1.021	4.621			
	2	-4.506	-1.021	4.621	0.000	0.016	

8	-55.343	-12.805	56.805			
3	-55.343	-12.805	56.805	0.062	2.487	
9	-272.575	-62.100	279.560			
4	-272.575	-62.100	279.560	1.808	72.305	
10	-155.845	-38.896	160.625			
5	-155.845	-38.896	160.625	0.519	20.757	
11	0.000	-75.776	75.776			
1	0.000	-75.776	75.776	0.112	4.478	
12	0.000	55.074	55.074			
2	0.000	55.074	55.074	0.051	2.053	
13	0.000	126.984	126.984			
3	-0.000	126.984	126.984	0.256	10.259	
14	0.000	153.728	153.728			
4	0.000	153.728	153.728	0.373	14.923	
15	0.000	117.171	117.171			
5	-0.000	117.171	117.171	0.218	8.717	
Total loss			72.635	347.512		

Power Flow Solution by Newton-Raphson Method
Maximum Power Mismatch = 3.68574e-005
No. of Iterations = 6

Bus No.	Voltage Mag.	Angle Degree	Load MW	Load Mvar	Generation MW	Generation Mvar	Injected Mvar
1	1.003	0.001	0.000	0.000	625.239	-23.250	230.000
2	0.932	-13.014	0.000	0.000	0.000	0.000	0.000
3	0.865	-35.348	0.000	0.000	0.000	0.000	0.000
4	0.823	-52.149	0.000	0.000	0.000	0.000	0.000
5	0.862	-62.219	0.000	0.000	0.000	0.000	0.000
6	0.997	-1.349	29.616	6.744	0.000	0.000	0.000
7	0.931	-13.250	4.506	1.021	0.000	0.000	0.000
8	0.850	-38.778	55.343	12.805	0.000	0.000	0.000
9	0.676	-75.105	272.575	62.100	0.000	0.000	0.000
10	0.805	-72.503	155.845	38.896	0.000	0.000	0.000
11	0.947	0.080	0.000	0.000	0.000	233.715	-300.000
12	1.001	-13.119	0.000	0.000	0.000	75.672	10.000
13	1.009	-35.586	0.000	0.000	0.000	141.665	40.000
14	1.005	-52.466	0.000	0.000	0.000	138.533	90.000
15	0.999	-62.447	0.000	0.000	0.000	140.759	30.000
Total			517.885	121.566	625.239	707.093	100.000

Line Flow and Losses

--Line-- from	to	Power at bus & line flow MW	Mvar	MVA	--Line loss-- MW	Mvar	Transformer tap
1		625.239	206.750	658.536			
	2	595.509	129.067	609.336	26.866	115.410	
	6	29.635	7.486	30.566	0.019	0.742	
	11	0.098	70.202	70.202	0.098	3.917	
2		0.000	0.000	0.000			
	1	-568.644	-13.657	568.808	26.866	115.410	
	3	563.990	92.427	571.513	41.597	184.569	
	7	4.507	1.041	4.626	0.000	0.020	
	12	0.147	-79.811	79.811	0.147	5.864	
3		0.000	0.000	0.000			
	2	-522.393	92.142	530.457	41.597	184.569	
	4	466.313	47.229	468.698	25.903	112.434	
	8	55.432	16.375	57.800	0.089	3.570	
	13	0.648	-155.747	155.748	0.648	25.925	
4		0.000	0.000	0.000			

	3	-440.410	65.205	445.211	25.903	112.434
	5	163.378	-77.055	180.637	6.152	-0.404
	9	275.997	198.986	340.249	3.422	136.885
	14	1.035	-187.135	187.138	1.035	41.408
5		0.000	0.000	0.000		
	4	-157.225	76.651	174.915	6.152	-0.404
	10	156.640	70.717	171.864	0.796	31.821
	15	0.585	-147.368	147.370	0.585	23.397
6		-29.616	-6.744	30.374		
	1	-29.616	-6.744	30.374	0.019	0.742
7		-4.506	-1.021	4.621		
	2	-4.506	-1.021	4.621	0.000	0.020
8		-55.343	-12.805	56.805		
	3	-55.343	-12.805	56.805	0.089	3.570
9		-272.575	-62.100	279.560		
	4	-272.575	-62.100	279.560	3.422	136.885
10		-155.845	-38.896	160.625		
	5	-155.845	-38.896	160.625	0.796	31.821
11		0.000	-66.285	66.285		
	1	0.000	-66.285	66.285	0.098	3.917
12		0.000	85.672	85.672		
	2	0.000	85.675	85.675	0.147	5.864
13		0.000	181.665	181.665		
	3	0.000	181.672	181.672	0.648	25.925
14		0.000	228.533	228.533		
	4	0.000	228.544	228.544	1.035	41.408
15		0.000	170.759	170.759		
	5	0.000	170.766	170.766	0.585	23.397
Total loss				107.357	685.560	

Power Flow Solution by Newton-Raphson Method
Maximum Power Mismatch = 3.79105e-005
No. of Iterations = 6

Bus No.	Voltage Mag.	Angle Degree	Load MW	Load Mvar	Generation MW	Generation Mvar	Injected Mvar
1	1.003	0.000	0.000	0.000	625.219	-23.355	230.000
2	0.932	-13.013	0.000	0.000	0.000	0.000	0.000
3	0.865	-35.343	0.000	0.000	0.000	0.000	0.000
4	0.822	-52.141	0.000	0.000	0.000	0.000	0.000
5	0.861	-62.215	0.000	0.000	0.000	0.000	0.000
6	0.997	-1.349	29.616	6.744	0.000	0.000	0.000
7	0.931	-13.250	4.506	1.021	0.000	0.000	0.000
8	0.850	-38.772	55.343	12.805	0.000	0.000	0.000
9	0.675	-75.115	272.575	62.100	0.000	0.000	0.000
10	0.805	-72.518	155.845	38.896	0.000	0.000	0.000
11	0.947	0.080	0.000	0.000	0.000	233.712	-300.000
12	1.001	-13.118	0.000	0.000	0.000	75.613	10.000
13	1.010	-35.582	0.000	0.000	0.000	142.588	40.000
14	1.005	-52.458	0.000	0.000	0.000	138.757	90.000
15	0.997	-62.442	0.000	0.000	0.000	140.010	30.000
Total			517.885	121.566	625.219	707.325	100.000

Line Flow and Losses

From	To	Power at bus & line flow MW	Mvar	MVA	Line loss MW	Mvar	Transformer tap
1		625.219	206.645	658.484			
	2	595.489	128.959	609.293	26.861	115.384	
	6	29.635	7.486	30.566	0.019	0.742	

```
   11  0.098  70.205  70.205   0.098   3.917

2      0.000   0.000   0.000
   1 -568.628 -13.575 568.790  26.861 115.384
   3  563.975  92.294 571.477  41.586 184.508
   7    4.507   1.041   4.626   0.000   0.020
  12    0.146 -79.760  79.760   0.146   5.856

3      0.000   0.000   0.000
   2 -522.388  92.213 530.465  41.586 184.508
   4  466.303  47.858 468.752  25.903 112.435
   8   55.432  16.374  57.800   0.089   3.569
  13    0.654 -156.445 156.447   0.654  26.150

4      0.000   0.000   0.000
   3 -440.400  64.577 445.109  25.903 112.435
   5  163.362 -76.423 180.354   6.139  -0.436
   9  276.000 199.122 340.332   3.426 137.022
  14    1.037 -187.276 187.279   1.037  41.492

5      0.000   0.000   0.000
   4 -157.223  75.987 174.623   6.139  -0.436
  10  156.642  70.782 171.892   0.797  31.886
  15    0.581 -146.770 146.771   0.581  23.247

6     -29.616  -6.744  30.374
   1  -29.616  -6.744  30.374   0.019   0.742

7      -4.506  -1.021   4.621
   2   -4.506  -1.021   4.621   0.000   0.020

8     -55.343 -12.805  56.805
   3  -55.343 -12.805  56.805   0.089   3.569

9    -272.575 -62.100 279.560
   4 -272.575 -62.100 279.560   3.426 137.022

10    -155.845 -38.896 160.625
   5 -155.845 -38.896 160.625   0.797  31.886

11     0.000 -66.288  66.288
   1   0.000 -66.288  66.288   0.098   3.917

12     0.000  85.613  85.613
   2   0.000  85.616  85.616   0.146   5.856

13     0.000 182.588 182.588
   3   0.000 182.595 182.595   0.654  26.150

14     0.000 228.757 228.757
   4   0.000 228.768 228.768   1.037  41.492

15     0.000 170.010 170.010
   5   0.000 170.017 170.017   0.581  23.247

Total loss                   107.336 685.793
```

Power Flow Solution by Newton-Raphson Method
Maximum Power Mismatch = 7.57149e-008
No. of Iterations = 5

Bus No.	Voltage Mag.	Angle Degree	Load MW	Load Mvar	Generation MW	Generation Mvar	Injected Mvar
1	1.073	0.000	0.000	0.000	590.523	-138.103	230.000
2	1.047	-10.605	0.000	0.000	0.000	0.000	0.000
3	1.031	-26.896	0.000	0.000	0.000	0.000	0.000
4	1.016	-38.194	0.000	0.000	0.000	0.000	0.000
5	1.039	-44.759	0.000	0.000	0.000	0.000	0.000
6	1.067	-1.179	29.616	6.744	0.000	0.000	0.000
7	1.046	-10.793	4.506	1.021	0.000	0.000	0.000
8	1.019	-29.299	55.343	12.667	0.000	0.000	0.000
9	0.930	-51.459	272.575	62.119	0.000	0.000	0.000
10	0.997	-51.632	155.846	39.224	0.000	0.000	0.000
11	1.013	0.080	0.000	0.000	0.000	224.224	-300.000
12	1.087	-10.661	0.000	0.000	0.000	45.073	10.000

13	1.121	-27.022	0.000	0.000	0.000	86.981	40.000
14	1.126	-38.348	0.000	0.000	0.000	63.810	90.000
15	1.122	-44.875	0.000	0.000	0.000	87.410	30.000
Total			517.887	121.776	590.523	369.395	100.000

Line Flow and Losses

--Line-- from	to	Power at bus & line flow MW	Mvar	MVA	--Line loss-- MW	Mvar	Transformer tap
1		590.523	91.897	597.631			
	2	560.779	4.250	560.795	19.751	74.416	
	6	29.632	7.393	30.541	0.016	0.648	
	11	0.112	80.254	80.254	0.112	4.478	
2		0.000	0.000	0.000			
	1	-541.027	70.166	545.558	19.751	74.416	
	3	536.469	-18.183	536.777	28.796	108.724	
	7	4.507	1.037	4.625	0.000	0.016	
	12	0.051	-53.020	53.020	0.051	2.053	
3		0.000	0.000	0.000			
	2	-507.673	126.907	523.294	28.796	108.724	
	4	452.011	-25.336	452.721	16.891	56.184	
	8	55.405	15.152	57.440	0.062	2.484	
	13	0.256	-116.723	116.723	0.256	10.258	
4		0.000	0.000	0.000			
	3	-435.120	81.520	442.691	16.891	56.184	
	5	160.363	-77.089	177.930	3.779	-28.452	
	9	274.383	134.440	305.549	1.808	72.321	
	14	0.373	-138.871	138.871	0.373	14.939	
5		0.000	0.000	0.000			
	4	-156.584	48.637	163.964	3.779	-28.452	
	10	156.366	60.020	167.489	0.520	20.797	
	15	0.219	-108.658	108.658	0.219	8.753	
6		-29.616	-6.744	30.374			
	1	-29.616	-6.744	30.374	0.016	0.648	
7		-4.506	-1.021	4.621			
	2	-4.506	-1.021	4.621	0.000	0.016	
8		-55.343	-12.667	56.774			
	3	-55.343	-12.667	56.774	0.062	2.484	
9		-272.575	-62.119	279.564			
	4	-272.575	-62.119	279.564	1.808	72.321	
10		-155.846	-39.224	160.706			
	5	-155.846	-39.224	160.706	0.520	20.797	
11		0.000	-75.776	75.776			
	1	0.000	-75.776	75.776	0.112	4.478	
12		0.000	55.073	55.073			
	2	0.000	55.073	55.073	0.051	2.053	
13		0.000	126.981	126.981			
	3	0.000	126.981	126.981	0.256	10.258	
14		0.000	153.810	153.810			
	4	-0.000	153.810	153.810	0.373	14.939	
15		0.000	117.410	117.410			
	5	0.000	117.410	117.410	0.219	8.753	
Total loss				72.636	347.620		

Power Flow Solution by Newton-Raphson Method
Maximum Power Mismatch = 3.79069e-005
No. of Iterations = 6

Bus No.	Voltage Mag.	Angle Degree	Load MW	Load Mvar	Generation MW	Generation Mvar	Injected Mvar
1	1.003	0.001	0.000	0.000	625.270	-23.186	230.000
2	0.932	-13.014	0.000	0.000	0.000	0.000	0.000
3	0.865	-35.351	0.000	0.000	0.000	0.000	0.000
4	0.822	-52.156	0.000	0.000	0.000	0.000	0.000
5	0.861	-62.231	0.000	0.000	0.000	0.000	0.000
6	0.997	-1.349	29.616	6.744	0.000	0.000	0.000
7	0.931	-13.251	4.506	1.021	0.000	0.000	0.000
8	0.850	-38.782	55.343	12.667	0.000	0.000	0.000
9	0.676	-75.129	272.575	62.119	0.000	0.000	0.000
10	0.805	-72.526	155.846	39.224	0.000	0.000	0.000
11	0.947	0.080	0.000	0.000	0.000	233.715	-300.000
12	1.001	-13.120	0.000	0.000	0.000	75.701	10.000
13	1.009	-35.590	0.000	0.000	0.000	141.739	40.000
14	1.005	-52.474	0.000	0.000	0.000	138.748	90.000
15	0.999	-62.459	0.000	0.000	0.000	141.125	30.000
Total			517.887	121.776	625.270	707.843	100.000

Line Flow and Losses

--Line-- from	to	Power at bus & line flow MW	Mvar	MVA	--Line loss-- MW	Mvar	Transformer tap
1		625.270	206.814	658.585			
	2	595.540	129.131	609.379	26.870	115.431	
	6	29.635	7.487	30.566	0.019	0.742	
	11	0.098	70.202	70.202	0.098	3.917	
2		0.000	0.000	0.000			
	1	-568.671	-13.700	568.836	26.870	115.431	
	3	564.017	92.495	571.551	41.605	184.612	
	7	4.507	1.041	4.626	0.000	0.020	
	12	0.147	-79.836	79.836	0.147	5.868	
3		0.000	0.000	0.000			
	2	-522.412	92.117	530.471	41.605	184.612	
	4	466.331	47.450	468.739	25.911	112.484	
	8	55.432	16.233	57.760	0.089	3.566	
	13	0.649	-155.800	155.802	0.649	25.946	
4		0.000	0.000	0.000			
	3	-440.420	65.034	445.196	25.911	112.484	
	5	163.382	-76.895	180.573	6.151	-0.391	
	9	276.001	199.133	340.339	3.425	137.014	
	14	1.037	-187.273	187.276	1.037	41.487	
5		0.000	0.000	0.000			
	4	-157.231	76.504	174.855	6.151	-0.391	
	10	156.643	71.131	172.037	0.798	31.907	
	15	0.587	-147.634	147.636	0.587	23.498	
6		-29.616	-6.744	30.374			
	1	-29.616	-6.744	30.374	0.019	0.742	
7		-4.506	-1.021	4.621			
	2	-4.506	-1.021	4.621	0.000	0.020	
8		-55.343	-12.667	56.774			
	3	-55.343	-12.667	56.774	0.089	3.566	
9		-272.575	-62.119	279.564			
	4	-272.575	-62.119	279.564	3.425	137.014	
10		-155.846	-39.224	160.706			
	5	-155.846	-39.224	160.706	0.798	31.907	
11		0.000	-66.285	66.285			
	1	0.000	-66.285	66.285	0.098	3.917	
12		0.000	85.701	85.701			
	2	0.000	85.704	85.704	0.147	5.868	
13		0.000	181.739	181.739			

	3	0.000	181.746	181.746	0.649	25.946
14		0.000	228.748	228.748		
	4	0.000	228.759	228.759	1.037	41.487
15		0.000	171.125	171.125		
	5	0.000	171.132	171.132	0.587	23.498
Total loss			107.386	686.101		

Power Flow Solution by Newton-Raphson Method
Maximum Power Mismatch = 3.8995e-005
No. of Iterations = 6

Bus No.	Voltage Mag.	Angle Degree	Load MW	Load Mvar	Generation MW	Generation Mvar	Injected Mvar
1	1.003	0.000	0.000	0.000	625.250	-23.291	230.000
2	0.932	-13.014	0.000	0.000	0.000	0.000	0.000
3	0.865	-35.347	0.000	0.000	0.000	0.000	0.000
4	0.822	-52.148	0.000	0.000	0.000	0.000	0.000
5	0.861	-62.226	0.000	0.000	0.000	0.000	0.000
6	0.997	-1.349	29.616	6.744	0.000	0.000	0.000
7	0.931	-13.251	4.506	1.021	0.000	0.000	0.000
8	0.850	-38.776	55.343	12.667	0.000	0.000	0.000
9	0.675	-75.139	272.575	62.119	0.000	0.000	0.000
10	0.804	-72.542	155.846	39.224	0.000	0.000	0.000
11	0.947	0.080	0.000	0.000	0.000	233.712	-300.000
12	1.001	-13.119	0.000	0.000	0.000	75.643	10.000
13	1.010	-35.586	0.000	0.000	0.000	142.663	40.000
14	1.005	-52.466	0.000	0.000	0.000	138.974	90.000
15	0.997	-62.454	0.000	0.000	0.000	140.377	30.000
Total			517.887	121.776	625.250	708.078	100.000

Line Flow and Losses

from	to	Power at bus & line flow MW	Mvar	MVA	Line loss MW	Line loss Mvar	Transformer tap
1		625.250	206.709	658.534			
	2	595.520	129.023	609.337	26.865	115.405	
	6	29.635	7.487	30.566	0.019	0.742	
	11	0.098	70.205	70.205	0.098	3.917	
2		0.000	0.000	0.000			
	1	-568.656	-13.618	568.819	26.865	115.405	
	3	564.002	92.363	571.515	41.594	184.551	
	7	4.507	1.041	4.626	0.000	0.020	
	12	0.146	-79.786	79.786	0.146	5.860	
3		0.000	0.000	0.000			
	2	-522.408	92.188	530.480	41.594	184.551	
	4	466.321	48.079	468.793	25.911	112.485	
	8	55.432	16.232	57.760	0.089	3.565	
	13	0.654	-156.499	156.500	0.654	26.171	
4		0.000	0.000	0.000			
	3	-440.410	64.407	445.095	25.911	112.485	
	5	163.367	-76.263	180.291	6.138	-0.423	
	9	276.004	199.271	340.422	3.429	137.152	
	14	1.039	-187.415	187.418	1.039	41.571	
5		0.000	0.000	0.000			
	4	-157.229	75.840	174.564	6.138	-0.423	
	10	156.645	71.196	172.066	0.799	31.973	
	15	0.584	-147.036	147.037	0.584	23.348	
6		-29.616	-6.744	30.374			
	1	-29.616	-6.744	30.374	0.019	0.742	
7		-4.506	-1.021	4.621			
	2	-4.506	-1.021	4.621	0.000	0.020	
8		-55.343	-12.667	56.774			

```
    3 -55.343 -12.667  56.774   0.089   3.565

 9    -272.575 -62.119 279.564
    4 -272.575 -62.119 279.564   3.429 137.152

10    -155.846 -39.224 160.706
    5 -155.846 -39.224 160.706   0.799  31.973

11       0.000 -66.288  66.288
    1    0.000 -66.288  66.288   0.098   3.917

12       0.000  85.643  85.643
    2    0.000  85.646  85.646   0.146   5.860

13       0.000 182.663 182.663
    3    0.000 182.670 182.670   0.654  26.171

14       0.000 228.974 228.974
    4    0.000 228.986 228.986   1.039  41.571

15       0.000 170.377 170.377
    5    0.000 170.384 170.384   0.584  23.348

Total loss                     107.366 686.337
```

Table E-1: Performance index information for initial- and suggested conditions.

Comparative results for all the buses and lines of Scenario 1 and the calculated index information for Scenario 1.

Bus Data

Swing Bus

	Measured by the Simulink model simulation.				Calculated from the developed MATLAB® Simulink model simulation results.							
					Total calculated rms		Fundamental		Harmonic		Total Harmonic Distortion	
	V_a (pu)	I_a (pu)	$P_{3\phi}$ (MW)	$Q_{3\phi}$ (Mvar)	V_a (pu)	I_a (pu)	V_{a1} (pu)	I_{a1} (pu)	V_{ah} (pu)	I_{ah} (pu)	V_aTHD (%)	I_aTHD (%)
Magnitude	1.003340	3.807780	573.06200	-1.550120	1.003300	3.807780	1.003320	3.807770	6.1226E-03	0.005602	0.612251	0.147321
Angle (deg or °)	-n.a.-	-n.a.-	-n.a.-	-n.a.-	0.000552	-n.a.-	0	-n.a.-	-n.a.-	-n.a.-	-n.a.-	-n.a.-

	Effective values analysis of the developed MATLAB® Simulink model simulation results.										
	Voltage (rms)				Current (rms)				Apparent power		
	V_a (pu)	V_{a1} (pu)	V_{ah} (pu)	$VTHD_a$ (%)	I_a (pu)	I_{a1} (pu)	I_{ah} (pu)	$ITHD_a$ (%)	S_a (pu)	S_{a1} (pu)	S_{ah} (pu)
Magnitude	1.003310	1.003320	0.006123	0.610230	3.807810	3.807770	0.005602	0.147121	1.910180	1.910210	0.011556

	Calculated three-phase power information.							Miscellaneous data			
	$S_{3\phi}$ (MVA)	$S_{3\phi1}$ (MVA)	$S_{3\phi N}$ (MVA)	$P_{3\phi}$ (MW)	$P_{3\phi1}$ (MW)	$P_{3\phiN}$ (MW)	$Q_{3\phi1}$ (Mvar)	$S_{a\phi}$ / S_{a1}	PF	DPF	Pollution indicator, true apparent- and displacement power factor.
Magnitude	576.679000	573.063111	3.615590	573.062000	573.061000	3.9882E-04	-1.555550	0.006277	0.993727	0.999996	

Bus 1 Load

	Measured by the Simulink model simulation.				Calculated from the developed MATLAB® Simulink model simulation results.							
					Total calculated rms		Fundamental		Harmonic		Total Harmonic Distortion	
	V_a (pu)	I_a (pu)	$P_{3\phi}$ (MW)	$Q_{3\phi}$ (Mvar)	V_a (pu)	I_a (pu)	V_{a1} (pu)	I_{a1} (pu)	V_{ah} (pu)	I_{ah} (pu)	V_aTHD (%)	I_aTHD (%)
Magnitude	0.947358	0.213752	29.61600	6.743860	0.947326	0.213751	0.947341	0.213751	5.6655E-03	0.000865	0.599992	0.405387
Angle (deg or °)	-n.a.-	-n.a.-	-n.a.-	-n.a.-	-0.422408	-n.a.-	-0.422959	-n.a.-	-n.a.-	-n.a.-	-n.a.-	-n.a.-

	Effective values analysis of the developed MATLAB® Simulink model simulation results.										
	Voltage (rms)				Current (rms)				Apparent power		
	V_a (pu)	V_{a1} (pu)	V_{ah} (pu)	$VTHD_a$ (%)	I_a (pu)	I_{a1} (pu)	I_{ah} (pu)	$ITHD_a$ (%)	S_a (pu)	S_{a1} (pu)	S_{ah} (pu)
Magnitude	0.947334	0.947341	0.005666	0.598047	0.213749	0.213751	0.000865	0.404551	0.101246	0.101247	0.000520

	Calculated three-phase power information.							Miscellaneous data			
	$S_{3\phi}$ (MVA)	$S_{3\phi1}$ (MVA)	$S_{3\phiN}$ (MVA)	$P_{3\phi}$ (MW)	$P_{3\phi1}$ (MW)	$P_{3\phiH}$ (MW)	$Q_{3\phi1}$ (Mvar)	$S_{a\phi}$ / S_{a1}	PF	DPF	Pollution indicator, true apparent- and displacement power factor.
Magnitude	30.594200	30.373754	0.220358	29.616000	29.615500	4.8856E-04	6.744410	0.007220	0.968029	0.975036	

Bus 2

	Measured by the Simulink model simulation.				Calculated from the developed MATLAB® Simulink model simulation results.							
					Total calculated rms		Fundamental		Harmonic		Total Harmonic Distortion	
	V_a (pu)	I_a (pu)	$P_{3\phi}$ (MW)	$Q_{3\phi}$ (Mvar)	V_a (pu)	I_a (pu)	V_{a1} (pu)	I_{a1} (pu)	V_{ah} (pu)	I_{ah} (pu)	V_aTHD (%)	I_aTHD (%)
Magnitude	0.998631	3.586410	527.17200	-102.902000	0.998596	3.586300	0.998609	3.585890	5.5243E-03	0.061115	0.654295	1.714030
Angle (deg or °)	-n.a.-	-n.a.-	-n.a.-	-n.a.-	-7.797420	-n.a.-	-7.79786	-n.a.-	-n.a.-	-n.a.-	-n.a.-	-n.a.-

	Effective values analysis of the developed MATLAB® Simulink model simulation results.										
	Voltage (rms)				Current (rms)				Apparent power		
	V_a (pu)	V_{a1} (pu)	V_{ah} (pu)	$VTHD_a$ (%)	I_a (pu)	I_{a1} (pu)	I_{ah} (pu)	$ITHD_a$ (%)	S_a (pu)	S_{a1} (pu)	S_{ah} (pu)
Magnitude	0.998603	0.998609	0.005524	0.553196	3.585920	3.585890	0.061115	1.704310	1.790630	1.790450	0.029988

	Calculated three-phase power information.							Miscellaneous data			
	$S_{3\phi}$ (MVA)	$S_{3\phi1}$ (MVA)	$S_{3\phiN}$ (MVA)	$P_{3\phi}$ (MW)	$P_{3\phi1}$ (MW)	$P_{3\phiH}$ (MW)	$Q_{3\phi1}$ (Mvar)	$S_{a\phi}$ / S_{a1}	PF	DPF	Pollution indicator, true apparent- and displacement power factor.
Magnitude	547.009000	537.136222	9.872320	527.172000	527.177000	-4.7552E-03	-102.955000	0.017919	0.963737	0.981458	

Bus 2 Load

	Measured by the Simulink model simulation.				Calculated from the developed MATLAB® Simulink model simulation results.							
					Total calculated rms		Fundamental		Harmonic		Total Harmonic Distortion	
	V_a (pu)	I_a (pu)	$P_{3\phi}$ (MW)	$Q_{3\phi}$ (Mvar)	V_a (pu)	I_a (pu)	V_{a1} (pu)	I_{a1} (pu)	V_{ah} (pu)	I_{ah} (pu)	V_aTHD (%)	I_aTHD (%)
Magnitude	1.000750	0.030783	4.50649	1.021350	1.000710	0.030783	1.000720	0.030783	4.7629E-03	0.000123	0.790580	0.467320
Angle (deg or °)	-n.a.-	-n.a.-	-n.a.-	-n.a.-	-7.901510	-n.a.-	-7.9019	-n.a.-	-n.a.-	-n.a.-	-n.a.-	-n.a.-

	Effective values analysis of the developed MATLAB® Simulink model simulation results.										
	Voltage (rms)				Current (rms)				Apparent power		
	V_a (pu)	V_{a1} (pu)	V_{ah} (pu)	$VTHD_a$ (%)	I_a (pu)	I_{a1} (pu)	I_{ah} (pu)	$ITHD_a$ (%)	S_a (pu)	S_{a1} (pu)	S_{ah} (pu)
Magnitude	1.000710	1.000720	0.004763	0.475948	0.030783	0.030783	0.000123	0.399622	0.015402	0.015403	0.000064

	Calculated three-phase power information.							Miscellaneous data			
	$S_{3\phi}$ (MVA)	$S_{3\phi1}$ (MVA)	$S_{3\phiN}$ (MVA)	$P_{3\phi}$ (MW)	$P_{3\phi1}$ (MW)	$P_{3\phiH}$ (MW)	$Q_{3\phi1}$ (Mvar)	$S_{a\phi}$ / S_{a1}	PF	DPF	Pollution indicator, true apparent- and displacement power factor.
Magnitude	4.663160	4.620709	0.042457	4.506480	4.506390	9.8649E-05	1.021470	0.006215	0.966401	0.975259	

Bus 3

	Measured by the Simulink model simulation.				Calculated from the developed MATLAB® Simulink model simulation results.							
					Total calculated rms		Fundamental		Harmonic		Total Harmonic Distortion	
	V_a (pu)	I_a (pu)	$P_{3\phi}$ (MW)	$Q_{3\phi}$ (Mvar)	V_a (pu)	I_a (pu)	V_{a1} (pu)	I_{a1} (pu)	V_{ah} (pu)	I_{ah} (pu)	V_aTHD (%)	I_aTHD (%)
Magnitude	1.004560	3.454620	501.66400	-138.306000	1.004130	3.454610	1.004340	3.454460	2.0518E-02	0.033488	2.102500	0.978204
Angle (deg or °)	-n.a.-	-n.a.-	-n.a.-	-n.a.-	-19.314700	-n.a.-	-19.3142	-n.a.-	-n.a.-	-n.a.-	-n.a.-	-n.a.-

	Effective values analysis of the developed MATLAB® Simulink model simulation results.										
	Voltage (rms)				Current (rms)				Apparent power		
	V_a (pu)	V_{a1} (pu)	V_{ah} (pu)	$VTHD_a$ (%)	I_a (pu)	I_{a1} (pu)	I_{ah} (pu)	$ITHD_a$ (%)	S_a (pu)	S_{a1} (pu)	S_{ah} (pu)
Magnitude	1.004330	1.004340	0.020518	2.042940	3.454490	3.454460	0.033488	0.969426	1.734440	1.734720	0.031399

	Calculated three-phase power information.							Miscellaneous data			
	$S_{3\phi}$ (MVA)	$S_{3\phi1}$ (MVA)	$S_{3\phiN}$ (MVA)	$P_{3\phi}$ (MW)	$P_{3\phi1}$ (MW)	$P_{3\phiH}$ (MW)	$Q_{3\phi1}$ (Mvar)	$S_{a\phi}$ / S_{a1}	PF	DPF	Pollution indicator, true apparent- and displacement power factor.

	Magnitude	532.508000	520.417532	12.090000	501.665000	501.674000	-9.5914E-03	-138.411000	0.022614	0.942080	0.963984	

Bus 3 Load

Measured by the Simulink model simulation.				Calculated from the developed MATLAB® Simulink model simulation results.							
				Total calculated rms		Fundamental		Harmonic		Total Harmonic Distortion	
V_a (pu)	I_a (pu)	$P_{3\Phi}$ (MW)	$Q_{3\Phi}$ (Mvar)	V_a (pu)	I_a (pu)	V_{a1} (pu)	I_{a1} (pu)	V_{aH} (pu)	I_{aH} (pu)	V_aTHD (%)	I_aTHD (%)
1.010760	0.376494	55.34300	12.804700	1.009200	0.375450	1.009950	0.375232	4.0000E-02	0.023605	3.997300	8.207450
-n.a.-	-n.a.-	-n.a.-	-n.a.-	-20.453700	-n.a.-	-20.4397	-n.a.-	-n.a.-	-n.a.-	-n.a.-	-n.a.-

Effective values analysis of the developed MATLAB® Simulink model simulation results.										
Voltage (rms)				Current (rms)				Apparent power		
V_e (pu)	V_{e1} (pu)	V_{eH} (pu)	$VTHD_e$ (%)	I_e (pu)	I_{e1} (pu)	I_{eH} (pu)	$ITHD_e$ (%)	S_e (pu)	S_{e1} (pu)	S_{eN} (pu)
1.009940	1.009950	0.040000	3.960600	0.375432	0.375232	0.023605	6.290730	0.189451	0.189483	0.012398

Calculated three-phase power information.							Miscellaneous data			Pollution indicator, true apparent- and displacement power factor.
$S_{3\Phi}$ (MVA)	$S_{3\Phi1}$ (MVA)	$S_{3\Phi N}$ (MVA)	$P_{3\Phi}$ (MW)	$P_{3\Phi1}$ (MW)	$P_{3\Phi H}$ (MW)	$Q_{3\Phi1}$ (Mvar)	S_{eN} / S_{e1}	PF	DPF	
62.034200	56.839348	5.194830	55.343100	55.409800	-6.6712E-02	12.667500	0.074379	0.892139	0.974850	

Bus 4

Measured by the Simulink model simulation.				Calculated from the developed MATLAB® Simulink model simulation results.							
				Total calculated rms		Fundamental		Harmonic		Total Harmonic Distortion	
V_a (pu)	I_a (pu)	$P_{3\Phi}$ (MW)	$Q_{3\Phi}$ (Mvar)	V_a (pu)	I_a (pu)	V_{a1} (pu)	I_{a1} (pu)	V_{aH} (pu)	I_{aH} (pu)	V_aTHD (%)	I_aTHD (%)
1.008610	2.953780	433.59600	-107.136000	1.008600	2.953760	1.008580	2.952000	6.1696E-03	0.102356	0.730376	3.474220
-n.a.-	-n.a.-	-n.a.-	-n.a.-	-27.141200	-n.a.-	-27.1413	-n.a.-	-n.a.-	-n.a.-	-n.a.-	-n.a.-

Effective values analysis of the developed MATLAB® Simulink model simulation results.										
Voltage (rms)				Current (rms)				Apparent power		
V_e (pu)	V_{e1} (pu)	V_{eH} (pu)	$VTHD_e$ (%)	I_e (pu)	I_{e1} (pu)	I_{eH} (pu)	$ITHD_e$ (%)	S_e (pu)	S_{e1} (pu)	S_{eN} (pu)
1.008580	1.008580	0.006170	0.611706	2.952070	2.952000	0.102356	3.467340	1.489580	1.488670	0.052395

Calculated three-phase power information.							Miscellaneous data			Pollution indicator, true apparent- and displacement power factor.
$S_{3\Phi}$ (MVA)	$S_{3\Phi1}$ (MVA)	$S_{3\Phi N}$ (MVA)	$P_{3\Phi}$ (MW)	$P_{3\Phi1}$ (MW)	$P_{3\Phi H}$ (MW)	$Q_{3\Phi1}$ (Mvar)	S_{eN} / S_{e1}	PF	DPF	
462.482000	446.607850	15.873600	433.595000	433.556000	3.8697E-02	-107.181000	0.035210	0.937540	0.970775	

Bus 4 Load

Measured by the Simulink model simulation.				Calculated from the developed MATLAB® Simulink model simulation results.							
				Total calculated rms		Fundamental		Harmonic		Total Harmonic Distortion	
V_a (pu)	I_a (pu)	$P_{3\Phi}$ (MW)	$Q_{3\Phi}$ (Mvar)	V_a (pu)	I_a (pu)	V_{a1} (pu)	I_{a1} (pu)	V_{aH} (pu)	I_{aH} (pu)	V_aTHD (%)	I_aTHD (%)
1.004560	1.855610	272.57500	62.100300	1.004550	1.855490	1.004520	1.855090	7.6346E-03	0.039166	0.929624	2.376790
-n.a.-	-n.a.-	-n.a.-	-n.a.-	-32.576400	-n.a.-	-32.5771	-n.a.-	-n.a.-	-n.a.-	-n.a.-	-n.a.-

Effective values analysis of the developed MATLAB® Simulink model simulation results.										
Voltage (rms)				Current (rms)				Apparent power		
V_e (pu)	V_{e1} (pu)	V_{eH} (pu)	$VTHD_e$ (%)	I_e (pu)	I_{e1} (pu)	I_{eH} (pu)	$ITHD_e$ (%)	S_e (pu)	S_{e1} (pu)	S_{eN} (pu)
1.004520	1.004520	0.007635	0.760025	1.855070	1.855090	0.039167	2.111300	0.931965	0.931737	0.020708

Calculated three-phase power information.							Miscellaneous data			Pollution indicator, true apparent- and displacement power factor.
$S_{3\Phi}$ (MVA)	$S_{3\Phi1}$ (MVA)	$S_{3\Phi N}$ (MVA)	$P_{3\Phi}$ (MW)	$P_{3\Phi1}$ (MW)	$P_{3\Phi H}$ (MW)	$Q_{3\Phi1}$ (Mvar)	S_{eN} / S_{e1}	PF	DPF	
286.651000	279.521799	7.129540	272.575000	272.532000	4.3240E-02	62.118800	0.022440	0.950895	0.974994	

Bus 6

Measured by the Simulink model simulation.				Calculated from the developed MATLAB® Simulink model simulation results.							
				Total calculated rms		Fundamental		Harmonic		Total Harmonic Distortion	
V_a (pu)	I_a (pu)	$P_{3\Phi}$ (MW)	$Q_{3\Phi}$ (Mvar)	V_a (pu)	I_a (pu)	V_{a1} (pu)	I_{a1} (pu)	V_{aH} (pu)	I_{aH} (pu)	V_aTHD (%)	I_aTHD (%)
1.007650	1.043420	156.99600	3.810890	1.007140	1.038380	1.006310	1.040560	5.1800E-02	0.076350	5.165220	7.428010
-n.a.-	-n.a.-	-n.a.-	-n.a.-	-31.521700	-n.a.-	-31.4625	-n.a.-	-n.a.-	-n.a.-	-n.a.-	-n.a.-

Effective values analysis of the developed MATLAB® Simulink model simulation results.										
Voltage (rms)				Current (rms)				Apparent power		
V_e (pu)	V_{e1} (pu)	V_{eH} (pu)	$VTHD_e$ (%)	I_e (pu)	I_{e1} (pu)	I_{eH} (pu)	$ITHD_e$ (%)	S_e (pu)	S_{e1} (pu)	S_{eN} (pu)
1.006310	1.006310	0.051800	5.147500	1.040590	1.040560	0.076350	7.337380	0.522898	0.523559	0.040638

Calculated three-phase power information.							Miscellaneous data			Pollution indicator, true apparent- and displacement power factor.
$S_{3\Phi}$ (MVA)	$S_{3\Phi1}$ (MVA)	$S_{3\Phi N}$ (MVA)	$P_{3\Phi}$ (MW)	$P_{3\Phi1}$ (MW)	$P_{3\Phi H}$ (MW)	$Q_{3\Phi1}$ (Mvar)	S_{eN} / S_{e1}	PF	DPF	
171.291000	157.072140	14.219300	156.994000	157.039000	-4.4468E-02	3.226380	0.089709	0.916534	0.999789	

Bus 5 Load

Measured by the Simulink model simulation.				Calculated from the developed MATLAB® Simulink model simulation results.							
				Total calculated rms		Fundamental		Harmonic		Total Harmonic Distortion	
V_a (pu)	I_a (pu)	$P_{3\Phi}$ (MW)	$Q_{3\Phi}$ (Mvar)	V_a (pu)	I_a (pu)	V_{a1} (pu)	I_{a1} (pu)	V_{aH} (pu)	I_{aH} (pu)	V_aTHD (%)	I_aTHD (%)
0.998968	1.075450	155.84500	38.896000	0.998536	1.073730	0.997357	1.074520	5.6499E-02	0.043192	5.686970	4.159440
-n.a.-	-n.a.-	-n.a.-	-n.a.-	-34.678700	-n.a.-	-34.6167	-n.a.-	-n.a.-	-n.a.-	-n.a.-	-n.a.-

Effective values analysis of the developed MATLAB® Simulink model simulation results.										
Voltage (rms)				Current (rms)				Apparent power		
V_e (pu)	V_{e1} (pu)	V_{eH} (pu)	$VTHD_e$ (%)	I_e (pu)	I_{e1} (pu)	I_{eH} (pu)	$ITHD_e$ (%)	S_e (pu)	S_{e1} (pu)	S_{eN} (pu)
0.997355	0.997357	0.056499	5.664860	1.074420	1.074520	0.043192	4.019670	0.536080	0.535840	0.029286

Calculated three-phase power information.							Miscellaneous data			Pollution indicator, true apparent- and displacement power factor.
$S_{3\Phi}$ (MVA)	$S_{3\Phi1}$ (MVA)	$S_{3\Phi N}$ (MVA)	$P_{3\Phi}$ (MW)	$P_{3\Phi1}$ (MW)	$P_{3\Phi H}$ (MW)	$Q_{3\Phi1}$ (Mvar)	S_{eN} / S_{e1}	PF	DPF	
172.084000	160.754638	11.329700	155.846000	155.896000	-5.0096E-02	39.223600	0.069498	0.905637	0.969776	

Line Data

Line 1

Calculated from the measured data as measured by the Simulink model simulation.											
Sending-end rms voltage and current						Receiving-end rms voltage and current					
Voltage (rms)			Current (rms)			Voltage (rms)			Current (rms)		
$V_{s\,a}$ (pu)	$V_{s\,a1}$ (pu)	$V_{s\,aH}$ (pu)	$I_{s\,a}$ (pu)	$I_{s\,a1}$ (pu)	$I_{s\,aH}$ (pu)	$V_{r\,a}$ (pu)	$V_{r\,a1}$ (pu)	$V_{r\,aH}$ (pu)	$I_{r\,a}$ (pu)	$I_{r\,a1}$ (pu)	$I_{r\,aH}$ (pu)
1.003302	1.003320	0.006123	3.624005	3.623648	0.060777	0.998599	0.998612	0.005524	3.586301	3.585885	0.061115

Calculated three-phase power line loss.			
$S_{line3\Phi}$ (MVA)	$P_{line3\Phi}$ (MW)	$N_{line3\Phi}$	
49.356686	11.022300	48.110200	

Line 2

Calculated from the measured data as measured by the Simulink model simulation.											
Sending-end rms voltage and current						Receiving-end rms voltage and current					
Voltage (rms)			Current (rms)			Voltage (rms)			Current (rms)		
$V_{s\,a}$ (pu)	$V_{s\,a1}$ (pu)	$V_{s\,aH}$ (pu)	$I_{s\,a}$ (pu)	$I_{s\,a1}$ (pu)	$I_{s\,aH}$ (pu)	$V_{r\,a}$ (pu)	$V_{r\,a1}$ (pu)	$V_{r\,aH}$ (pu)	$I_{r\,a}$ (pu)	$I_{r\,a1}$ (pu)	$I_{r\,aH}$ (pu)
0.998599	0.998612	0.005524	3.534941	3.534550	0.057833	1.004126	1.004335	0.020518	3.454610	3.454460	0.033488

Calculated three-phase power line loss.			
$S_{line3\Phi}$ (MVA)	$P_{line3\Phi}$ (MW)	$N_{line3\Phi}$	
71.057134	17.075700	68.974900	

Line 3

Calculated from the measured data as measured by the Simulink model simulation.											
Sending-end rms voltage and current						Receiving-end rms voltage and current					
Voltage (rms)			Current (rms)			Voltage (rms)			Current (rms)		
$V_{s\,a}$ (pu)	$V_{s\,a1}$ (pu)	$V_{s\,aH}$ (pu)	$I_{s\,a}$ (pu)	$I_{s\,a1}$ (pu)	$I_{s\,aH}$ (pu)	$V_{r\,a}$ (pu)	$V_{r\,a1}$ (pu)	$V_{r\,aH}$ (pu)	$I_{r\,a}$ (pu)	$I_{r\,a1}$ (pu)	$I_{r\,aH}$ (pu)
1.004126	1.004335	0.020518	3.018583	3.017271	0.089117	1.008602	1.008583	0.006170	2.953756	2.952001	0.102356

Calculated three-phase power line loss.			
$S_{line3\Phi}$ (MVA)	$P_{line3\Phi}$ (MW)	$N_{line3\Phi}$	
41.475306	9.849550	40.288800	

Line 4

Calculated from the measured data as measured by the Simulink model simulation.											
Sending-end rms voltage and current						Receiving-end rms voltage and current					
Voltage (rms)			Current (rms)			Voltage (rms)			Current (rms)		
$V_{s\,a}$ (pu)	$V_{s\,a1}$ (pu)	$V_{s\,aH}$ (pu)	$I_{s\,a}$ (pu)	$I_{s\,a1}$ (pu)	$I_{s\,aH}$ (pu)	$V_{r\,a}$ (pu)	$V_{r\,a1}$ (pu)	$V_{r\,aH}$ (pu)	$I_{r\,a}$ (pu)	$I_{r\,a1}$ (pu)	$I_{r\,aH}$ (pu)
1.008602	1.008583	0.006170	1.113126	1.112591	0.139994	1.007139	1.006307	0.051800	1.038387	1.040557	0.076350

Calculated three-phase power line loss.			
$S_{line3\Phi}$ (MVA)	$P_{line3\Phi}$ (MW)	$N_{line3\Phi}$	
8.457248	3.264740	7.801700	

Performance

Calculated index measures for the scenario.			
$Index_{performance}$	$Index_V$	$Index_{THD}$	$Index_{P\,loss}$
0.936598	0.017450	0.045952	1.1410E-07

Bibliography

[1] CIRED, Dispersed generation, CIRED report (International Conference on Electricity Distribution), Working Group WG04, Brussels, Belgium, June 1999.

[2] H. Lee Willis and Walter G. Scott, "Distributed Power Generation: Planning and Evaluation", Marcell Dekker, 2000.

[3] Visit the web page at http://grouper.ieee.org/groups/td/pq/ for the relevant standards.

[4] Anne-Marie Borbely and Jan F. Kreider, "Distributed Generation: The Power Paradigm for the New Millennium", CRC Press, 2001.

[5] Richard P. Bingham, "Power Quality – A Critical Element for Distributed Generation", February 2001.

[6] See the "Distributed Generation" website at www.distributed-generation.com.

[7] DG Monitor, Volume II, Issue 6, November/December 2002, various authors.

[8] DG Monitor, Volume II, Issue 5 September/October 2002, Resource Dynamics Corporation, various authors.

[9] N. Richard Friedman – Resource Dynamics Corporation, "Distributed Generation & On-Site Power Conference", March 12, 2002, Atlanta, Georgia.

[10] "Distributed Generation Interconnection Manual", Public Utility Commission of Texas U.S. Department of Energy, Office of Energy Efficiency and Renewable Energy, 2001.

[11] Gray Davis, "California Energy Commission, Distributed Generation Strategic Plan", June 2002.

[12] See the "Electric Power Research Institute (EPRI)" web page http://www.epri.com/gg/newgen/disgen/index.html.

[13] Gas Research Institute, "Distributed Power Generation: A strategy for a competitive energy industry", Gas Research Institute, Chicago, USA 1998.

[14] D. Sharma, R. Bartels, "Distributed electricity generation in competitive energy markets", in: "The Energy Journal: Distributed Resources: Toward a new paradigm of the electricity business", Cleveland, Ohio, USA 1998.

[15] J. Cardell, R Tabors, "Operation and control in competitive energy markets, distributed generation in a restructured industry", in: "The Energy Journal: Distributed Resources: Toward a new paradigm of the electricity business", Cleveland, Ohio, USA 1998, p.111–134.

[16] CIRED, "Impact of increasing contribution of dispersed generation on power systems", CIGRE Study Committee no 37, September 1998.

[17] See the "Institute of Electrical and Electronic Engineers" web page http://grouper.ieee.org/groups/scc21/1547/archives/.

[18] H.R. Linden, Distributed Power Generation, "The logical response to restructuring and convergence", see web page http://www.dpc.org/publications/index.html.

[19] International Energy Agency (IEA), "Enhancing the market deployment of energy technology", Paris 1997, p.64.

[20] J.A. Duffie, "Solar engineering of thermal processes", John Wiley & Sons, New York, USA, 1991, p.638.

[21] Anis Ibrahim, M.M. Morcos, "Electric power quality and artificial intelligence: Overview and applicability", IEEE Power engineering review, 5-10 June 1999.

[22] R.C. Dugan, M.F. McGranaghan, H.W. Beaty, "Electric Power Systems Quality", McGraw-Hill, 1996.

[23] A.P. George, "Introduction to the Pebble Bed Modular reactor (PBMR)", PBMR, Pretoria, Tech. Rep. 2001.

[24] M.C. Nieuwoudt and W Kriel, "PBMR operability summary", PBMR, Pretoria, Tech. Rep. Revision: 2D, 2001.
[25] See the "RReDC Glossary of Solar Radiation Resource Terms" web page at http://rredc.nrel.gov/solar/glossary (sections "A-Z").
[26] Glover J. Duncan – Failure Analysis Associates, Inc., Sarma Mulukutla – Northeastern University, "Power System Analysis and Design", PWS Publishing Company, Boston, USA, 1994.
[27] See the "Current Technology: Harmonix" web page at http://www.psihq.com/harmonic/harmonix.htm.
[28] See the "Harmonics Limited | What Are Harmonic Currents?" web page at http://www.harmonicslimited.com/docs/tech/what_r.html.
[29] Rens A.P.J., "Validation of popular non-sinusoidal power theories for the analysis and management of modern power systems", PhD thesis, North-West University, South Africa, 2005.
[30] W. Mack Grady and Surya Santoso, "Understanding Power System Harmonics", USA, September 2001.
[31] Mack Grady – University of Texas at Austin, "Understanding Power System Harmonics", September 2000.
[32] NRS 048-2:1996 – 1st Edition, "Electricity Supply – Quality of Supply", South Africa, 1996.
[33] NRS 048-4:1999 – 1st Edition, Draft 2a of NRS 048-4:1999, "Electricity Supply – Quality of Supply", South Africa, 1999.
[34] Electrical Power Research Institute (EPRI), "Power quality impacts of distributed generation: Guidelines", Final Report, California, USA, December 2000.
[35] Saadat Hadi, "Power System Analysis", Milwaukee School of Engineering, WCB/McGraw-Hill, Singapore, 1999.
[36] Institute of Electrical and Electronic Engineers – IEEE, P1433/D5A, "A Draft Standard Glossary of Power Quality Terminology", July 15, 1999.
[37] Ned Mohan, Tore M. Undeland, William P. Robbins, "Power Electronics – Converters, Applications and Design", John Wiley & Sons, New York, USA, 1995.
[38] IEEE Working Group on Non-sinusoidal Situations: "Effects on Meter Performance and Definitions of Power; Practical Definitions for Power in Systems with Non-sinusoidal Waveforms and Unbalanced Loads: A Discussion"; IEEE Transactions on Power Delivery, Vol. 11, No 1, January 1996; pp 79-101.
[39] Caldon R., Rossetto F., Scala A. "Reactive power control in distribution networks with dispersed generators: a cost based method", Electric Power Systems Research vol. 64, p.209–217, 2003.